# Mathematical Analysis of Malaria Transmission Dynamics

by

Ashrafi Meher Niger

A Thesis submitted to the Faculty of Graduate Studies of

The University of Manitoba

in partial fulfilment of the requirements of the degree of

MASTER OF SCIENCE

Department of Mathematics

University of Manitoba

Winnipeg

# Mathematical Analysis of Malaria Transmission Dynamics

By

**Ashrafi Meher Niger**

A Thesis/Practicum submitted to the Faculty of Graduate Studies of The University of Manitoba in partial fulfillment of the requirement of the degree

Of

**Master of Science**

# Abstract

The thesis is based on using mathematical approaches to gain insights into the transmission dynamics of malaria, a disease of major public health significance. Since mosquito vector is critically important to malaria dynamics, a model for the population dynamics of the malaria vector is considered first of all. The model takes the form of a system of delay differential equations. The asymptotic stability of the associated equilibria as well as the existence of Hopf bifurcation are established using various mathematical techniques and theories (such as the fluctuation method, Fatou's lemma and Hopf bifurcation theory).

A model assessing the impact of immune response and a potential anti-malaria vaccine on controlling malaria dynamics in an infected host is developed and rigorously analysed. The model, which is derived based on progressive refinements of some existing models, has a globally-asymptotically stable disease-free equilibrium (for a special case) when the associated reproduction threshold is less than unity. The model allows for the assessment of various assumed vaccine characteristics.

Finally, the thesis addresses the problem of the role of repeated malaria exposure on the transmission dynamics of the disease in a population. It is shown that such repeated exposure induces the phenomenon of backward bifurcation, the epidemiological consequence of which is that the classical requirement of having the associated reproduction number less than unity becomes only necessary, but not sufficient, for the effective control of malaria in a population. Numerical simulations of the model

show that the size of the backward bifurcation region increases with increasing rate of re-infection of first-time infected individuals.

# Acknowledgement

I would like to take this opportunity to express my homage and deep sense of gratitude to my honourable supervisor Professor Abba B. Gumel of the Department of Mathematics, University of Manitoba, whose kind and sympathetic guidance, warm advice and encouragement have enabled me to successfully carry out this work. I am greatly indebted to Chandra Nath Podder, a fellow graduate student, for always been there for me. I am grateful to Oluwaseun Sharomi for his help and support.

I wish to express my profound gratitude to the Department of Mathematics, together with the Faculty of Graduate Studies and the Faculty of Science, of the University of Manitoba, for the financial support during my M.Sc. program. I am grateful to my Thesis Committee members, namely Dr. J. Arino (Department of Mathematics), Dr. C. Bowman (Institute for Biodiagnostics) and Dr. J. Williams (Department of Mathematics) for their valuable comments and suggestions.

I am also grateful to the teaching and secretarial staff of the department, especially Professors T. Berry and T. Kucera, for their support. I am thankful to the graduate students in the department for their friendship and support, particularly the members of our research group (S. M. Garba, D. Melesse, M. Safi and A. Sunday).

Finally, I acknowledge the invaluable support, love and inspiration of my family, which has been very helpful in the successful completion of the thesis.

# Dedication

To my lovely parents.

# Contents

# List of Tables

# List of Figures

# Glossary

| Abbreviation | Meaning |
|---|---|
| DDE | Delay differential equation |
| DFE | Disease-free equilibrium |
| EEP | Endemic equilibrium point |
| GAS | Globally-asymptotically stable |
| IRBC | Infected red blood cell |
| LAS | Locally-asymptotically stable |
| ODE | Ordinary differential equation |
| RBC | Red blood cell |

# Chapter 1

# Introduction

## 1.1 Public Health and Socio-economic Impact

Malaria is a parasitic vector-borne disease that is endemic in many parts of the world. Currently, up to 300 million people are affected worldwide (with about 2 million malaria-related deaths recorded annually) [139]. Although malaria has been successfully controlled in most developed areas of the world, it remains a major public health burden in many of the developing parts of the globe, particularly in some regions within Africa, Asia and South America. For instance, malaria represents 10% of Africa's overall disease burden [139]. In malaria endemic areas, the heaviest toll of morbidity and mortality falls on young children (in the year 2000, malaria was the principal cause of around 18% of deaths of children under 5 years of age in sub-Saharan Africa [121]). Unfortunately, however, in the past three decades, there has been a resurgence of malaria in areas where it had been eradicated or had been successfully controlled [12].

This is largely attributed to global warming, resistance to anti-malarial drugs (such as Chloroquine), inadequate vector control programmes, migration etc. [12].

## 1.2 Transmission of Malaria

The malaria parasite is primarily transmitted from person-to-person by an infected female *Anopheles* mosquito when it takes a blood meal from the host. It can also be transmitted through blood transfusion from donors with parasitaemia [48]. Transplacental malaria (i.e., congenital malaria) occurs in malaria-endemic areas in population with partial immunity to malaria [48]. The symptoms of malaria in an infected human include fever and anaemia. On average, the incubation period is about 12 days in humans and about 10 days in mosquitoes. The period can be longer depending on the strain of the parasite. In this thesis, malaria transmission through mosquito bites (by female Anopheles mosquitoes) is considered.

The *Anopheles* mosquito goes through several distinct stages of development. The eggs are laid on water. After about 2-3 days, they hatch into larvae. This process is temperature-dependent, and can take up to 2-3 weeks in cold weather. In about 4-10 days, the larvae mature into pupae. The pupae then metamorphose into adult mosquitoes in about 2-4 days. The duration of the whole cycle varies between 7 and 20 days, depending on the ambient temperature and the mosquito species [47].

The four species that cause malaria in humans are the protozoan parasites of the genus *Plasmodium* (*Plasmodium vivax*, *Plasmodium malariae*, *Plasmodium ovale* and *Plasmodium falciparum*). These protozoan parasites are transmitted by the bite of a

female *Anopheles* mosquito. The species *P. falciparum* accounts for the most severe and often potentially lethal forms of malaria. This thesis will focus on transmission by the *P. falciparum* species.

Once inside a human host, the parasite develops and multiplies, causing flu-like symptoms such as fever, headache and chills. The developing parasites destroy red blood cells (RBCs), which may cause death by severe anemia as well as by the clogging of capillaries that supply the brain, or other vital organs, with blood [92].

*Plasmodium* has a complex life style, alternating between human and mosquito hosts. The infected female Anopheles mosquito injects the parasite, in the form of *sporozoite*, into the host's bloodstream when taking a blood meal. Then, the *sporozoite* enters a liver cell and produce thousands of *merozoites* (another form of the parasite) and releases them into the bloodstream. In the bloodstream, *merozoites* infect red blood cells, reproduce there and burst out of the infected cells (following the rupture of the host cells). The resulting *merozoites* can infect other red blood cells, yielding a cycle of infection and eruption. This cycle, known as the *erythrocytic* stage, causes the pathological hallmarks of a malaria infection [51]. Some of the *merozoites* develop into sexual forms, called *gametocytes*, which are either male or female [30]. The ingestion of these *gametocytes* (following a blood meal) by a mosquito initiates the next stage of the *Plasmodium* life cycle. In the mosquito's gut, *gametocytes* produce *gametes*. *Zygotes*, produced from *gametes*, develop into *ookinete* and then *oocyst*. The *oocyst* rupture and release *sporozoites*, which migrate to the salivary gland of mosquito, infect humans and repeat the *Plasmodium* life cycle [92].

## 1.3 Control Strategies Against Malaria

The World Health Organization (WHO), in conjunction with the United Nations Children's Fund (UNICEF), the United Nations Development Programme (UNDP), and the World Bank launched the Roll Back Malaria Global Partnership (RBM) in 1998, with the goal of halving the worldwide burden of malaria by 2010 [139]. In line with this laudable initiative, numerous control and therapeutic strategies have been set up including larval control, indoor residual spraying, insecticide-treated bed nets (ITNs), prompt and effective case management, personal protection against mosquito bite (*via* the use of insect repellents), using DNA technology to modify the vector's ability to transmit infection, the use of antibiotics, etc. [120]. Furthermore, although concerted efforts are embarked upon to design a suitable malaria vaccine, no such vaccine is currently available for use in humans. Consequently, anti-malaria strategies are focussed on vector-reduction and personal protection strategies. However, in order to choose the most effective vector control strategy (or combination of strategies), it is necessary to understand the population dynamics of the mosquito vector. A sizable part of this thesis is devoted to the mathematical analysis of the population dynamics of the malaria vector.

## 1.4 Thesis Outline

The thesis is organized as follows. In Chapter 2, some basic mathematical preliminaries, relevant to the thesis, are described. In Chapter 3, a population model for the

dynamics of the malaria vector is formulated. The model, which takes the form of a deterministic system of non-linear delay differential equations, is qualitatively and numerically analysed subject to two types of birth rate functions, in the absence of delay. The vector population model with time delay is studied in Chapter 4. Chapter 5 addresses some in-host models for malaria, with the aim of gaining insight into the effect of immune response and potential vaccination on malaria transmission dynamics *in vivo*. In Chapter 6, the role of infection-acquired immunity due to repeated exposure to malaria is investigated using a deterministic model. The main mathematical and epidemiological contributions of the thesis are summarized in Chapter 7.

# Chapter 2

# Mathematical Preliminaries

This chapter introduces some of the key mathematical theories and methodologies relevant to the thesis.

## 2.1 Equilibria of Linear and Non-linear Autonomous Systems

Consider the equation below

$$\dot{x} = f(x, t; \mu), \quad x \in U \subset \mathbb{R}^n, \quad t \in \mathbb{R}^1, \quad \text{and} \quad \mu \in V \subset \mathbb{R}^p, \tag{2.1}$$

where, $U$ and $V$ are open sets in $\mathbb{R}^n$ and $\mathbb{R}^p$, respectively, and $\mu$ is a parameter. The overdot in (2.1) represents differentiation with respect to time ($\frac{d}{dt}$). The equation (2.1) is an *ordinary differential equation* (ODE) and the right-hand side function, $f(x, t; \mu)$, is called a *vector field*. ODEs which explicitly depend on time are called *non-autonomous*,

while those that are independent of time are called *autonomous.* This thesis focusses on autonomous systems of differential equations.

Consider the following general autonomous system

$$\dot{x} = f(x), \quad x \in \mathbb{R}^n. \tag{2.2}$$

**Definition 2.1.** *An equilibrium solution of* (2.2) *is given by* $x = \bar{x} \in \mathbb{R}^n$ *where* $f(\bar{x}) = 0$. *The number* $\bar{x}$ *is called an equilibrium point.*

**Theorem 2.1.** (Fundamental Existence-Uniqueness Theorem [113]). *Let* $E$ *be an open subset of* $\mathbb{R}^n$ *containing* $x_0$ *and assume that* $f \in C^1(E)$. *Then there exists an* $a > 0$ *such that the initial value problem (IVP)*

$$\dot{x} = f(x), \;\; x(0) = x_0$$

*has a unique solution* $x(t)$ *on the interval* $[-a, a]$.

**Lemma 2.1.** [113]. *Let* $E$ *be an open subset of* $\mathbb{R}^n$ *and let* $f : E \to \mathbb{R}^n$. *Then if* $f \in C^1(E)$, $f$ *is locally Lipschitz on* $E$.

*Proof.* The proof is given in [113], and is reproduced below for completeness. Since $E$ is an open subset of $\mathbb{R}^n$, given $x_0 \in E$, there is an $\epsilon > 0$ such that $N_\epsilon(x_0) \subset E$. Let

$$K = \max_{|x|<\epsilon/2} \|Df(x)\|,$$

the maximum of the continuous function $Df(x)$ on the compact set $|x| \leq \epsilon/2$, where

$Df(x)$ represents the derivative (or Jacobian) of $f(x)$. Let $N_0$ denote the $\epsilon/2$-neighbourhood of $x_0$, $N_{\epsilon/2}(x_0)$. Then for $x, y \in N_0$, set $u = y - x$. It follows that $x + su \in N_0$ for $0 \leq \delta \leq 1$ since $N_0$ is a convex set. Define the function $F : [0,1] \to \mathbb{R}^n$ by

$$F(s) = f(x + su).$$

Then, by the chain rule,

$$F'(s) = Df(x + su)u,$$

and therefore

$$\begin{aligned} f(y) - f(x) &= F(1) - F(0), \\ &= \int_0^1 F'(s)ds = \int_0^1 Df(x + su)uds. \end{aligned}$$

It follows that

$$\begin{aligned} |f(y) - f(x)| &\leq \int_0^1 |Df(x + su)u|ds, \\ &\leq \int_0^1 \|Df(x + su)\||u|ds, \\ &\leq K|u| = K|y - x|. \end{aligned}$$

This proves the Lemma. □

## 2.2 Hartman-Grobman Theorem

**Definition 2.2.** *The Jacobian matrix of $f$ at the equilibrium $\bar{x}$, denoted by $Df(\bar{x})$, is the matrix*

$$\begin{pmatrix} \frac{\partial f_1}{\partial x_1}(\bar{x}) & \cdots & \frac{\partial f_1}{\partial x_n}(\bar{x}) \\ \vdots & \vdots & \vdots \\ \frac{\partial f_n}{\partial x_1}(\bar{x}) & \cdots & \frac{\partial f_n}{\partial x_n}(\bar{x}) \end{pmatrix}$$

*of partial derivatives evaluated at $\bar{x}$.*

**Definition 2.3.** *Let $x = \bar{x}$ be an equilibrium solution of (2.2). Then $\bar{x}$ is called hyperbolic if none of the eigenvalues of $Df(\bar{x})$ have zero real part. An equilibrium point that is not hyperbolic is called non-hyperbolic.*

Consider the systems

$$\begin{aligned} \dot{x} &= f(x), \quad x \in \mathbb{R}^n, \\ \dot{y} &= g(y), \quad y \in \mathbb{R}^n, \end{aligned} \tag{2.3}$$

where $f$ and $g$ are two $C^r$ $(r \geq 1)$ ODEs defined on $\mathbb{R}^n$.

**Definition 2.4.** [138]. *The dynamics generated by the vector fields $f$ and $g$ of (2.3) are said to be locally $C^k$ conjugate $(k \leq r)$ if there exist a $C^k$ diffeomorphism $h$ which takes the orbits of the flow generated by $f$, $\phi(t,x)$, to the orbits of the flow generated by $g$, $\psi(t,y)$, preserving orientation and parametrization by time.*

**Theorem 2.2.** (Hartman and Grobman [138]). *Consider a $C^r(r \geq 1)$ vector field $f$*

*and the system*

$$\dot{x} = f(x), \quad x \in \mathbb{R}^n, \tag{2.4}$$

*with domain of $f$ an open subset of $\mathbb{R}^n$. Suppose also that* (2.4) *has equilibrium solutions which are hyperbolic. Consider the associated linear ODE system*

$$\dot{\xi} = Df(\bar{x})\xi, \quad \xi \in \mathbb{R}^n. \tag{2.5}$$

*Then the flow generated by* (2.4) *is $C^0$ conjugate to the flow generated by the linearized system* (2.5) *in a neighbourhood of the equilibrium point.*

A direct application of the Hartman-Grobman Theorem is that an orbit structure near a hyperbolic equilibrium solution is qualitatively the same as the orbit structure given by the associated linearized (around the equilibrium) dynamical system.

## 2.3 Stability of Solutions

The following are standard definitions and theorems required to analyze the stability of an equilibrium of an autonomous system. Let $\bar{x}(t)$ be any solution of (2.2). Then, $\bar{x}(t)$ is *stable* if solutions starting "close" to $\bar{x}(t)$ at a given time remain close to $\bar{x}(t)$ for all later times. It is *asymptotically stable* if nearby solutions converge to $\bar{x}(t)$ as $t \to \infty$. These concepts are formally defined below:

**Definition 2.5.** [138]. *The equilibrium $\bar{x}(t)$ is said to be stable if given $\epsilon > 0$, there exists a $\delta = \delta(\epsilon) > 0$ such that, for any solution $y(t)$ of (2.2) satisfying $|\bar{x}(t_0) - y(t_0)| < \delta$, $|\bar{x}(t) - y(t)| < \epsilon$ for $t > t_0$, $t_0 \in \mathbb{R}$.*

**Definition 2.6.** [138]. *The equilibrium $\bar{x}(t)$ is said to be asymptotically stable if (i) it is stable and (ii) there exists a constant $c > 0$ such that, for any solution $y(t)$ of (2.2) satisfying $|\bar{x}(t_0) - y(t_0)| < c$, then $\lim_{t\to\infty} |\bar{x}(t) - y(t)| = 0$.*

**Definition 2.7.** *A solution which is not stable is said to be unstable.*

**Theorem 2.3.** [138]. *Suppose all the eigenvalues of $Df(\bar{x})$ have negative real parts. Then the equilibrium solution $x = \bar{x}$ of the system (2.2) is locally asymptotically stable, and unstable if at least one of the eigenvalues has positive real part.*

## 2.4 Bifurcation Theory

In general, systems of physical interest typically have parameters which appear in the defining (governing) systems of equations. As these parameters are varied, changes may occur in the qualitative structures of the solutions for certain parameter values. These changes are called *bifurcations.* The parameter values where bifurcation occurs are called *bifurcation values.* A standard definition of bifurcation at a point is given below.

**Definition 2.8.** *Let*

$$\dot{x} = f(x, \mu), \quad x \in \mathbb{R}, \quad \mu \in \mathbb{R}, \tag{2.6}$$

*be a one-parameter family of one-dimensional ODEs. An equilibrium solution of* (2.6) *given by* $(x, \mu) = (0, 0)$ *is said to undergo bifurcation at* $\mu = 0$ *if the flow for* $\mu$ *near zero and* $x$ *near zero is not qualitatively the same as the flow near* $x = 0$ *at* $\mu = 0$.

There are various types of bifurcations, including saddle-node, transcritical, pitchfork, backward, Bogdanov-Takens and Hopf bifurcations [138]. Three of these, forward, backward and Hopf bifurcations, are relevant to this thesis.

### 2.4.1 Hopf bifurcation

This entails the bifurcation of an equilibrium solution into a periodic solution. A formal definition, for planar systems, is given below.

**Theorem 2.4.** (Andronov-Hopf bifurcation [118]). *Let* $\dot{\mathbf{x}} = \mathbf{F}_\mu(\mathbf{x})$ *be a system of differential equations in the plane, depending on a parameter* $\mu$. *Assume that there is a fixed point* $\mathbf{x}_\mu$ *for the parameter value* $\mu$, *with eigenvalues* $\lambda_\mu = \alpha_\mu \pm i\beta_\mu$. *Assume that* $\beta_\mu \neq 0$, $\alpha_{\mu_0} = 0$, *and*

$$\frac{d}{d\mu}(\alpha_\mu)\bigg|_{\mu=\mu_0} > 0.$$

*(a) (Supercritical bifurcation). If* $\mathbf{x}_{\mu_0}$ *is weakly attracting for* $\mu = \mu_0$, *then there is an attracting periodic orbit for* $|\mu - \mu_0|$ *small and* $\mu > \mu_0$. *The period of the orbit is equal to* $2\pi/\beta_{\mu_0}$ *plus terms which go to zero as* $\mu$ *goes to* $\mu_0$.

*(b) (Subcritical bifurcation). If* $\mathbf{x}_{\mu_0}$ *is weakly repelling for* $\mu = \mu_0$, *then there is a repelling periodic orbit for* $|\mu - \mu_0|$ *small and* $\mu < \mu_0$. *The period of the orbit is equal to* $2\pi/\beta_{\mu_0}$ *plus terms which go to zero as* $\mu$ *goes to* $\mu_0$.

**Remark:** If the rest of the assumptions of the theorem are true, but

$$\frac{d}{d\mu}(\alpha_\mu)\Big|_{\mu=\mu_0} < 0,$$

then the periodic orbit appears for the parameter values on the opposite side of the bifurcation value (see [68, 94] for generalized version of Hopf bifurcation theorem).

## 2.5 Non-existence of Periodic Solutions

Generally, models of disease transmission may have solutions that differ from the associated equilibrium solutions. Such solutions affect the stability of the equilibria. These kinds of solutions are generally referred to as closed orbits. In order to establish global properties of equilibria, it is sometimes necessary to show the non-existence of closed orbits in the feasible region of the model. One method for ruling out closed orbits is described below.

**Definition 2.9.** (Periodic solution). *A solution $x(t)$ is said to be periodic if $x(t+T) = x(t)$ for all $t$, for some $T > 0$.*

### 2.5.1 Lyapunov functions and LaSalle's Invariance Principle

#### Lyapunov Functions

A powerful method for analyzing the stability of an equilibrium point is based on the use of Lyapunov functions. Lyapunov functions are energy-like functions that decrease along trajectories [130].

**Definition 2.10.** *A function $V : \mathbb{R}^n \to \mathbb{R}$ is said to be a positive definite function if*

- $V(x) > 0$ *for all* $x \neq 0$,
- $V(x) = 0$ *if and only if* $x = 0$,
- $V(x) \to \infty$ *as* $x \to \infty$.

The general Lyapunov Function Theorem is given below.

**Theorem 2.5.** [138]. *Consider the following system*

$$\dot{x} = f(x), \quad x \in \mathbb{R}^n. \tag{2.7}$$

*Let $\bar{x}$ be an equilibrium solution of (2.7) and let $V : U \to \mathbb{R}$ be a $C^1$ function defined on some neighbourhood $U$ of $\bar{x}$ such that*

i) *$V$ is positive definite*

ii) *$\dot{V}(x) \leq 0$ in $U \backslash \{\bar{x}\}$.*

*Then $\bar{x}$ is stable. Moreover, if*

iii) *$\dot{V}(x) < 0$ in $U \backslash \{\bar{x}\}$*

*then $\bar{x}$ is asymptotically-stable.*

Any function $V$ that satisfies the above is called a *Lyapunov function* [68, 138]. If $U = \mathbb{R}^n$, then $\bar{x}$ is globally-asymptotically stable (GAS) whenever (i) and (iii) hold.

**Example 1:**

Consider the following system,

$$\begin{aligned} \dot{x} &= y - x^3, \\ \dot{y} &= -x - y^3. \end{aligned}$$

The system has a non-hyperbolic equilibrium solution at $(x, y) = (0, 0)$. Let $V(x, y) = x^2 + y^2$. Clearly $V(0, 0) = 0$ and $V(x, y) > 0$ in any deleted neighbourhood of $(0, 0)$. Further,

$$\begin{aligned} \dot{V}(x, y) &= 2x\dot{x} + 2y\dot{y} \\ &= 2x(y - x^3) + 2y(-x - y^3) \\ &= -2(x^4 + y^4) < 0. \end{aligned}$$

Hence, $\dot{V} < 0$ if $(x, y) \neq (0, 0)$. Thus, by the Lyapunov Function Theorem 2.5 above, the equilibrium $(0, 0)$ is asymptotically-stable.

**Limit Sets and Invariance Principle**

Since general population biology models (e.g., those arising in epidemiology, immunology, vector dynamics etc.) monitor human, cell or vector populations, it is necessary to consider that associated population sizes can never be negative. Thus, population dynamics models should be considered in (feasible) regions where such property (non-negativity) is preserved.

**Definition 2.11.** *A point $x_0 \in \mathbb{R}^n$ is called an $\omega-$limit point of $x \in \mathbb{R}^n$, denoted by $\omega(x)$, if there exists a sequence $\{t_i\}$, $t_i \to \infty$ such that*

$$\phi(t_i, x) \to x_0.$$

**Definition 2.12.** *A point $x_0 \in \mathbb{R}^n$ is called an $\alpha-$limit point of $x \in \mathbb{R}^n$, denoted by $\alpha(x)$, if there exists a sequence $\{t_i\}$, $t_i \to -\infty$ such that*

$$\phi(t_i, x) \to x_0.$$

**Definition 2.13.** [138]. *The set of all $\omega-$limit points of a flow is called the $\omega-$limit set. Similarly, the set of all $\alpha-$limit points of a flow is called the $\alpha-$limit set.*

**Definition 2.14.** [138]. *Let $S \subset \mathbb{R}^n$ be a set. Then, $S$ is said to be invariant under the flow generated by $\dot{x} = f(x)$ if for any $x_0 \in S$ we have $x(t, 0, x_0) \in S$ for all $t \in \mathbb{R}$.*

If we restrict the region to positive times (i.e., $t \geq 0$), then $S$ is said to be a *positively-invariant set.* In other words, solutions in a positively-invariant set remain there for all time. The set is negatively-invariant if we go backward in time.

**Theorem 2.6.** (LaSalle's Invariance Principle [56, 86]). *Suppose there is a continuously differentiable, positive definite, and radially unbounded function $V : \mathbb{R}^n \to \mathbb{R}$, such that*

$$\frac{\partial V}{\partial x}(x - \bar{x})f(x) \leq W(x) \leq 0, \ \ \forall\, x \in \mathbb{R}^n.$$

*Then, $\bar{x}$ is a globally-stable equilibrium. The solution $x(t)$ converges to the largest invariant set $S$ contained in $E = \{x \in \mathbb{R}^n : W(x) = 0\}$.*

## 2.6 Methods for Local Asymptotic Stability of Equilibria

Here, two standard methods for analyzing the local stability of the equilibria of disease transmission models are briefly described.

### 2.6.1 Linearization

Determining the stability of an equilibrium $\bar{x}(t)$ generally requires an understanding of the nature of solutions near $\bar{x}(t)$. Let

$$x = \bar{x}(t) + \epsilon, \tag{2.8}$$

and suppose that equation (2.8) is substituted into the general autonomous system $\dot{x} = f(x)$, $x \in \mathbb{R}^n$ and $f$ is twice differentiable. The Taylor series expansion about $\bar{x}(t)$ gives

$$\dot{x} = \dot{\bar{x}}(t) + \dot{\epsilon} = f(\bar{x}(t)) + Df(\bar{x}(t))\epsilon + O(|\epsilon|^2),$$

where, $|\cdot|$ denotes norm on $\mathbb{R}^n$. Hence,

$$\dot{\epsilon} = Df(\bar{x}(t))\epsilon + O(|\epsilon|^2). \tag{2.9}$$

Equation (2.9) above describes the evolution of orbits near $\bar{x}(t)$. The behavior of solutions arbitrarily close to $\bar{x}(t)$ is obtained by studying the associated linear system

$$\dot{\epsilon} = Df(\bar{x}(t))\epsilon. \tag{2.10}$$

However, if $\bar{x}(t)$ is an equilibrium solution, i.e., $\bar{x}(t) = \bar{x}$, then $Df(\bar{x}(t)) = Df(\bar{x})$ is a matrix with constant entries, and the solution of (2.10) through the point $\epsilon_0 \in \mathbb{R}^n$ at $t = 0$ is given by

$$\epsilon(t) = \exp(Df(\bar{x})t)\epsilon_0. \tag{2.11}$$

**Theorem 2.7.** *Suppose all of the eigenvalues of $Df(\bar{x})$ have negative real parts. Then, the equilibrium solution $x = \bar{x}$ of the non-linear ODE $\dot{x} = f(x)$, $x \in \mathbb{R}^n$ is asymptotically-stable.*

### Example 2

Consider the ODE system

$$\begin{aligned} \dot{x} &\equiv f_1(x, y) = y^3 - x, \\ \dot{y} &\equiv f_2(x, y) = x^2 - 2y. \end{aligned}$$

The system has an equilibrium point $\bar{x} = (0, 0)$. The Jacobian $J$ of the system is given by

$$J(x, y) = Df(x) = \begin{pmatrix} \frac{\partial f_1}{\partial x} & \frac{\partial f_1}{\partial y} \\ \\ \frac{\partial f_2}{\partial x} & \frac{\partial f_2}{\partial y} \end{pmatrix} = \begin{pmatrix} -1 & 3y^2 \\ \\ 2x & -2 \end{pmatrix}.$$

Evaluating $J$ at $\bar{x}$ gives

$$J(0, 0) = \begin{pmatrix} -1 & 0 \\ \\ 0 & -2 \end{pmatrix},$$

so that the eigenvalues of $J(0, 0)$, $\lambda_1 = -1$, $\lambda_2 = -2$, have negative real parts. Hence, the equilibrium $\bar{x} = (0, 0)$ is asymptotically stable.

### 2.6.2 Next generation method

Whilst the standard linearization method described above applies to analyzing the local stability of equilibria in general, the *next generation method*, which is also a linearization method, is used to establish the local asymptotic stability of the DFE (or a boundary equilibrium). The method was first introduced by Diekmann and Hesterbeek [31] and refined for epidemiological models by van den Driessche and Watmough [136].

Epidemiological models, of Kermack and Mckendrick type [74], typically sub-divide the total population ($N$) into a number of mutually exclusive compartments, depending on their disease status. The formulation in [136] is now described.

Suppose the given disease transmission model, with non-negative initial conditions,

can be written in terms of the following system:

$$\dot{x}_i = f(x_i) = \mathrm{F}_i(x) - \mathrm{V}_i(x), \quad i = 1, \cdots, n, \tag{2.12}$$

where $\mathrm{V}_i = \mathrm{V}_i^- - \mathrm{V}_i^+$ and the function satisfy the following axioms below. First of all, $X_s = \{x \geq 0 | x_i = 0,\ i = 1, \cdots, m\}$ is defined as the disease-free states (non-infected state variables) of the model, where $x = (x_1, \cdots, x_n)^t, x_i \geq 0$ represents the number of individuals in each compartment of the model.

**(A1)** if $x \geq 0$, then $\mathrm{F}_i, \mathrm{V}_i^+, \mathrm{V}_i^- \geq 0$ for $i = 1, \cdots, m$.

**(A2)** if $x_i = 0$, then $\mathrm{V}_i^- = 0$. In particular, if $x \in X_s$ then $\mathrm{V}_i^- = 0$ for $i = 1, \cdots, m$.

**(A3)** $\mathrm{F}_i = 0$ if $i > m$.

**(A4)** if $x \in X_s$, then $\mathrm{F}_i(x) = 0$ and $\mathrm{V}_i^+(x) = 0$ for $i = 1, \cdots, m$.

**(A5)** If $\mathrm{F}(x)$ is set to zero, then all eigenvalues of $Df(x_0)$ have negative real part.

Here, $\mathrm{F}_i(x)$ represents the rate of appearance of new infections in compartment $i$; $\mathrm{V}_i^+(x)$ represents the rate of transfer of individuals into compartment $i$ by all other means, and $\mathrm{V}_i^-(x)$ represents the rate of transfer of individuals out of compartment $i$. It is assumed that these functions are at least twice continuously differentiable in each variable [136].

**Definition 2.15.** ($M-$Matrix) *An $n \times n$ matrix $A$ is an $M-$matrix if and only if every off-diagonal entry of $A$ is non-positive and the diagonal entries are all positive.*

**Lemma 2.2.** (van den Driessche and Watmough [136]). *If $\bar{x}$ is a DFE of* (2.12) *and $f_i(x)$ satisfy* $(A1)-(A5)$*, then the derivatives* $D\mathrm{F}(\bar{x})$ *and* $D\mathrm{V}(\bar{x})$ *are partitioned as*

$$D\mathrm{F}(\bar{x}) = \begin{pmatrix} F & 0 \\ 0 & 0 \end{pmatrix}, \; D\mathrm{V}(\bar{x}) = \begin{pmatrix} V & 0 \\ J_3 & J_4 \end{pmatrix},$$

*where $F$ and $V$ are the $m \times m$ matrices defined by,*

$$F = \left[\frac{\partial \mathrm{F}_i}{\partial x_j}(\bar{x})\right] \text{ and } V = \left[\frac{\partial \mathrm{V}_i}{\partial x_j}(\bar{x})\right] \text{ with } 1 \leq i, j \leq m.$$

*Further, $F$ is non-negative, $V$ is a non-singular $M-$matrix and $J_3, J_4$ are matrices associated with the transition terms of the model, and all eigenvalues of $J_4$ have positive real parts.*

**Theorem 2.8.** (van den Driessche and Watmough [136]). *Consider the disease transmission model given by* (2.12) *with $f(x)$ satisfying axioms* $(A1)-(A5)$*. If $\bar{x}$ is a DFE of the model, then $\bar{x}$ is LAS if $\mathcal{R}_0 = \rho(FV^{-1}) < 1$ (where $\rho$ is spectral radius), but unstable if $\mathcal{R}_0 > 1$.*

## 2.7 Delay Differential Equations

Time delays are used to model several different mechanisms in the dynamics of epidemics. These include incubation periods, latent periods, age structure and seasonal variations. A brief introduction and basic properties of delay differential equations are given below.

### 2.7.1 Existence and uniqueness of solutions of delay differential equations

Suppose $\tau \geq 0$ is a given real number, $\mathbb{R}^n$ is an $n$-dimensional linear vector space over the real numbers with norm $|.|$, $C = C([-\tau, 0], \mathbb{R}^n)$ is the Banach space of continuous functions mapping the interval $[-\tau, 0]$ into $\mathbb{R}^n$ with the topology of uniform convergence. If $\phi \in C$, then the norm $\|\phi\| = \sup_{\theta \in [-\tau, 0]} |\phi(\theta)|$. If

$$\sigma \in \mathbb{R}, \quad A \geq 0 \quad \text{and} \quad x \in C([\sigma - \tau, \sigma + A], \mathbb{R}^n),$$

then for any $t \in [\sigma, \sigma + A]$, let $x_t$ be defined by

$$x_t(\theta) = x(t + \theta), \quad -\tau \leq \theta \leq 0.$$

If $D$ is a subset of $\mathbb{R} \times C$, $f : D \to \mathbb{R}^n$ then the delay differential equation on $D$ is given by

$$\dot{x}(t) = f(t, x_t). \tag{2.13}$$

The existence and uniqueness of solutions of the delay differential equation (2.13) are stated below.

**Theorem 2.9.** [57]. *Suppose $\Omega$ is an open subset of $\mathbb{R} \times C$ and $f^0 \in C(\Omega, \mathbb{R}^n)$. If $(\sigma, \phi) \in \Omega$, then there is a solution of the delay differential equation* (2.13) *passing through $(\sigma, \phi)$.*

*More generally, if $W \subseteq \Omega$ is compact and $f^0 \in C(\Omega, \mathbb{R}^n)$ is given, then there is a*

*neighbourhood $V \subseteq \Omega$ of $W$ such that $f^0 \in C^0(V, \mathbb{R}^n)$, there is a neighbourhood $U \subseteq C^0(V, \mathbb{R}^n)$ of $f^0$ and an $\alpha > 0$ and $r > 0$ such that, for any $(\sigma, \phi) \in W$, $f \in U$, there is a solution $x(\sigma, \phi, f)$ of the equation (2.13) through $(\sigma, \phi)$ which exists on $[\sigma - r, \sigma + \alpha]$.*

**Theorem 2.10.** [57]. *Suppose $\Omega$ is an open set in $\mathbb{R} \times C$, $f : \Omega \to \mathbb{R}^n$ is continuous, and $f(t, \phi)$ is Lipschitzian in $\phi$ on each compact set in $\Omega$. If $(\sigma, \phi) \in \Omega$, then there is a unique solution of equation (2.13) through $(\sigma, \phi)$.*

The delay differential equation (2.13) can contain distributed delay or discrete delay. A distributed delay differential equation has the form

$$\dot{x} = f\left(t, x(t), \int_{-\infty}^{0} x(t+\tau) d\mu(\tau)\right),$$

where $f$ depends on $x$ computed on a continuum, possibly unbounded set of past values, whereas, discrete delay differential equation has the form

$$\dot{x} = f(t, x(t), x(t-\tau_1), \cdots, x(t-\tau_n)) \quad \text{for} \quad \tau_1, \cdots, \tau_n \geq 0,$$

where only a finite number of past values of state variables $x$ are involved. In this thesis, only the discrete delay will be considered.

### 2.7.2 Linearization of delay differential equation

Consider a discrete delay differential equation (DDE) in the form

$$\dot{\mathbf{x}} = f(\mathbf{x}(t), \mathbf{x}(t-\tau_1), \mathbf{x}(t-\tau_2), \cdots, \mathbf{x}(t-\tau_n)), \tag{2.14}$$

where the quantities $\tau_i$ are positive constants.

An equilibrium point is a point in the state space for which $\mathbf{x}(t) = \mathbf{x}^*$ is a solution for all $t$. Thus, for a DDE of the form (2.14), equilibrium points satisfy

$$f(\mathbf{x}^*, \mathbf{x}^*, \cdots, \mathbf{x}^*) = 0.$$

For the stability of the equilibrium points of ODEs, we assume that the system has been displaced by a small distance in phase space from the equilibrium. With ODEs, the phase space is a finite-dimensional coordinate space, whereas with DDEs, the phase space is an infinite-dimensional function space. In other words, displacements are time-dependent functions $\delta\mathbf{x}(t)$ persisting over an interval of at least $\tau_{max}$, the longest delay. Before proceeding further, it is convenient to introduce some new notation. It is a common convention for DDEs that variables without subscripts are instantaneous (i.e., $\mathbf{x} \equiv \mathbf{x}(t)$ ) while delayed variables are indicated by the subscripted value of the delay $\mathbf{x}_\tau \equiv \mathbf{x}(t - \tau)$. Henceforth, this convention will be used.

Let $\mathbf{x}^*$ be an equilibrium of equation (2.14), and let the system be perturbed from equilibrium by a small perturbation which lasts from $t = t_0 - \tau_{max}$ to $t_0$. Let $\delta\mathbf{x}(t)$ be the displacement from equilibrium, assumed small, at any time in the open interval $[t_0 - \tau_{max}, \infty)$. Accordingly,

$$\mathbf{x} = \mathbf{x}^* + \delta\mathbf{x}$$

and

$$\dot{\mathbf{x}} = \dot{\delta\mathbf{x}} = f(\mathbf{x}^* + \delta\mathbf{x}, \mathbf{x}^* + \delta\mathbf{x}_{\tau_1}, \mathbf{x}^* + \delta\mathbf{x}_{\tau_2}, \cdots, \mathbf{x}^* + \delta\mathbf{x}_{\tau_n}).$$

Since each of the quantities $\delta\mathbf{x}, \delta\mathbf{x}_{\tau_1}, \delta\mathbf{x}_{\tau_2}, \cdots, \delta\mathbf{x}_{\tau_n}$ is small, linearizing the differential equation about the equilibrium point using Taylor series gives:

$$\dot{\delta\mathbf{x}} \approx J_0\delta\mathbf{x} + J_{\tau_1}\delta\mathbf{x}_{\tau_1} + J_{\tau_2}\delta\mathbf{x}_{\tau_2} + \cdots + J_{\tau_n}\delta\mathbf{x}_{\tau_n}. \tag{2.15}$$

To obtain equation (2.15), the following fact is used.

$$f(\mathbf{x}^*, \mathbf{x}^*, \cdots, \mathbf{x}^*) = 0.$$

The quantity $J_0$ is the usual Jacobian with respect to $\mathbf{x}$ evaluated at the equilibrium point, while the matrices $J_{\tau_i}$ are the Jacobians with respect to the corresponding $\mathbf{x}_{\tau_i}$ evaluated at $\mathbf{x} = \mathbf{x}_{\tau_1} = \mathbf{x}_{\tau_2} = \cdots = \mathbf{x}_{\tau_n} = \mathbf{x}^*$. In linear ODEs, the solutions are exponential functions of time, with exponents given by the eigenvalues of the Jacobian matrix.

Suppose that the linear DDE (2.15) also has exponential solutions. That is,

$$\delta\mathbf{x}(t) = \mathbf{A}e^{\lambda t}. \tag{2.16}$$

Substituting (2.16) into equation (2.15), and rearranging gives

$$\lambda\mathbf{A} = (J_0 + e^{-\lambda\tau_1}J_{\tau_1} + e^{-\lambda\tau_2}J_{\tau_2} + \cdots + e^{-\lambda\tau_n}J_{\tau_n})\mathbf{A}. \tag{2.17}$$

This equation can only be satisfied with non-zero displacement amplitude $\mathbf{A}$ if

$$\left| J_0 + e^{-\lambda\tau_1} J_{\tau_1} + e^{-\lambda\tau_2} J_{\tau_2} + \cdots + e^{-\lambda\tau_n} J_{\tau_n} - \lambda I \right| = 0, \tag{2.18}$$

where $I$ is the identity matrix of order $n$. Equation (2.18) is called the characteristic equation of the equilibrium point of the DDE system (2.14).

**Definition 2.1.** [82]. *An equilibrium of a system of delay differential equations is absolutely-stable if it is asymptotically-stable for all delays $T \geq 0$ and is conditionally-stable if it is asymptotically-stable for $T$ in some finite interval.*

## 2.8 Global Asymptotic Stability of Equilibria

An equilibrium $\mathbf{x}^*$ is locally-asymptotically stable if it attracts solutions within a neighbourhood (in a feasible region) containing $\mathbf{x}^*$ (Figure 2.1(a)). It is globally-asymptotically stable if it attracts all solutions in the feasible region (Figure 2.1(b)).

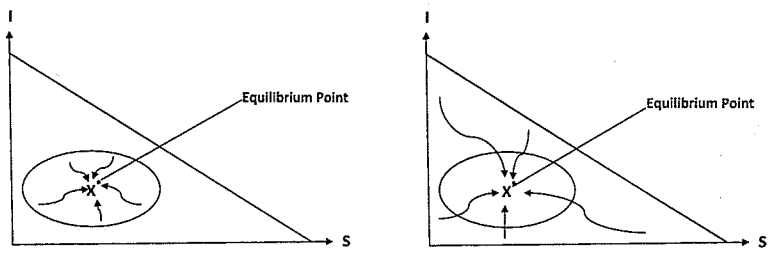


(a) (b)

Figure 2.1: Diagram illustrating (a) local-asymptotic stability, (b) global-asymptotic stability of an equilibrium point.

There are numerous methods for establishing GAS of an equilibrium point. One of these methods (relevant to the thesis) is described below (another method, based on the use of Lyapunov function and LaSalle's Invariance Principle, is briefly described in Section 2.5.1 ).

### 2.8.1 Fluctuation method

**Properties of** lim sup

The operations lim sup and lim inf on sequences $\{a_n\}$ and $\{b_n\}$ in $\mathbb{R}^* = \mathbb{R} \bigcup \{-\infty\} \bigcup \{\infty\}$ have the following properties.

(a) if $a_n \leq b_n$ for all $n$, then $\limsup a_n \leq \limsup b_n$ and $\liminf a_n \leq \liminf b_n$.

(b) $\liminf a_n \leq \limsup a_n$.

(c) $\limsup a_n b_n \leq \limsup a_n \limsup b_n$.

(d) $\liminf a_n = -\limsup(-a_n)$.

(e) the sequence $\{a_n\}$ in $\mathbb{R}^*$ converges in $\mathbb{R}^*$ if and only if $\liminf a_n = \limsup a_n$.

**Lemma 2.3.** (Thieme [133]). *Let $f : (t_0, \infty) \to \mathbb{R}$ be a differentiable function that has no limit as $t \to \infty$. Then there are sequences $s_n, t_n \to \infty$ with the following properties:*

$$f(s_n) \to f_\infty, \quad f'(s_n) = 0,$$

$$f(t_n) \to f_\infty, \quad f'(t_n) = 0,$$

*for $n \to \infty$, where, $f^\infty = \limsup_{t\to\infty} f(t)$ and $f_\infty = \liminf_{t\to\infty} f(t)$.*

If $f$ has no limit for $t \to \infty$, it has to oscillate between $f_\infty$ and $f^\infty$. So appropriate sequences of local minima $f(s_n)$ and local maxima $f(t_n)$ can be chosen that have the desired properties.

**Proposition 2.1.** (Thieme [133]). *Let $f : (t_0, \infty) \to \mathbb{R}$ be bounded and continuously differentiable. Then there are sequences $s_n, t_n \to \infty$ with the following properties:*

$$f(s_n) \to f_\infty, \quad f'(s_n) \to 0,$$

$$f(t_n) \to f_\infty, \quad f'(t_n) \to 0,$$

*for $n \to \infty$, where, $f^\infty = \limsup_{t\to\infty} f(t)$ and $f_\infty = \liminf_{t\to\infty} f(t)$.*

The global stability of equilibria can be established using the fluctuation method [66, 133]. The method is based on using the following Theorem and Corollary.

**Theorem 2.11.** (Thieme [133]). *Let $D$ be a bounded interval in $\mathbb{R}$ and $g : (t_0, \infty) \times D \to \mathbb{R}$ be bounded and uniformly continuous. Further, let $x : (t_0, \infty) \to D$ be a*

*solution of* $\dot{x} = g(t, x)$*, which is defined on the whole interval* $(t_0, \infty)$*. Then, there exist sequences* $s_n, t_n \to \infty$ *such that*

$$\lim_{n\to\infty} g(s_n, x_\infty) = 0 = \lim_{n\to\infty} g(t_n, x^\infty),$$

*where,* $x^\infty = \limsup_{t\to\infty} x(t)$ *and* $x_\infty = \liminf_{t\to\infty} x(t)$.

**Corollary 2.1.** (Thieme [133]). *Let the assumptions of Theorem 2.11 be satisfied. Then,*

*(a)* $\liminf_{t\to\infty} g(t, x_\infty) \leq 0 \leq \limsup_{t\to\infty} g(t, x_\infty)$,

*(b)* $\liminf_{t\to\infty} g(t, x^\infty) \leq 0 \leq \limsup_{t\to\infty} g(t, x^\infty)$.

## 2.9 Epidemiological Preliminaries

### 2.9.1 Incidence functions

Disease incidence in a community is defined in terms of the number of new infections generated per unit time in that community. Incidence, in disease models, is generally characterized by an incidence function (a function that describes the mixing pattern within the community). Various types of incidence functions have been used in disease modelling (see, for example, [63] for general discussion), and the choice of such function can play an important role in the dynamics of the disease. Here, a general construction of incidence function required for modelling is given.

Let $S(t)$, $I(t)$ and $N(t)$ denote the number of susceptible individuals, infected individuals and the total population size at time $t$, respectively. Suppose $\beta(N)$ is the effective contact rate (i.e., the average number of contacts sufficient to transmit infection) *per* person *per* unit time. Then, $\beta(N)I/N$ is the average number of contacts with infectious individuals a susceptible individual makes per unit time. Thus, the number of new cases coming from all susceptible individuals ($S$) is $\lambda S$, where $\lambda = \beta(N)I/N$ is the force of infection. If $\beta(N) = \beta$, a constant, then $\lambda S$ is referred to as a *standard incidence function.* When $\beta(N) = \beta N$ (that is, the contact rate depends on the total population), then $\lambda S$ is called *mass action incidence* [60, 62, 63]. It is worth stating that standard incidence models with constant total population ($N(t)$), such as the model in [81], are essentially mass action models.

The aforementioned two incidence formulations (standard and mass action incidence) appear to be the most widely used in the mathematical biology literature. Although some studies have suggested that the standard incidence formulation is more realistic for human diseases [2, 4], the choice of one over the other really depends on the disease being modeled and, in some cases, the need for analytical tractability.

### 2.9.2 Reproduction numbers

Compartmental mathematical models have been widely used to gain insight into the spread and control of emerging and re-emerging human diseases, dating back to the pioneering work of Bernoulli (on modelling the transmission dynamics of smallpox) in 1760 and the likes of Ross, Kermack and McKendrick and others (see [2, 4, 63] and

the references therein). The dynamics of these models tend generally to be completely determined by a threshold quantity, known as the *basic reproduction number* (denoted by $\mathcal{R}_0$), which measures the average number of new cases an index case can generate in a completely susceptible population [4, 33, 63]. Typically, when $\mathcal{R}_0$ is less than unity, a small influx of infected individuals will not generate large outbreaks, and the disease dies out in time (in this case, the corresponding disease-free equilibrium (DFE) is LAS). On the other hand, the disease will persist if $\mathcal{R}_0$ exceeds unity, where a stable endemic equilibrium point (EEP) exists. This phenomenon, where the DFE and an EEP exchange their stability at $\mathcal{R}_0 = 1$, is known as *forward bifurcation* (or transcritical bifurcation). A schematic description is given in Figure 2.2.

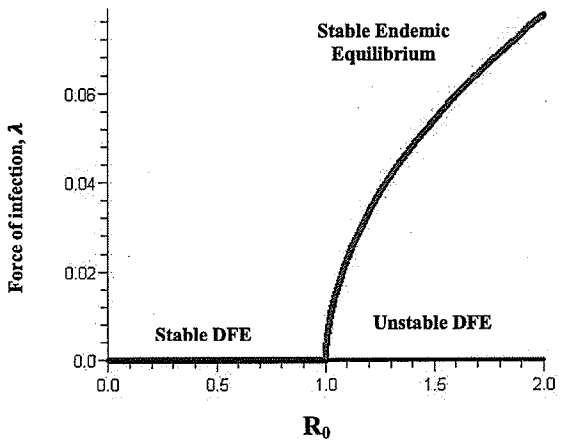


Figure 2.2: Forward bifurcation diagram.

The forward bifurcation phenomenon was first noted by Kermack and McKendrick [74], and has been observed in many disease transmission models ever since (see [19, 20, 21, 61, 63] and the references therein). In general, for models that exhibit forward

bifurcation, the requirement $\mathcal{R}_0 < 1$ is necessary and sufficient for disease elimination (i.e., the number of infectives at steady state depends continuously on $\mathcal{R}_0$). In the presence of a control measure, such as the use of a vaccine in the community, the dynamics of the model is governed by another threshold quantity, known as the *effective reproduction number*, denoted by $\mathcal{R}_{eff}$. The threshold, $\mathcal{R}_{eff}$, represents the average number of secondary cases a typical infected individual will generate in a population where a fraction of the susceptible individuals are vaccinated.

A number of studies have shown that whilst $\mathcal{R}_0 < 1$ is necessary for disease elimination, this requirement may not be sufficient. This is owing to the phenomenon of *backward bifurcation*, where a stable endemic equilibrium co-exists with a stable disease-free equilibrium for $\mathcal{R}_0 < 1$. This phenomenon has been observed in numerous disease transmission models such as those for behavioural responses to perceived risks [55], multiple groups [19, 20, 127], vaccination [37, 81], vector-borne diseases [43, 105] and transmission of *mycobacterium tuberculosis* with exogenous re-infection [21, 40, 126]. The phenomenon of backward bifurcation has important public health implication, since it renders the classical requirement of reproduction number being less than unity to be insufficient (in general) for disease elimination. A schematic description of the backward bifurcation phenomenon is given in Figure 2.3 (in a backward bifurcation situation, global asymptotic stability of the DFE is only feasible outside the region of the co-existence of the two stable attractors, such as the region $0 < \mathcal{R}_0 \leq 0.82$ in Figure 2.3).

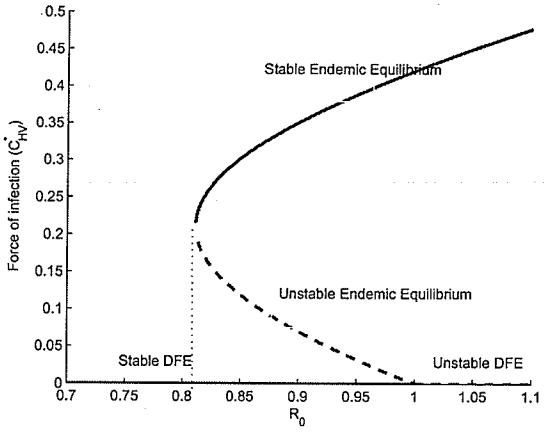


Figure 2.3: Backward bifurcation diagram showing the co-existence of a stable DFE and two branches of endemic equilibria (a stable and an unstable branch).

Numerical simulations in this thesis are carried out using two Matlab routines, namely ODE45 (for the non-delayed systems in Chapters 3, 5 and 6) and DDE23 (for the delayed model in Chapter 4).

# Chapter 3

# Analysis of Vector Dynamics Model

## 3.1 Introduction

Malaria is one of the oldest and deadliest infectious diseases in humans. The malaria parasite is transmitted between people by female *Anopheles* mosquitoes. More than 60 species are known to transmit the infection. Some species are more significant than others as vectors because of variations in susceptibility to the parasite or the propensity of mosquito to bite humans and to enter houses when looking for a blood meal [92]. Both the male and female mosquitoes feed on nectar. However, only the female mosquitoes feed on animal blood to provide proteins for their eggs. Thus, the transmission of malaria is essentially driven by the human biting habit of the mosquito. Transmission of most indirectly transmitted diseases of humans follow the same pattern: the vector, in most cases an insect, interacts with a human and, depending on the disease status of the mosquito and the human, will either infect or be infected. In the

process of this interaction, the vector may lose its life. For a disease vector to feed on a human, it must actively seek the human host. Thus, mosquito can systematically target and identify human beings [47, 95]. Once a blood meal is taken, the vector moves to a convenient breeding site, usually a swamp or humid area.

The *Anopheles* mosquito has several stages of development (metamorphosis). Female mosquitoes lay their eggs in batches of 70-100 on the surface of water and in tropical temperatures the eggs hatch into larvae after 2-3 days. After 7-14 days, the larvae turn into pupae. The pupa is comma-shaped and is the least active stage of the *Anopheles* life cycle. After 2-4 days, the pupa metamorphoses into an adult mosquito. The adult mosquitoes emerge during late evening, and are able to fly within minutes. The duration of the whole cycle, from egg laying to an adult mosquito eclosion, varies between 7 and 20 days, depending on the ambient temperature of the swamp and the mosquito species involved [47].

A basic ecological requirement for all organisms is to maintain an appropriate seasonality to optimize the chance of survival of the species. In warmer regions, seasonal rainfall can increase the abundance of mosquitoes and other vectors with aquatic larval stages, where reproduction depends on the availability of breeding sites [88, 104]. Furthermore, mosquitoes reach sexual maturity earlier and feed more frequently at warmer temperatures, potentially increasing the rate of parasite transmission. Powell and Logan [116] reviewed the mathematical relationship between environmental temperatures and development timing. Raffy and Tran [119] modelled vector dynamics using a diffusion equation. Porphyre *et al.* [115] developed and studied a model that assesses

and characterizes the abundance of vectors that can be produced in one breeding site as a function of the variation of the environmental conditions of the breeding site. Takahashi *et al.* [132] presented models for the vital and dispersal dynamics of *Aedes aegypti*, a dengue vector. Some other vector population models have been presented in [18, 26, 29, 103, 140], but with emphasis in different directions.

The knowledge of the population structure of the major vector species is fundamental to the sound understanding of malaria epidemiology and assessment of the effects of many vector control strategies. The distribution of disease vectors in different regions of the world depends on the prevailing local climatic and environmental conditions. Due to global warming, there is a risk of the emergence of malaria in new regions (where malaria has not been endemic). Thus, the complete understanding of the vector population dynamics is necessary for gaining insight into the disease spread and the design of effective vector control strategies.

In this chapter, the model presented in [109] will be considered. The model is a demographic model for vector population assuming the mass action contact. Due to human biting habit of mosquitoes, a restricted form of homogeneous mixing is assumed. This model captures the biology of the *Anopheles* mosquito from the behavioural ecology perspective. The model parameters are based on simplified assumptions that can apply to most insect vectors with a similar life style.

The objective of this chapter is to rigorously analyse the model given in [109], aimed at extending some of the theoretical results given in [109], using two different forms of the vector birth rate function.

## 3.2 Model Formulation

The vector dynamics model presented by Ngwa [109] is considered. Although detailed formulation of the model is given in [109], the same is repeated here for completeness. The total female mosquito population is sub-divided into three compartments based on the physiological status of the mosquito. At any time $t_1$, the density of the total adult mosquito population, denoted by $N_v(t_1)$, is sub-divided into three sub-populations, namely

(i) $U(t_1)$: population of fertilized, well-nourished (with blood) and reproducing female vectors;

(ii) $V(t_1)$: population of all previously-fertilized female vectors at the breeding site that have just laid their eggs but are still resting at the breeding site together with all unfertilized female vectors that are not fed with blood and are not questing for blood but are swarming at the breeding site;

(iii) $W(t_1)$: population of fertilized but non-reproducing vectors that have left the breeding site and are questing for a blood meal.

Thus, $N_v(t_1) = V(t_1) + U(t_1) + W(t_1)$.

### 3.2.1 Birth rate function

The *per capita* birth rate *per* reproducing vector in class $U$ is denoted by $B(U)$, where $B$ is assumed to be a non-negative strictly monotone decreasing, continuously-

differentiable function. We assume the following conditions on the function $B : [0, \infty) \rightarrow [0, \infty)$ (see also [25]).

**Definition 3.1.** *A function $B : [0, \infty) \rightarrow \mathbb{R}$ is a suitable birth rate function for the vector if it satisfies the following three conditions (where a prime represents a derivative with respect to $U$):*

***A1:*** $B(U) > 0, \ \forall \ U \geq 0$;

***A2:*** *$B(U)$ is continuously-differentiable with $B'(U) < 0, \ \forall \ U \geq 0$;*

***A3:*** *There exists a positive number, called the vectorial basic reproduction number (denoted by $\mathcal{R}_0$), such that $B(\infty) < \frac{B(0+)}{\mathcal{R}_0} < B(0+) = B_0$.*

Assumptions **A1** and **A2** ensure that $B^{-1}(x)$ exists for $x > 0$ with $B(\infty) < x < B_0$, while condition **A3** ensures the existence of a threshold parameter, $\mathcal{R}_0$, with the property that, when $\mathcal{R}_0 > 1$, a positive non-trivial equilibrium, given by $U^{**} = B^{-1}(x)$, with $x \in (B(\infty), B_0)$, exists. This equilibrium does not exist if $\mathcal{R}_0 \leq 1$.

The functional form of $B(U)$ is chosen based on the fact that, in ecology, non-linearity in the dynamics of the population of a single species arises due to the competition (for resources) between members of the population. Generally, when members of the same species compete for a common resource, two types of competition can be identified, namely *contest competition* and *scramble competition* [73]. In a scramble competition, members of the species compete for a resource that is inadequate for the needs of all, but is partitioned equally among contestants. Thus, in such a case, no competitor obtains the amount it needs and, in extreme cases, all the members of the

species may die. In a contest competition scenario, competition is for a resource that is partitioned unequally, so that some competitors obtain all they need and others less than they need (i.e., there are "winners" and "losers"). In the case of the mosquito, it is logical to assume that there is an abundance of humans from which to draw much needed blood meals, and that some of the mosquitoes succeed in the quest for blood ("winners") and some die in the process ("losers"). Hence, it seems plausible to assume a contest type competition for modelling the population dynamics of mosquitoes.

In this chapter, the following forms of birth functions, which satisfy Assumptions **A1** – **A3**, will be used.

$$\begin{aligned} &\textbf{B1}:\ B(U) = B_0\left(1-\frac{U}{L}\right),\ \ U\in[0,L); \\ &\textbf{B2}:\ B(U) = \frac{B_0}{1+\left(\frac{U}{L}\right)^n},\ \ n>0. \end{aligned} \tag{3.1}$$

The functional form **B1** was used in [109], and is commonly known in the literature as the Verhulst-Pearl logistic growth model. It should be mentioned that for this type of birth function, condition **A1** will hold only when $U < L$. Hence, $L$ is assumed to be large and can be considered as the environmental carrying capacity. Since there is a possibility for $U > L$, because of the possibility that fluctuations (oscillations) in vector population can induce some numerical instabilities (e.g. causing negative solutions in the simulations of the malaria vector population dynamics). However, we continue to use it for comparison purpose, since it is linear and is, in fact, a general form, for a first linear approximation near $U = 0$, to any form of birth rate function

satisfying Assumptions **A1** – **A3**. In each form of the birth rate function, $B_0$ may be identified as the limiting birth rate when the population numbers become very small. The birth rate form **B2**, known as the Beverton-Holt function, is an example of a birth rate function for a contest competition [16]. This is, perhaps, the first time the form **B2** is used to model the population dynamics of the mosquito vector. A plot of the birth rate functions **B1** and **B2** is depicted in Figure 3.2, from which it is evident that while **B1** is a linear decreasing function of $U$, **B2** is a non-linear and concave upward decreasing function of $U$.

### 3.2.2 Model equations

Before deriving the equations of the model, it is worth stating that the breeding ground for the vector is assumed to be distinct from the resting place of the humans (i.e., human habitat site). In a general setting, it is natural to consider several such breeding sites and human habitats. In this study, only one breeding site and human habitat is considered.

The population of fertilized, well-nourished and reproducing female vectors ($U$) is generated when vectors of class $W$ successfully take a blood meal from humans (where the density of human population is $H$) at a rate $\tau$ and with probability $p$. This population is decreased by the return of these vectors to the breeding site (at a rate $a$) and natural death (at a rate $\mu$). Thus,

$$\frac{dU}{dt_1} = p\tau HW - (a+\mu)U.$$

The population of all previously-fertilized female vectors at the breeding site that have just laid their eggs ($V$) is generated by the birth of new vectors (with density $\chi(U)$) and by the return of vectors of type $U$ to the breeding site. The functional form of $\chi(U)$ is derived as follows (as given in [25, 109])

At the breeding site, fed and reproducing vectors lay eggs that hatch into larvae. The larvae then mature into pupae which, in turn, produce adult vectors. Thus, there is a time delay from oviposition to adult mosquito eclosion. Suppose the fertilized and fed vectors lay eggs at a rate $B(U)$ *per* fed vector. Then, the density of eggs laid *per* unit time at the breeding site is given by $aB(U(t_1))U(t_1)$. Further, let $E_\pi(t_1)$ be the density of eggs initially present at the breeding site at time $\pi$; and assume that these eggs are still present at the breeding site at time $t_1 \geq \pi$. In the absence of any new eggs laid by fed vectors, and in the absence of any other sources of loss of eggs, the density of eggs present at time $t_1 \geq \pi$ is given by

$$E_\pi(t_1) = E_\pi(\pi)e^{-\mu_e(t_1-\pi)},$$

where, $\mu_e$ is the constant natural death rate in the embryo stage at the breeding site. The time $T_e$ spent by eggs at the breeding site is an exponentially distributed random variable. Survival to time $t_1$, for a cohort born at time $\pi$ is then defined as $S(\tilde{t_1}) = 1 - F(\tilde{t_1})$, where $F$ is the cumulative distribution function and $\tilde{t_1} = t_1 - \pi$ [7, 8], so that

$$S(\tilde{t_1}) = Pr(T_e \geq \tilde{t_1}) = 1 - Pr(T_e \leq \tilde{t_1}) = 1 - \int_0^{\tilde{t_1}} \mu_e e^{-\mu_e s} ds = e^{-\mu_e \tilde{t_1}} = e^{-\mu_e(t_1-\pi)}.$$

Therefore, $e^{-\mu_e(t_1-\pi)}$ is the proportion of eggs initially present at the breeding site at time $\pi$ that are still present at time $t_1 \geq \pi$; and $t_1 - \pi$ is the time duration the eggs have survived for until the present time $t_1$. Let $q(t_1)$ be the probability that eggs will remain unhatched $t_1$ time units after they were laid. Then, the density of eggs at the breeding site initially present at time $\pi$, that remain unhatched at time $t_1 \geq \pi$, now becomes

$$E_\pi(t_1) = E_\pi(\pi)q(t_1 - \pi)e^{-\mu_e(t_1-\pi)}.$$

Thus, the term $q(t_1-\pi)e^{-\mu_e(t_1-\pi)}$ represents the survival probability of eggs in the time interval $[\pi, t_1]$ [64].

Suppose that a fed and fertilized vector arriving at the breeding site laid its eggs at time $\nu \in [\pi, t_1]$. Then, the density of eggs at the breeding site (i.e., eggs initially present and new eggs laid by vectors returning to breeding site), at time $t_1$, is

$$E(t_1) = E_\pi(t_1) + \int_\pi^{t_1} aB(U(\nu))U(\nu)q(t_1 - \nu)e^{-\mu_e(t_1-\nu)}d\nu, \tag{3.2}$$

where the integral is taken over all eggs laid at time $\nu \in [\pi, t_1]$ that have survived and are present at time $t_1$. For simplicity, set $\pi = 0$ and assume that the maturation period of eggs is constant, denoted by $T_e$. It follows that, for $t \geq T_e$,

$$\begin{aligned} E(t_1) = E_0(t_1) &+ \int_0^{t_1-T_e} aB(U(\nu))U(\nu)q(t_1 - \nu)e^{-\mu_e(t_1-\nu)}d\nu \\ &+ \int_{t_1-T_e}^{t_1} aB(U(\nu))U(\nu)q(t_1 - \nu)e^{-\mu_e(t_1-\nu)}d\nu. \end{aligned} \tag{3.3}$$

Since $E_0(t_1) = 0$ (because it is assumed that no eggs were present at time $t_1 = 0$), for

$t_1 \geq T_e$, and

$$q(t_1) = \begin{cases} 1 & t_1 \in [0, T_e] \\ 0 & t_1 \in (T_e, \infty), \end{cases}$$

then,

$$q(t_1 - \nu) = \begin{cases} 1 & t_1 \in [t_1 - T_e, t_1], \\ 0 & t_1 \in [0, t_1 - T_e). \end{cases} \tag{3.4}$$

Using (3.4) in (3.3) for $t_1 \in [0, t_1 - T_e)$, and noting that $E_0(t_1) = 0$, gives

$$E(t_1) = \int_{t_1 - T_e}^{t_1} aB(U(\nu))U(\nu)q(t_1 - \nu)e^{-\mu_e(t_1 - \nu)}d\nu. \tag{3.5}$$

Differentiating (3.5) with respect to $t_1$ (noting (3.4)) gives

$$\frac{dE}{dt_1} = aB(U(t_1))U(t_1) - aB(U(t_1 - T_e))U(t_1 - T_e)e^{-\mu_e T_e} - \mu_e E(t_1). \tag{3.6}$$

It follows then that the density of larvae that would have hatched at time $t_1$, from eggs laid $T_e$ units of time earlier, is given by

$$aB(U(t_1 - T_e))U(t_1 - T_e)e^{-\mu_e T_e}, \tag{3.7}$$

where, $T_e$ is the maturation period of eggs.

Considering all the developmental stages of the vector (egg, larva, pupa), the density

of new vectors emerging at time $t_1$, $\chi(U)$, is then given by equation (3.7). That is,

$$\chi(U) = aB(U(t_1 - T))U(t_1 - T)e^{-\mu_e T}, \tag{3.8}$$

where, $T = T_e + T_l + T_p$, with $T_i$, $i = e, l, p$ being the respective maturation time of egg, larva and pupa and $\mu_e$ is the constant natural death rate of vectors in earlier life stages. Thus, at the breeding site, new vectors emerge at the rate

$$\chi(U) = aB(U(t_1 - T))U(t_1 - T)e^{-\mu_e T}.$$

The population of all previously-fertilized vectors that have just laid their eggs ($V$) is decreased by natural death (at the rate $\mu$) and by questing for human blood meal (at a rate $b$, which is scaled by $\frac{H}{H+K}$ to account for the preference of these vectors to human blood rather the blood of other animals). Note that $K$ is a positive constant representing a constant alternative food source for the mosquitoes. Thus, the rate of change of the population of vectors of type $V$ is given by

$$\frac{dV}{dt_1} = \chi(U) + aU - \left(\mu + \frac{bH}{H+K}\right)V.$$

The population of fertilized but non-reproducing vectors questing for blood meal ($W$) is increased at the rate $\frac{bH}{H+K}$ and is diminished by natural death (at the rate $\mu$) and by taking blood successfully (at a rate $\tau H$). Thus, the rate of change of vectors

in the class $W$ is

$$\frac{dW}{dt_1} = \left(\frac{bH}{H+K}\right)V - (\mu + \tau H)W.$$

In summary, the vector population dynamics in a single human habitat site and breeding site can be represented by the following non-linear system of delay differential equations [109]

$$\begin{aligned}
\frac{dU}{dt_1} &= p\tau HW - (a+\mu)U, \\
\frac{dV}{dt_1} &= aB(U(t_1-T))U(t_1-T)e^{-\mu_e T} + aU - \left(\mu + \frac{bH}{H+K}\right)V, \\
\frac{dW}{dt_1} &= \left(\frac{bH}{H+K}\right)V - (\mu+\tau H)W,
\end{aligned} \tag{3.9}$$

with initial data,

$$(U(t_1), V(t_1), W(t_1)) = (u_0(t_1), v_0(t_1), w_0(t_1)), \quad t_1 \in [-T, 0], \tag{3.10}$$

where, $u_0(t_1)$, $v_0(t_1)$ and $w_0(t_1)$ are continuously differentiable functions on the interval $[-T, 0]$. A flow diagram of the model (3.9) is given in Figure 3.1. The model variables and parameters are described in Tables 3.1 and 3.2.

The model (3.9) will be analysed for its dynamical features subject to the two birth functions **B1** and **B2**. In [109], the mathematical analysis of (3.9) was carried out subject to the birth function **B1**, establishing the local asymptotic stability of the associated trivial and non-trivial equilibria as well as the presence of Hopf bifurcation under certain conditions. The aim of this chapter is to, first of all, extend the analysis

in [109] for the case when no time delay ($T = 0$) is present for the birth function **B2** (the analysis for the case with $T \neq 0$ is carried out in Chapter 4 subject to the birth functions **B1** and **B2**. It should be noted that the birth function **B2** was not considered in [109]). The second objective is to investigate the effect of the functional form of $B(U)$ on the vector dynamics. In other words, the effect of using the forms **B1** and **B2** on the dynamics of the mosquito vector will be compared.

### 3.2.3 Basic properties of the model without delay ($T = 0$)

**Lemma 3.1.** *Consider the model* (3.9) *in the absence of delay* ($T = 0$). *The region* $\mathbb{R}^3_+$ *is positively-invariant.*

*Proof.* Consider the initial conditions $U(0) > 0$, $V(0) > 0$ and $W(0) > 0$. Suppose there exists a $t_2$ such that $U(t_2) = 0$. Thus,

$$\frac{dU}{dt_1}(t_2) = p\tau HW(t_2) > 0.$$

It follows that a $t_2 > t_1$ can be chosen such that $W(t_2) > 0$, so that $\frac{dU}{dt_1}(t_2) > 0$. But this contradicts the fact that $U(t_2) = 0$. Thus, no such $t_2$ exists. Using similar argument for $V(t_1)$ and $W(t_1)$, it can be shown that the solutions with positive initial conditions remain positive (in $\mathbb{R}^3_+$) for all $t_1 > 0$. That is, the region $\mathbb{R}^3_+$ is positively-invariant. □

**Lemma 3.2.** *The solutions of the system* (3.9) *in the absence of delay are bounded provided* $\mu - aB_0 > 0$.

*Proof.* In the absence of delay ($T = 0$), it can be shown from (3.9) that the rate of change of the total vector population, $N_v(t_1)$, is given by

$$\frac{dN_v(t_1)}{dt_1} = aB(U(t_1))U(t_1) - (1-p)\tau HW(t_1) - \mu N_v(t_1),$$

$$\leq aB(U(t_1))U(t_1) - \mu N_v(t_1),$$

$$\leq aB(U(t_1))N_v(t_1) - \mu N_v(t_1),$$

$$\leq aB_0 N_v(t_1) - \mu N_v(t_1).$$

Thus,

$$N_v(t_1) \leq N_v(0)e^{-(\mu - aB_0)t_1}.$$

Hence, the total vector population is bounded if $\mu - aB_0 > 0$. Since the total vector population is bounded (for $\mu - aB_0 > 0$), it follows that all the sub-populations of the model, namely $U(t_1)$, $V(t_1)$ and $W(t_1)$, are also bounded. □

From now on, it is assumed that $\mu - aB_0 > 0$, so that the system (3.9) is bounded.

### 3.2.4 Change of variables and parameters

Before proceeding with the mathematical analysis of the model (3.9), it is convenient to carry out the following change of parameters:

$$\begin{aligned} &\tau^* = \tau H, \;\; b^* = \frac{bH}{H+K}, \;\; C = (a+\mu)(b^*+\mu)(\tau^*+\mu), \;\; M = ab^*p\tau^*, \\ &N = \mu^3 + (b^*+a+\tau^*)\mu^2 + (ab^*+a\tau^*+b^*\tau^*)\mu + (1-p)b^*a\tau^*, \end{aligned} \tag{3.11}$$

and change of variables:

$$u = \frac{U}{U_0}, \;\; v = \frac{V}{V_0}, \;\; w = \frac{W}{W_0}, \;\; t = \frac{t_1}{T_0}, \tag{3.12}$$

where,

$$W_0 = \frac{(a+\mu)}{p\tau^*}U_0, \;\; V_0 = \frac{(a+\mu)(\tau^*+\mu)}{p\tau H\frac{bH}{H+K}}U_0, \;\; U_0 = L, \text{ and } T_0 = \frac{1}{a+\mu}. \tag{3.13}$$

It follows that, using (3.11), (3.12) and (3.13), the model (3.9) reduces to

$$\begin{aligned} \frac{du}{dt} &= w(t) - u(t), \\ \frac{dv}{dt} &= \alpha B(Lu(t-T))u(t-T)e^{-\mu_s T} + \alpha u(t) - \rho v(t), \\ \frac{dw}{dt} &= \gamma[v(t) - w(t)], \end{aligned} \tag{3.14}$$

with initial data,

$$(u(t), v(t), w(t)) = (u_0(t), v_0(t), w_0(t)), \;\; t \in [-T, 0], \tag{3.15}$$

where, $u_0(t)$, $v_0(t)$ and $w_0(t)$ are continuously differentiable functions on the interval $[-T, 0]$ and,

$$\alpha = \frac{aU_0T_0}{V_0}, \quad \rho = \frac{\frac{bH}{H+K} + \mu}{a+\mu}, \quad \gamma = \frac{\tau^* + \mu}{a+\mu}, \quad \mu_s = \frac{\mu_e}{a+\mu}. \tag{3.16}$$

For mathematical tractability, the analysis will be done for the scaled model (3.14). In the absence of delay ($T = 0$), the scaled system (3.14) reduces to,

$$\begin{aligned} \frac{du}{dt} &= w(t) - u(t), \\ \frac{dv}{dt} &= \alpha B(Lu(t))u(t) + \alpha u(t) - \rho v(t), \\ \frac{dw}{dt} &= \gamma[v(t) - w(t)]. \end{aligned} \tag{3.17}$$

It is easy to see that, using the above scaling, the birth rate functions **B1** and **B2** now take the forms:

$$B(U) = B(Lu) = \hat{B}(u) = \begin{cases} B_0(1-u); \ 0 < u \leq 1; & \text{Type} \quad \mathbf{B1}, \\ \\ \dfrac{B_0}{1+u^n}; & \text{Type} \quad \mathbf{B2}. \end{cases} \tag{3.18}$$

For notational convenience, we shall simply write $B(u)$ in place of $\hat{B}(u)$ for each of the birth functions (**B1** and **B2**) given in (3.18).

Using the above definitions, it is easy to show that

$$\alpha = \left(\frac{\frac{bH}{H+K} + \mu}{a+\mu}\right)\left(\frac{a}{a+\mu}\right)\left(\frac{\frac{bH}{H+K}}{\frac{bH}{H+K} + \mu}\right)\left(\frac{\tau^*}{\tau^* + \mu}\right)p < \left(\frac{\frac{bH}{H+K} + \mu}{a+\mu}\right) = \rho, \tag{3.19}$$

from which it follows that,

$$\alpha(\tau^*) = \frac{\alpha_0 \tau^*}{\tau^* + \mu}, \tag{3.20}$$

where,

$$\alpha_0 = \left(\frac{\frac{bH}{H+K}+\mu}{a+\mu}\right)\left(\frac{a}{a+\mu}\right)\left(\frac{\frac{bH}{H+K}}{\frac{bH}{H+K}+\mu}\right)p.$$

Further, it can be noted that

$$\gamma(\tau^*) = \frac{\tau^* + \mu}{a+\mu} > 0; \quad \text{since } 0 < \tau^* = \tau H < \infty.$$

It is convenient to define

$$Q(\tau^*) = 1 + \gamma(\tau^*) + \rho, \; R(\tau^*) = \gamma(\tau^*) + \rho + \rho\gamma(\tau^*). \tag{3.21}$$

Henceforth, we ignore referring to the explicit dependence of the parameters on $\tau^*$ and simply write $Q$, $\gamma$, $R$, etc.

## 3.3 Existence and Stability of Equilibria

The existence and asymptotic stability of the equilibria of the scaled system (3.17), for any arbitrary birth rate function $B(u)$, are explored as follows.

### 3.3.1 Local asymptotic stability of the trivial equilibrium

The system (3.17) has a trivial equilibrium, denoted by $E_0 = (u^*, v^*, w^*) = (0, 0, 0)$, which exists for all parameter regimes. The local asymptotic stability of $E_0$ is determined by linearizing the system (3.12) around $E_0$. This entails computing the Jacobian of the system (3.17) at $E_0$, given by

$$J(E_0) = \begin{pmatrix} -1 & 0 & 1 \\ \alpha(1+B_0) & -\rho & 0 \\ 0 & \gamma & -\gamma \end{pmatrix}. \tag{3.22}$$

The eigenvalues of $J(E_0)$ satisfy the characteristic equation:

$$G(\lambda) = \lambda^3 + Q\lambda^2 + R\lambda - \gamma[\alpha B_0 - (\rho - \alpha)] = 0,$$

where, $Q > 0$, $R > 0$ and $B_0 > 0$ as defined in Section 3.2.4. The roots of $G(\lambda)$ have negative real parts if and only if

$$\gamma[\alpha B_0 - (\rho - \alpha)] < 0, \tag{3.23}$$

so that,

$$\mathcal{R}_0 = \frac{\alpha B_0}{\rho - \alpha} < 1. \tag{3.24}$$

It should be noted that $\rho - \alpha > 0$ from (3.19), so that $\mathcal{R}_0 > 0$. Thus, the following result is established.

**Lemma 3.3.** *Consider the model* (3.17) *with* $B : [0, \infty) \to \mathbb{R}$ *satisfying Assumptions* ***A1 – A3****. The trivial equilibrium of the system* (3.17), $E_0$, *is locally-asymptotically stable (LAS) if* $\mathcal{R}_0 < 1$, *and unstable if* $\mathcal{R}_0 > 1$.

The threshold quantity, $\mathcal{R}_0$, is the *vectorial reproduction number* associated with the model (3.17). It measures the average number of new adult mosquitoes (offspring) produced by one reproductive mosquito during its entire reproductive period. The concept of the existence of a vectorial reproduction number in the study of the population dynamics of mosquito vectors has also been addressed by Porphyre *et al.* [115].

The ecological implication of the above local stability result of the trivial equilibrium ($E_0$) is that if the initial vector population is in the basin of attraction of the trivial equilibrium, then the vector population can be eradicated provided $\mathcal{R}_0 < 1$. To ensure that such eradication is independent of the initial population of the vector, a global asymptotic stability result must be established for the trivial equilibrium. This is considered below for a general birth function satisfying **A1-A3** (using the fluctuation method [66, 133]). It should be mentioned that although the above local stability result was also established in [109], no global asymptotic stability (GAS) result for the trivial equilibrium ($E_0$) was provided in that study.

### 3.3.2 Global asymptotic stability of the trivial equilibrium

We claim the following:

**Theorem 3.1.** *Consider the model* (3.17) *with* $B : [0, \infty) \to \mathbb{R}$ *satisfying Assumptions* ***A1 – A3****. The trivial equilibrium,* $E_0$*, of the model* (3.17) *is GAS in* $\mathbb{R}^3_+$ *whenever* $\mathcal{R}_0 < 1$.

*Proof.* The proof is based on using the fluctuation method (see Section 2.8.1). First of all, a sequence $t_k$ is chosen such that $\lim_{k\to\infty} v(t_k) = v^\infty$ and $dv(t_k)/dt \to 0$ (Proposition 2.1). It follows then that, by Theorem 2.11 and Corollary 2.1,

$$0 = \lim_{k\to\infty} [\alpha B(u(t_k))u(t_k) + \alpha u(t_k)] - \rho v^\infty,$$

so that,

$$\begin{aligned} \rho v^\infty &= \lim_{k\to\infty} [\alpha B(u(t_k))u(t_k) + \alpha u(t_k)], \\ &\leq \alpha B_0 u^\infty + \alpha u^\infty, \text{ by Assumption } \mathbf{A3}, \\ &= \alpha u^\infty (B_0 + 1). \end{aligned} \tag{3.25}$$

Thus,

$$v^\infty \leq \frac{\alpha u^\infty (B_0 + 1)}{\rho}. \tag{3.26}$$

Similarly, a sequence $s_k$ can be chosen such that $\lim_{k\to\infty} w(s_k) = w^\infty$ and $dw(s_k)/dt \to 0$. Hence,

$$0 = \gamma \left[ \lim_{k\to\infty} v(s_k) - w^\infty \right],$$

so that,

$$0 \leq \gamma(v^{\infty} - w^{\infty}). \tag{3.27}$$

It follows from (3.26) and (3.27) that

$$w^{\infty} \leq v^{\infty} \leq \frac{\alpha u^{\infty}(B_0 + 1)}{\rho}.$$

Furthermore, choosing a sequence $r_k$ such that $\lim_{k\to\infty} u(r_k) = u^{\infty}$ and $du(r_k)/dt \to 0$ leads to

$$\begin{aligned} 0 &= \lim_{k\to\infty} w(r_k) - u^{\infty}, \\ 0 &\leq w^{\infty} - u^{\infty}, \end{aligned} \tag{3.28}$$

so that,

$$u^{\infty} \leq w^{\infty} \leq v^{\infty} \leq \frac{\alpha u^{\infty}(B_0 + 1)}{\rho}.$$

Thus,

$$0 \leq \left[\frac{\alpha B_0 - (\rho - \alpha)}{\rho}\right] u^{\infty},$$

which can be re-written as

$$0 \leq \frac{\rho - \alpha}{\rho}(\mathcal{R}_0 - 1)u^{\infty}.$$

This implies that $u^{\infty} \leq 0$ whenever $\mathcal{R}_0 < 1$. Since $u^{\infty} \geq 0$, it follows that $u^{\infty} = 0$.

Using this fact in (3.26) and (3.27), also leads to the conclusion that $v^{\infty} = 0$ and $w^{\infty} = 0$ whenever $\mathcal{R}_0 < 1$. Hence, $E_0$ is GAS in $\mathbb{R}^3_+$ whenever $\mathcal{R}_0 < 1$. □

The result of Theorem 3.1 is illustrated numerically, by simulating the model (3.17) with appropriate parameter values (so that $\mathcal{R}_0 < 1$), using the Verhulst-Pearl logistic growth function (Figure 3.3) and the Beverton-Holt function (Figure 3.4) as birth functions. It is evident from the numerical simulations that for both birth functions, all the solution profiles of the model (3.17) converge to the trivial equilibrium whenever $\mathcal{R}_0 < 1$, (i.e., the model has the same qualitative dynamics, using any of the two birth functions, if $\mathcal{R}_0 < 1$). Thus, the result of local asymptotic stability of the trivial equilibrium $E_0$ for the birth function **B1** obtained in [109] is extended in this thesis to that of global asymptotic stability of $E_0$ for any arbitrary birth function satisfying **A1 – A3**.

### 3.3.3 Existence and local stability of non-trivial equilibrium

#### Existence

The system (3.17) has a unique non-trivial equilibrium given by (see also [109])

$$E_1 = (u^{**}, v^{**}, w^{**}) = (1, 1, 1)u^{**}, \tag{3.29}$$

where, $u^{**} > 0$ is obtained as follows. It can be shown, by setting the right-hand sides of the equations in (3.17) to zero, that (at the non-trivial steady state)

$$\alpha u^{**}[1 + B(u^{**})] = \rho v^{**} = \rho u^{**},$$

so that,

$$B(u^{**}) = \frac{\rho - \alpha}{\alpha} = \frac{B_0}{\mathcal{R}_0}. \tag{3.30}$$

Hence,

$$u^{**} = B^{-1}\left(\frac{B_0}{\mathcal{R}_0}\right) > 0,$$

where $B(u)$ is any arbitrary birth function satisfying Assumptions $\mathbf{A1} - \mathbf{A3}$. It should be recalled that Assumptions **A1** and **A2** guarantee that the function $B^{-1}$ exists. Further, Assumption **A3**, with $B(0+) = B_0$, assures the existence of $u^{**}$ whenever $\mathcal{R}_0 > 1$. Thus, the following result holds.

**Lemma 3.4.** *Consider the model* (3.17) *with* $B : [0, \infty) \to \mathbb{R}$ *satisfying Assumptions* $\boldsymbol{A1 - A3}$. *The unique non-trivial equilibrium of* (3.17), *given by* $E_1$, *exists whenever* $\mathcal{R}_0 > 1$.

### Local stability

The Jacobian of the system (3.17), evaluated at $E_1$, is given by

$$J(E_1) = \begin{pmatrix} -1 & 0 & 1 \\ \alpha[1+\Psi(u^{**})] & -\rho & 0 \\ 0 & \gamma & -\gamma \end{pmatrix}, \tag{3.31}$$

with the following characteristic equation

$$\lambda^3 + Q\lambda^2 + R\lambda + P = \Psi(u^{**})A, \tag{3.32}$$

where $Q$ and $R$ are as defined in Section 3.2.4, and

$$P = \gamma(\rho - \alpha), \quad A = \alpha\gamma, \quad \Psi(u^{**}) = B(u^{**}) + B'(u^{**})u^{**}. \tag{3.33}$$

The following result can be established (see also [109]).

**Theorem 3.2.** *Consider the model* (3.17) *with* $B : [0, \infty) \to \mathbb{R}$ *satisfying Assumptions* ***A1*** $-$ ***A3***. *The non-trivial equilibrium,* $E_1$, *of the system* (3.17) *is LAS whenever* $\mathcal{R}_0 > 1$ *and* $\dfrac{-AB'(u^{**})u^{**}}{QR} < 1$.

*Proof.* Let $\mathcal{R}_0 > 1$, so that the non-trivial equilibrium $E_1$ exists (Lemma 3.4). Using (3.33) and (3.30) in (3.32) gives

$$\lambda^3 + Q\lambda^2 + R\lambda + P = A\left[\frac{P}{A} + B'(u^{**})u^{**}\right],$$

so that

$$\lambda^3 + Q\lambda^2 + R\lambda - AB'(u^{**})u^{**} = 0. \tag{3.34}$$

The coefficients of the cubic (3.34) are non-negative, since $Q = 1 + \gamma + \rho > 0$, $R = \gamma + \rho + \rho\gamma > 0$ and $-AB'(u^{**})u^{**} \geq 0$ (noting that $B$ is monotone decreasing). It follows, by the Routh-Hurwitz criterion [85], that the roots of the polynomial (3.34) have negative real parts if and only if

$$QR + AB'(u^{**})u^{**} > 0. \tag{3.35}$$

The inequality (3.35) implies that

$$\frac{-AB'(u^{**})u^{**}}{QR} < 1. \tag{3.36}$$

Thus, $E_1$ is LAS if $\dfrac{-AB'(u^{**})u^{**}}{QR} < 1$ and $\mathcal{R}_0 > 1$. □

This result (Theorem 3.2) holds for any birth function $B(u)$ satisfying **A1** – **A3**. It is illustrated numerically, by simulating the model (3.17) with appropriate parameter values, using the Verhulst-Pearl logistic growth function (Figures 3.5 and 3.6) and the Beverton-Holt birth function (Figures 3.7 and 3.8). Simulation results show that for both birth functions (**B1** and **B2**), the non-trivial equilibrium becomes a stable spiral if $\mathcal{R}_0 > 1$ and the inequality (3.36) holds. The results in Lemma 3.4 and Theorem 3.2

are also shown in [109].

In summary, these analyses reveal that the model (3.17) exhibits the same equilibrium dynamics (convergence to $E_0$ for $\mathcal{R}_0 < 1$ and to $E_1$ for $\mathcal{R}_0 > 1$, and $\frac{-AB'(u^{**})u^{**}}{QR} < 1$) regardless of which of the two birth functions is used.

## 3.4 Hopf Bifurcation

In this section, the existence of Hopf bifurcation (i.e., bifurcation of the non-trivial equilibrium into a limit cycle [58, 68, 94]) will be explored for each of the two birth functions.

It is worth stating that Ngwa [109] also showed the presence of Hopf bifurcation in (3.9), subject to general birth function satisfying **A1** – **A3**, using a perturbation argument. In this thesis, the phenomenon of Hopf bifurcation will be shown using a different (but standard) method, based on the direct application of Hopf bifurcation theory [58, 68, 94], for the two birth functions (**B1** and **B2**). It follows from Theorem 3.2 that the roots of the characteristic polynomial have negative real parts whenever the inequality (3.36) holds. Consider the case when the inequality (3.36) becomes equality. That is, let

$$\frac{-AB'(u^{**})u^{**}}{QR} = 1.$$

Then,

$$-AB'(u^{**})u^{**} = QR.$$

Thus, equation (3.34) becomes

$$\lambda^3 + Q\lambda^2 + R\lambda + QR = 0,$$

so that

$$(\lambda^2 + R)(\lambda + Q) = 0. \tag{3.37}$$

It follows that the characteristic equation (3.37) has a pair of purely imaginary eigenvalues, given by $\lambda = \pm i\sqrt{R}$, and a negative real eigenvalue $\lambda = -Q$, suggesting that system (3.17) may undergo a Hopf bifurcation at the point in parameter space where $-AB'(u^{**})u^{**} = QR$. We claim the following

**Lemma 3.5.** *For the two birth rate functions **B1** and **B2**, and for every given parameter grouping, there exists a positive number $\gamma^*$ such that*

$$-\frac{\alpha\gamma^* u^{**} B'(u^{**})}{Q(\gamma^*)R(\gamma^*)} = 1.$$

*Proof.* Consider the bifurcation condition $-\dfrac{\alpha\gamma^* u^{**} B'(u^{**})}{Q(\gamma^*)R(\gamma^*)} = 1$. Thus, $\gamma^*$ is determined by finding the fixed-point of the map

$$f : x \mapsto -\frac{(1+\rho+x)[\rho+(1+\rho)x]}{\alpha u^{**} B'(u^{**})},$$

such that $x \in (0, \infty)$. In other words, the required value of $\gamma^*$ at the bifurcation point

is given by a positive real solution, $(x)$, of the non-linear equation

$$x + \frac{(1+\rho+x)[\rho+(1+\rho)x]}{\alpha u^{**} B'(u^{**})} = 0. \tag{3.38}$$

Simplifying (3.38) gives

$$a_1 x^2 + b_1 x + c_1 = 0, \tag{3.39}$$

where,

$$a_1 = (1+\rho),$$

$$b_1 = [(1+\rho)^2 + \rho + \alpha u^{**} B'(u^{**})],$$

$$c_1 = \rho(1+\rho).$$

Clearly, the constants $a_1$ and $c_1$ are positive. Thus, the quadratic (3.39) will have two positive roots if

$$b_1 < 0 \quad \text{and} \quad b_1^2 - 4a_1c_1 \geq 0.$$

The positive solutions of the quadratic (3.39) are then given by

$$\gamma_1^* = x_1 = \frac{-b_1 - \sqrt{b_1^2 - 4a_1c_1}}{2a_1}, \tag{3.40}$$

$$\gamma_2^* = x_2 = \frac{-b_1 + \sqrt{b_1^2 - 4a_1c_1}}{2a_1}.$$

In particular, $\gamma_1^*$ takes the following forms for the birth functions **B1** and **B2**.

(i) For **B1**:

$$b_1 = (1+\rho)^2 + \rho - \alpha B_0\left(1 - \frac{1}{\mathcal{R}_0}\right).$$

Thus,

$$\gamma_1^* = \frac{1}{2(1+\rho)}\left\{-\left[(1+\rho)^2 + \rho - \alpha B_0\left(1 - \frac{1}{\mathcal{R}_0}\right)\right] - \sqrt{\left[(1+\rho)^2 + \rho - \alpha B_0\left(1 - \frac{1}{\mathcal{R}_0}\right)\right]^2 - 4\rho(1+\rho)^2}\right\}. \tag{3.41}$$

(ii) For **B2**:

$$b_1 = (1+\rho)^2 + \rho - \alpha n B_0\left(\frac{1}{\mathcal{R}_0} - \frac{1}{\mathcal{R}_0^2}\right).$$

Hence,

$$\gamma_1^* = \frac{1}{2(1+\rho)}\left\{-\left[(1+\rho)^2 + \rho - \alpha n B_0\left(\frac{1}{\mathcal{R}_0} - \frac{1}{\mathcal{R}_0^2}\right)\right] - \sqrt{\left[(1+\rho)^2 + \rho - \alpha n B_0\left(\frac{1}{\mathcal{R}_0} - \frac{1}{\mathcal{R}_0^2}\right)\right]^2 - 4\rho(1+\rho)^2}\right\}. \tag{3.42}$$

□

### 3.4.1 Hopf bifurcation: Verhulst-Pearl logistic growth function

To establish the presence of Hopf bifurcation using the Verhulst-Pearl logistic growth function, we consider the birth function **B1** (defined in (3.18))

$$B(u) = B_0(1-u), \tag{3.43}$$

where, $B_0 > 0$ is a constant. With the given $B(u)$, it is easy to show (using (3.29) and (3.43)) that the non-trivial equilibrium of the system (3.17) takes the form

$$(u^{**},\ v^{**},\ w^{**}) = \left[(1,1,1)\left(1-\frac{1}{\mathcal{R}_0}\right)\right],$$

where, $B(u)$ satisfies Assumptions $\mathbf{A1}-\mathbf{A3}$.

Using (3.43) in the associated local stability condition (3.36), for the non-trivial equilibrium ($E_1$), gives

$$\frac{\alpha\gamma B_0\left(1-\frac{1}{\mathcal{R}_0}\right)}{QR} < 1, \tag{3.44}$$

which implies that

$$\frac{\alpha\gamma\left(\frac{\rho-\alpha}{\alpha}\right)\left(1-\frac{1}{\mathcal{R}_0}\right)\mathcal{R}_0}{QR} < 1.$$

Thus,

$$\frac{\gamma(\rho-\alpha)(\mathcal{R}_0-1)}{QR} < 1,$$

so that

$$\mathcal{R}_0 < 1 + \frac{QR}{\gamma(\rho - \alpha)},$$

or, equivalently,

$$B_0 < \frac{\rho - \alpha}{\alpha} + \frac{QR}{\alpha\gamma}.$$

We claim the following result.

**Theorem 3.3.** *Consider $\gamma_1^*$ as defined in* (3.41). *The system* (3.17) *with $B(u) = B_0(1-u)$ undergoes a Hopf bifurcation at $\gamma_1^*$.*

*Proof.* Consider $\gamma$ as the bifurcation parameter and $\gamma_1^*$ as given in (3.41). The characteristic equation (3.32) now becomes (since $QR = \alpha\gamma B_0(1 - \frac{1}{\mathcal{R}_0})$)

$$\lambda^3 + Q\lambda^2 + R\lambda + \alpha\gamma B_0\left(1 - \frac{1}{\mathcal{R}_0}\right) = 0. \tag{3.45}$$

At $\gamma = \gamma_1^*$, the cubic (3.45) has a pair of purely imaginary roots, given by $\lambda = \pm i\sqrt{R}$. Substituting $\lambda = \pm i\omega$ (with $\omega > 0$) in (3.45) gives

$$-i\omega^3 - Q\omega^2 + iR\omega + \alpha\gamma B_0\left(1 - \frac{1}{\mathcal{R}_0}\right) = 0. \tag{3.46}$$

Separating the real and imaginary parts of (3.46) gives

$$\begin{aligned} Q\omega^2 - \alpha\gamma B_0\left(1 - \frac{1}{\mathcal{R}_0}\right) &= 0, \\ \omega(R - \omega^2) &= 0. \end{aligned} \tag{3.47}$$

Hence,

$$\left.\frac{\partial Re(\lambda)}{\partial \gamma}\right|_{\gamma=\gamma_1^*} = \omega^2 - \alpha B_0\left(1-\frac{1}{\mathcal{R}_0}\right),$$

$$= R - \alpha B_0\left(1-\frac{1}{\mathcal{R}_0}\right), \text{ since } R=\omega^2,$$

$$= \rho + \gamma_1^*(1+\rho) - \alpha B_0\left(1-\frac{1}{\mathcal{R}_0}\right),$$

$$= \rho + (1+\rho)\frac{1}{2(1+\rho)}\left\{-\left[(1+\rho)^2+\rho-\alpha B_0\left(1-\frac{1}{\mathcal{R}_0}\right)\right]\right.$$

$$\left. - \sqrt{\left[(1+\rho)^2+\rho-\alpha B_0\left(1-\frac{1}{\mathcal{R}_0}\right)\right]^2 - 4\rho(1+\rho)^2}\right\} - \alpha B_0\left(1-\frac{1}{\mathcal{R}_0}\right),$$

$$= \frac{1}{2}\left\{-(1+\rho+\rho^2) - \sqrt{\left[(1+\rho)^2+\rho-\alpha B_0\left(1-\frac{1}{\mathcal{R}_0}\right)\right]^2 - 4\rho(1+\rho)^2}\right.$$

$$\left. - \alpha B_0\left(1-\frac{1}{\mathcal{R}_0}\right)\right\},$$

$$< 0 \text{ (since } b_1^2 - 4a_1c_1 > 0, \alpha > 0, B_0 > 0 \text{ and } \mathcal{R}_0 > 1).$$

Thus, a Hopf bifurcation occurs at $\gamma = \gamma_1^*$ defined in (3.41). □

The result in Theorem 3.3 is illustrated numerically, by simulating the model (3.17) with **B1**, as depicted in Figures 3.9 and 3.10.

In summary, we have established the following results for the system (3.17) subject to the Verhulst-Pearl logistic growth function **B1**:

(i) the model has a trivial equilibrium solution $E_0 = (0,0,0)$, which is GAS in $\mathbb{R}^3_+$ if $\mathcal{R}_0 < 1$ (or, $B_0 \leq \frac{\rho-\alpha}{\alpha}$). This result holds for any arbitrary birth function

satisfying **A1 – A3**;

(ii) if $\mathcal{R}_0 > 1$ (or, $B_0 > \frac{\rho-\alpha}{\alpha}$), then the model has a non-trivial equilibrium solution given by $E_1 = (u^{**}, v^{**}, w^{**}) = (1,1,1)\left(1 - \frac{1}{\mathcal{R}_0}\right)$. This equilibrium is locally-asymptotically stable (stable spiral) if $1 < \mathcal{R}_0 < 1 + \frac{QR}{\gamma(\rho-\alpha)}$ (or, $\frac{\rho-\alpha}{\alpha} < B_0 < \frac{\rho-\alpha}{\alpha} + \frac{QR}{\alpha\gamma}$);

(iii) a Hopf bifurcation occurs at $\gamma = \gamma_1^*$ given by (3.41) (or, $B_0 = \frac{\rho-\alpha}{\alpha} + \frac{QR}{\alpha\gamma}$). In other words, if $\mathcal{R}_0 > 1 + \frac{QR}{\gamma(\rho-\alpha)}$ (or, $B_0 > \frac{\rho-\alpha}{\alpha} + \frac{QR}{\alpha\gamma}$), the stable spiral loses its stability and a limit cycle emerges *via* a Hopf bifurcation.

It should be noted that when $b_1^2 - 4a_1c_1 = 0$, then $b_1 = -2\sqrt{a_1c_1}$ (as $b_1 < 0$). Thus, it follows from (3.40), that $\gamma_1^* = \gamma_2^* = \frac{-b_1}{2a_1}$ (at which the Hopf bifurcation is possible).

### 3.4.2 Hopf bifurcation: Beverton-Holt function

Here, we consider the Beverton-Holt function (given in (3.18))

$$B(u) = \frac{B_0}{1+u^n}, \tag{3.48}$$

where, $B_0 > 0$ is a constant and $B(u)$ satisfies Assumptions **A1 – A3**. Using (3.29) and (3.48), it can be shown that the non-trivial equilibrium of the system (3.17) is given by

$$(u^{**},\ v^{**},\ w^{**}) = \left[(1,1,1)(\mathcal{R}_0 - 1)^{1/n}\right].$$

Using (3.48) in the local stability condition (3.36), for the non-trivial equilibrium, gives

$$\frac{\gamma n(\rho-\alpha)^2\left(\frac{1}{\rho-\alpha}-\frac{1}{\alpha B_0}\right)}{QR}<1, \tag{3.49}$$

which implies that

$$1-\frac{\rho-\alpha}{\alpha B_0}<\frac{QR}{\gamma n(\rho-\alpha)},$$

so that

$$1-\frac{\rho-\alpha}{\mathcal{R}_0(\rho-\alpha)}<\frac{QR}{\gamma n(\rho-\alpha)},$$

which can be re-written as

$$1-\frac{QR}{\gamma n(\rho-\alpha)}<\frac{1}{\mathcal{R}_0}.$$

Hence,

$$\mathcal{R}_0<\frac{\gamma n(\rho-\alpha)}{\gamma n(\rho-\alpha)-QR},$$

or, equivalently,

$$B_0<\frac{\gamma n(\rho-\alpha)^2}{\alpha[\gamma n(\rho-\alpha)-QR]}.$$

We claim the following.

**Theorem 3.4.** *Consider the system* (3.17) *with* $B(u)=\dfrac{B_0}{1+u^n}$ *and* $\gamma_1^*$ *as defined in* (3.42). *The system undergoes a Hopf bifurcation at* $\gamma_1^*$.

*Proof.* Consider $\gamma$ as the bifurcation parameter and $\gamma_1^*$ as in equation (3.42). The characteristic equation (3.32) becomes (since $QR = \frac{n\gamma(\rho-\alpha)^2(\mathcal{R}_0-1)}{\alpha B_0}$)

$$\lambda^3 + Q\lambda^2 + R\lambda + \frac{n\gamma(\rho-\alpha)^2(\mathcal{R}_0-1)}{\alpha B_0} = 0. \tag{3.50}$$

At $\gamma = \gamma_1^*$ given in (3.42), the cubic (3.50) has a pair of purely imaginary roots given by $\lambda = \pm i\sqrt{R}$. Substituting $\lambda = \pm i\omega$ in (3.50) gives

$$-i\omega^3 - Q\omega^2 + iR\omega + \frac{n\gamma(\rho-\alpha)^2(\mathcal{R}_0-1)}{\alpha B_0} = 0. \tag{3.51}$$

Separating the real and imaginary parts of (3.51) gives

$$Q\omega^2 - \frac{n\gamma(\rho-\alpha)^2(\mathcal{R}_0-1)}{\alpha B_0} = 0,$$

$$\omega(R-\omega^2) = 0,$$

so that

$$\left.\frac{\partial Re(\lambda)}{\partial \gamma}\right|_{\gamma=\gamma_1^*} = \omega^2 - \frac{n(\rho-\alpha)^2(\mathcal{R}_0-1)}{\alpha B_0},$$

$$= R - \frac{n(\rho-\alpha)^2(\mathcal{R}_0-1)}{\alpha B_0}, \text{ since } \omega^2 = R,$$

$$= \rho + \gamma_1^*(1+\rho) - \frac{n(\rho-\alpha)^2(\mathcal{R}_0-1)}{\alpha B_0},$$

$$= \rho + (1+\rho)\frac{1}{2(1+\rho)}\left\{-\left[(1+\rho)^2+\rho-\alpha n B_0\left(\frac{1}{\mathcal{R}_0}-\frac{1}{\mathcal{R}_0^2}\right)\right]\right.$$
$$\left.-\sqrt{\left[(1+\rho)^2+\rho-\alpha n B_0\left(\frac{1}{\mathcal{R}_0}-\frac{1}{\mathcal{R}_0^2}\right)\right]^2-4\rho(1+\rho)^2}\right\} - \frac{n(\rho-\alpha)^2(\mathcal{R}_0-1)}{\alpha B_0},$$

$$= \frac{1}{2}\left\{-(1+\rho+\rho^2) - \sqrt{\left[(1+\rho)^2+\rho-\frac{n(\rho-\alpha)^2(\mathcal{R}_0-1)}{\alpha B_0}\right]^2-4\rho(1+\rho)^2}\right.$$
$$\left.-\frac{n(\rho-\alpha)^2(\mathcal{R}_0-1)}{\alpha B_0}\right\} < 0, \text{ since the discriminant } b_1^2 - 4a_1c_1 > 0.$$

Thus, a Hopf bifurcation occurs at $\gamma = \gamma_1^*$, given by (3.42). □

The result in Theorem 3.4 is illustrated numerically, by simulating the model (3.17) subject to **B2**, as depicted in Figures 3.11 and 3.12.

In summary, we have established the following results for the system (3.17) subject to the Beverton-Holt function:

(i) the model has a trivial equilibrium solution $E_0 = (0,0,0)$ which is GAS in $\mathbb{R}^3_+$ if $\mathcal{R}_0 < 1$ (or, $B_0 \leq \frac{\rho-\alpha}{\alpha}$). This result holds for any arbitrary birth function satisfying **A1** – **A3**;

(ii) if $\mathcal{R}_0 > 1$, (or, $B_0 > \frac{\rho-\alpha}{\alpha}$), then the model has a non-trivial equilibrium solution given by $E_1 = (u^{**},\ v^{**},\ w^{**}) = \left[(1,1,1)(\mathcal{R}_0 - 1)^{1/n}\right]$. This equilibrium is locally-asymptotically stable (stable spiral) if $1 < \mathcal{R}_0 < \frac{\gamma n(\rho-\alpha)}{\gamma n(\rho-\alpha)-QR}$ (or, $\frac{\rho-\alpha}{\alpha} < B_0 < \frac{\gamma n(\rho-\alpha)^2}{\alpha[\gamma n(\rho-\alpha)-QR]}$ where $n > \frac{QR}{\gamma(\rho-\alpha)}$);

(iii) a Hopf bifurcation occurs at $\gamma = \gamma_1^*$ given by (3.42) (or, $B_0 = \frac{\gamma n(\rho-\alpha)^2}{\alpha[\gamma n(\rho-\alpha)-QR]}$). That is, if $\mathcal{R}_0 > \frac{\gamma n(\rho-\alpha)}{\gamma n(\rho-\alpha)-QR}$ (or, $B_0 > \frac{\gamma n(\rho-\alpha)^2}{\alpha[\gamma n(\rho-\alpha)-QR]}$), the stable spiral loses its stability and a limit cycle appears *via* a Hopf bifurcation.

The stability regions of the various solutions are tabulated in terms of $\mathcal{R}_0$ and $B_0$ in Tables 3.3 and 3.4, respectively.

### 3.4.3 Summary of stability regions

For the system (3.17), with $B(u)$ satisfying Assumptions $\mathbf{A1}-\mathbf{A3}$, the boundary curve in parameter space that separates the associated periodic solution from the stable spiral is given by the equation

$$-\frac{\alpha\gamma u^{**}B'(u^{**})}{QR} = 1. \tag{3.52}$$

On this curve, the linearized system would have a pair of purely imaginary eigenvalues, and on either side of it, the system exhibits qualitatively different dynamic behaviours.

The regions labeled I, II and III in Tables 3.3 and 3.4 represent areas in parameter space where the model exhibits different qualitative dynamics. Since the bifurcation parameter $\gamma$ is a function of $\tau^*$, it changes as $\tau^*$ changes. These regions are best

observed by plotting the boundary curves defining $B_0$ as a function of $\tau^*$ at the limits shown in column two of Table 3.4 (see Figure 3.13). The model dynamics at the various regions is summarized below.

**Region I.** In this region, the system has only the trivial equilibrium ($E_0$), which is globally asymptotically stable for $\mathcal{R}_0 < 1$ (Theorem 3.1).

**Region II.** As $\tau^*$ increases from zero, the system eventually enters Region II, wherein $B_0(\tau^*) > \frac{\rho - \alpha(\tau^*)}{\alpha(\tau^*)}$ but bounded as shown in Table 3.4. Here, an additional steady state, the non-trivial equilibrium ($E_1$), emerges. The non-trivial equilibrium is locally-asymptotically stable for each of the birth functions (**B1** and **B2**) under certain conditions (Theorem 3.2).

**Region III.** As $\tau^*$ increases further, the stable non-trivial equilibrium can be driven into instability *via* a Hopf bifurcation (Theorems 3.3 and 3.4), for the two birth rate functions **B1** and **B2**, respectively.

Extensive numerical simulations suggest that the size of the instability window (of $E_1$) can be different for the different forms of the birth rate functions. This observation is explored rigorously below.

### 3.4.4 Birth functions and periodic solutions

To understand how the functional form of the birth rate function $B(u)$ affects the dynamics of the mosquito population, we examine either the threshold condition (Column Two of Table 3.3) or the region of parameter space (Column Two of Table 3.4) in the

$(B_0, \tau^*)$-plane generated using the two birth functions **B1** and **B2**. There are several distinct possibilities to consider, as follows:

Suppose that $n = \kappa \frac{QR}{\gamma(\rho-\alpha)}$ for some positive constant $\kappa$. Then, referring to Regions II and III for birth function type **B2**, we have

$$\frac{\gamma(\rho-\alpha)n}{\gamma(\rho-\alpha)n - QR} = \frac{\kappa}{\kappa - 1} = 1 + \frac{1}{\kappa - 1},$$

so that if $\kappa > 1$ is fixed, the threshold condition for a stable spiral is then given by

$$1 < \mathcal{R}_0 < 1 + \frac{1}{\kappa - 1},$$

or, equivalently,

$$\frac{\rho - \alpha}{\alpha} < B_0 < \frac{\rho - \alpha}{\alpha}\left(1 + \frac{1}{\kappa - 1}\right).$$

For a sufficiently large, but fixed, $B_0$, as $\tau^*$ is increased from zero, the $(B_0, \tau^*)$-plane is traversed in the following order: Region $I \rightarrow II \rightarrow III$. For intermediate values of $B_0$, the $(B_0, \tau^*)$-plane is traversed in the order Region: $I \rightarrow II$, while for low values of $B_0$, where $\mathcal{R}_0 < 1$, the system stays in Region I.

For the birth rate function of type **B1**, a somewhat different scenario arises. For a sufficiently large, but fixed, $B_0$, as $\tau^*$ is increased from zero, the $(B_0, \tau^*)$-plane is traversed in the order: Region $I \rightarrow II \rightarrow III \rightarrow II$. For intermediate values of $B_0$, the $(B_0, \tau^*)$-plane is traversed in the order Region $I \rightarrow II$, while for low values of $B_0$, where $\mathcal{R}_0 < 1$, we stay in Region I. The possibility of the system going from stable

equilibrium solutions through limit cycles and then back to equilibrium solutions is shown in Figure 3.14.

### The size of the instability window

We can order the delimiters of the size of the stability window by observing that for moderately large values of $\tau^* \in (0, \infty)$, and fixed $\kappa$,

$$\frac{\rho - \alpha(\tau^*)}{\alpha(\tau^*)} \frac{\kappa}{\kappa - 1} < \frac{\rho - \alpha(\tau^*)}{\alpha(\tau^*)} + \frac{Q(\tau^*)R(\tau^*)}{\alpha(\tau^*)\gamma(\tau^*)}. \tag{3.53}$$

If the inequality (3.53) is viewed as a function of $\tau^*$, as $h(\tau^*) < g(\tau^*)$, then the degree of concavity of $h$ and $g$ can be measured by computing the second derivatives of $h$ and $g$. That is,

$$h(\tau^*) = \frac{\rho - \alpha(\tau^*)}{\alpha(\tau^*)},$$

$$h''(\tau^*) = -\left( \frac{\rho\alpha''(\tau^*)\alpha(\tau^*) - 2\alpha'(\tau^*)^2\rho}{\alpha(\tau^*)^3} \right).$$

But,

$$\alpha(\tau^*) = \frac{\alpha_0\tau^*}{\mu + \tau^*} \text{ and } \alpha''(\tau^*) = \frac{-2\mu\alpha_0}{(\mu + \tau^*)^3} < 0.$$

Hence, $h''(\tau^*) > 0$. Thus, $h$ is a concave upward function of $\tau^*$. Furthermore, $g''(\tau^*) > h''(\tau^*)$. It is then a simple matter to see, using the parameter groupings as shown in equations (3.20) and (3.21) that the delimiting curves, as functions of $\tau^*$, are parabolas that are concave upwards with increasingly narrow arms as we move from left to right

along the inequality (3.53). That is, the stability window of non-trivial equilibrium of the system subject to **B2** is smaller than that of the system subject to **B1**. In other words, the model with **B2** has a higher probability of undergoing oscillations, *via* bifurcation of the non-trivial equilibrium into a limit cycle (since it is easier for the non-trivial equilibrium of the model with **B2** to lose its stability than the case with **B1**), than the case when **B1** is used. Hence, the model with **B2** can be expected to induce more sustained oscillations than with **B1**. Consequently, the birth rate form of type **B2** is a more suitable candidate for the birth rate function for mosquitoes as the model solutions associated with it lead to more sustained oscillations (it is of ecological interest to have the vector dynamics persist).

## 3.5 Summary

A deterministic model for the population dynamics of the malaria vector was described in this chapter. The model in the absence of delay is rigorously analysed subject to two different birth functions (**B1** and **B2**). The main results of this chapter, which hold for each of the two birth rate functions, are as follows:

(i) the model, with any arbitrary birth function satisfying **A1** – **A3**, has a globally-asymptotically stable trivial equilibrium ($E_0$) whenever the vectorial reproduction threshold ($\mathcal{R}_0$) is less than unity;

(ii) for values of $\mathcal{R}_0 > 1$, the model can have a stable non-trivial equilibrium or a limit cycle (arising *via* a Hopf bifurcation);

(iii) it is shown that the Beverton-Holt birth function is a more suitable birth function for modelling vector dynamics than the Verhulst-Pearl logistic growth function, since the former generates more sustained oscillations (known to be a desirable ecological process) than the latter.

The main mathematical novelties presented in this chapter are:

(a) establishing the global asymptotic stability of the trivial equilibrium ($E_0$) subject to any birth rate function satisfying **A1**-**A3**;

(b) using a standard (and, arguably, simpler) method (direct application of the Hopf bifurcation theorem) to prove the presence of Hopf bifurcation in the model (3.17) subject to the birth rate functions **B1** and **B2**. Perturbation arguments were used to show these results in [109];

(c) expressing the associated bifurcation thresholds in terms of both the vectorial reproduction number ($\mathcal{R}_0$) and the birth constant ($B_0$);

(d) determining which of the two birth rate functions is more suitable for modelling vector dynamics, by way of providing an analysis of the size of the associated instability window.

| Variables and Parameters | Description |
|---|---|
| $U(t_1)$ | Population of fertilized, well-nourished with blood and reproducing female vectors |
| $V(t_1)$ | Population of fertilized female vectors that have laid eggs |
| $W(t_1)$ | Population of fertilized but non-reproducing female vectors questing for blood |
| $p$ | Probability of successfully taking a blood meal |
| $\tau$ | Contact rate between vectors of type $W$ and humans |
| $\mu$ | Natural death rate of adult vectors |
| $\mu_e$ | Natural death rate of vectors in earlier developmental stages |
| $H$ | Population density of humans at human habitat sites |
| $a$ | Rate of return of vectors to the vector breeding site |
| $b$ | Rate at which vectors of type $V$ visit human habitat sites |
| $K$ | Constant alternative food source for vectors |
| $B$ | Rate at which fertilized and fed vectors lay eggs |

Table 3.1: Description of variables and parameters of the model (3.9).

| Scaled Variables |
|---|
| $u(t) = \dfrac{U}{U_0}$ |
| $v(t) = \dfrac{V}{V_0}$ |
| $w(t) = \dfrac{W}{W_0}$ |
| $t = \dfrac{t_1}{T_0}$ |
| **Scaled Parameters** |
| $\alpha = \dfrac{aU_0T_0}{V_0}$ |
| $\rho = \dfrac{\frac{bH}{H+K} + \mu}{a+\mu}$ |
| $\gamma = \dfrac{\tau H + \mu}{a+\mu}$ |
| $\mu_s = \dfrac{\mu_e}{a+\mu}$ |
| $\mathcal{R}_0 = \dfrac{\alpha B_0}{\rho - \alpha}$ |

Table 3.2: Description of variables and parameters of the scaled model (3.17).

| Birth Rate Function Type | Threshold Condition | Region I: Trivial Equilibrium | Region II: Non-trivial Equilibrium | Region III: Limit Cycle |
|---|---|---|---|---|
| **B1** | | $(0,0,0)$ | $(1,1,1)(1-\frac{1}{\mathcal{R}_0})$ | |
| | $\mathcal{R}_0 \leq 1$ | GAS | DNE | DNE |
| | $1 < \mathcal{R}_0 < 1 + \frac{QR}{\gamma(\rho-\alpha)}$ | Unstable | LAS | DNE |
| | $\mathcal{R}_0 > 1 + \frac{QR}{\gamma(\rho-\alpha)}$ | Unstable | Unstable | Stable |
| **B2** | | $(0,0,0)$ | $(1,1,1)(\mathcal{R}_0-1)^{\frac{1}{n}}$ | |
| | $\mathcal{R}_0 \leq 1$ | GAS | DNE | DNE |
| | $1 < \mathcal{R}_0 < \frac{\gamma(\rho-\alpha)n}{\gamma(\rho-\alpha)n-QR}$, $n > \frac{QR}{\gamma(\rho-\alpha)}$ | Unstable | LAS | DNE |
| | $\mathcal{R}_0 > \frac{\gamma(\rho-\alpha)n}{\gamma(\rho-\alpha)n-QR}$, $n > \frac{QR}{\gamma(\rho-\alpha)}$ | Unstable | Unstable | Stable |

*DNE: does not exist.

Table 3.3: The stability properties of the model (3.17) in terms of $\mathcal{R}_0$ for the birth rate functions **B1** and **B2**.

| Birth Rate Function Type | Threshold Region in terms of $B_0$ | Region I: Trivial Equilibrium | Region II: Non-trivial Equilibrium | Region III: Limit Cycle |
|---|---|---|---|---|
| **B1** | | $(0,0,0)$ | $(1,1,1)(1-\frac{1}{\mathcal{R}_0})$ | |
| | $B_0 \leq \frac{\rho-\alpha}{\alpha}$ | GAS | DNE | DNE |
| | $\frac{\rho-\alpha}{\alpha} < B_0 < \frac{\rho-\alpha}{\alpha} + \frac{QR}{\alpha\gamma}$ | Unstable | LAS | DNE |
| | $B_0 > \frac{\rho-\alpha}{\alpha} + \frac{QR}{\alpha\gamma}$ | Unstable | Unstable | Stable |
| **B2** | | $(0,0,0)$ | $(1,1,1)(\mathcal{R}_0-1)^{\frac{1}{n}}$ | |
| | $B_0 \leq \frac{\rho-\alpha}{\alpha}$ | GAS | DNE | DNE |
| | $\frac{\rho-\alpha}{\alpha} < B_0 < \frac{\gamma(\rho-\alpha)^2 n}{\alpha(\gamma(\rho-\alpha)n-QR)}$, $n > \frac{QR}{\gamma(\rho-\alpha)}$ | Unstable | LAS | DNE |
| | $B_0 > \frac{\gamma(\rho-\alpha)^2 n}{\alpha(\gamma(\rho-\alpha)n-QR)}$, $n > \frac{QR}{\gamma(\rho-\alpha)}$ | Unstable | Unstable | Stable |

Table 3.4: The stability properties of the model (3.17) in terms of $B_0$ for the birth rate functions **B1** and **B2**.

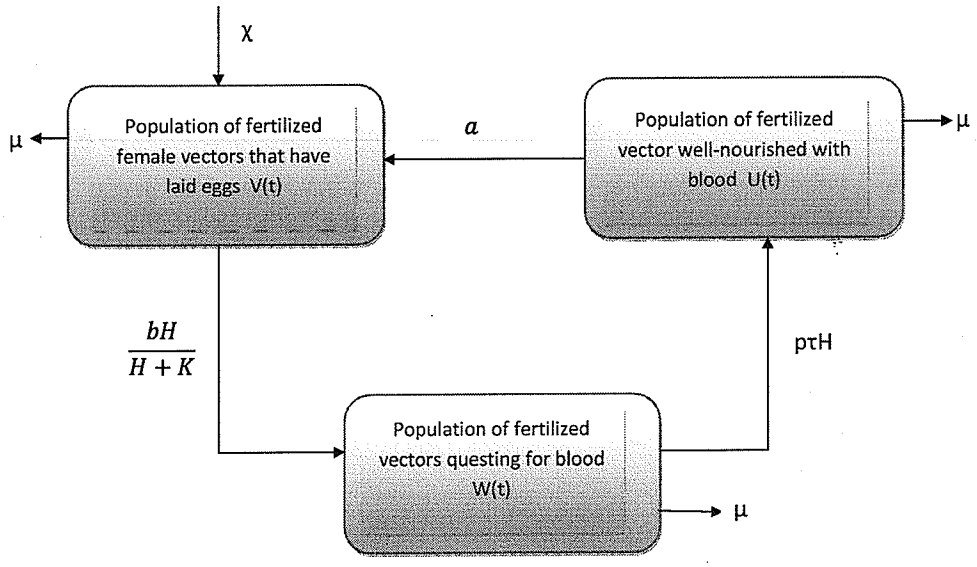


Figure 3.1: Schematic diagram of the model (3.9).

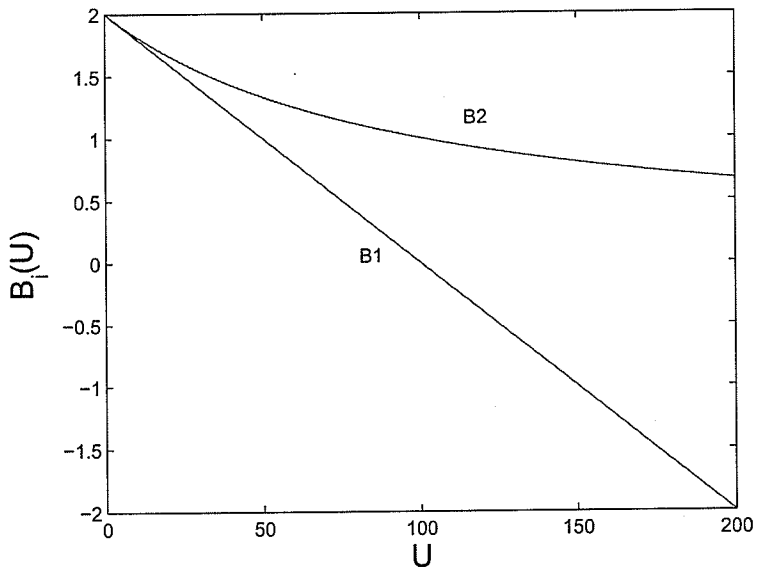


Figure 3.2: Graph of birth rate functions **B1** and **B2**. Parameter values used are: $B_0 = 2$, $L = 100$ and for **B2**, $n = 2$.

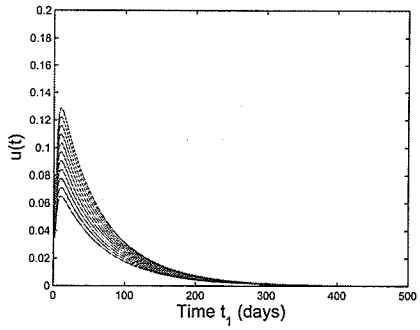


(a)

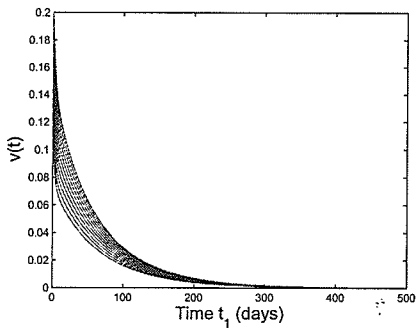


(b)

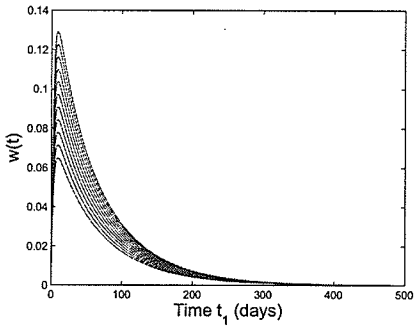


(c)

Figure 3.3: Simulations of the model (3.17), using Verhulst-Pearl logistic growth function **B1**, showing the state variables converging to the trivial equilibrium for $B_0 < \frac{\rho-\alpha}{\alpha}$. Parameter values used are: $a = 1$, $\mu = 0.042$, $B_0 = 1$, $\alpha = 0.0393$, $\rho = 0.0979$, and $\gamma = 0.2322$ (so that, $\mathcal{R}_0 = \frac{\alpha B_0}{\rho-\alpha} = 0.6701 < 1$).

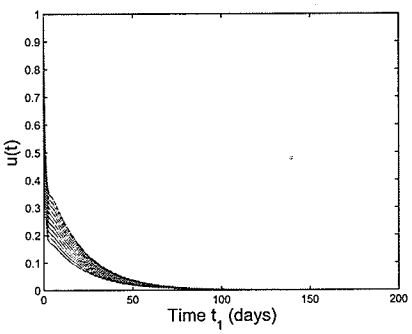


(a)

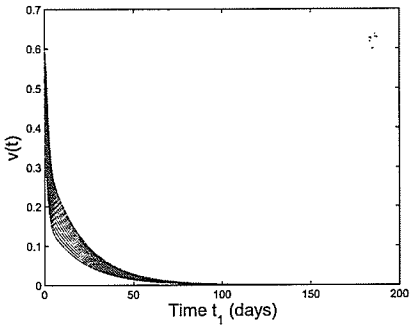


(b)

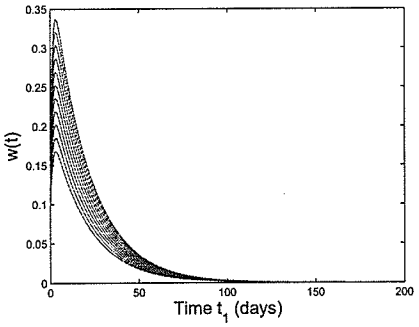


(c)

Figure 3.4: Simulations of the model (3.17), using Beverton-Holt function **B2**, showing the state variables converging to the trivial equilibrium for $B_0 < \frac{\rho-\alpha}{\alpha}$. Parameter values used are: $a = 1$, $\mu = 0.042$, $B_0 = 0.1$, $\alpha = 0.0393$, $\rho = 0.0979$, $\gamma = 0.2322$, and $n = 70$ (so that, $\mathcal{R}_0 = \frac{\alpha B_0}{\rho-\alpha} = 0.0670 < 1$).

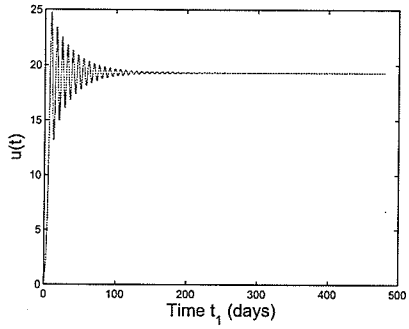


(a) $t-u$ plane

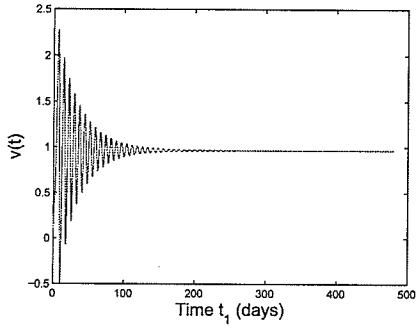


(b) $t-v$ plane

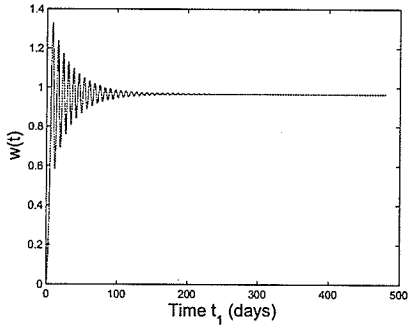


(c) $t-w$ plane

Figure 3.5: Simulations of the model (3.17), using Verhulst-Pearl logistic growth function **B1**, showing the time series of the state variables for $\frac{\rho-\alpha}{\alpha} < B_0 < \frac{\rho-\alpha}{\alpha} + \frac{QR}{\alpha\gamma}$. Parameter values used are $a = 1$, $\mu = 0.042$, $B_0 = 18$, $\alpha = 0.2618$, $\gamma = 0.2322$, and $\rho = 0.4242$ (so that, $1 < \mathcal{R}_0 = \frac{\alpha B_0}{\rho-\alpha} = 29.0319 < 1 + \frac{QR}{\gamma(\rho-\alpha)} = 34.1670$).

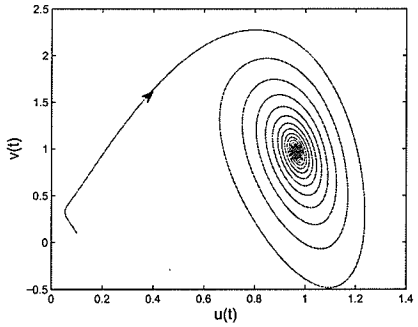


(a) $u - v$ plane

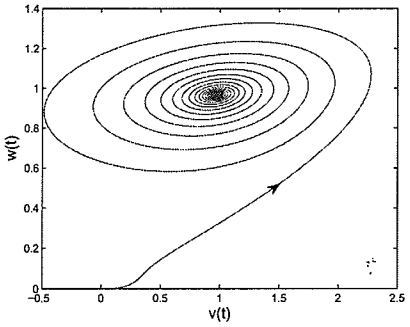


(b) $v - w$ plane

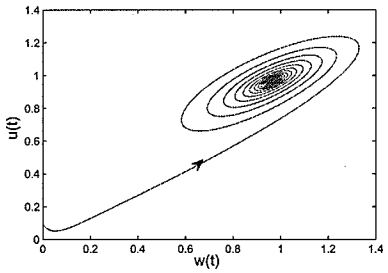


(c) $w - u$ plane

Figure 3.6: Simulations of the model (3.17), using Verhulst-Pearl logistic growth function **B1**, showing stable spiral for $\frac{\rho-\alpha}{\alpha} < B_0 < \frac{\rho-\alpha}{\alpha} + \frac{QR}{\alpha\gamma}$. Parameter values used are $a = 1$, $\mu = 0.042$, $B_0 = 18$, $\alpha = 0.2618$, $\gamma = 0.2322$, and $\rho = 0.4242$ (so that, $1 < \mathcal{R}_0 = \frac{\alpha B_0}{\rho-\alpha} = 29.0319 < 1 + \frac{QR}{\gamma(\rho-\alpha)} = 34.1670$).

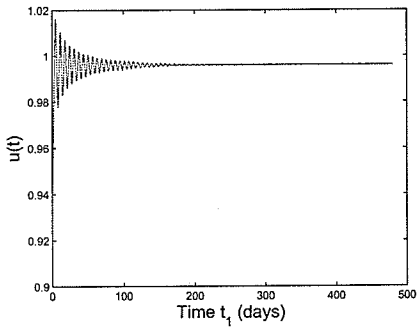


(a) $t-u$ plane

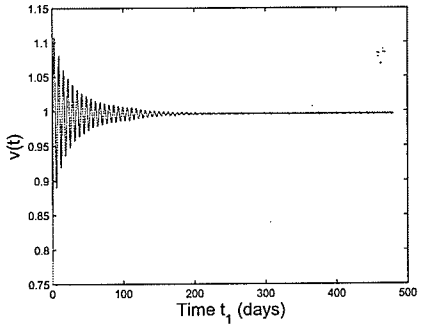


(b) $t-v$ plane

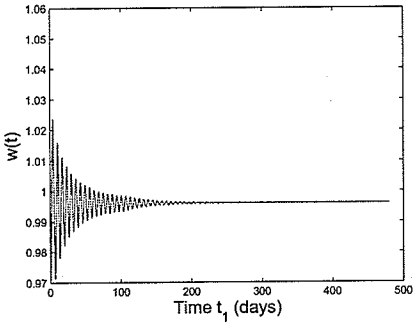


(c) $t-w$ plane

Figure 3.7: Simulations of the model (3.17), using Beverton-Holt function **B2**, showing the time series of the state variables for $\frac{\rho-\alpha}{\alpha} < B_0 < \frac{\gamma(\rho-\alpha)^2 n}{\alpha(\gamma(\rho-\alpha)n-QR)}$. Parameter values used are $a = 1,\ \mu = 0.042,\ B_0 = 1,\ \alpha = 0.3928,\ \gamma = 0.2322,$ and $\rho = 0.6161$ (so that, $1 < \mathcal{R}_0 = \frac{\alpha B_0}{\rho-\alpha} = 1.7584 < \frac{\gamma(\rho-\alpha)n}{\gamma(\rho-\alpha)n-QR} = 2.0189$).

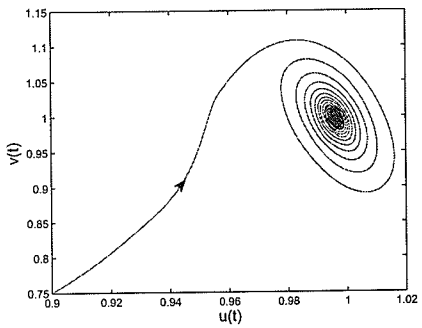


(a) $u - v$ plane

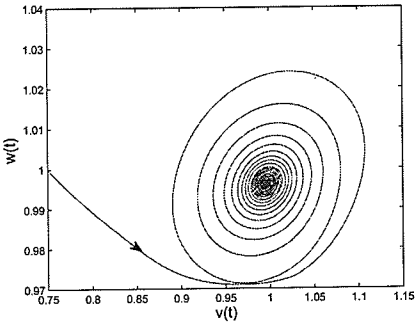


(b) $v - w$ plane

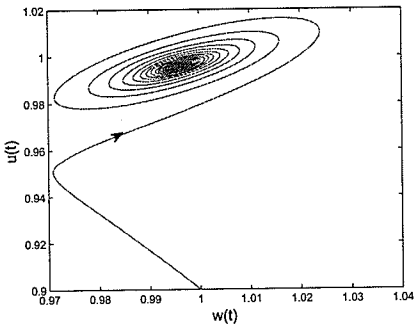


(c) $w - u$ plane

Figure 3.8: Simulations of the model (3.17), using Beverton-Holt function **B2**, showing stable spiral for $\frac{\rho-\alpha}{\alpha} < B_0 < \frac{\gamma(\rho-\alpha)^2 n}{\alpha(\gamma(\rho-\alpha)n-QR)}$. Parameter values used are $a = 1$, $\mu = 0.042$, $B_0 = 1$, $\alpha = 0.3928$, $\gamma = 0.2322$, and $\rho = 0.6161$ (so that, $1 < \mathcal{R}_0 = \frac{\alpha B_0}{\rho-\alpha} = 1.7584 < \frac{\gamma(\rho-\alpha)n}{\gamma(\rho-\alpha)n-QR} = 2.0189$).

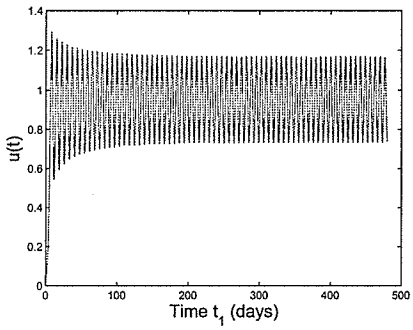


(a) $t-u$ plane

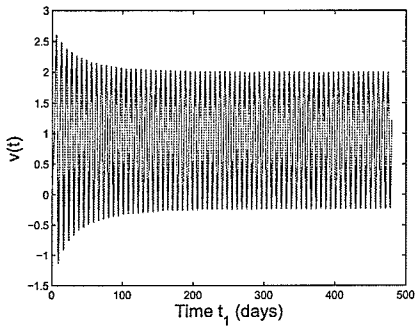


(b) $t-v$ plane

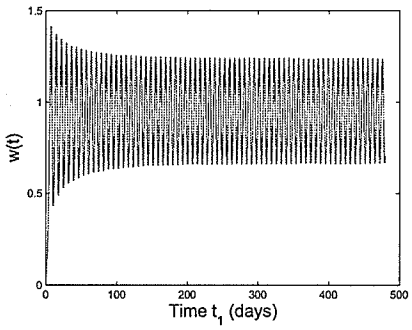


(c) $t-w$ plane

Figure 3.9: Simulations of the model (3.17), using Verhulst-Pearl logistic growth function **B1**, showing the time series of the state variables for $B_0 > \frac{\rho-\alpha}{\alpha} + \frac{QR}{\alpha\gamma}$. Parameter values used are $a = 1$, $\mu = 0.042$, $B_0 = 22$, $\alpha = 0.2618$, $\gamma = 0.2322$, and $\rho = 0.4242$ (so that, $1 < \mathcal{R}_0 = \frac{\alpha B_0}{\rho-\alpha} = 35.4835 > 1 + \frac{QR}{\gamma(\rho-\alpha)} = 34.1670$).

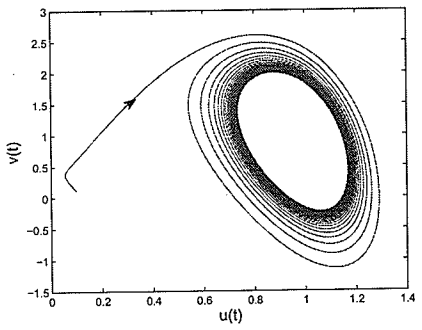


(a) $u - v$ plane

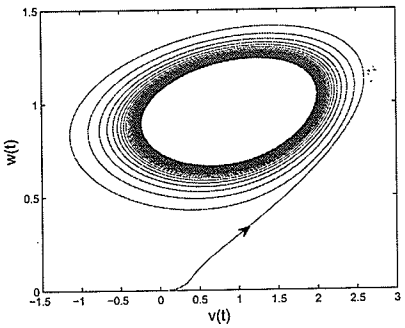


(b) $v - w$ plane

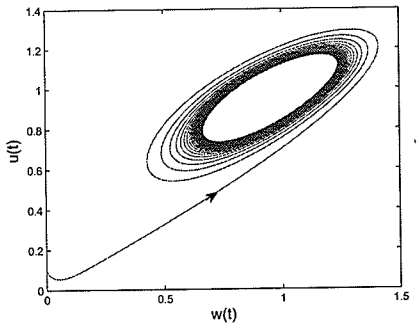


(c) $w - u$ plane

Figure 3.10: Simulations of the model (3.17), using Verhulst-Pearl logistic growth function **B1**, showing a stable limit cycle for $B_0 > \frac{\rho-\alpha}{\alpha} + \frac{QR}{\alpha\gamma}$. Parameter values used are $a = 1$, $\mu = 0.042$, $B_0 = 22$, $\alpha = 0.2618$, $\gamma = 0.2322$, and $\rho = 0.4242$ (so that, $1 < \mathcal{R}_0 = \frac{\alpha B_0}{\rho-\alpha} = 35.4835 > 1 + \frac{QR}{\gamma(\rho-\alpha)} = 34.1670$).

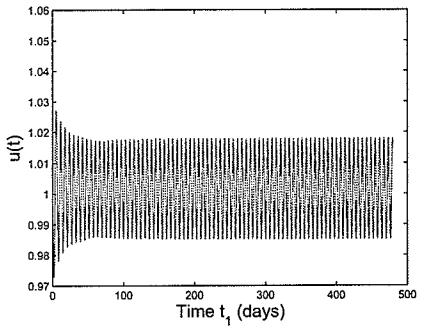


(a) $t-u$ plane

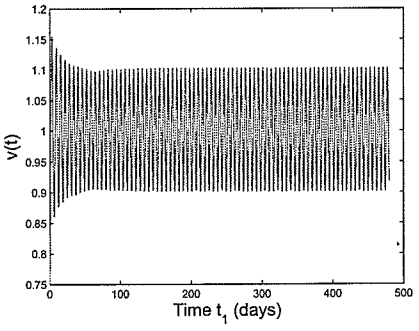


(b) $t-v$ plane

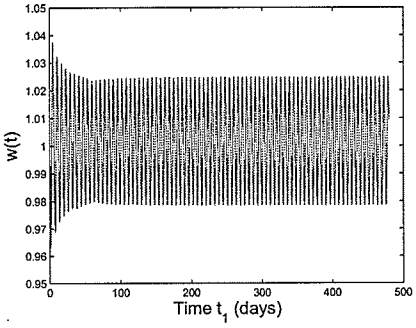


(c) $t-w$ plane

Figure 3.11: Simulations of the model (3.17), using Beverton-Holt function **B2**, showing the time series of the state variables for $B_0 > \frac{\rho-\alpha}{\alpha} + \frac{QR}{\alpha\gamma}$. Parameter values used are $a = 1,\ \mu = 0.042,\ B_0 = 1.2,\ \alpha = 0.3928,\ \gamma = 0.2322,\ \rho = 0.6161,$ and $n = 70$ (so that, $\mathcal{R}_0 = 2.1101 > \frac{\gamma(\rho-\alpha)n}{\gamma(\rho-\alpha)n-QR} = 2.0189$).

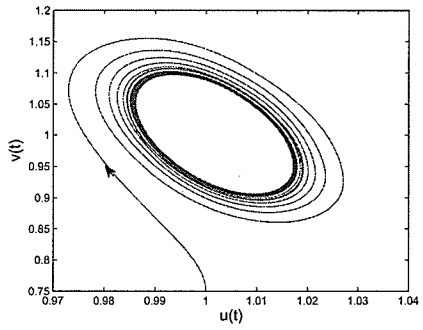


(a) $u - v$ plane

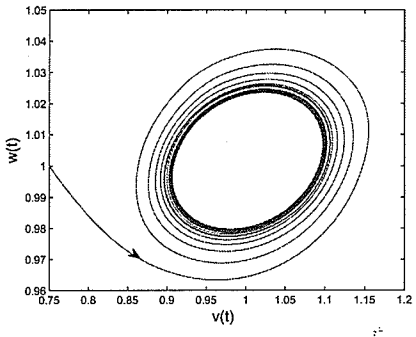


(b) $v - w$ plane

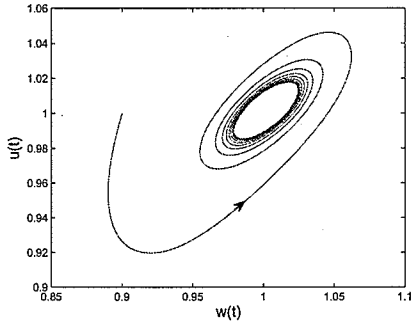


(c) $w - u$ plane

Figure 3.12: Simulations of the model (3.17), using Beverton-Holt function **B2**, showing stable limit cycle for $B_0 > \frac{\rho-\alpha}{\alpha} + \frac{QR}{\alpha\gamma}$. Parameter values used are $a = 1$, $\mu = 0.042$, $B_0 = 1.2$, $\alpha = 0.3928$, $\gamma = 0.2322$, $\rho = 0.6161$, and $n = 70$ (so that, $\mathcal{R}_0 = 2.1101 > \frac{\gamma(\rho-\alpha)n}{\gamma(\rho-\alpha)n-QR} = 2.0189$).

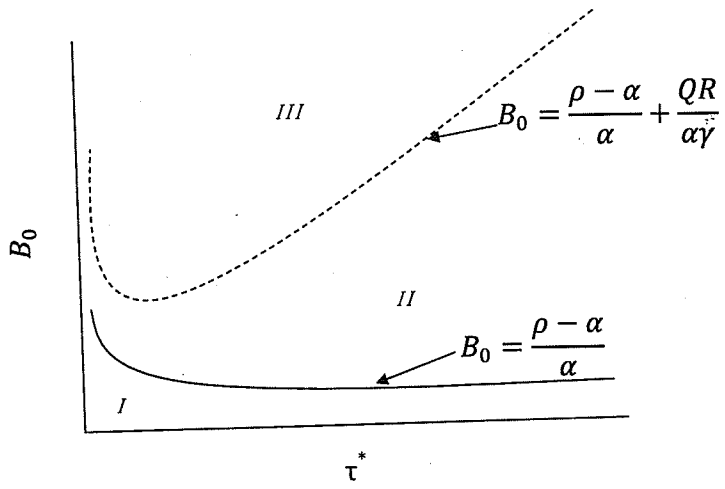


Figure 3.13: Diagram showing the different stability regions in parameter space of the model (3.17). Parameter values used are: $a = 1$, $b^* = 0.06$, $\mu = 0.042$, $p = 0.86$, and $L = 20$.

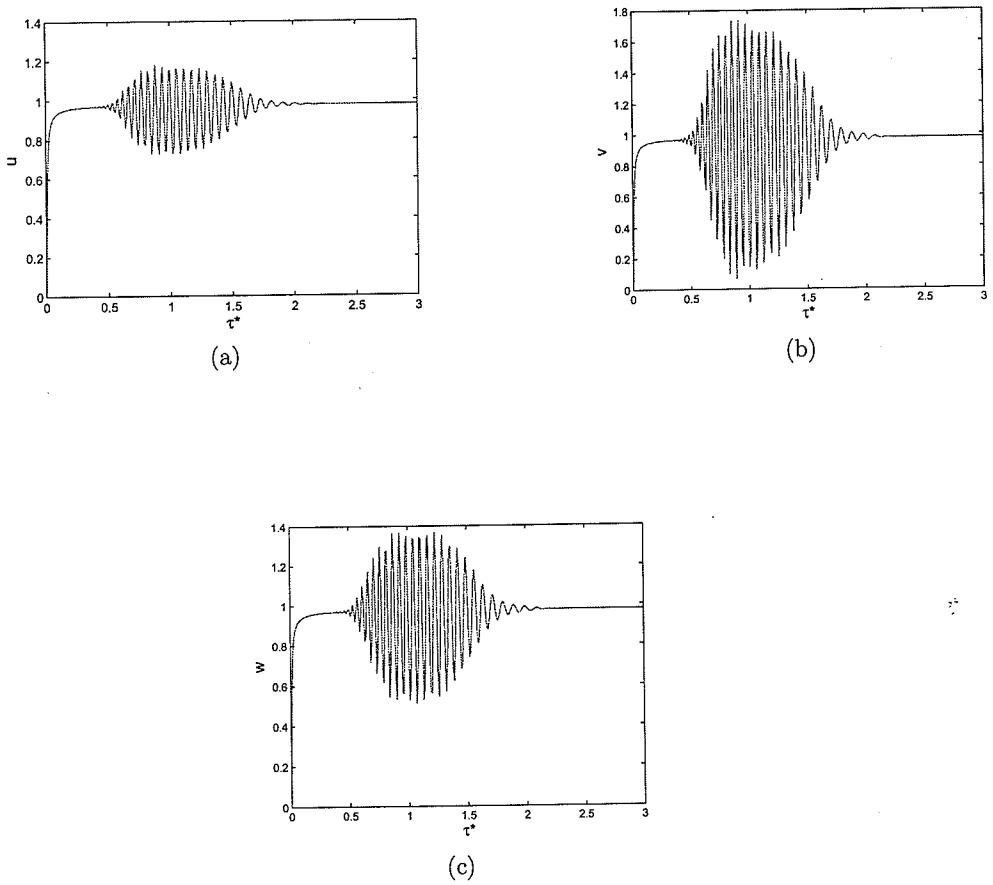


Figure 3.14: Simulations of the model (3.17). The bundle of long-term solutions for a fixed value of $B_0$ as a function of $\tau^*$. Parameter values used are: $a = 1$, $b^* = 0.06$, $\mu = 0.042$, $p = 0.86$, $L = 20$, and $B_0 = 13$.

# Chapter 4

# Analysis of Vector Dynamics Model with Time Delay

## 4.1 Introduction

In this chapter, the vector population model (3.9) with discrete time delay ($T > 0$), given below,

$$\begin{aligned}
\frac{dU}{dt_1} &= p\tau HW - (a+\mu)U, \\
\frac{dV}{dt_1} &= aB(U(t_1-T))U(t_1-T)e^{-\mu_e T} + aU - \left(\mu + \frac{bH}{H+K}\right)V, \\
\frac{dW}{dt_1} &= \left(\frac{bH}{H+K}\right)V - (\mu+\tau H)W,
\end{aligned} \tag{4.1}$$

will be rigorously analysed subject to the associated initial data,

$$(U(t_1), V(t_1), W(t_1)) = (u_0(t_1), v_0(t_1), w_0(t_1)), \;\; t_1 \in [-T, 0], \tag{4.2}$$

where, $u_0(t_1)$, $v_0(t_1)$ and $w_0(t_1)$ are continuously-differentiable functions on the interval $[-T, 0]$. The system above will be considered subject to birth functions satisfying **A1** – **A3** (given in Chapter 3). The basic features of the model (4.1), subject to (4.2), will now be discussed.

## 4.2 Basic Properties

### 4.2.1 Existence and uniqueness of solutions

Let,

$$C = \{\phi : [-T, 0] \to \mathbb{R}^3_+\}$$

be the Banach space of continuous functions mapping the interval $[-T, 0]$ into $\mathbb{R}^3_+$ with the topology of uniform convergence. That is, for $\phi \in C$, the norm of $\phi$ is defined as $\|\phi\| = \sup_{\theta\in[-T,0]} |\phi(\theta)|$, where $|.|$ is the norm in $\mathbb{R}^3$. The system (4.1) can be written as

$$\dot{X}(t_1) = f(t_1, X_{t_1}).$$

Since $f$ is continuously differentiable, it is Lipschitzian (Lemma 2.1). An alternative proof of the Lipschitzian property of $f$ is given in Appendix A.

As $f$ is continuous and Lipschitzian, it follows from Theorem 2.10 that the delay differential equation system (4.1) has a unique solution through the given initial data (4.2).

### 4.2.2 Positivity of solutions

Suppose there exists a $t_2 > 0$ such that $U(t_2) = 0$, $U'(t_2) \leq 0$ and

$$U(t_1) > 0, \quad V(t_1) > 0, \quad W(t_1) > 0 \quad \text{for} \quad 0 < t_1 < t_2.$$

Then,

$$\frac{dU}{dt_1}(t_2) = p\tau HW(t_2) - (a+\mu)U(t_2) = p\tau HW(t_2) > 0,$$

which contradicts the assumption that $U'(t_2) \leq 0$. Hence, no such $t_2$ exists. Furthermore, suppose there exists a $t_3 > 0$ such that $V(t_3) = 0$, $V'(t_3) \leq 0$ and

$$U(t_1) > 0, \quad V(t_1) > 0, \quad W(t_1) > 0 \quad \text{for} \quad 0 < t_1 < t_3.$$

It follows that

$$\frac{dV}{dt_1}(t_3) = aB(U(t_3 - T))U(t_3 - T)e^{-\mu_e T} + aU(t_3) - \left(\mu + \frac{bH}{H+K}\right)V(t_3) > 0,$$

contradicting the fact that $V'(t_3) \leq 0$. A similar argument can be made for $W(t_1)$. Hence, it can be concluded that starting the system (4.1) with non-negative initial data in $\mathbb{R}^3_+$ will generate non-negative solutions for all $t_1 > 0$.

### 4.2.3 Uniform boundedness of solutions

To show the uniform boundedness of the solutions of the system (4.1), consider the equation for the rate of change of the total vector population, given by

$$\frac{dN_v(t_1)}{dt_1} = aB(U(t_1 - T))U(t_1 - T)e^{-\mu_e T} - (1-p)\tau HW(t_1) - \mu N_v(t_1), \quad t_1 > 0, \tag{4.3}$$

with initial data,

$$N_v(t_1) = u_0(t_1) + v_0(t_1) + w_0(t_1), \quad t_1 \in [-T, 0].$$

It follows from (4.3) that

$$\frac{dN_v}{dt_1} \leq aB_0 N_v(t_1 - T)e^{-\mu_e T} - \mu N_v(t_1); \quad \text{by Assumption } \mathbf{A3}. \tag{4.4}$$

Consider, now, the delay differential equation (obtained by using equality in (4.4))

$$\begin{aligned} \frac{dN_v}{dt_1} &= aB_0 N_v(t_1 - T)e^{-\mu_e T} - \mu N_v(t_1), \\ \phi_0(t_1) &= N_v(t_1) = u_0(t_1) + v_0(t_1) + w_0(t_1), \quad t_1 \in [-T, 0], \end{aligned} \tag{4.5}$$

where the initial data $\phi_0(t_1)$ is assumed to be positive, continuous and bounded on $[-T, 0]$. The solution will be constructed using the *method of steps* [56]. The delay differential equation (4.5) can be considered as a non-delayed IVP on the interval $[0, T]$

given by (note that $\phi_0(t_1 - T)$ is known from (4.5))

$$\begin{aligned} \frac{dN_v}{dt_1} &= aB_0\phi_0(t_1 - T)e^{-\mu_e T} - \mu N_v(t_1), \\ N_v(0) &= \phi_0, \quad t_1 \in [0, T]. \end{aligned} \tag{4.6}$$

The solution to the IVP (4.6) is

$$\phi_1(t_1) = \phi_0(0)e^{-\mu t_1} + e^{-\mu t_1}\int_0^{t_1} e^{\mu s} aB_0\phi_0(s - T)e^{-\mu_e T} ds, \quad t_1 \in [0, T]. \tag{4.7}$$

It follows from (4.7) that the solution $\phi_1(t_1)$ is bounded, since $\phi_0(t_1)$ is bounded. Using the principle of mathematical induction, the boundedness of solutions of (4.1) will be proved for all $t_1 \geq 0$. To do so, let (the induction step)

$$\phi_k(t_1) = \phi_{k-1}((k-1)T)e^{-\mu t_1} + e^{-\mu t_1}\int_{(k-1)T}^{t_1} e^{\mu s} aB_0\phi_{k-1}(s-T)e^{-\mu_e T} ds, \quad t_1 \in [(k-1)T, kT] \tag{4.8}$$

be bounded for some $k \in \mathbb{Z}_+$. The goal is to show that $\phi_{k+1}(t_1)$ is also bounded.

The solution $\phi_{k+1}(t_1)$ is given by

$$\phi_{k+1}(t_1) = \phi_k(kT)e^{-\mu t_1} + e^{-\mu t_1}\int_{kT}^{t_1} e^{\mu s} aB_0\phi_K(s-T)e^{-\mu_e T} ds, \quad t_1 \in [kT, (k+1)T]. \tag{4.9}$$

Since $\phi_k(t_1)$ is bounded, it follows from (4.9) that $\phi_{k+1}(t_1)$ is also bounded. Thus, by mathematical induction, the total vector population $N_v(t_1)$ is bounded for all $t_1 \geq 0$.

Let $\phi_0(0) \leq \bar{N}_v$, for some $\bar{N}_v > 0$. Then it follows from (4.7) that

$$\phi_1(t_1) \leq \bar{N}_v e^{-\mu t_1} + e^{-\mu t_1} \int_0^{t_1} e^{\mu s} a B_0 \bar{N}_v e^{-\mu_e T} ds, \quad t_1 \in [0, T],$$

$$= \bar{N}_v e^{-\mu t_1} + a B_0 \bar{N}_v e^{-\mu t_1} e^{-\mu_e T} \left( \frac{e^{\mu t_1} - 1}{\mu} \right),$$

$$\leq \bar{N}_v e^{-\mu T} + a B_0 \bar{N}_v e^{-\mu T} e^{-\mu_e T} \left( \frac{e^{\mu T} - 1}{\mu} \right), \quad \text{for} \quad t_1 \in [0, T],$$

$$= \left[ e^{-\mu T} + e^{-\mu_e T} (1 - e^{-\mu T}) \frac{a B_0}{\mu} \right] \bar{N}_v.$$

Further, it is easy to see that

$$e^{-\mu T} + e^{-\mu_e T} (1 - e^{-\mu T}) \frac{a B_0}{\mu} < 1 \quad \text{if} \quad \mu - a B_0 > 0.$$

Proceeding in time steps of length $T$, it can be shown that $N_v(t_1)$ is uniformly-bounded by $\bar{N}_v$ for all $t_1 \geq 0$ if $\mu - a B_0 > 0$. Thus, the components $U(t_1)$, $V(t_1)$ are $W(t_1)$ are uniformly-bounded for all $t_1 \geq 0$ if $\mu - a B_0 > 0$. This result is summarized below:

**Theorem 4.1.** *The solutions of the system* (4.1) *are uniformly-bounded if* $\mu - a B_0 > 0$.

It is worth recalling that the condition $\mu - a B_0 > 0$ was also needed for the boundedness of the solutions of the non-delayed system (Lemma 3.2).

As in [109], the scaled system of delay differential equations will be used for mathematical convenience (where all the parameters are as defined in Section 3.2.4). It is

given below.

$$\begin{aligned}
\frac{du}{dt} &= w(t) - u(t), \\
\frac{dv}{dt} &= \alpha B(Lu(t-T))u(t-T)e^{-\mu_s T} + \alpha u(t) - \rho v(t), \\
\frac{dw}{dt} &= \gamma[v(t) - w(t)],
\end{aligned} \tag{4.10}$$

with initial data,

$$(u(t), v(t), w(t)) = (u_0(t), v_0(t), w_0(t)), \quad t \in [-T, 0], \tag{4.11}$$

where, $u_0(t)$, $v_0(t)$ and $w_0(t)$ are continuously-differentiable functions on the interval $[-T, 0]$, and the function $B(u)$ is given by

$$B(u) = \begin{cases} B_0(1-u);\ 0 < u \leq 1; & \text{Type } \mathbf{B1}, \\ \dfrac{B_0}{1+u^n}; & \text{Type } \mathbf{B2}. \end{cases} \tag{4.12}$$

Furthermore, the scaled parameters $\alpha$, $\rho$, $\gamma$ and $\mu_s$ are, respectively, given by:

$$\alpha = \frac{aU_0T_0}{V_0}, \quad \rho = \frac{\frac{bH}{H+K} + \mu}{a+\mu}, \quad \gamma = \frac{\tau H + \mu}{a+\mu}, \quad \mu_s = \frac{\mu_e}{a+\mu}. \tag{4.13}$$

It should be recalled that the birth rate function $B(u)$ is defined as follows:

**Definition 4.1.** *A function $B : [0, \infty) \to \mathbb{R}$ is a suitable birth rate function for the vector if it satisfies the following three conditions (where prime represents a derivative with respect to $u$):*

***A1:*** $B(u) > 0,\ \forall\ u \geq 0$;

***A2:*** *$B(u)$ is continuously-differentiable with $B'(u) < 0,\ \forall\ u \geq 0$;*

***A3:*** *There exists a positive number, called the vectorial basic reproduction number (denoted by $\mathcal{R}_{0d}$), such that $B(\infty) < \frac{B(0+)}{\mathcal{R}_{0d}} < B(0+) = B_0$.*

## 4.3 Existence and Stability of Equilibria

The system (4.10) has a trivial equilibrium, denoted by $E_0 = (u^*, v^*, w^*) = (0, 0, 0)$, which exists for all parameter regimes. Let $E_1 = (u^{**}, v^{**}, w^{**})$ be any non-trivial equilibrium of the system (4.10). Setting the right-hand sides of the equations in the system (4.10) to zero, and solving the resulting system at the non-trivial equilibrium $E_1$, gives

$$\begin{aligned} w^{**} &= v^{**} = u^{**}, \\ \alpha u^{**}[B(u^{**})e^{-\mu_s T} + 1] &= \rho v^{**}. \end{aligned} \tag{4.14}$$

It follows from the second equation of (4.14) that

$$B(u^{**})e^{-\mu_s T} + 1 = \frac{\rho}{\alpha},$$

so that

$$B(u^{**}) = \frac{\rho - \alpha}{\alpha e^{-\mu_s T}}. \tag{4.15}$$

Using the expression for the birth rate function **B1** given in (4.12) into (4.15) gives

$$B_0(1-u^{**}) = \frac{\rho-\alpha}{\alpha e^{-\mu_s T}}.$$

Hence,

$$u^{**} = 1 - \frac{\rho-\alpha}{\alpha B_0 e^{-\mu_s T}}. \tag{4.16}$$

It follows from (4.16) that $u^{**} > 0$ if and only if (note that $\rho - \alpha > 0$ as shown in Section 3.2.4)

$$\mathcal{R}_{0d} = \frac{\alpha B_0 e^{-\mu_s T}}{\rho-\alpha} > 1. \tag{4.17}$$

In other words, the *vectorial reproduction number* for the vector population model (4.10) with time delay is given by $\mathcal{R}_{0d}$ (note that $\mathcal{R}_{0d}$ reduces to $\mathcal{R}_0$, given in Section 3.3.1, if $T = 0$). The term $e^{-\mu_s T}$ in $\mathcal{R}_{0d}$ accounts for the survival to death for the $T$ time units that the cohort is supposed to spend before *eclosion*. It can be shown, in a similar manner, that the $\mathcal{R}_{0d}$ expression remains the same if the birth rate function **B2** is used in (4.15).

### 4.3.1 Local asymptotic stability of the trivial equilibrium

The local asymptotic stability property of the equilibrium $E_0$ is determined by linearizing the system (4.10) around $E_0$. It is convenient to write the following perturbation

equations,

$$\begin{aligned} u(t) &= u^* + \hat{u}(t), \\ v(t) &= v^* + \hat{v}(t), \\ w(t) &= w^* + \hat{w}(t), \end{aligned} \tag{4.18}$$

where, $\hat{u}(t)$, $\hat{v}(t)$, and $\hat{w}(t)$ are small positive perturbations from $u^*$, $v^*$ and $w^*$ respectively.

Substituting (4.18) into the right-hand sides of the equations in (4.10) and expanding in a Taylor series about $(u^*, v^*, w^*)$ (and retaining only the first-order terms in $\hat{u}(t)$, $\hat{v}(t)$ and $\hat{w}(t)$) gives the following linear approximation (where the symbol prime denotes differentiation with respect to $t$).

$$\begin{aligned} \hat{u}'(t) &= \hat{w}(t) - \hat{u}(t), \\ \hat{v}'(t) &= \alpha\Psi(u^*)e^{-\mu_s T}\hat{u}(t-T) + \alpha\hat{u}(t) - \rho\hat{v}(t), \\ \hat{w}'(t) &= \gamma[\hat{v}(t) - \hat{w}(t)]. \end{aligned} \tag{4.19}$$

Next, we seek solutions for the perturbed system (4.19) of the form

$$\hat{v}(t) = c_v e^{\lambda t}, \quad \hat{w}(t) = c_w e^{\lambda t}, \quad \hat{u}(t) = c_u e^{\lambda t}, \tag{4.20}$$

where, $c_v$, $c_w$, $c_u$ are constants which determine the eigenvectors that span the null space of the linearized system, and $\lambda$ is the eigenvalue that measures the time evolutionary growth of a linear solution of the form (4.20).

Substituting (4.20) into (4.19), and simplifying, shows that, for trivial solutions, we must have

$$|J_0 + e^{-\lambda T} J_T - \lambda I| = 0, \tag{4.21}$$

where, $J_0$ is the Jacobian with respect to $\mathbf{U}(t) = (u(t), v(t), w(t))$ evaluated at the trivial equilibrium $E_0$, $J_T$ is the Jacobian with respect to $\mathbf{U}(t-T) = (u(t-T), v(t-T), w(t-T))$ evaluated at $E_0$ and $I$ is the identity matrix of order 3.

Thus, equation (4.21) can be expressed as

$$\begin{vmatrix} -(\lambda+1) & 0 & 1 \\ \alpha\Psi(u^*)e^{-(\mu_s+\lambda)T} + \alpha & -(\lambda+\rho) & 0 \\ 0 & \gamma & -(\lambda+\gamma) \end{vmatrix} = 0, \tag{4.22}$$

where, $\Psi(u^*) = B(u^*) + B'(u^*)u^*$. The associated characteristic equation of (4.22) is

$$G(\lambda) := \lambda^3 + Q\lambda^2 + R\lambda + P = A\Psi(u^*)e^{-(\mu_s+\lambda)T}, \tag{4.23}$$

with, $Q = 1 + \gamma + \rho$, $R = \gamma + \rho + \rho\gamma$, $P = \gamma(\rho - \alpha)$ and $A = \alpha\gamma$.

Using $\Psi(u^*) = B_0$ (since $u^* = 0$ at $E_0$) in (4.23), and simplifying, gives

$$G(\lambda) = \lambda^3 + Q\lambda^2 + R\lambda + P(1 - \mathcal{R}_{0d}e^{-\lambda T}) = 0, \tag{4.24}$$

from which it follows that all the roots of $G(\lambda)$, with $T = 0$, have negative real parts

whenever $\mathcal{R}_{0d} < 1$. Hence, by Rouché's Theorem [34] and the continuity in $T$, the transcendental equation (4.24) has roots with positive real parts if and only if it has purely imaginary roots.

Assume that there exist $T_c > 0$ and $\omega_c > 0$ such that $\lambda = i\omega$, where $\omega > 0$ is a root of (4.24). Thus, substituting $\lambda = i\omega$ in (4.24) gives

$$-i\omega^3 - Q\omega^2 + i\omega R + P = P\mathcal{R}_{0d}e^{-i\omega T}. \tag{4.25}$$

Separating the real and imaginary parts of (4.25) gives

$$\begin{aligned} -Q\omega^2 + P &= P\mathcal{R}_{0d}\cos\omega T, \\ -\omega^3 + R\omega &= -P\mathcal{R}_{0d}\sin\omega T. \end{aligned} \tag{4.26}$$

Squaring and adding the two equations in (4.26) gives

$$\omega^6 + (Q^2 - 2R)\omega^4 + (R^2 - 2PQ)\omega^2 + P^2[1 - (\mathcal{R}_{0d})^2] = 0. \tag{4.27}$$

Let $z = \omega^2$. Hence, equation (4.27) becomes

$$z^3 + (Q^2 - 2R)z^2 + (R^2 - 2PQ)z + P^2[1 - (\mathcal{R}_{0d})^2] = 0. \tag{4.28}$$

The coefficients of the cubic (4.28) are all positive (for $\mathcal{R}_{0d} < 1$), since

$$\begin{aligned} Q^2 - 2R &= (1+\gamma+\rho)^2 - 2(\gamma+\rho+\rho\gamma) > 0, \\ R^2 - 2PQ &= (\gamma+\rho+\rho\gamma)^2 - 2\gamma(\rho-\alpha)(1+\gamma+\rho) > 0, \end{aligned} \tag{4.29}$$

and,

$$P^2[1-(\mathcal{R}_{0d})^2] > 0 \quad \text{for} \quad \mathcal{R}_{0d} < 1.$$

Thus, the cubic (4.28) has no positive real root. That is, the characteristic equation (4.24) has no purely imaginary roots. Therefore, the real parts of all the eigenvalues of (4.24) are negative for all $T \geq 0$. Hence, the following result is established.

**Lemma 4.1.** *The trivial equilibrium of the system* (4.10)*, denoted by* $E_0$*, is LAS for all* $T \geq 0$ *whenever* $\mathcal{R}_{0d} < 1$.

The above local stability result of the trivial equilibrium ($E_0$) means that if the initial vector population is in the basin of attraction of the trivial equilibrium, then the vector population can be eradicated provided $\mathcal{R}_{0d} < 1$. To ensure that such eradication is independent of the initial population of the vector, a global asymptotic stability result must be established for the trivial equilibrium.

### 4.3.2 Global stability of the trivial equilibrium

As the solutions of the non-scaled model (4.1) are uniformly bounded, the solutions of scaled model (4.10) are also uniformly bounded. We claim the following.

**Theorem 4.2.** *The trivial equilibrium, $E_0$, of the model* (4.10) *is GAS in* $\mathbb{R}^3_+$ *whenever* $\mathcal{R}_{0d} < 1$.

*Proof.* To prove the global asymptotic stability of the trivial equilibrium of the delayed system (4.10), the system is expressed in terms of integral equations as follows:

$$\begin{aligned} u(t) &= \int_{-\infty}^{t} w(\theta)e^{-(t-\theta)}d\theta, \\ v(t) &= \int_{-\infty}^{t} [\alpha B(u(\theta - T))u(\theta - T)e^{-\mu_s T} + \alpha u(\theta)]e^{-\rho(t-\theta)}d\theta, \\ w(t) &= \int_{-\infty}^{t} \gamma v(\theta)e^{-\gamma(t-\theta)}d\theta. \end{aligned} \tag{4.30}$$

Using the substitution $x = t - \theta$, taking the lim sup of the first equation of (4.30) and applying the fact that $\limsup \int f \leq \int \limsup f$ [80] (and noting that the solutions to (4.30) are uniformly-bounded as shown in Theorem 4.1), gives

$$\begin{aligned} \limsup_{t\to\infty} u(t) &= \limsup_{t\to\infty} \int_0^{\infty} w(t-x)e^{-x}dx, \\ &\leq \int_0^{\infty} \limsup_{t\to\infty} w(t-x)e^{-x}dx, \\ &\leq \limsup_{t\to\infty} w(t) \int_0^{\infty} e^{-x}dx, \\ &\leq \limsup_{t\to\infty} w(t). \end{aligned} \tag{4.31}$$

Similarly, for the third equation of the system (4.30), we have

$$\begin{aligned}
\limsup_{t\to\infty} w(t) &= \limsup_{t\to\infty} \int_0^\infty \gamma v(t-x)e^{-\gamma x}dx, \\
&\leq \int_0^\infty \limsup_{t\to\infty} \gamma v(t-x)e^{-\gamma x}dx, \\
&\leq \limsup_{t\to\infty} \gamma v(t) \int_0^\infty e^{-\gamma x}dx, \\
&= \limsup_{t\to\infty} v(t).
\end{aligned} \tag{4.32}$$

The last equality holds because $\int_0^\infty \gamma e^{-\gamma x}dx = 1$, since the latter is the integral of the probability distribution function of an exponentially-distributed random variable. Taking the lim sup of the second equation of (4.30) gives

$$\limsup_{t\to\infty} v(t) = \limsup_{t\to\infty} \int_0^\infty [\alpha B(u(t-x-T))u(t-x-T)e^{-\mu_s T} + \alpha u(t-x)]e^{-\rho x}dx,$$

$$\leq \int_0^\infty \limsup_{t\to\infty} [\alpha B(u(t-x-T))u(t-x-T)e^{-\mu_s T} + \alpha u(t-x)]e^{-\rho x}dx,$$

$$\leq \int_0^\infty \limsup_{t\to\infty} [\alpha B(u(t-x))u(t-x)e^{-\mu_s T} + \alpha u(t-x)]e^{-\rho x}dx, \tag{4.33}$$

$$\leq \limsup_{t\to\infty} \alpha B(u(t))u(t)e^{-\mu_s T} \int_0^\infty e^{-\rho x}dx + \limsup_{t\to\infty} \alpha u(t) \int_0^\infty e^{-\rho x}dx,$$

$$\leq \frac{\alpha e^{-\mu_s T}}{\rho} \limsup_{t\to\infty} B(u(t)) \limsup_{t\to\infty} u(t) + \frac{\alpha}{\rho} \limsup_{t\to\infty} u(t).$$

It follows from (4.31), (4.32) and (4.33) that

$$\begin{aligned}
\limsup_{t\to\infty} u(t) &\leq \frac{\alpha e^{-\mu_s T}}{\rho} \limsup_{t\to\infty} B(u(t)) \limsup_{t\to\infty} u(t) + \frac{\alpha}{\rho} \limsup_{t\to\infty} u(t), \\
&\leq \frac{\alpha e^{-\mu_s T}}{\rho} B_0 \limsup_{t\to\infty} u(t) + \frac{\alpha}{\rho} \limsup_{t\to\infty} u(t), \text{ by Assumption } \mathbf{A3}, \\
&\leq \left[\frac{\alpha e^{-\mu_s T}}{\rho} B_0 + \frac{\alpha}{\rho}\right] \limsup_{t\to\infty} u(t), \\
0 &\leq \frac{\rho - \alpha}{\rho}(\mathcal{R}_{0d} - 1) \limsup_{t\to\infty} u(t).
\end{aligned} \tag{4.34}$$

This implies that $\limsup_{t\to\infty} u(t) \leq 0$ whenever $\mathcal{R}_{0d} < 1$. Since $\limsup_{t\to\infty} u(t) \geq 0$, it follows that $\limsup_{t\to\infty} u(t) = 0$. Using this fact in (4.31) and (4.32) also leads to the conclusion that $\limsup_{t\to\infty} v(t) = 0$ and $\limsup_{t\to\infty} w(t) = 0$ whenever $\mathcal{R}_{0d} < 1$. Hence, $E_0$ is GAS whenever $\mathcal{R}_{0d} < 1$. □

The result of Theorem 4.2 is illustrated numerically, by simulating the model (4.10) with appropriate parameter values so that $\mathcal{R}_{0d} < 1$, using the Verhulst-Pearl logistic growth function (Figure 4.1) and the Beverton-Holt function (Figure 4.2). It is evident from the numerical simulations that for both birth functions, all the solution profiles of the model (4.10) converge to the trivial equilibrium whenever $\mathcal{R}_{0d} < 1$, (i.e., the model has the same qualitative dynamics, using any of the two birth functions, for the case when $\mathcal{R}_{0d} < 1$). It is worth stating that such (global stability) result was not proven in [109].

### 4.3.3 Existence and local stability of a non-trivial equilibrium

#### Existence

The system (4.10) has a unique non-trivial equilibrium given by

$$E_1 = (u^{**}, v^{**}, w^{**}) = (1, 1, 1)u^{**},$$

where,

$$u^{**}(T) = B^{-1}\left(\frac{B_0}{\mathcal{R}_{0d}}\right).$$

It should be recalled that Assumptions **A1-A3** (on the birth function $B(u)$) assure the existence of $u^{**}(T)$ whenever $\mathcal{R}_{0d} > 1$.

#### Local stability

To prove the stability of the non-trivial equilibrium ($E_1$) of the system (4.10), the following results by Song *et al.* [129] will be used.

**Lemma 4.2.** (Song *et al.* [129]). *Consider the transcendental equation*

$$\lambda^3 + m_2\lambda^2 + m_1\lambda + m_0 + (n_2\lambda^2 + n_1\lambda + n_0)e^{-\lambda\tau} = 0, \tag{4.35}$$

*where* $m_i, n_i \in \mathbb{R}$ $(i = 0, 1, 2)$ *and* $\sum_{i=0}^{2} n_i^2 \neq 0$. *Further, consider the polynomial equation*

$$z^3 + pz^2 + qz + r = 0, \tag{4.36}$$

*where*

$$p = m_2^2 - 2m_1 - n_2^2,$$

$$q = m_1^2 - 2m_0m_2 + 2n_0n_2 - n_1^2,$$

$$r = m_0^2 - n_0^2.$$

*(i) If* $r < 0$, *then* (4.36) *has at least one positive root;*

*(ii) If* $r \geq 0$ *and* $\triangle = p^2 - 3q \leq 0$, *then* (4.36) *has no positive roots;*

*(iii) If* $r \geq 0$ *and* $\triangle = p^2 - 3q > 0$, *then* (4.36) *has positive roots if and only if* $z_1^* = \frac{-p+\sqrt{\triangle}}{3}$ *and* $h(z_1^*) \leq 0$, *where* $h(z) = z^3 + pz^2 + qz + r$.

**Lemma 4.3.** (Song *et al.* [129]). *For the transcendental equation* (4.35)

*(i) If* $r \geq 0$ *and* $\triangle = p^2 - 3q \leq 0$, *then all roots with positive real parts of* (4.35) *has the same sum as those of the polynomial equation* (4.36) *for all* $\tau$;

*(ii) If* $r < 0$ *or* $r \geq 0$ *and* $\triangle = p^2 - 3q > 0$, $z_1^* = \frac{-p+\sqrt{\triangle}}{3} > 0$ *and* $h(z_1^*) \leq 0$ *then all roots with positive real parts of* (4.35) *has the same sum as those of the polynomial equation* (4.36) *for all* $\tau \in [0, \tau_0)$.

As in the case of the stability of the trivial equilibrium $E_0$, characterizing the local asymptotic stability of $E_1$ entails solving the equation

$$|J_0 + e^{-\lambda T} J_T - \lambda I| = 0, \tag{4.37}$$

where, now, $J_0$ is the Jacobian with respect to $\mathbf{U}(t) = (u(t), v(t), w(t))$ evaluated at

the non-trivial equilibrium $E_1$ and $J_T$ is the Jacobian with respect to $\mathbf{U}(t-T) = (u(t-T), v(t-T), w(t-T))$ evaluated at $E_1$. It is easy to show that equation (4.37) can be expressed as

$$\begin{vmatrix} -(\lambda+1) & 0 & 1 \\ \alpha\Psi(u^{**})e^{-(\mu_s+\lambda)T} + \alpha & -(\lambda+\rho) & 0 \\ 0 & \gamma & -(\lambda+\gamma) \end{vmatrix} = 0, \tag{4.38}$$

which has the following characteristic equation

$$(\lambda+1)(\lambda+\rho)(\lambda+\gamma) - [\Psi(u^{**})e^{-(\mu_s+\lambda)T} + 1]\alpha\gamma = 0. \tag{4.39}$$

Equation (4.39) may be written in expanded form as

$$\lambda^3 + Q\lambda^2 + R\lambda + P = AS(T)e^{-(\mu_s+\lambda)T}, \tag{4.40}$$

where

$$S(T) = \Psi(u^{**}(T)) = B(u^{**}(T)) + B'(u^{**}(T))u^{**}(T). \tag{4.41}$$

It should be recalled that the non-trivial equilibrium ($E_1$) takes the form (as shown in

Chapter 3)

$$E_1 = (1,1,1)\left(1 - \frac{1}{\mathcal{R}_{0d}}\right), \quad \text{For } \mathbf{B1},$$

$$E_1 = (1,1,1)(\mathcal{R}_{0d} - 1)^{\frac{1}{n}}, \quad \text{For } \mathbf{B2}.$$

For the two types of birth rate functions, the term $AS(T)e^{-\mu_s T}$ can be written, for $u^{**}(T) \neq 0$, as follows.

(i) **B1**:

$$\begin{aligned}
&A[B(u^{**}) + B'(u^{**})u^{**}]e^{-\mu_s T} \\
&= A[B_0(1-u^{**}) - B_0 u^{**}]e^{-\mu_s T}, \\
&= AB_0(1-2u^{**})e^{-\mu_s T}, \\
&= AB_0\left[1 - 2\left(1 - \frac{1}{\mathcal{R}_{0d}}\right)\right]e^{-\mu_s T}, \\
&= \frac{AB_0}{\mathcal{R}_{0d}}(2 - \mathcal{R}_{0d})e^{-\mu_s T}, \\
&= P(2 - \mathcal{R}_{0d}).
\end{aligned} \tag{4.42}$$

(ii) **B2**:

$$
\begin{aligned}
&A[B(u^{**}) + B'(u^{**})u^{**}]e^{-\mu_s T} \\
&= A\left[\frac{B_0}{1+(u^{**})^n} - \frac{B_0 n (u^{**})^{(n-1)}}{[1+(u^{**})^n]^2}u^{**}\right]e^{-\mu_s T}, \\
&= A\left\{\frac{B_0}{1+(\mathcal{R}_{0d}-1)^{n/n}} - \frac{B_0 n (\mathcal{R}_{0d}-1)^{\frac{n-1}{n}}}{[1+(\mathcal{R}_{0d}-1)^{n/n}]^2}(\mathcal{R}_{0d}-1)^{1/n}\right\}e^{-\mu_s T}, \\
&= AB_0\left[\frac{1}{\mathcal{R}_{0d}} - \frac{n(\mathcal{R}_{0d}-1)}{\mathcal{R}_{0d}^2}\right]e^{-\mu_s T}, \\
&= \frac{AB_0}{\mathcal{R}_{0d}}\left[1 - \frac{n(\mathcal{R}_{0d}-1)}{\mathcal{R}_{0d}}\right]e^{-\mu_s T}, \\
&= P\left[1 - \frac{n(\mathcal{R}_{0d}-1)}{\mathcal{R}_{0d}}\right].
\end{aligned}
\tag{4.43}
$$

Thus, it follows, using (4.41), (4.42) and (4.43), that

$$
AS(T)e^{-\mu_s T} = \begin{cases} P[2 - \mathcal{R}_{0d}(T)] & \text{for } \mathbf{B1}, \\ P\left[1 - n\frac{\mathcal{R}_{0d}(T)-1}{\mathcal{R}_{0d}(T)}\right] & \text{for } \mathbf{B2}. \end{cases} \tag{4.44}
$$

On the other hand, for $u^{**}(T) = 0$, it can be shown that, for each of the two birth functions,

$$
AS(T)e^{-\mu_s T} = P\mathcal{R}_{0d}(T). \tag{4.45}
$$

Equation (4.44) shows that, for each form of the birth rate function, as $\mathcal{R}_{0d}(T)$ increases from unity, $AS(T)e^{-\mu_s T}$ decreases and can change sign from positive to negative. We claim the following result.

**Theorem 4.3.** *The positive equilibrium, $E_1$, of the system* (4.10) *is conditionally-stable*

*if and only if all the roots of the characteristic equation* (4.40) *have negative real parts at* $T = 0$ *and there exists some positive value* $T$ *such that the characteristic equation* (4.40) *has a pair of purely imaginary roots* $\pm i\omega_c$.

*Proof.* It should be recalled that all the roots of the characteristic equation (4.40) have negative real parts when $T = 0$ (Theorem 3 of Section 3.3.3). The next task is to show that the characteristic equation (4.40) has a unique pair of purely imaginary roots $\pm i\omega$, with $\omega > 0$. Assume that for some $T > 0$ and $\omega > 0$, the quantity $i\omega$ is a root of the characteristic equation (4.40). Then, substituting $i\omega$ into (4.40) gives

$$(i\omega)^3 + Q(i\omega)^2 + R(i\omega) + P = AS(T)e^{-(\mu_s + i\omega)T}, \tag{4.46}$$

where, $Q$, $R$, $P$ and $A$ are as defined in Section 4.3.1. Equation (4.46) can be re-written as

$$-i\omega^3 - Q\omega^2 + Ri\omega + P = AS(T)e^{-\mu_s T}(\cos\omega T - i\sin\omega T). \tag{4.47}$$

Separating the real and imaginary parts of (4.47) gives

$$-Q\omega^2 + P = AS(T)e^{-\mu_s T}\cos\omega T, \tag{4.48}$$

$$-\omega^3 + R\omega = -AS(T)e^{-\mu_s T}\sin\omega T. \tag{4.49}$$

Squaring and adding the equations in (4.48) and (4.49) gives

$$(-Q\omega^2 + P)^2 + (-\omega^3 + R\omega)^2 = A^2S^2(T)e^{-2\mu_s T}, \tag{4.50}$$

which is equivalent to

$$\omega^6 + c_1\omega^4 + c_2\omega^2 + c_3 = 0. \tag{4.51}$$

Setting $\omega^2 = z$ in (4.51) gives

$$z^3 + c_1 z^2 + c_2 z + c_3 = 0, \tag{4.52}$$

where

$$\begin{aligned} c_1 &= Q^2 - 2R = (1+\gamma+\rho)^2 - 2(\gamma+\rho+\rho\gamma) > 0, \\ c_2 &= R^2 - 2PQ = (\gamma+\rho+\rho\gamma)^2 - 2\gamma(\rho-\alpha)(1+\gamma+\rho) > 0, \\ c_3 &= P^2 - A^2S^2(T)e^{-2\mu_s T}. \end{aligned} \tag{4.53}$$

Clearly, the coefficient $c_3$ is negative if

$$P^2 < A^2S^2(T)e^{-2\mu_s T}. \tag{4.54}$$

It then follows from Lemma 4.2 that there exists a unique positive root, $\omega_c$, satisfying (4.52). That is, the characteristic equation (4.40) has a pair of purely imaginary roots of the form $\pm i\omega_c$, with $\omega_c > 0$.

Dividing equation (4.49) by equation (4.48) gives

$$\tan(\omega_c T_c) = \frac{\omega_c(\omega_c^2 - R)}{P - Q\omega_c^2},\ \omega_c > 0. \tag{4.55}$$

Then, the quantities $\omega_c$ and $T_c$ can be obtained by solving equations (4.52) and (4.55) simultaneously. It follows from (4.55) that

$$T_c = \frac{1}{\omega_c}\tan^{-1}\left(\frac{\omega_c(\omega_c^2 - R)}{P - Q\omega_c^2}\right),\ \omega_c > 0. \tag{4.56}$$

□

Theorem 4.3 can be written in the following (simpler) form:

**Theorem 4.4.** *If $P^2 < A^2S^2(T)e^{-2\mu_s T}$, then the non-trivial equilibrium, $E_1$, of the system* (4.10)*, is conditionally-stable.*

Further, for the value of $T_c$, given in (4.56), equation (4.50) becomes

$$AS(T_c)e^{-\mu_s T_c} \ = \ \pm\sqrt{(P - Q\omega_c^2)^2 + (R\omega_c - \omega_c^3)^2}. \tag{4.57}$$

Note that the sign of the square root must be chosen such that $\omega_c$ has a positive value. Observe that the left-hand side of (4.57) has been completely characterized in terms of $\mathcal{R}_{0d}$, for any of the two forms of the birth rate function, by equations (4.44) and (4.45).

It is worth stating that, for the two birth rate functions **B1** and **B2**, the condition

(4.54) takes the following forms:

(i) For **B1**:

$$AS(T)e^{-\mu_s T} = P[2 - \mathcal{R}_{0d}(T)].$$

Thus,

$$c_3 < 0 \Rightarrow P^2\{1 - [2 - \mathcal{R}_{0d}(T)]^2\} < 0,$$

so that

$$\mathcal{R}_{0d} > 3. \tag{4.58}$$

(ii) For **B2**:

$$AS(T)e^{-\mu_s T} = P\left[1 - n\frac{\mathcal{R}_{0d}(T) - 1}{\mathcal{R}_{0d}(T)}\right].$$

Hence,

$$c_3 < 0 \Rightarrow P^2\left\{1 - \left[1 - n\frac{\mathcal{R}_{0d}(T) - 1}{\mathcal{R}_{0d}(T)}\right]^2\right\} < 0,$$

so that

$$n\left(1 - \frac{1}{\mathcal{R}_{0d}}\right) > 2,$$

or, equivalently,

$$\mathcal{R}_{0d} > \frac{n}{n-2},\ n > 2. \tag{4.59}$$

**Lemma 4.4.** *A realistic value for $T_c$, as given by equation* (4.56)*, exists only for values*

*of* $\omega_c$ *such that* $\sqrt{\frac{P}{Q}} \leq \omega_c \leq \sqrt{R}$.

*Proof.* A value of $T_c$ must be non-negative (to be ecologically-realistic). Observe that

$$\frac{P}{Q} = \frac{\gamma(\rho - \alpha)}{1 + \rho + \gamma} < \rho - \alpha < \rho + \gamma + \rho\gamma = R.$$

Therefore,

$$\sqrt{P/Q} < \sqrt{R}.$$

It is easy to see from (4.56) that

$$T_c(\omega_c) < 0 \text{ for } 0 < \omega_c < \sqrt{P/Q}, \text{ or } \omega_c > \sqrt{R}.$$

The threshold $T_c$, as a function of $\omega_c$, is continuous at each $\omega_c \in (0, \infty)$ except at $\omega_c = \sqrt{P/Q}$, where it has a jump discontinuity of size

$$T_c((\sqrt{P/Q})^+) - T_c((\sqrt{P/Q})^-) = \pi\sqrt{Q/P}.$$

Hence, there exists a unique point $\omega_c = \omega_c^* = \sqrt{R}$, where $T_c(\omega_c^*) = 0$.

Finally,

$$\lim_{\omega_c \to \infty} T_c(\omega_c) = 0^- = 0.$$

Therefore, the only ecologically-acceptable set of $\omega_c$ values, where non-negative values for $T_c$ can exist, is given by

$$\sqrt{P/Q} \leq \omega_c \leq \sqrt{R}.$$

□

We claim the following.

**Lemma 4.5.** *The largest possible value of $T_c$ for which periodic solutions can be observed is in the set $\{T_{c,k} = \sqrt{Q/P}(\frac{\pi}{2} + k\pi), k = 0, \pm 1, \pm 2, \pm 3, \cdots\}$ with corresponding wave number $\omega_c = \sqrt{P/Q}$. Also, the smallest possible value of $T_c$ for which the periodic solutions can be observed is in the set $\{T_{c,k} = k\pi/\sqrt{R}, k = 0, \pm 1, \pm 2, \cdots\}$, corresponding to the wave number $\omega_c = \sqrt{R}$. In this second case, when $k = 0$, $T_c = T_{c,0} = 0$ and $\omega_c = \sqrt{R}$ coinciding with the wave number from the Hopf Bifurcation derived in without delay ($T = 0$) case.*

*Proof.* The threshold $T_c$, as a function of $\omega_c$ given by (4.56), is monotone decreasing for $\omega \in [\sqrt{P/Q}, \sqrt{R}]$ with $\lim_{\omega_c \to (\sqrt{P/Q})^+} T_c(\omega_c) = \frac{\pi}{2}\sqrt{Q/P}$.

If $\omega_c = \sqrt{P/Q}$, then from the equation (4.48), either $\cos(\omega_c T_c) = 0$ or $AS(T_c)e^{-\mu_s T_c} = 0$. But $AS(T_c)e^{-\mu_s T_c} \neq 0$, since if it is zero, the equation (4.49) is not satisfied for all parameters. Thus,

$$\cos(\omega_c T_c) = 0 \Rightarrow \omega_c T_c = \frac{\pi}{2} + k\pi, \ k = 0, \pm 1, \pm 2, \cdots,$$

from which a set of possible $T_c$ values can be obtained. Then $\sin(\omega_c T_c) = (-1)^k$ and we have, the relation

$$\sqrt{\frac{P}{Q}}\left(R - \frac{P}{Q}\right) = (-1)^{k+1} S(T_c) A e^{-\mu_s T_c}, \ k = 0, \pm 1, \pm 2, \cdots, \tag{4.60}$$

which now contains only the one unknown $B_0$ to be determined.

Similarly, if $\omega_c = \sqrt{R}$, then from the equation (4.49), either $\sin(\omega_c T_c) = 0$ or $AS(T_c)e^{-\mu_s T_c} = 0$. But $AS(T_c)e^{-\mu_s T_c} \neq 0$, since if it is zero, equation (4.48) will not be satisfied for all parameters. Thus,

$$\sin(\omega_c T_c) = 0 \Rightarrow \omega_c T_c = k\pi,\ k = 0, \pm 1, \pm 2, \cdots,$$

from which a set of possible $T_c$ values can be obtained as postulated. Then

$$\cos(\omega_c T_c) = (-1)^k,$$

and

$$P - QR = (-1)^k S(T_c) A e^{-\mu_s T_c},\ k = 0, \pm 1, \pm 2, \cdots \tag{4.61}$$

□

### 4.3.4 Hopf bifurcation

The technique in [131] (see also [22, 28, 41]) will be used in this section to establish the presence of Hopf bifurcation in (4.10) subject to the two birth functions **B1** and **B2**.

### Verhulst-Pearl logistic growth function (B1)

We claim the following:

**Theorem 4.5.** *The non-trivial equilibrium $E_1$ of the system* (4.10) *with birth function* ***B1*** *is conditionally-stable when $T < T_c$, and unstable when $T > T_c$, where*

$$T_c = \frac{1}{\omega_c} \tan^{-1}\left(\frac{\omega_c(\omega_c^2 - R)}{P - Q\omega_c^2}\right), \ \omega_c > 0.$$

*When $T = T_c$, a Hopf bifurcation occurs (i.e., a family of periodic solutions bifurcates from $E_1$ as $T$ passes through the critical value $T_c$).*

*Proof.* The non-trivial equilibrium, $E_1$, is conditionally-stable for $0 < T < T_c$ (Theorem 4.3). Further, the characteristic equation (4.40) has a pair of purely imaginary eigenvalues at $T = T_c$. Now the transversality condition is shown by proving the following Lemma:

**Lemma 4.6.** *Consider the model* (4.10) *subject to the Verhulst-Pearl logistic growth function* ***B1****. The transversality condition* $\left\{\frac{d(\mathrm{Re}\lambda)}{dT}\right\}_{T=T_c} > 0$ *if the following inequalities hold.*

$$R - 3\omega_c^2 + T_c(P - Q\omega_c^2) > 0,$$

$$\frac{\omega_c(P - Q\omega_c^2)(2 - \mathcal{R}_{0d})}{\mathcal{R}_{0d}\mu_s\omega_c(R - \omega_c^2)} > 1. \tag{4.62}$$

The proof of Lemma 4.6 is given in Appendix B.

Hence, by Theorem 4.3 and Lemma 4.6, a Hopf bifurcation occurs at $T = T_c$. □

The result of Theorem 4.5 is illustrated numerically by simulating the model (4.10) subject to **B1** with appropriate parameter values as depicted in Figures 4.3 and 4.4 (it is worth stating that the corresponding values of $\omega_c$ and $T_c$ are obtained by solving equations (4.52) and (4.55) simultaneously using Newton's method for a system of nonlinear equations).

### Beverton-Holt function (B2)

Consider the model (4.10) subject to the Beverton-Holt birth function **B2**. We claim the following.

**Theorem 4.6.** *The non-trivial equilibrium, $E_1$, of the system* (4.10) *with birth function* ***B2****, is conditionally-stable when $T < T_c$, and unstable when $T > T_c$, where*

$$T_c = \frac{1}{\omega_c} \tan^{-1}\left(\frac{\omega_c(\omega_c^2 - R)}{P - Q\omega_c^2}\right), \ \omega_c > 0.$$

*When $T = T_c$, a Hopf bifurcation occurs (i.e., a family of periodic solution bifurcates from $E_1$ as $T$ passes through the critical value $T_c$).*

*Proof.* By Theorem 4.3, the non-trivial equilibrium, $E_1$, is conditionally-stable for $0 < T < T_c$. Here, too, the characteristic equation (4.40) has a pair of purely imaginary eigenvalues at $T = T_c$. The transversality condition is shown as follows:

**Lemma 4.7.** *The transversality condition* $\left\{\frac{d(\mathrm{Re}\lambda)}{dT}\right\}_{T=T_c} > 0$ *for the birth function*

***B2*** *if the following condition holds.*

$$\frac{F_1}{F_2} < 1, \tag{4.63}$$

*where*

$$F_1 = n\mu_s T_c(P - Q\omega_c^2)^2 + n\mu_s T_c\omega_c^2(R - \omega_c^2)^2 + 2Qn\mu_s\omega_c^2(R - \omega_c^2)$$
$$- 3\omega_c^2\{n\mu_s(P - Q\omega_c^2) + \omega_c^2(R - \omega_c^2)[\mathcal{R}_{0d}(1 - n) + n]\},$$

*and*

$$F_2 = \omega_c^2[\mathcal{R}_{0d}(1 - n) + n][2Q(P - Q\omega_c^2) - R(R - \omega_c^2)] - n\mu_s R(P - Q\omega_c^2).$$

The proof of Lemma 4.7 is given in Appendix C.

Hence, it follows from Theorem 4.3 and Lemma 4.7 that a Hopf bifurcation occurs at $T = T_c$. □

The result of Theorem 4.6 is illustrated by simulating the model (4.10) with appropriate parameter values as depicted in Figures 4.5 and 4.6. Further numerical simulations were carried out for different values of $T > T_c$ showing an increase in the amplitude of the oscillation with the increasing values of $T$ (Figures 4.7 and 4.8). Thus, the larger the chosen $T$ value is from the critical value $T_c$, the larger the resulting amplitude of oscillation. Hence, the use of time delay contributes in sustaining vector dynamics (by way of increasing sustained oscillation for values of $T > T_c$).

## 4.4 Summary

A deterministic model, with discrete delay, for the vector population dynamics of malaria is analysed. The following results, which hold for any of the two birth rate functions, are shown.

(i) the system, with any arbitrary birth function satisfying $\mathbf{A1}-\mathbf{A3}$, has a globally-asymptotically stable trivial equilibrium ($E_0$) whenever the vectorial reproduction number ($\mathcal{R}_{0d}$) is less than unity;

(ii) for the case when the vectorial threshold ($\mathcal{R}_{0d}$) exceeds unity, the system can have a stable non-trivial equilibrium or a limit cycle (which arises *via* a Hopf bifurcation);

(iii) the amplitude of oscillation increases with increasing values of $T > T_c$;

(iv) the use of time delay in modelling vector population dynamics contributes in sustaining vector dynamics.

Some of the main novel contributions of this chapter are as follows:

(a) establishing the well-posedness of the delayed system (4.1);

(b) establishing the global asymptotic stability of the trivial equilibrium ($E_0$) subject to any birth rate function satisfying **A1-A3**;

(c) proving the existence of Hopf bifurcation, for each of the two birth rate functions (**B1** and **B2**), using Hopf bifurcation theorem.

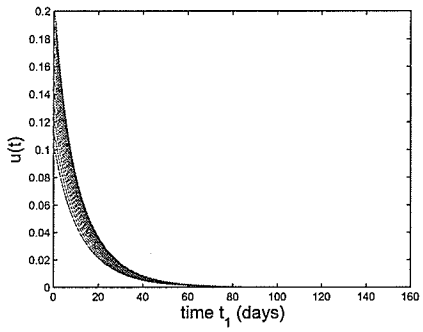


(a)

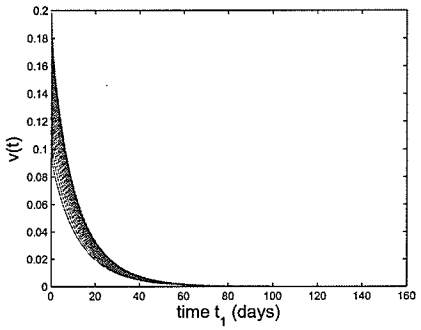


(b)

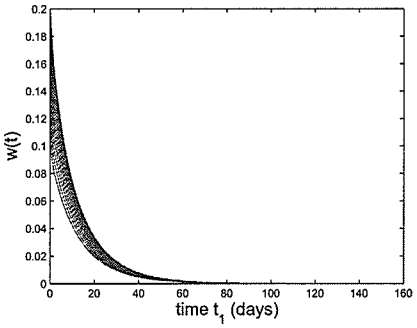


(c)

Figure 4.1: Simulations of the model (4.10), using the Verhulst-Pearl logistic growth function **B1**, showing the state variables converging to the trivial equilibrium. Parameter values used are: $a = 1$, $\mu = 0.042$, $B_0 = 1.07$, $\alpha = 0.33$, $\gamma = 3.88$, $\rho = 0.81$, $\mu_s = 0.07$, and $T = 1.3$ (so that, $\mathcal{R}_{0d} = 0.6716 < 1$).

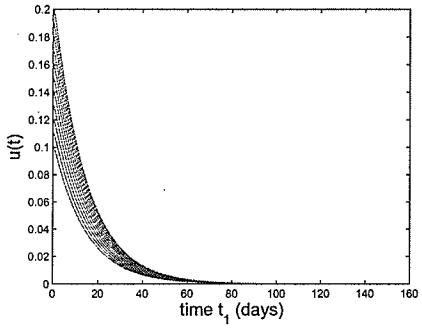


(a)

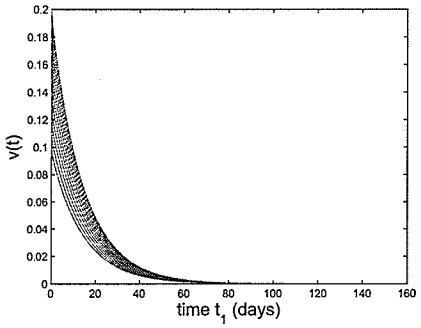


(b)

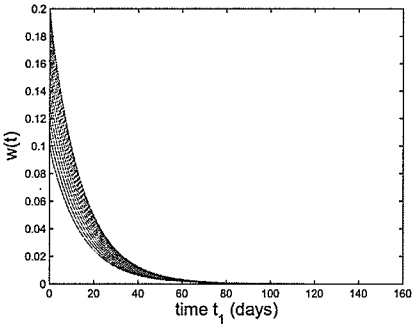


(c)

Figure 4.2: Simulations of the model (4.10), using the Beverton-Holt function **B2**, showing the state variables converging to the trivial equilibrium. Parameter values used are: $a = 1$, $\mu = 0.042$, $B_0 = 1.07$, $\alpha = 0.33$, $\gamma = 3.88$, $\rho = 0.81$, $\mu_s = 0.07$, $n = 30$, and $T = 0.3$ (so that, $\mathcal{R}_{0d} = 0.7203 < 1$).

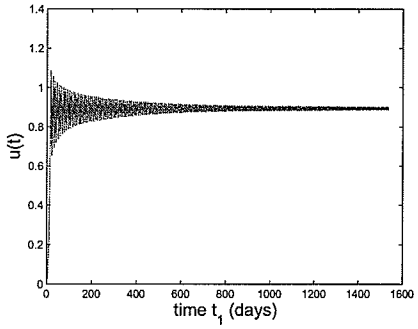


(a) $t-u$ plane

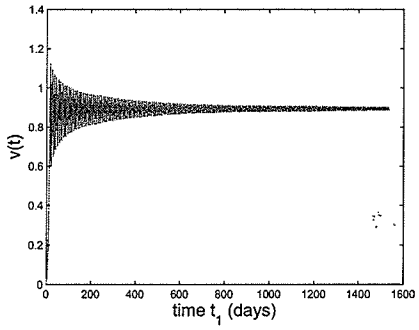


(b) $t-v$ plane

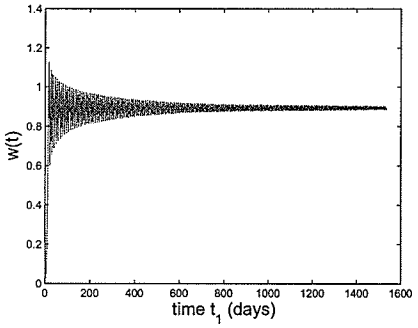


(c) $t-w$ plane

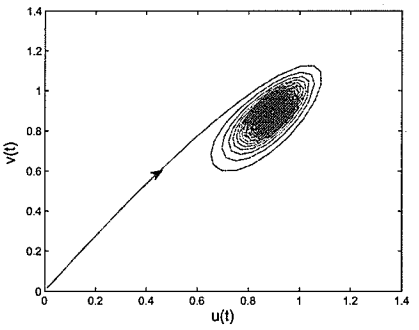


(d) a stable spiral

Figure 4.3: Simulations of the model (4.10), using the Verhulst-Pearl logistic growth function **B1**, showing the time series of the state variables for $T = 1.84 < T_c = 1.8502$ converging to a stable spiral. Parameter values used are: $a = 1$, $\mu = 0.042$, $B_0 = 3.07$, $\alpha = 0.63$, $\gamma = 3.88$, $\rho = 0.81$, and $\mu_s = 0.07$ (so that, $1 < \mathcal{R}_{0d} = 9.4465$).

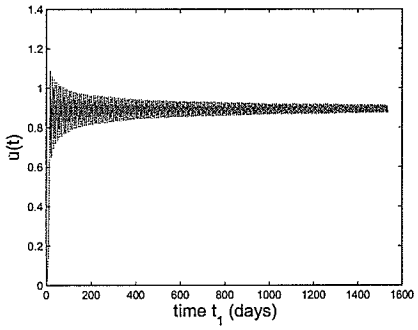


(a) $t - u$ plane

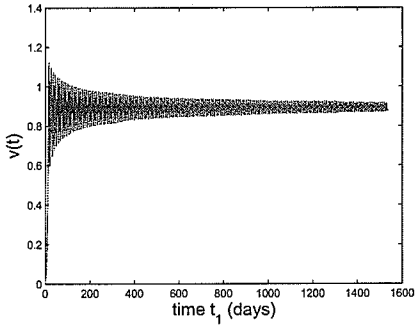


(b) $t - v$ plane

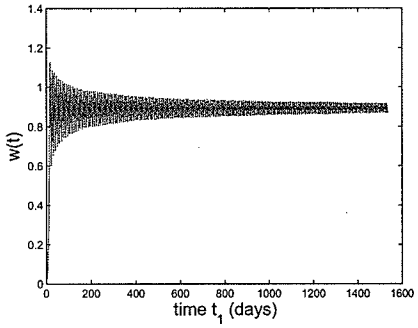


(c) $t - w$ plane

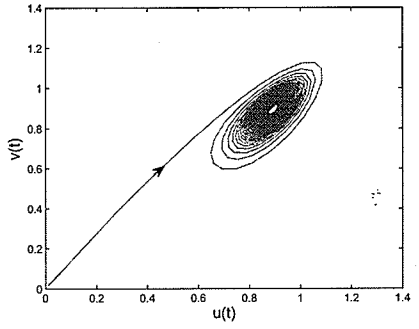


(d) a stable limit cycle

Figure 4.4: Simulations of the model (4.10), using the Verhulst-Pearl logistic growth function **B1**, showing the time series of the state variables for $T = 1.86 > T_c = 1.8502$ converging to a stable limit cycle. Parameter values used are: $a = 1$, $\mu = 0.042$, $B_0 = 3.07$, $\alpha = 0.63$, $\gamma = 3.88$, $\rho = 0.81$, and $\mu_s = 0.07$ (so that, $1 < \mathcal{R}_{0d} = 9.4332$).

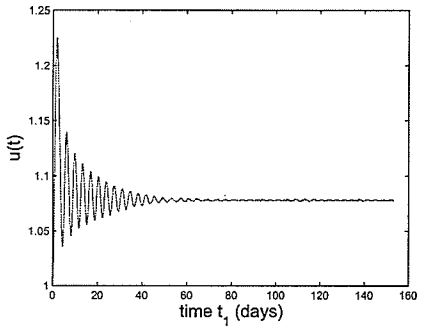


(a) $t - u$ plane

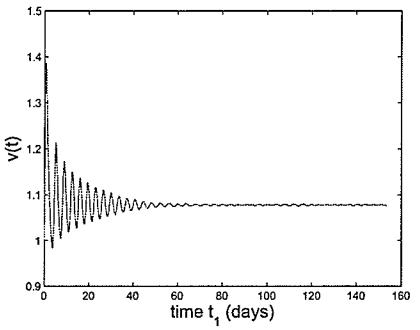


(b) $t - v$ plane

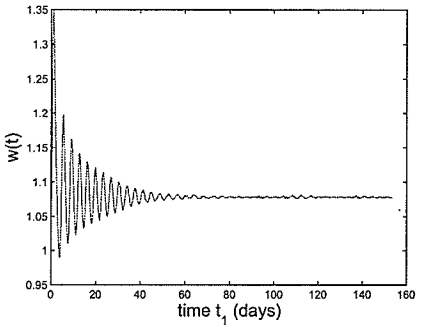


(c) $t - w$ plane

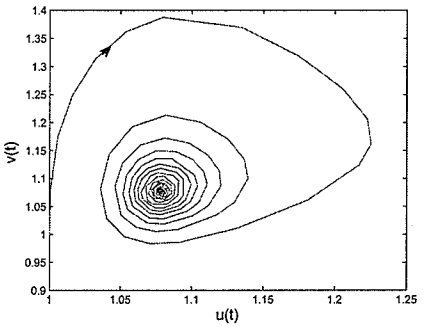


(d) a stable spiral

Figure 4.5: Simulations of the model (4.10), using Beverton-Holt function **B2**, showing the time series of the state variables for $T = 0.25 < T_c = 0.27628$ converging to a stable spiral. Parameter values used are: $a = 1$, $\mu = 0.042$, $B_0 = 3.07$, $\alpha = 0.63$, $\gamma = 3.88$, $\mu_s = 0.07$, $\rho = 0.81$, and $n = 30$ (so that, $1 < \mathcal{R}_{0d} = 10.5586$).

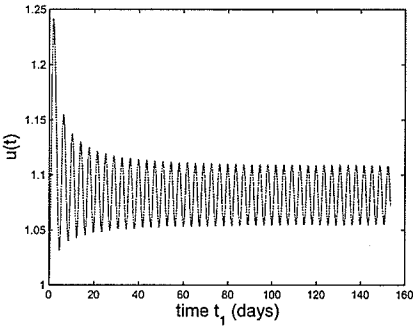


(a) $t-u$ plane

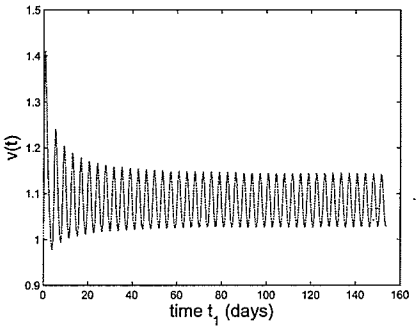


(b) $t-v$ plane

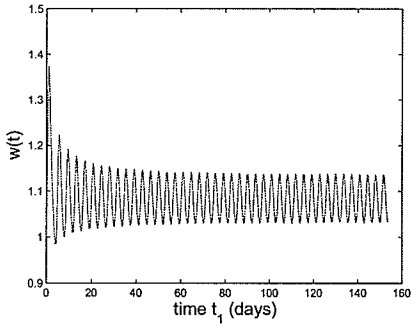


(c) $t-w$ plane

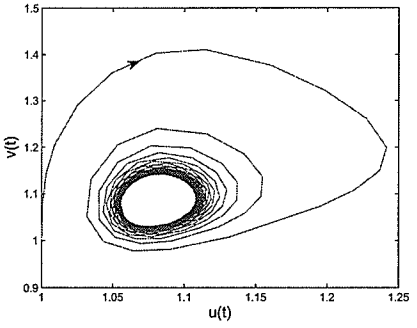


(d) a stable limit cycle

Figure 4.6: Simulations of the model (4.10), using the Beverton-Holt function **B2**, showing the time series of the state variables for $T = 0.30 > T_c = 0.27628$ converging to a stable limit cycle. Parameter values used are: $a = 1$, $\mu = 0.042$, $B_0 = 3.07$, $\alpha = 0.63$, $\gamma = 3.88$, $\mu_s = 0.07$, $\rho = 0.81$, and $n = 30$ (so that, $1 < \mathcal{R}_{0d} = 10.5217$).

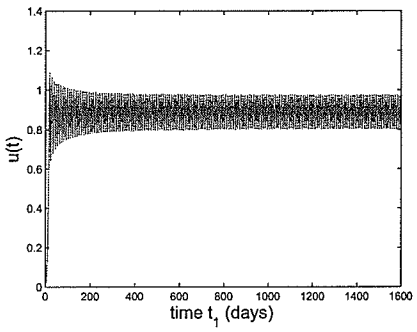


(a) $t - u$ plane for $T = 1.9$

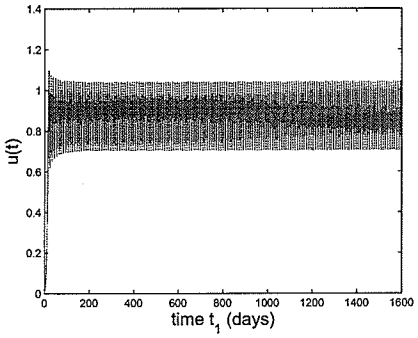


(b) $t - u$ plane for $T = 2$

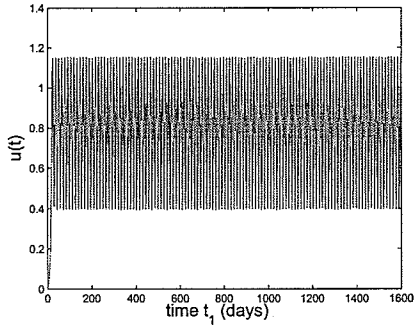


(c) $t - u$ plane for $T = 3$

Figure 4.7: Simulations of the model (4.10), using the Verhulst-Pearl logistic growth function **B1**, showing the time series of the state variable $u$ for (a) $T = 1.9$, (b) $T = 2$ and (c) $T = 3$. Parameter values used are: $a = 1$, $\mu = 0.042$, $B_0 = 3.07$, $\alpha = 0.63$, $\gamma = 3.88$, $\mu_s = 0.007$, and $\rho = 0.81$.

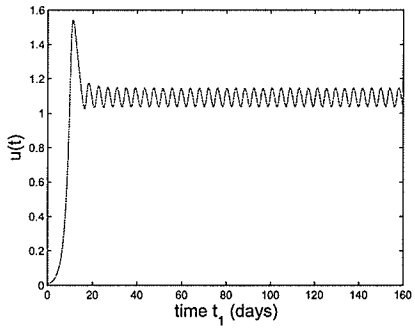


(a) $t-u$ plane for $T=0.35$

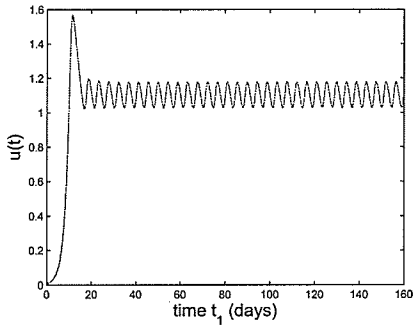


(b) $t-u$ plane for $T=0.4$

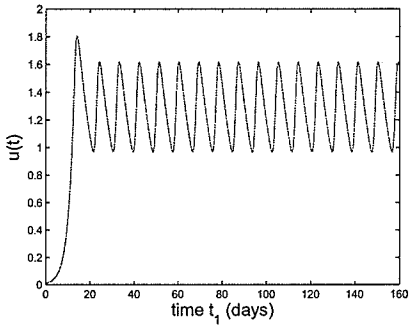


(c) $t-u$ plane for $T=1$

Figure 4.8: Simulations of the model (4.10), using the Beverton-Holt function **B2**, showing the time series of the state variable $u$ for (a) $T=0.35$, (b) $T=0.4$ and (c) $T=1$. Parameter values used are: $a=1$, $\mu=0.042$, $B_0=3.07$, $\alpha=0.63$, $\gamma=3.88$, $\mu_s=0.007$, $\rho=0.81$, and $n=30$.

# Chapter 5

# In-host Models for Malaria

## 5.1 Introduction

Malaria in humans develops *via* two phases, namely *exoerythrocytic* (that is, mainly in the liver) and *erythrocytic* phase. When an infected female *Anopheles* mosquito pierces a person's skin to take a blood meal, *sporozoites* in the mosquito's saliva enter the bloodstream and migrate to the liver. Within less than an hour of being introduced into the human host, they infect *hepatocytes*, multiplying asexually and asymptomatically for a period of 6-15 days [11, 97]. Once in the liver, these organisms differentiate to yield thousands of *merozoites* which, following the rupture of their host cells, escape into the blood and infect red blood cells, thus beginning the erythrocytic stage of the life cycle.

After about 48 hours, for *Plasmodium falciparum*, the infected erythrocyte ruptures releasing 8-32 merozoites daughter parasites that quickly invade fresh erythrocytes

to renew the cycle [30, 69]. This erythrocytic cycle maintains infection and directly generates disease symptoms [51]. This blood cycle can be repeated many times and some merozoites develop into the sexual form of the parasites called gametocytes. If a mosquito pierces the skin of an infected person, it potentially picks up gametocytes within the blood [92]. Fertilization and sexual recombination of the parasite occurs in the mosquito's gut. Successive erythrocytic cycles result in an increase in parasitaemia until the immune response begins. Detailed reviews of host immune response to malaria infection are available in [38, 83, 114], and a general summary is provided in [91]. As noted by Engwerda and Good [38], "understanding host immune response to the malaria parasite is crucial to the design and implementation of new vaccines and drugs". This chapter considers the problem of modelling the in-host dynamics of malaria subject to host immune response and a potential malaria vaccine.

A number of modelling studies have been conducted to gain insight into the intra-host dynamics of the malaria parasite (see, for instance, the models given in [30, 51, 69, 101, 102]). These models typically describe the dynamics of the blood stages of the parasite (*Plasmodium falciparum*) and their interaction with host cells (RBCs) and immune cells. Molineaux and Dietz [102] provided a review of some earlier in-host models of malaria. Models for assessing the effect of host immune response to malaria infection are presented in [24, 98]. Kwiatkowski and Nowak [84] presented a discrete-time model for studying the periodic and chaotic host-parasite interactions in human malaria. Most of the aforementioned models, with the exception of the model in [98], considered a single stage for the infected red blood cells (IRBCs). The

objective of this chapter is to carry out a detailed mathematical analysis of a new in-host malaria model that takes into account multiple ($n$) stages for the IRBCs. The model incorporates the effect of immune response on the parasite dynamics *in vivo*, by adding two state variables for the associated immune cells and antibodies, as well as a potential anti-malaria vaccine. Before formulating the model, some earlier in-host models for malaria will be considered first of all.

## 5.2 Some Earlier Models

### 5.2.1 Anderson *et al.* model

The first mathematical model of the *erythrocyte cycle* was proposed by Anderson *et al.* [3], and is given by the following system of differential equations:

$$\begin{aligned} \frac{dX}{dt} &= \lambda_X - \beta XM - \mu_X X, \\ \frac{dY}{dt} &= \beta XM - \mu_Y Y, \\ \frac{dM}{dt} &= r\mu_Y Y - \mu_M M - \beta XM, \end{aligned} \tag{5.1}$$

where $X(t)$ and $Y(t)$ are the concentrations of uninfected RBCs and IRBCs at time $t$, respectively. The variable $M(t)$ represents the concentration of the free merozoites in the blood at time $t$. The parameters $\mu_X$, $\mu_Y$ and $\mu_M$ are the death rates of the RBCs, IRBCs and free merozoites, respectively. Uninfected red blood cells are generated from the bone marrow at a constant rate $\lambda_X$, and become infected, by coming in contact with free merozoites, at a rate $\beta$. The parameter $r$ models the average number of

merozoites released per each bursting IRBC. Free merozoites die (at a rate $\mu_M$) or successively invade RBCs, at the rate $\beta$.

The model (5.1) will now be qualitatively analysed to gain insight into its dynamical features.

### Stability of DFE

The DFE of the model (5.1) is given by

$$E_{00} = (X^*,\ Y^*,\ M^*) = (\lambda_X/\mu_X,\ 0,\ 0). \tag{5.2}$$

The local stability of $E_{00}$ will be explored using the next generation operator method [31, 136]. Here, the non-negative matrix, $F_1$, of the new infection terms, and the $M$-matrix, $V_1$, of the transition terms associated with the model (5.1), are given, respectively, by

$$F_1 = \begin{pmatrix} 0 & \frac{\beta\lambda_X}{\mu_X} \\ 0 & 0 \end{pmatrix},$$

and,

$$V_1 = \begin{pmatrix} \mu_Y & 0 \\ -r\mu_Y & \mu_M + \frac{\beta\lambda_X}{\mu_X} \end{pmatrix}.$$

It follows that the *basic reproduction number*, denoted by $\mathcal{R}_A = \rho(F_1V_1^{-1})$, is given by

$$\mathcal{R}_A = \frac{\beta\lambda_X r}{\mu_X\mu_M + \beta\lambda_X}. \tag{5.3}$$

Using Theorem 2 of [136], the following result is established.

**Lemma 5.1.** *The DFE of the model* (5.1)*, given by* $E_{00}$*, is LAS if* $\mathcal{R}_A < 1$*, and unstable if* $\mathcal{R}_A > 1$.

The threshold quantity, $\mathcal{R}_A$, measures the number of secondary IRBCs produced per primary IRBC in a host at the onset of infection [102].

The above local stability result of the DFE ($E_{00}$) shows that if the initial sub-populations of the model are in the basin of attraction of the DFE, then the parasite can be cleared from the bloodstream if $\mathcal{R}_A < 1$. To ensure that such clearance is independent of the initial concentrations of RBCs, IRBCs and merozoites, a global asymptotic stability result must be established for the DFE. This is explored below.

### Global stability of DFE

Consider the region

$$\Omega = \left\{(X, Y, M) \in \mathbb{R}^3_+ : X + Y \leq \frac{\lambda_X}{\mu_{min}}, M \leq \bar{M}\right\}, \tag{5.4}$$

where $\bar{M} = r\mu_Y\lambda_X/\mu_M\mu_{min}$ with $\mu_{min} = \min\{\mu_X, \mu_Y\}$. Before proving the global stability of the DFE, the following results will first be established.

**Lemma 5.2.** *The region* $\Omega$ *given by* (5.4) *is positively-invariant and attracting for the model* (5.1).

*Proof.* Let,

$$(X(t), Y(t), M(t)) \in \mathbb{R}^3_+, \tag{5.5}$$

be any solution of the system (5.1) with non-negative initial conditions. Adding the first two equations of the model (5.1) gives

$$\frac{d(X+Y)}{dt} = \lambda_X - (\mu_X X + \mu_Y Y). \tag{5.6}$$

Thus,

$$\frac{d(X+Y)}{dt} \leq \lambda_X - \mu_{min}(X+Y), \tag{5.7}$$

so that

$$\limsup_{t\to\infty}(X+Y) \leq \frac{\lambda_X}{\mu_{min}}.$$

Furthermore, it can be shown from the last equation of (5.1) that

$$\limsup_{t\to\infty} M \leq \frac{r\mu_Y\lambda_X}{\mu_M\mu_{min}}.$$

It follows from (5.7) that $\frac{d(X+Y)}{dt} < 0$ if $(X+Y) > \frac{\lambda_X}{\mu_{min}}$. Similarly, it follows from the equation for $\frac{dM}{dt}$ in (5.1) that $\frac{dM}{dt} < 0$ whenever $M > \bar{M}$. Thus, the vector field of (5.1) points inward (into $\Omega$). Thus, $\Omega$ is positively-invariant and attracting for the model (5.1). □

**Lemma 5.3.** *The region* $\Omega^* = \left\{(X,Y,M) \in \Omega : X \leq X^*\right\}$ *is positively-invariant and attracting for the model* (5.1).

*Proof.* It follows from the first equation of (5.1) that

$$\frac{dX}{dt} = \lambda_X - \beta XM - \mu_X X \leq \lambda_X - \mu_X X = \mu_X(X^* - X).$$

Hence, $X \leq X^* - [X^* - X(0)]e^{-\mu_X t}$. Thus, either $X(t)$ approaches $X^*$ asymptotically, or there is some finite time after which $X(t) \leq X^*$ (see also [52]). Therefore, all feasible solutions of the RBC and merozoite component of the system (5.1) enter the region $\Omega^*$. Thus, the region $\Omega^*$ is positively-invariant and attracting. □

We claim the following result.

**Theorem 5.1.** *The DFE, $E_{00}$, of the model* (5.1)*, given by* (5.2)*, is GAS in $\Omega^*$ if $\mathcal{R}_A \leq 1$.*

*Proof.* Consider the Lyapunov function

$$\mathcal{F}_1 = rY + M,$$

with Lyapunov derivative given by (where a dot represents differentiation with respect

to $t$)

$$\begin{aligned}
\dot{\mathcal{F}}_1 &= r\dot{Y} + \dot{M}, \\
&= r(\beta XM - \mu_Y Y) + r\mu_Y Y - \mu_M M - \beta XM, \\
&= (r\beta X - \beta X - \mu_M)M, \\
&\leq (r\beta X^* - \beta X^* - \mu_M)M, \text{ since } X \leq X^* \text{ in } \Omega^*, \\
&= \left(\frac{r\beta\lambda_X}{\mu_X} - \frac{\beta\lambda_X + \mu_X\mu_M}{\mu_X}\right)M, \\
&= \frac{1}{\mu_X}(\beta\lambda_X + \mu_X\mu_M)(\mathcal{R}_A - 1)M.
\end{aligned}$$

Thus, $\dot{\mathcal{F}}_1 \leq 0$ if $\mathcal{R}_A \leq 1$ with $\dot{\mathcal{F}}_1 = 0$ if and only if $M = 0$. Further, the largest compact invariant set in $\{(X, Y, M) \in \Omega^* : \dot{\mathcal{F}}_1 = 0\}$ is the singleton $\{E_{00}\}$. It follows from the LaSalle's Invariance Principle [56, 86] that every solution to the system (5.1) with initial conditions in $\Omega^*$ converge to the DFE $E_{00}$ as $t \to \infty$. That is, $(Y(t), M(t)) \to (0, 0)$ as $t \to \infty$. Substituting $Y(t) = M(t) = 0$ in the equation for $dX/dt$ in (5.1) gives $X(t) \to X^*$ as $t \to \infty$. Thus, the DFE, $E_{00}$, is GAS in $\Omega^*$ if $\mathcal{R}_A \leq 1$. □

This result shows that the parasite can be cleared from the bloodstream, regardless of the initial concentrations of RBCs, IRBCs and merozoites, whenever $\mathcal{R}_A \leq 1$.

### Existence of endemic equilibria

To find conditions for the existence of an equilibrium of the form $E_{e0} = (X^{**}, Y^{**}, M^{**})$, of the model (5.1), for which the disease is endemic (i.e., at least one of $Y^{**}$ and $M^{**}$ is non-zero), the equations in (5.1) are solved at steady-state giving the unique endemic

(positive) equilibrium point ($E_{e0}$), with components:

$$X^{**} = \frac{\mu_M}{\beta(r-1)}, \quad Y^{**} = \frac{(\mu_X\mu_M + \beta\lambda_X)(\mathcal{R}_A - 1)}{\beta\mu_Y(r-1)}, \quad M^{**} = \frac{(\mu_X\mu_M + \beta\lambda_X)(\mathcal{R}_A - 1)}{\beta\mu_M}. \tag{5.8}$$

It is clear from (5.8) that this EEP ($E_{e0}$) exists if and only if $\mathcal{R}_A > 1$ and $r > 1$. It should be noted that if $\mathcal{R}_A > 1$, then $\beta\lambda_X(r-1) > \mu_X\mu_M > 0$, which requires $r > 1$. Thus, from now on, we consider $r > 1$. Further, if $\mathcal{R}_A < 1$, then the aforementioned $Y^{**}$ and $M^{**}$ components of the EEP ($E_{e0}$) are negative. Thus, the model (5.1) has no positive endemic equilibrium whenever $\mathcal{R}_A < 1$. When $\mathcal{R}_A = 1$, the EEP ($E_{e0}$) corresponds to the DFE ($E_{00}$). These results are summarized below.

**Theorem 5.2.** *The model* (5.1) *has a unique positive endemic equilibrium, given by* $E_{e0}$, *whenever* $\mathcal{R}_A > 1$, *and no positive endemic equilibrium otherwise.*

### Local stability of EEP

The stability of the EEP ($E_{e0}$) is explored evaluating the Jacobian of (5.1) at $E_{e0}$, giving

$$J(E_{e0}) = \begin{pmatrix} -\mu_X - \dfrac{\lambda_X\beta r - \lambda_X\beta - \mu_X\mu_M}{\mu_M} & 0 & -\dfrac{\mu_M}{r-1} \\ \dfrac{\lambda_X\beta r - \lambda_X\beta - \mu_X\mu_M}{\mu_M} & -\mu_Y & \dfrac{\mu_M}{r-1} \\ \dfrac{\lambda_X\beta r - \lambda_X\beta - \mu_X\mu_M}{\mu_M} & r\mu_Y & -\mu_M - \dfrac{\mu_M}{r-1} \end{pmatrix}.$$

The eigenvalues of $J(E_{e0})$ are the roots of the polynomial

$$a_0\lambda^3 + a_1\lambda^2 + a_2\lambda + a_3 = 0, \tag{5.9}$$

with,

$$a_0 = 1,$$

$$a_1 = \frac{1}{\mu_M}\left[\lambda_X\beta(r-1) + \mu_M\mu_Y + \frac{\mu_M^2 r}{r-1}\right],$$

$$a_2 = \frac{1}{\mu_M}\left[\lambda_X\beta(r-1)(\mu_Y + \mu_M) + \frac{\mu_X\mu_M^2}{r-1}\right],$$

$$a_3 = \mu_Y(\lambda_X\beta + \mu_X\mu_M)(\mathcal{R}_A - 1).$$

Thus, the coefficients $a_i$ (with $i = 0, \ldots, 3$) of the cubic (5.9) are all positive if $\mathcal{R}_A > 1$ (note that $r > 1$, as shown in Section 5.2.1). It follows that

$$\begin{aligned}
a_1a_2 - a_3a_0 = \frac{1}{\mu_M^2(r-1)^2}\Big[&(\lambda_X^2\beta^2\mu_M + \lambda_X^2\beta^2\mu_Y)r^4 + (\mu_M^2\mu_Y\lambda_X\beta - 4\lambda_X^2\beta^2\mu_Y \\
&- 4\lambda_X^2\beta^2\mu_M + \mu_M^3\lambda_X\beta + \mu_M\mu_Y^2\lambda_X\beta)r^3 + (-3\mu_M\mu_Y^2\lambda_X\beta + \lambda_X\beta\mu_X\mu_M^2 \\
&- 2\mu_M^2\mu_Y\lambda_X\beta - 2\mu_M^3\lambda_X\beta + \mu_M^3\mu_Y\mu_X + 6\lambda_X^2\beta^2\mu_M + 6\lambda_X^2\beta^2\mu_Y)r^2 \\
&+ (\mu_M^2\mu_Y\lambda_X\beta + \mu_M^4\mu_X - 2\lambda_X\beta\mu_X\mu_M^2 - 4\lambda_X^2\beta^2\mu_Y - \mu_M^3\mu_Y\mu_X \\
&+ \mu_M^3\lambda_X\beta - 4\lambda_X^2\beta^2\mu_M + 3\mu_M\mu_Y^2\lambda_X\beta)r + \lambda_X^2\beta^2\mu_Y + \lambda_X^2\beta^2\mu_M \\
&- \mu_M\mu_Y^2\lambda_X\beta + \lambda_X\beta\mu_X\mu_M^2\Big], \\
= \frac{1}{\mu_M^2(r-1)^2}\Big[&\mu_M^2\mu_Y\lambda_X\beta r(r-1)^2 + \mu_M^3\lambda_X\beta r(r-1)^2 + \lambda_X\beta\mu_X\mu_M^2(r-1)^2 \\
&+ \lambda_X^2\beta^2\mu_Y(r-1)[r(r^2+r+1) - 1 + 2r - 4r^2] + \lambda_X^2\beta^2\mu_M(r-1)[r(r^2+r+1) \\
&- 1 - 2r - 4r^2] + \mu_M\mu_Y^2\lambda_X\beta(r-1)(r^2+r+1-3r) + \mu_M^3\mu_X\mu_Y r(r-1) + \mu_M^4\mu_X r\Big], \\
= \frac{1}{\mu_M^2(r-1)^2}\Big[&\mu_M^2\mu_Y\lambda_X\beta r(r-1)^2 + \mu_M^3\lambda_X\beta r(r-1)^2 + \lambda_X\beta\mu_X\mu_M^2(r-1)^2 \\
&+ \lambda_X^2\beta^2\mu_Y(r-1)^4 + \lambda_X^2\beta^2\mu_M(r-1)^4 + \mu_M\mu_Y^2\lambda_X\beta(r-1)^3 \\
&+ \mu_M^3\mu_X\mu_Y r(r-1) + \mu_M^4\mu_X r\Big].
\end{aligned}$$

Since $r > 1$, it follows that $a_1a_2 - a_3a_0 > 0$. Hence, by Routh-Hurwitz criterion [85], all the eigenvalues of $J(E_{e0})$ have negative real parts whenever $\mathcal{R}_A > 1$. This result is summarized below.

**Theorem 5.3.** *The unique endemic equilibrium of the model* (5.1)*, denoted by* $E_{e0}$*, is LAS if* $\mathcal{R}_A > 1$.

### Global stability of EEP

Define the region (the stable manifold of the DFE, $E_{00}$)

$$\Omega_0 = \Big\{(X, Y, M) \in \Omega^* : Y = M = 0\Big\}.$$

We claim the following.

**Theorem 5.4.** *The unique endemic equilibrium of the model* (5.1)*, given by* $E_{e0}$*, is GAS in* $\Omega^* \setminus \Omega_0$ *if*

*(i)* $\mathcal{R}_A > 1$,

*(ii)* $\text{sign}(1 - \frac{\text{M}}{\text{M}^{**}}) = \text{sign}(1 - \frac{\text{X}}{\text{X}^{**}})$ .

*Proof.* Let $\mathcal{R}_A > 1$, so that the EEP, $E_{e0}$, exists (by Theorem 5.2). Further, let $\text{sign}(1 - \frac{M}{M^{**}}) = \text{sign}(1 - \frac{X}{X^{**}})$. Consider the following non-linear Lyapunov function of Volterra-type (functions of this type have been used in mathematical ecology [42, 117]; and more recently in mathematical epidemiology and immunology [39, 53, 54, 71, 77, 78, 79, 96]):

$$\mathcal{F}_2 = X - X^{**} - X^{**} \ln\left(\frac{X}{X^{**}}\right) + Y - Y^{**} - Y^{**} \ln\left(\frac{Y}{Y^{**}}\right) + \frac{1}{r}\left[M - M^{**} - M^{**} \ln\left(\frac{M}{M^{**}}\right)\right],$$

with Lyapunov derivative

$$\dot{\mathcal{F}}_2 = \lambda_X - \beta XM - \mu_X X - \frac{X^{**}}{X}(\lambda_X - \beta XM - \mu_X X) + \beta XM - \mu_Y Y$$
$$+ \frac{Y^{**}}{Y}(\beta XM - \mu_Y Y) + \frac{1}{r}\left[r\mu_Y Y - \mu_M M - \beta XM - \frac{M^{**}}{M}(r\mu_Y Y - \mu_M M - \beta XM)\right],$$

$$= \lambda_X - \lambda_X \frac{X^{**}}{X} + \mu_X X^{**}\left(1 - \frac{X^{**}}{X}\right) + \beta X^{**}M - \beta XM\frac{Y^{**}}{Y} + \mu_Y Y^{**}$$
$$- \frac{1}{r}\mu_M M - \frac{1}{r}\beta XM - \mu_Y Y\frac{M^{**}}{M} + \frac{1}{r}\mu_M M^{**} + \frac{1}{r}\beta XM^{**},$$

$$= (\beta X^{**}M^{**} + \mu_X X^{**}) - (\beta X^{**}M^{**} + \mu_X X^{**})\frac{X^{**}}{X} + \mu_X X^{**}\left(1 - \frac{X^{**}}{X}\right)$$
$$+ \beta X^{**}M - \beta XM\frac{Y^{**}}{Y} + \beta X^{**}M^{**} + \frac{1}{r}\mu_M M^{**}\left(1 - \frac{M}{M^{**}}\right)$$
$$+ \frac{1}{r}\beta XM^{**}\left(1 - \frac{M}{M^{**}}\right) - \mu_Y Y\frac{M^{**}}{M},$$

$$= \beta X^{**}M^{**}\left(2 - \frac{X^{**}}{X} - \frac{Y}{Y^{**}}\frac{M^{**}}{M} - \frac{X}{X^{**}}\frac{Y^{**}}{Y}\frac{M}{M^{**}}\right)$$
$$+ \mu_X X^{**}\left(2 - \frac{X^{**}}{X} - \frac{X}{X^{**}}\right) + \beta X^{**}M + \frac{1}{r}\left(1 - \frac{M}{M^{**}}\right)$$
$$\times (r\mu_Y Y^{**} - \beta X^{**}M^{**} + \beta XM^{**}),$$

$$= \beta X^{**}M^{**}\left(3 - \frac{X^{**}}{X} - \frac{Y}{Y^{**}}\frac{M^{**}}{M} - \frac{X}{X^{**}}\frac{Y^{**}}{Y}\frac{M}{M^{**}}\right)$$
$$+ \mu_X X^{**}\left(2 - \frac{X^{**}}{X} - \frac{X}{X^{**}}\right) - \frac{1}{r}\beta X^{**}M^{**}\left(1 - \frac{X}{X^{**}}\right)\left(1 - \frac{M}{M^{**}}\right).$$

Since the arithmetic mean exceeds the geometric mean, then

$$3 - \frac{X^{**}}{X} - \frac{Y}{Y^{**}}\frac{M^{**}}{M} - \frac{X}{X^{**}}\frac{Y^{**}}{Y}\frac{M}{M^{**}} \leq 0 \text{ and } 2 - \frac{X^{**}}{X} - \frac{X}{X^{**}} \leq 0.$$

Owing to the fact that all the model parameters are non-negative, it follows that $\dot{\mathcal{F}}_2 \leq 0$ for $\mathcal{R}_A > 1$ and $(1 - \frac{X}{X^{**}})$ and $(1 - \frac{M}{M^{**}})$ have the same sign. Hence, $\mathcal{F}_2$ is a Lyapunov function on $\Omega^*$. Therefore, by the LaSalle's Invariance Principle [56, 86], every solution to the equations of the model with initial condition in $\Omega^* \setminus \Omega_0$ , approaches $E_{e0}$ as $t \to \infty$ for $\mathcal{R}_A > 1$. □

It should be stated that Chiyaka *et al.* [24] also proved global asymptotic stability of the EEP ($E_{e0}$) using the compound matrix technique of Li and Muldowney [87, 106], subject to $\mathcal{R}_A > 1$ and some conditions (which differ from Item (ii) of Theorem 5.4). This result is proven here, using a non-linear Lyapunov function and LaSalle's Invariance Principle, for the sake of completeness. In summary, the basic Anderson *et al.* model (5.1) has the following qualitative properties:

(i) It has a globally-asymptotically stable DFE whenever the associated basic reproduction number, $R_A$, is less than unity;

(ii) It has a unique endemic equilibrium point, which is globally-asymptotically stable when it exists and when another condition (given by Item (ii) of Theorem 5.4) holds.

### 5.2.2 Model with multiple parasitic stages

Considerable modelling work has been done on extending the basic model (5.1) in different directions (see, for instance, [5, 24, 49, 50, 59, 65, 69, 71, 122]). Saul [122] showed that the model (5.1) can exhibit unrealistically large growth rates, and suggested the replacement of the merozoite release parameter, $r$, with a non-linear term $\ln r + 1$. This reformulation ensures that if all merozoites re-invade, the parasite population increases by a factor $r$ over one generation. However, as noted by Gravenor and Lloyd [50], the replacement of $r$ by $\ln r + 1$ will not remedy the problem of unrealistically large growth rate. In [49], Gravenor *et al.* considered the situation where a parasite can produce the observed number of merozoites, $r$, many of which do not re-invade.

Further, as noted by Gravenor [50], in both the original model (5.1) and Saul's suggested model [122], growth rate of the parasite is the same, and they both have the same distributional assumptions concerning parasite life-span. Two solutions to the large growth rate problem were suggested by Gravenor and Lloyd [50], namely:

(i) to replace the term describing parasite life-span by a term that incorporates a time delay;

(ii) to add more age compartments to the intracellular parasite stage.

Option (ii) is the simpler alternative. Under this scenario, as a parasite matures, it passes through the aforementioned compartments in sequence (denoted by $Y_i$; with $i = 1, 2, \cdots, n$), and constant rates govern the transition between these compartments. Consequently, the overall parasite life-span is now described by a sum of several expo-

nential distributions. If $\gamma_1 = \gamma_2 = \cdots = \gamma_n = \gamma$ then it is a gamma distribution. It is noteworthy that different numbers of stages, ranging from 5 to 48, are used in [49, 51].

Taking the above assumptions into consideration, we consider the following model for the intra-host dynamics of malaria:

$$\begin{aligned}
\frac{dX}{dt} &= \lambda_X - \beta XM - \mu_X X, \\
\frac{dY_1}{dt} &= \beta XM - \mu_1 Y_1 - \gamma_1 Y_1, \\
\frac{dY_2}{dt} &= \gamma_1 Y_1 - \mu_2 Y_2 - \gamma_2 Y_2, \\
\frac{dY_3}{dt} &= \gamma_2 Y_2 - \mu_3 Y_3 - \gamma_3 Y_3, \\
&\cdots \quad \cdots \quad \cdots \\
\frac{dY_n}{dt} &= \gamma_{n-1} Y_{n-1} - \mu_n Y_n - \gamma_n Y_n, \\
\frac{dM}{dt} &= r(\mu_n + \gamma_n) Y_n - \mu_M M - u\beta XM,
\end{aligned} \tag{5.10}$$

where, $X$, $Y$, and $M$ are as defined as in Section 5.2.1 and $\gamma_i$ (with $i = 1, 2, \cdots, n$) represent the transmission rates from compartment $Y_i$ to the next compartment $Y_{i+1}$. The model (5.10) is a slight modification of the models in [50, 71], by

(i) using a constant growth rate for the uninfected RBCs ($\lambda_X$); whereas density-

dependent growth rate was used in [71];

(ii) modelling the growth rate of merozoites by the term $r(\gamma_n + \mu_n)$, whereas the rate $r\gamma_n$ was used in [50, 71].

It should be stated that a parameter $u$ is used in the loss term, $-\beta XM$, in the equation for the merozoites, where $u = 0$ when the loss of the merozoites entering the RBCs is ignored; and $u = 1$ when the loss is not ignored [71]. Further, it should be mentioned that Iggidr *et al.* [71] provided a complete analysis for the existence and global asymptotic stability of the equilibria of a variant of (5.10), with density-dependent growth rate of RBCs ($f(x)$ instead of the constant rate, $\lambda_X$, in (5.10)) and growth rate of merozoites $\gamma_n$, instead of $\gamma_n + \mu_n$ in (5.10).

The main objective of this chapter is to extend the model given in (5.10), by including two new dynamic compartments for the concentration of immune cells and antibodies, to incorporate the effect of the immune response on merozoite invasion of erythrocytes and suppression of parasite production by antibodies; and to also explore the potential impact of an imperfect malaria vaccine. In both cases, the resulting model will be rigorously analysed. Before making the aforementioned extensions, the qualitative features of the model (5.10) will be rigorously analysed. It should be stated that although the method and results we will give for the analysis of the model (5.10) closely follow the approach in Iggidr *et al.* [71], the model (5.10) is analysed for the sake of completeness since it contains some modifications (albeit minor) from the model presented by Iggidr *et al.* [71] (as stated above). Further, some of the results obtained would be used in the analysis in some of the subsequent sections.

### Local stability of DFE

Consider the region of the model (5.10)

$$\mathcal{D}_1 = \left\{(X(t), Y_1(t), Y_2(t), \cdots, Y_n(t), M(t)) \in \mathbb{R}_+^{n+2} : X + \sum_{i=1}^{n} Y_i \leq \frac{\lambda_X}{\mu_{min}}, M \leq \bar{M}\right\}, \tag{5.11}$$

where, now, $\bar{M} = \dfrac{r(\mu_n + \gamma_n)\lambda_X}{\mu_{min}\mu_M}$ and $\mu_{min} = \min\{\mu_X, \mu_1, \cdots, \mu_n\}$. We claim the following

**Lemma 5.4.** *The region $\mathcal{D}_1$, given in* (5.11)*, is positively-invariant and attracting for the model* (5.10)*.*

*Proof.* Let,

$$(X(t), Y_1(t), \cdots, Y_n(t), M(t)) \in \mathbb{R}_+^{n+2}, \tag{5.12}$$

be any solution of the system (5.10) with non-negative initial conditions. It can be shown, by adding the first $n+1$ equations of the model (5.10) (*i.e.*, the equations for $dX/dt$ and $dY_i/dt$ for $i = 1, \cdots, n$), that

$$\frac{d}{dt}\left(X + \sum_{i=1}^{n} Y_i\right) \leq \lambda_X - \mu_{min}\left(X + \sum_{i=1}^{n} Y_i\right). \tag{5.13}$$

Thus,

$$\limsup_{t\to\infty}\left(X + \sum_{i=1}^{n} Y_i\right) \leq \frac{\lambda_X}{\mu_{min}}.$$

Further, it follows from the last equation of (5.10) that

$$\limsup_{t\to\infty} M \leq \frac{r(\mu_n+\gamma_n)\lambda_X}{\mu_M\mu_{min}}.$$

Since $\frac{d}{dt}\left(X+\sum_{i=1}^{n}Y_i\right) < 0$ if $(X+\sum_{i=1}^{n}Y_i) > \frac{\lambda_X}{\mu_{min}}$ and $\frac{dM}{dt} < 0$ whenever $M > \bar{M}$, the vector field points inward (into $\mathcal{D}_1$) on the boundary. Thus, $\mathcal{D}_1$ is positively-invariant and attracting. □

The DFE of the system (5.10) is given by

$$E_{01} = (X^*,\ Y_1^*,\ Y_2^*,\ \cdots,\ Y_n^*,\ M^*) = (\lambda_X/\mu_X,\ 0,\ 0,\ \cdots, 0). \tag{5.14}$$

The local stability of $E_{01}$ will be explored using the next generation operator method [31, 136]. The associated next generation matrices, $F_2$ and $V_2$, are given, respectively, by

$$F_2 = \begin{pmatrix} 0 & 0 & 0 & \cdots & 0 & 0 & \frac{\beta\lambda_X}{\mu_X} \\ 0 & 0 & 0 & \cdots & 0 & 0 & 0 \\ 0 & 0 & 0 & \cdots & 0 & 0 & 0 \\ \vdots & \vdots & \vdots & \cdots & \vdots & \vdots & \vdots \\ 0 & 0 & 0 & \cdots & 0 & 0 & 0 \\ 0 & 0 & 0 & \cdots & 0 & 0 & 0 \end{pmatrix},$$

and,

$$V_2 = \begin{pmatrix} Q_1 & 0 & 0 & \cdots & 0 & 0 & 0 \\ -\gamma_1 & Q_2 & 0 & \cdots & 0 & 0 & 0 \\ 0 & -\gamma_2 & Q_3 & \cdots & 0 & 0 & 0 \\ \vdots & \vdots & \vdots & \cdots & \vdots & \vdots & \vdots \\ 0 & 0 & 0 & \cdots & -\gamma_{n-1} & Q_n & 0 \\ 0 & 0 & 0 & \cdots & 0 & -r(\mu_n + \gamma_n) & \mu_M + u\beta X^* \end{pmatrix},$$

where, $Q_i = \mu_i + \gamma_i$ for $i = 1, \cdots, n$. It follows that the basic reproduction number of the model (5.10), denoted by $\mathcal{R}_S = \rho(F_2 V_2^{-1})$, is given by

$$\mathcal{R}_S = \frac{\beta r \gamma_1 \gamma_2 \cdots \gamma_{n-1} X^*}{(\mu_M + u\beta X^*) Q_1 Q_2 \cdots Q_{n-1}}. \tag{5.15}$$

Using Theorem 2 of [136], the following result is established.

**Lemma 5.5.** *The DFE of the multiple parasitic stage model* (5.10)*, given by* $E_{01}$*, is LAS if* $\mathcal{R}_S < 1$*, and unstable if* $\mathcal{R}_S > 1$.

### Existence of endemic equilibrium

Consider the matrix

$$A = \begin{pmatrix} -Q_1 & 0 & 0 & \cdots & 0 \\ \gamma_1 & -Q_2 & 0 & \cdots & 0 \\ 0 & \gamma_2 & -Q_3 & \cdots & 0 \\ \vdots & \ddots & \ddots & \ddots & \vdots \\ 0 & \cdots & 0 & \gamma_{n-1} & -Q_n \end{pmatrix}.$$

Following Iggidr *et al.* [71], the system (5.10) can be re-written as:

$$\begin{aligned} \dot{X} &= \lambda_X - \mu_X X - \beta X M = \phi(X) - \mu_X X, \\ \dot{\mathbf{Y}} &= \beta X M \mathbf{e_1} + A\mathbf{Y}, \\ \dot{M} &= r(\mu_n + \gamma_n)\mathbf{e}_n^T \mathbf{Y} - \mu_M M - u\beta X M, \end{aligned} \tag{5.16}$$

where $\mathbf{e}_1 = (1, 0, \cdots, 0)^T$, $\mathbf{e}_n = (0, \cdots, 0, 1)^T$, $\mathbf{Y} = (Y_1, Y_2, \cdots, Y_n)^T$ and $\phi(X) = \lambda_X - \beta X M$. The following result can easily be shown (by solving the system (5.16) at steady-state).

**Lemma 5.6.** *The model* (5.10) *has a unique EEP given by*

$$E_{e1} = (X^{**}, Y_1^{**}, Y_2^{**}, \cdots, Y_n^{**}, M^{**}) = (X^{**}, Y^{**}, M^{**}),$$

*with*

$$X^{**} = \frac{\mu_M}{\beta\left(\frac{r\gamma_1\gamma_2\cdots\gamma_{n-1}}{Q_1Q_2\cdots Q_{n-1}} - u\right)}, \quad Y^{**} = \phi(X^{**})(-A^{-1})\mathbf{e_1}, \quad M^{**} = \frac{\phi(X^{**})}{\beta X^{**}}, \tag{5.17}$$

*whenever* $\mathcal{R}_S > 1$.

Further, it can be shown from (5.15) that

$$\mathcal{R}_S < 1 \Rightarrow \beta X^*\left(\frac{r\gamma_1\cdots\gamma_{n-1}}{Q_1\cdots Q_{n-1}} - u\right) < \mu_M,$$

so tha,t

$$\frac{\beta X^*\left(\frac{r\gamma_1\gamma_2\cdots\gamma_{n-1}}{Q_1Q_2\cdots Q_{n-1}} - u\right)}{\mu_M} < 1.$$

Hence, using the expression for $X^{**}$ from (5.17), it follows that $X^*/X^{**} < 1$. In other words,

$$\mathcal{R}_S < 1 \ \Rightarrow \frac{X^*}{X^{**}} < 1. \tag{5.18}$$

The result in (5.18) will be used in the proof of Theorem 5.6.

### Global stability of DFE

Define the region

$$\mathcal{D}_1^* = \left\{(X(t), Y_1(t), Y_2(t), \cdots, Y_n(t), M(t)) \in \mathcal{D}_1 : X(t) \leq X^*\right\}. \tag{5.19}$$

It is easy to show (using the approach in Section 5.2.1) that the region $\mathcal{D}_1^*$ is positively-invariant. We claim the following result.

**Theorem 5.5.** *The DFE, $E_{01}$, of the model* (5.10) *is GAS in $\mathcal{D}_1^*$ if $\mathcal{R}_S \leq 1$.*

The proof of Theorem 5.5 is given in Appendix D.

It should be stated that the Lyapunov function $\mathcal{F}_3$, used to prove Theorem 5.5 in Appendix D, takes the same form as that used by Iggidr *et al.* [71] to prove the global asymptotic stability of the DFE of their model (the main difference is a few minor, but necessary, modifications we made for some of the coefficients of the variables in $\mathcal{F}_3$).

### Global stability of EEP

Define the region (the stable manifold of the DFE, $E_{01}$)

$$\mathcal{D}_0 = \Big\{(X, Y_1, \cdots, Y_n, M) \in \mathcal{D}_1^* : Y_1 = \cdots = Y_n = M = 0\Big\}.$$

We claim the following.

**Theorem 5.6.** *The EEP, $E_{e1}$, of the model* (5.10) *is GAS in $\mathcal{D}_1 \setminus \mathcal{D}_0$ if $\mathcal{R}_S \geq 1$ and $b_1 \geq \frac{u\lambda_X}{\mu_X X^{**}}$.*

The proof of Theorem 5.6 is given in Appendix E.

It should also be mentioned that the Lyapunov function $\mathcal{F}_4$, used to prove Theorem 5.6 in Appendix E, is similar to the one used in [71], except for a few necessary modifications made to the coefficients of $\mathcal{F}_4$. Furthermore, the condition obtained here

for global stability is in line with that in [71], although a constant rate is used for the concentration of susceptible RBCs.

In summary, the model (5.10) exhibits global asymptotic dynamics at $\mathcal{R}_S = 1$. Thus, the slight change we made to the model in [71], to obtain the model (5.10), does not alter the main qualitative (equilibrium) dynamics of the original model given in [71].

## 5.3 Formulation of Extended Model with Immune Response

The multiple parasitic stage model (5.10) is now extended to incorporate the role of immune response as follows. In addition to the compartments for uninfected RBCs ($X(t)$), $n$ compartments of IRBCs with $n$ different stages of the parasite evolution ($Y_i(t);\ i = 1, \cdots n$), and the compartment for merozoites ($M(t)$), two new compartments of immune cells ($B(t)$) and antibodies ($A(t)$) are added.

The concentration of uninfected RBCs ($X(t)$) is increased by the production of RBCs from the bone marrow (at a rate $\lambda_X$) and decreased by natural death (at a rate $\mu_X$) and infection of RBCs by merozoites (at a rate $\beta$). IRBCs with parasites in stage 1 ($Y_1(t)$) are increased due to the infection of RBCs (at a rate $\beta$) and reduced by natural death (at a rate $\mu_1$), by progression to the compartment of IRBCs infected with the second stage of parasites (at a rate $\gamma_1$) and by killing by immune cells (at a rate $k_1$, where $k_1$ is the immunosensitivity of IRBCs infected with parasites in stage 1) [102].

IRBCs infected with parasites in stage $i$ ($Y_i(t),\ i = 2, \cdots n$) are increased (at a rate $\gamma_i,\ i = 1, \cdots n-1$) and diminished by natural death (at a rate $\mu_i,\ i = 2, \cdots n$), by moving to next stage (at a rate $\gamma_i,\ i = 2, \cdots n$) and by destruction by immune cells (at a rate $k_i,\ i = 2, \cdots n$ where $k_i$ represents the immunosensitivity of IRBCs infected with parasites in stage $i$). The rupture of IRBCs infected with parasites in stage $n$ release merozoites in the bloodstream and $r$ is the average number of merozoites released *per* each bursting IRBC. Merozoites ($M(t)$) are reduced by natural death (at a rate $\mu_M$), by the effect of immune cells (at a rate $k_M$) and by the process of invasion of RBCs by merozoites (at a rate $\beta$).

Immune cells ($B(t)$) are recruited (at a rate $\lambda_B$) and the production of immune cells is stimulated in the presence of IRBCs and merozoites. The parameter $\rho_i$ ($i = 1, \cdots n$) represent the immunogenicity of IRBCs infected with parasites in stage $i$, and $\rho_{n+1}$ models the immunogenicity of merozoites. Immune cells are diminished by natural death (at a rate $\mu_B$). Immune cells secret antibodies in the presence of merozoites, which inhibit the invasion of RBCs by merozoites. The parameter $\eta$ represents the maximum rate of increase of antibodies. It is assumed that antibodies decay at a rate $\mu_A$.

Thus, the extended intra-host model for malaria is given by the following system

of non-linear differential equations.

$$
\begin{aligned}
\frac{dX}{dt} &= \lambda_X - \beta XM - \mu_X X, \\
\frac{dY_1}{dt} &= \beta XM - \mu_1 Y_1 - \gamma_1 Y_1 - k_1 BY_1, \\
\frac{dY_2}{dt} &= \gamma_1 Y_1 - \mu_2 Y_2 - \gamma_2 Y_2 - k_2 BY_2, \\
\frac{dY_3}{dt} &= \gamma_2 Y_2 - \mu_3 Y_3 - \gamma_3 Y_3 - k_3 BY_3, \\
&\cdots \quad \cdots \quad \cdots \\
\frac{dY_n}{dt} &= \gamma_{n-1} Y_{n-1} - \mu_n Y_n - \gamma_n Y_n - k_n BY_n, \\
\frac{dM}{dt} &= r(\mu_n + \gamma_n) Y_n - \mu_M M - k_M BM - u\beta XM, \\
\frac{dB}{dt} &= \lambda_B + B(\rho_1 Y_1 + \rho_2 Y_2 + \cdots + \rho_n Y_n + \rho_{n+1} M) - \mu_B B, \\
\frac{dA}{dt} &= \eta BM - \mu_A A.
\end{aligned}
\tag{5.20}
$$

In summary, the model (5.20) is an extension of the model in [71] by

(a) incorporating two new compartments for the dynamics of immune cells ($B(t)$) and antibodies ($A(t)$);

(b) using a constant growth rate of uninfected RBCs ($\lambda_X$); whereas density-dependent growth rate was used in [71];

(c) using the growth rate of merozoites, given by $r(\gamma_n + \mu_n)$; whereas the rate $r\gamma_n$ was used in [50, 71].

It should be stated that the extended model (5.20) only offers a simple formulation of the immune response to malaria infection *in vivo*. A more detailed formulation, taking

into account a fast-activating but short-acting innate response and a slower-activating but long-acting antibody-like response, is given in [98] (but no mathematical analysis of the resulting model is provided therein).

### 5.3.1 Basic properties

For mathematical convenience, the system (5.20) is split into two parts, namely the RBC and merozoite component (with a total population at time $t$ denoted by $N_1(t)$) and the immune cells and antibodies component (with a total population at time $t$ denoted by $N_2(t)$), so that

$$N_1(t) = X(t) + Y_1(t) + Y_2(t) + \cdots + Y_n(t) + M(t), \tag{5.21}$$

and,

$$N_2(t) = B(t) + A(t). \tag{5.22}$$

Define the following region

$$\mathcal{D}_2 = \left\{(B(t), A(t)) \in \mathbb{R}^2_+ : B \leq \bar{B}, A \leq \bar{A}\right\},$$

where, $\bar{B} = \dfrac{\lambda_B}{\mu_B - K}$, with $K = \rho_{max}\left(\frac{\lambda_X}{\mu_{min}} + \bar{M}\right)$, $\rho_{max} = \max\{\rho_1, \cdots, \rho_{n+1}\}$, $\mu_B > K$ and $\bar{A} = \dfrac{\eta \bar{B} \bar{M}}{\mu_A}$.

**Theorem 5.7.** *The region $\mathcal{D}_E = \mathcal{D}_1 \cup \mathcal{D}_2 \subset \mathbb{R}^{n+2}_+ \times \mathbb{R}^2_+$ is positively-invariant and attracting for the model* (5.20).

*Proof.* Let,

$$(X(t), Y_1(t), Y_2(t), \cdots, Y_n(t), M(t)) \in \mathbb{R}^{n+2}_+, \tag{5.23}$$

be any solution of the RBC and merozoite component of the model (5.20) (*i.e.*, the first $n+1$ equations of (5.20)) with non-negative initial conditions. By Lemma 5.4, $\mathcal{D}_1$ is positively-invariant. A similar reasoning, for the immune cells and antibodies for any non-negative initial solution in $\mathbb{R}^2_+$, yields

$$\limsup_{t\to\infty} B(t) \leq \frac{\lambda_B}{\mu_B - K} = \bar{B}, \tag{5.24}$$

and,

$$\limsup_{t\to\infty} A(t) \leq \frac{\eta \bar{B}\bar{M}}{\mu_A} = \bar{A}. \tag{5.25}$$

It follows from the equation for $\frac{dB}{dt}$ in (5.20) that, if $B > \bar{B}$, then $\frac{dB}{dt} < 0$. Furthermore, it follows from the equation for $\frac{dA}{dt}$ in (5.20) that $\frac{dA}{dt} < 0$ if $A > \bar{A}$. Thus, the vector field (corresponding to the last two equations in (5.20)) points inward (into $\mathcal{D}_2$). Thus, all feasible solutions of the immune cells and antibodies component of the system (5.20) enter the region $\mathcal{D}_2$.

Combining the above results show that all possible solutions of the system (5.20) will enter the region (as $t \to \infty$)

$$\mathcal{D}_E = \mathcal{D}_1 \cup \mathcal{D}_2 \subset \mathbb{R}^{n+2}_+ \times \mathbb{R}^2_+. \tag{5.26}$$

Hence, the region $\mathcal{D}_E$ is positively-invariant and attracting under the flow induced by

the system (5.20). □

### 5.3.2 Stability of DFE

#### Local stability of DFE

The DFE of the extended model (5.20) is given by

$$E_0 = (X^*,\ Y_1^*,\ Y_2^*,\ \cdots,\ Y_n^*,\ \ M^*,\ B^*,\ A^*) = (\lambda_X/\mu_X,\ 0,\ 0,\ \cdots, 0, 0,\ \lambda_B/\mu_B,\ 0). \tag{5.27}$$

The associated non-negative matrix $F_3$ (of new infection terms) and the M-matrix $V_3$ (of the transition terms) of the model (5.20) are given, respectively, by

$$F_3 = \begin{pmatrix} 0 & 0 & 0 & \cdots & 0 & 0 & \frac{\beta\lambda_X}{\mu_X} \\ 0 & 0 & 0 & \cdots & 0 & 0 & 0 \\ 0 & 0 & 0 & \cdots & 0 & 0 & 0 \\ \vdots & \vdots & \vdots & \cdots & \vdots & \vdots & \vdots \\ 0 & 0 & 0 & \cdots & 0 & 0 & 0 \\ 0 & 0 & 0 & \cdots & 0 & 0 & 0 \end{pmatrix},$$

and,

$$V_3 = \begin{pmatrix} P_1 & 0 & 0 & \cdots & 0 & 0 & 0 \\ -\gamma_1 & P_2 & 0 & \cdots & 0 & 0 & 0 \\ 0 & -\gamma_2 & P_3 & \cdots & 0 & 0 & 0 \\ \vdots & \vdots & \vdots & \cdots & \vdots & \vdots & \vdots \\ 0 & 0 & 0 & \cdots & -\gamma_{n-1} & P_n & 0 \\ 0 & 0 & 0 & \cdots & 0 & -r(\mu_n + \gamma_n) & \mu_M + k_M B^* + u\beta X^* \end{pmatrix},$$

where, $P_i = \mu_i + \gamma_i + k_i B^*;\ i = 1, \cdots, n$.

It follows that $\mathcal{R}_0 = \rho(F_3 V_3^{-1})$, where

$$\mathcal{R}_0 = \frac{\beta r \gamma_1 \gamma_2 \cdots \gamma_{n-1}(\gamma_n + \mu_n) X^*}{(\mu_M + k_M B^* + u\beta X^*) P_1 P_2 \cdots P_n}. \tag{5.28}$$

Using Theorem 2 of [136], the following result is established.

**Lemma 5.7.** *The DFE of the extended model* (5.20)*, given by* $E_0$*, is LAS if* $\mathcal{R}_0 < 1$*, and unstable if* $\mathcal{R}_0 > 1$.

Lemma 5.7 implies that the parasite can be cleared from the bloodstream (when $\mathcal{R}_0 < 1$) if the initial sizes of the sub-population of the model are in the basin of attraction of $E_0$. To ensure that clearance of the parasite is independent of the initial sizes of the sub-population, it is necessary to show that the DFE of the model (5.20) given by $E_0$ is GAS in $\mathcal{D}_E$.

**Global stability of DFE for a special case ($k_i = 0$ and $k_M = 0$)**

Here, a global asymptotic stability result will be given for the special case where $k_i(\ i = 1, \cdots, n) = k_M = 0$ (corresponding to the case where the immune response is completely ineffective). It should be noted that the associated reproduction threshold ($\mathcal{R}_0$), given in (5.28), reduces to $\mathcal{R}_S$, given in (5.15), when $k_i\ (i = 1, \cdots, n) = k_M = 0$.

**Theorem 5.8.** *The DFE, $E_0$, of the extended model* (5.20) *is GAS in $\mathcal{D}_E$ if $\mathcal{R}_S \leq 1$ and $k_i\ (i = 1, \cdots, n) = k_M = 0$.*

*Proof.* Using the same Lyapunov function $\mathcal{F}_3$ (for the proof of Theorem 5.5 given in Appendix D), it can be shown that $(X, Y_1, \cdots, Y_n, M)$ converges to $(X^*, 0, \cdots, 0, 0)$ as $t \to \infty$ whenever $\mathcal{R}_S \leq 1$. Using $Y_1 = Y_2 = \cdots = Y_n = 0$ in the equation for $dB/dt$ shows that $B(t) \to B^*$ as $t \to \infty$. Furthermore, using $M = 0$ in the equation for $dA/dt$ shows that $A(t) \to 0$ as $t \to \infty$. Thus, the DFE ($E_0$) of the extended model (5.20) is GAS in $\mathcal{D}_E$ whenever $\mathcal{R}_S \leq 1$ and $k_i\ (i = 1, \cdots, n) = k_M = 0$. □

The above result shows that, for the extended model (5.20) with $k_i = 0$ $(i = 1, \cdots, n)$ and $k_M = 0$, the malaria parasite can be cleared from the bloodstream if the threshold quantity, $\mathcal{R}_S$, can be brought to a value less than unity.

Numerical simulations of the extended model (5.20) (for the aforementioned special case) show convergence to the DFE (Figure 5.2) when $\mathcal{R}_S < 1$ (in line with Theorem 5.8) and to an endemic equilibrium (Figure 5.3; these simulations are for $k_i \neq 0$ and $k_M \neq 0$) when $\mathcal{R}_0 > 1$. Although not established rigorously, these simulation results suggest that the extended model (5.20) has a stable EEP whenever $\mathcal{R}_0 > 1$.

## 5.4 Extended Model with Vaccination

Although there is currently no effective anti-malaria vaccine for humans, a number of candidate vaccines (of varying types and characteristics) are undergoing various stages of clinical trials (see, for instance, [36, 45, 93, 99, 123, 125, 135, 137]). Owing to the numerous failed attempts to design such a vaccine, a future malaria vaccine is expected to be imperfect. However, as noted by [13, 128], even a partially-protective vaccine may be a cost-effective and a critically important public health tool for combatting malaria. As stated above, future malaria vaccines can be of various types with varying characteristics. A few of such potential vaccines are itemized below.

- **Pre-erythrocytic vaccines**

  These vaccines, designed to target sporozoites or *schizont*-infected liver cells, prevent the release of primary merozoites from infected hepatocytes. Preclinical studies indicate that such a vaccine can be designed based on the secretion of antibodies that target sporozoites and block their ability to infect liver cells or by cell-mediated responses that kill parasite-infected hepatocytes before they can release infectious merozoites [67, 111] (see also Sharma and Pathak [125] for a review).

- **Asexual stage vaccines**

  These vaccines target immune responses against the asexual stage (blood stage) of the parasite [35]. The justification for this approach is based on the following observations [14]:

(a) maternal antibodies passively transferred to the fetus may provide a window of protection against clinical malaria;

(b) following repeated attacks of malaria, a majority of infected individuals living in endemic areas acquire the ability to control parasite replication to levels below those that result in clinical disease;

(c) hyper-immune globulin prepared from the sera of individuals chronically infected with malaria can eliminate circulating parasites from *P. falciparum*-infected individuals.

(These vaccines primarily target merozoites).

- **Transmission blocking vaccines**

  Preclinical studies have shown that antibodies directed against several sexual stage antigens can prevent the development of infectious sporozoites in the salivary glands of *Anopheles* mosquitoes [14]. This suggests that such a vaccine may offer an effective mechanism to combat malaria.

In this section, the model (5.20) is extended to include a potential imperfect malaria vaccine with the following assumed characteristics [13, 35, 67, 111]:

(i) blocks transmission of infection (with an efficacy $0 < \tau \leq 1$);

(ii) enhances immune response (at a rate $\theta_B K_i$; with $\theta_B > 1$);

(iii) reduces the number of merozoites released per burst of an IRBC. The modification parameter $0 < \psi < 1$ accounts for this reduction;

(iv) enhances the production of antibodies (at a rate $p\lambda_B$; with $p > 1$).

The effectiveness of these vaccine characteristics (in curtailing the parasite load *in vivo*) will be assessed in Section 5.4.1. Using the above assumptions, the extended model (5.20) can be re-written as

$$\begin{aligned}
\frac{dX}{dt} &= \lambda_X - (1-\tau)\beta XM - \mu_X X,\\
\frac{dY_1}{dt} &= (1-\tau)\beta XM - \mu_1 Y_1 - \gamma_1 Y_1 - \theta_B k_1 B Y_1,\\
\frac{dY_2}{dt} &= \gamma_1 Y_1 - \mu_2 Y_2 - \gamma_2 Y_2 - \theta_B k_2 B Y_2,\\
\frac{dY_3}{dt} &= \gamma_2 Y_2 - \mu_3 Y_3 - \gamma_3 Y_3 - \theta_B k_3 B Y_3,\\
&\cdots \quad \cdots \quad \cdots \qquad (5.29)\\
\frac{dY_n}{dt} &= \gamma_{n-1} Y_{n-1} - \mu_n Y_n - \gamma_n Y_n - \theta_B k_n B Y_n,\\
\frac{dM}{dt} &= r(1-\psi)(\mu_n + \gamma_n) Y_n - \mu_M M - \theta_B k_M B M - u\beta XM,\\
\frac{dB}{dt} &= p\lambda_B + B(\rho_1 Y_1 + + \rho_2 Y_2 + \cdots + \rho_n Y_n + \rho_{n+1} M) - \mu_B B,\\
\frac{dA}{dt} &= \eta BM - \mu_A A,
\end{aligned}$$

where, $0 < \tau < 1$ is the efficacy of vaccine, $\theta_B > 1$ accounts for the assumed vaccine-induced increase in immune response by antibodies. The modification parameter $0 < \psi < 1$ incorporates the reduction of the release of merozoites from hepatocytes due to vaccine and $p > 1$ accounts for the vaccine-induced increase in the production rate of antibodies (see Figure 5.1 for a flow diagram, and Table 5.1 for the description of the variables and parameters of the vaccination model (5.29)).

### 5.4.1 Stability of DFE

#### Local stability of DFE

The DFE of the extended model with vaccination (5.29) is given by

$$E_{0v} = (X^*,\ Y_1^*,\ Y_2^*,\ \cdots,\ Y_n^*,\ M^*,\ B^*,\ A^*) = (\lambda_X/\mu_X,\ 0,\ 0,\ \cdots, 0, 0,\ p\lambda_B/\mu_B,\ 0). \tag{5.30}$$

The associated next generation matrices, $F_4$ and $V_4$, of the model (5.29) are given, respectively, by

$$F_4 = \begin{pmatrix} 0 & 0 & 0 & \cdots & 0 & 0 & \frac{(1-\tau)\beta\lambda_X}{\mu_X} \\ 0 & 0 & 0 & \cdots & 0 & 0 & 0 \\ 0 & 0 & 0 & \cdots & 0 & 0 & 0 \\ \vdots & \vdots & \vdots & \cdots & \vdots & \vdots & \vdots \\ 0 & 0 & 0 & \cdots & 0 & 0 & 0 \\ 0 & 0 & 0 & \cdots & 0 & 0 & 0 \end{pmatrix},$$

and,

$$V_4 = \begin{pmatrix} L_1 & 0 & 0 & \cdots & 0 & 0 & 0 \\ -\gamma_1 & L_2 & 0 & \cdots & 0 & 0 & 0 \\ 0 & -\gamma_2 & L_3 & \cdots & 0 & 0 & 0 \\ \vdots & \vdots & \vdots & \cdots & \vdots & \vdots & \vdots \\ 0 & 0 & 0 & \cdots & -\gamma_{n-1} & L_n & 0 \\ 0 & 0 & 0 & \cdots & 0 & -r(1-\psi)(\mu_n+\gamma_n) & \mu_M + \theta_B k_M B^* + u\beta X^* \end{pmatrix},$$

where, $L_i = \mu_i + \gamma_i + \theta_B k_i B^*$ for $i = 1, \cdots, n$.

It follows that the *vaccination reproduction number*, denoted by $\mathcal{R}_{0v} = \rho(F_4 V_4^{-1})$, is given by

$$\mathcal{R}_{0v} = \frac{(1-\tau)(1-\psi)\beta r \gamma_1 \gamma_2 \cdots \gamma_{n-1}(\gamma_n + \mu_n)X^*}{(\mu_M + \theta_B k_M B^* + u\beta X^*)L_1 L_2 \cdots L_n}. \tag{5.31}$$

Using Theorem 2 of [136], the following result is established.

**Lemma 5.8.** *The DFE of the extended model* (5.29)*, given by* $E_{0v}$*, is LAS if* $\mathcal{R}_{0v} < 1$*, and unstable if* $\mathcal{R}_{0v} > 1$.

### Global stability of DFE for a special case ($k_i$ $(i = 1, \cdots, n) = k_M = u = 0$)

The global asymptotic stability property of the DFE, $E_{0v}$, will be explored for a special case $k_i$ $(i = 1, \cdots, n) = k_M = u = 0$. For this special case, the reproduction number $(\mathcal{R}_{0v})$ reduces to

$$\tilde{\mathcal{R}}_{0v} = \frac{(1-\tau)(1-\psi)\beta r \gamma_1 \gamma_2 \cdots \gamma_{n-1} X^*}{\mu_M Q_1 \cdots Q_{n-1}},$$

where, $Q_i = \gamma_i + \mu_i$ $(i = 1, \cdots, n)$. We claim the following.

**Theorem 5.9.** *Consider the vaccination model* (5.29) *with* $k_i$ $(i = 1, \cdots, n) = k_M = u = 0$*. The DFE,* $E_{0v}$*, is GAS in* $\mathcal{D}_E$ *if* $\tilde{\mathcal{R}}_{0v} \leq 1$.

*Proof.* Consider the Lyapunov function

$$\mathcal{F}_5 = M + r(1-\psi)Y_n + \sum_{m=1}^{n-1} r \prod_{i=m}^{n-1} \frac{\gamma_i(1-\psi)}{Q_i} Y_m,$$

with Lyapunov derivative given by,

$$\dot{\mathcal{F}}_5 = r(1-\psi)(\mu_n+\gamma_n)Y_n - \mu_M M + r(1-\psi)(\gamma_{n-1}Y_{n-1} - Q_nY_n)$$

$$+\left[\frac{r(1-\psi)\gamma_1\gamma_2\cdots\gamma_{n-1}}{Q_1Q_2\cdots Q_{n-1}}\right][(1-\tau)\beta XM - Q_1Y_1] + \left[\frac{r(1-\psi)\gamma_2\gamma_3\cdots\gamma_{n-1}}{Q_2Q_3\cdots Q_{n-1}}\right](\gamma_1Y_1 - Q_2Y_2)$$

$$+\cdots+\left[\frac{r(1-\psi)\gamma_{n-1}}{Q_{n-1}}\right](\gamma_{n-2}Y_{n-2} - Q_{n-1}Y_{n-1}),$$

$$\leq \left[\frac{(1-\tau)(1-\psi)\beta r\gamma_1\gamma_2\cdots\gamma_{n-1}X^*}{Q_1Q_2\cdots Q_{n-1}} - \mu_M\right]M,$$

$$\leq \mu_M\left(\tilde{\mathcal{R}}_{0v} - 1\right)M.$$

Thus, $\dot{\mathcal{F}}_5 \leq 0$ if $\tilde{\mathcal{R}}_{0v} \leq 1$ with $\dot{\mathcal{F}}_5 = 0$ if and only if $M = 0$. Hence, $Y_i$, $(i = 1,\cdots,n) \to 0$ as $t \to \infty$. Using this fact in the equation for $\frac{dB}{dt}$ in (5.29) shows that $B(t) \to B^* = \frac{p\lambda_B}{\mu_B}$ as $t \to \infty$. Further, it follows from the equation for $\frac{dA}{dt}$ in (5.29) that $A(t) \to 0$ as $t \to \infty$. Thus, the DFE $(E_{0v})$ of the extended model (5.29) is GAS in $\mathcal{D}_E$ whenever $\tilde{\mathcal{R}}_{0v} \leq 1$ and $k_i$ $(i = 1,\cdots,n) = k_M = 0 = u = 0$. □

### Critical vaccine efficacy

Solving for $\tau$ from the expression for $\tilde{\mathcal{R}}_{0v} = 1$ gives

$$\tau_c = 1 - \frac{\mu_M Q_1 \cdots Q_{n-1}}{(1-\psi)\beta r \gamma_1 \gamma_2 \cdots \gamma_{n-1} X^*}.$$

We have the following result.

**Lemma 5.9.** *The reproduction threshold $\tilde{\mathcal{R}}_{0v} < 1$ whenever $\tau > \tau_c$.*

The implication of this result is that if the efficacy of the vaccine is greater than $\tau_c$, then the parasite can be cleared from the blood stream (since $\tilde{\mathcal{R}}_{0v} < 1$ in this case, and Theorem 5.9 guarantees the clearance of the parasite *in vivo* if $\tilde{\mathcal{R}}_{0v} < 1$). This result (Lemma 5.9) is illustrated in Figure 5.4 using different $\tau$ values. Based on the parameter values used to generate Figure 5.4, a vaccine with a minimum efficacy of 87.85% is needed to effectively control the parasite load *in vivo*.

### Assessment of vaccine impact

To see the effect of various vaccine parameters on the vaccinated reproduction number, $\mathcal{R}_{0v}$, associated with the vaccination model (5.29), an analysis on the associated reproduction threshold ($\mathcal{R}_{0v}$) is carried out as follows. Differentiating $\mathcal{R}_{0v}$ partially with respect to vaccine efficacy ($\tau$) gives (note that $0 < \psi < 1$)

$$\frac{\partial \mathcal{R}_{0v}}{\partial \tau} = \frac{-\gamma_1 \gamma_2 \cdots \gamma_{n-1} \beta r (1-\psi)(\gamma_n + \mu_n) X^*}{L_1 L_2 \cdots L_n (\mu_M + \theta_B k_M B^* + u\beta X^*)} < 0,$$

from which it follows that $\mathcal{R}_{0v}$ is a decreasing function of $\tau$ (i.e., $\mathcal{R}_{0v}$ decreases as the vaccine efficacy, $0 < \tau < 1$, increases). Since a reduction in $\mathcal{R}_{0v}$ implies a reduction in the concentration of IRBCs, it follows that a vaccine with high enough efficacy will significantly reduce the concentration of IRBCs *in vivo*. Figure 5.5 shows the profiles of the total concentration of infected RBCs as a function of $\tau$, from which it is evident that the number of IRBCs decreases with increasing values of $\tau$.

Furthermore, the effect of vaccine-induced reduction of merozoite is monitored by differentiating $\mathcal{R}_{0v}$ partially with respect to the associated parameter $\psi$. This gives (note that $0 < \tau < 1$)

$$\frac{\partial \mathcal{R}_{0v}}{\partial \psi} = \frac{-\gamma_1\gamma_2\cdots\gamma_{n-1}\beta r(1-\tau)(\gamma_n+\mu_n)X^*}{L_1L_2\cdots L_n(\mu_M+\theta_B k_M B^*+u\beta X^*)} < 0.$$

Thus, $\mathcal{R}_{0v}$ decreases with increasing $\psi$. That is, if the vaccine reduces the number of merozoites released per burst of an IRBC, the reproduction number $\mathcal{R}_{0v}$ decreases. The effect of such a vaccine-induced reduction of merozoites released on the total concentration of IRBCs is depicted in Figure 5.6. (showing a marked decrease in the concentration of IRBCs with increasing $\psi$).

Finally, the effect of vaccine-induced enhanced immune response is monitored by differentiating $\mathcal{R}_{0v}$ partially with respect to $\theta_B$ giving

$$\frac{\partial \mathcal{R}_{0v}}{\partial \theta_B} = \frac{-H_1H_3}{H_4} < 0,$$

where,

$$H_1 = (1-\tau)(1-\psi)\beta r\gamma_1\gamma_2\cdots\gamma_{n-1}(\gamma_n+\mu_n)X^* > 0,$$

$$H_2 = \mu_M + \theta_B k_M B^* + u\beta X^* > 0,$$

$$H_3 = k_M B^* L_1 L_2 \cdots L_n + H_2 B^*(k_1 L_2 \cdots L_n + k_2 L_1 L_3 \cdots L_n + \cdots + k_n L_1 \cdots L_{n-1}) > 0,$$

$$H_4 = H_2 L_1 L_2 \cdots L_n > 0.$$

Thus, $\mathcal{R}_{0v}$ decreases with increasing $\theta_B$. Figure 5.7 shows a reduction of the total concentration of IRBCs with increasing $\theta_B$.

## 5.5 Summary

The chapter considers the problem of the modelling and analysis of the in-host dynamics of malaria. The basic model of Anderson *et al.* [3] was considered first of all, where a complete rigorous analysis of its associated equilibria was provided. The model was then extended along the lines of the Iggidr *et al.* [71] formulation, which incorporates multiple parasitic stages. Here, too, detailed analyses are given. Finally, the extended model was further extended to incorporate the roles of immune response and a potential (imperfect) vaccine on malaria dynamics *in vivo*. The main theoretical and numerical results obtained are itemized below.

(i) the Anderson *et al.* model (5.1) has a globally-asymptotically stable disease-free equilibrium whenever the associated reproduction threshold ($\mathcal{R}_A$) is less than unity; and it has a unique and globally-asymptotically stable endemic equilibrium

whenever $\mathcal{R}_A$ exceeds unity;

(ii) the model with multiple parasitic stages, but without immune and antibody responses, given by (5.10), exhibits global dynamics at $\mathcal{R}_S = 1$ (i.e., the model without antibodies and immune cells has a globally-asymptotically stable disease-free equilibrium whenever $\mathcal{R}_S < 1$; and a globally-asymptotically stable endemic equilibrium whenever $\mathcal{R}_S > 1$);

(iii) the extended model with immune response, given by (5.20), has a globally-asymptotically stable disease-free equilibrium whenever the associated reproduction number ($\mathcal{R}_S$) is less than unity and $k_i$ $(i = 1, \cdots, n) = k_M = 0$. Further, numerical simulations suggest that this model with immune response (5.20) has a stable endemic equilibrium whenever $\mathcal{R}_0 > 1$;

(iv) the extended model with immune response and vaccination, given by (5.29), has a globally-asymptotically stable disease-free equilibrium whenever the associated reproduction number ($\tilde{\mathcal{R}}_{0v}$) is less than unity and $k_i$ $(i = 1, \cdots, n) = k_M = u = 0$;

(v) an analysis of the threshold ($\mathcal{R}_{0v}$) of the extended vaccination model with immune response (5.29) shows the following.

  (a) a future malaria vaccine with efficacy $0 < \tau < 1$ will reduce IRBC concentration; and such reduction increases with increasing values of vaccine efficacy ($\tau$). Numerical simulations show that a vaccine efficacy of at least 87.85% is needed to effectively control the malaria parasite load *in vivo*;

(b) a malaria vaccine that decreases the number of merozoites released per bursting IRBC will reduce IRBC concentration *in vivo*;

(c) a malaria vaccine that increases immune response will decrease IRBC concentration *in vivo*.

| Variables and Parameters | Description |
|---|---|
| $X(t)$ | Concentration of uninfected red blood cells |
| $Y_i(t)$ | Concentration of infected red blood cells with parasite in stage $i$ |
| $M(t)$ | Concentration of merozoites |
| $B(t)$ | Concentration of immune cells |
| $A(t)$ | Concentration of antibodies |
| $\lambda_X$ | Production rate of RBCs from the bone marrow |
| $\lambda_B$ | Production rate of immune cells |
| $\mu_X$ | Natural death rate of uninfected RBCs |
| $\mu_{Y_i}$ | Natural death rate of infected RBCs |
| $\mu_M$ | Natural death rate of merozoites |
| $\mu_B$ | Death rate of immune cells |
| $\mu_A$ | Deterioration rate of antibodies |
| $\beta$ | Rate of infection |
| $\gamma_i$ | Progression rate of IRBCs from Stage $(i)$ to Stage $(i+1)$ |
| $k_i$ | Immunosensitivity of IRBCs |
| $k_M$ | Immunosensitivity of merozoites |
| $\rho_i$ | immunogenicity of IRBCs and merozoites |
| $\eta$ | Maximum rate of increase of antibodies |
| $r$ | Number of merozoites released per bursting IRBC |
| Vaccine-related Parameters | |
| $\tau$ | Efficacy of vaccine |
| $\psi$ | Modification parameter accounting for vaccine-induced reduction of merozoites released per bursting IRBC |
| $\theta_B$ | Modification parameter accounting for vaccine-induced enhanced immune response |
| $p$ | Modification parameter accounting for vaccine-induced enhanced production of antibodies |

Table 5.1: Description of variables and parameters of the model (5.29).

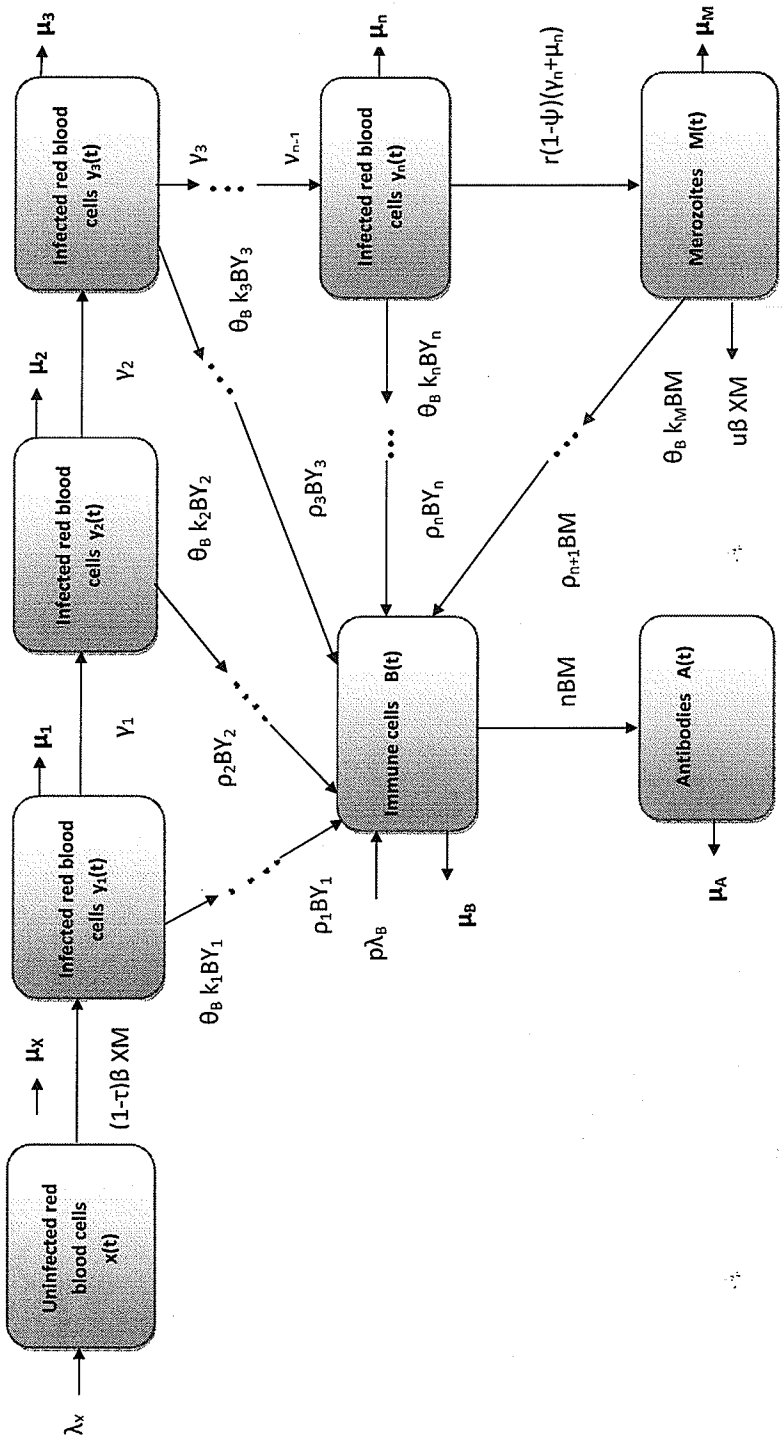


Figure 5.1: Schematic diagram of the extended vaccination model (5.29).

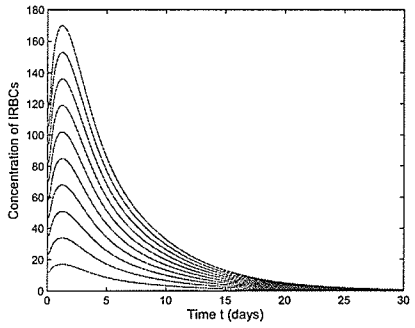


(a)

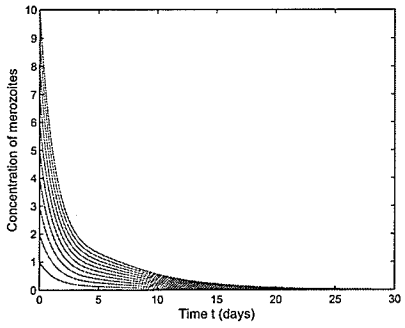


(b)

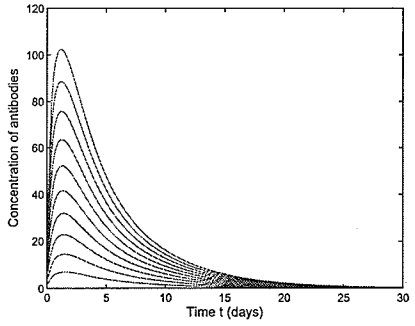


(c)

Figure 5.2: Simulations of the model (5.20) (with $k_i = 0,\ i = 1, \cdots, 5$ and $k_M = 0$) showing the concentrations of (a) IRBCs (b) merozoites and (c) antibodies as a function of time for $\mathcal{R}_S < 1$. Parameter values used are: $\lambda_X = 41664,\ \beta = 0.0008,\ \mu_X = 0.8,\ \mu_1 = 0.5,\ \mu_2 = 0.5,\ \mu_3 = 0.5,\ \mu_4 = 0.5,\ \mu_5 = 1.0,\ \mu_M = 3.0,\ \mu_B = 1.53,\ \mu_A = 0.4,\ \gamma_1 = 0.3,\ \gamma_2 = 0.3,\ \gamma_3 = 0.3,\ \gamma_4 = 0.3,\ \gamma_5 = 0.3,\ \rho_1 = 0.001,\ \rho_2 = 0.00001,\ \rho_3 = 0.00001,\ \rho_4 = 0.00001,\ \rho_5 = 0.00001,\ \rho_6 = 0.00001,\ \eta = 0.6,\ \lambda_B = 30,\ r = 16$ and $u = 1$ (so that, $\mathcal{R}_S = 0.2952$).

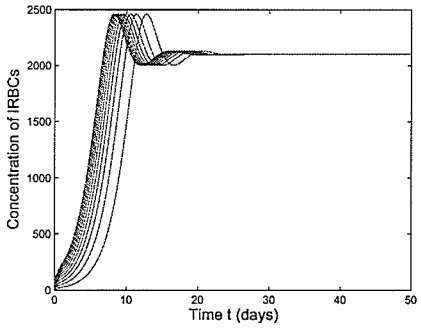


(a)

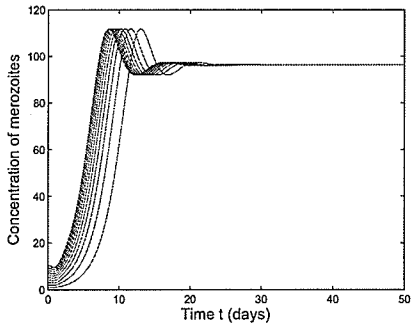


(b)

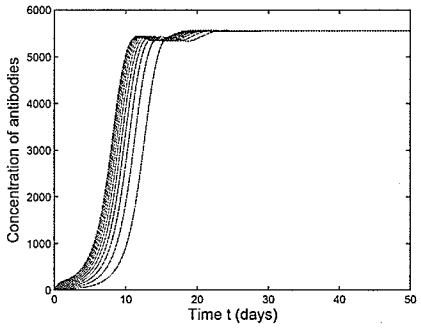


(c)

Figure 5.3: Simulations of the model (5.20) showing the concentrations of (a) IRBCs (b) merozoites and (c) antibodies as a function of time for $\mathcal{R}_0 > 1$. Parameter values used are: $\lambda_X = 41664$, $\beta = 0.0008$, $\mu_X = 0.8$, $\mu_1 = 0.5$, $\mu_2 = 0.5$, $\mu_3 = 0.5$, $\mu_4 = 0.5$, $\mu_5 = 1.0$, $\mu_M = 3.0$, $\mu_B = 1.53$, $\mu_A = 0.4$, $k_1 = 0.01$, $k_2 = 0.01$, $k_3 = 0.01$, $k_4 = 0.01$, $k_5 = 0.01$, $k_M = 0.3$, $\gamma_1 = 1.5$, $\gamma_2 = 1.5$, $\gamma_3 = 1.5$, $\gamma_4 = 1.5$, $\gamma_5 = 1.5$, $\rho_1 = 0.001$, $\rho_2 = 0.00001$, $\rho_3 = 0.00001$, $\rho_4 = 0.00001$, $\rho_5 = 0.00001$, $\rho_6 = 0.00001$, $\eta = 0.6$, $\lambda_B = 30$, $r = 16$ and $u = 1$ (so that, $\mathcal{R}_0 = 2.6618$).

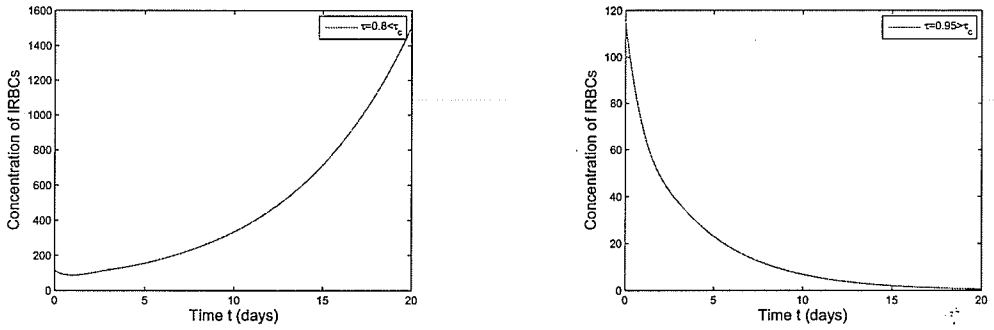


(a) $\tau < \tau_c$ (b) $\tau > \tau_c$

Figure 5.4: Simulations of the model (5.29) showing the concentrations of IRBCs for (a) $\tau = 0.8 < \tau_c = 0.8785$ and (b) $\tau = 0.95 > \tau_c = 0.8785$ using: $\lambda_X = 41664$, $\beta = 0.0005$, $\mu_X = 0.8$, $\mu_1 = 0.5$, $\mu_2 = 0.5$, $\mu_3 = 0.5$, $\mu_4 = 0.5$, $\mu_5 = 1.0$, $\mu_M = 5.0$, $\mu_B = 1.53$, $\mu_A = 0.4$, $k_i = 0$, $\gamma_1 = 1$, $\gamma_2 = 1$, $\gamma_3 = 1$, $\gamma_4 = 1$, $\gamma_5 = 1$, $\rho_1 = 0.001$, $\rho_2 = 0.00001$, $\rho_3 = 0.00001$, $\rho_4 = 0.00001$, $\rho_5 = 0.00001$, $\rho_6 = 0.00001$, $\eta = 0.6$, $\lambda_B = 30$, $r = 16$ $\theta_B = 1.5$, $p = 1.2$, $\psi = 0.5$ and $u = 0$.

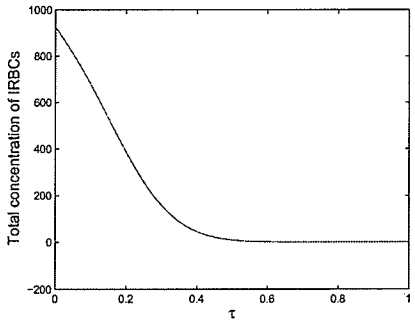


Figure 5.5: Simulations of the model (5.29) showing the total concentration of IRBCs as a function of vaccine efficacy ($0 < \tau < 1$). Parameter values used are: $\lambda_X = 41664$, $\beta = 0.0008$, $\mu_X = 0.8$, $\mu_1 = 0.5$, $\mu_2 = 0.5$, $\mu_3 = 0.5$, $\mu_4 = 0.5$, $\mu_5 = 1.0$, $\mu_M = 3.0$, $\mu_B = 1.53$, $\mu_A = 0.4$, $k_1 = 0.01$, $k_2 = 0.01$, $k_3 = 0.01$, $k_4 = 0.01$, $k_5 = 0.01$, $k_M = 0.3$, $\gamma_1 = 1.5$, $\gamma_2 = 1.5$, $\gamma_3 = 1.5$, $\gamma_4 = 1.5$, $\gamma_5 = 1.5$, $\rho_1 = 0.001$, $\rho_2 = 0.00001$, $\rho_3 = 0.00001$, $\rho_4 = 0.00001$, $\rho_5 = 0.00001$, $\rho_6 = 0.00001$, $\eta = 0.6$, $\lambda_B = 30$, $\psi = 0.2$, $\theta_B = 1.2$, $p = 1.5$, $r = 16$ and $u = 1$.

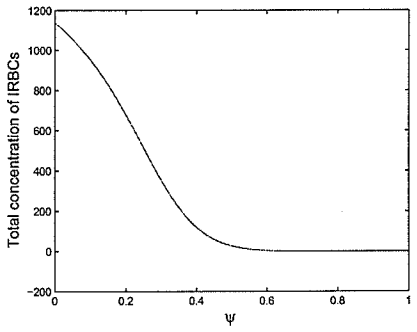


Figure 5.6: Simulations of the model (5.29) showing the total concentration of IRBCs as a function of accounting for vaccine-induced reduction of merozoite released $0 < \psi < 1$. Parameter values used are: $\lambda_X = 41664$, $\beta = 0.0008$, $\mu_X = 0.8$, $\mu_1 = 0.5$, $\mu_2 = 0.5$, $\mu_3 = 0.5$, $\mu_4 = 0.5$, $\mu_5 = 1.0$, $\mu_M = 3.0$, $\mu_B = 1.53$, $\mu_A = 0.4$, $k_1 = 0.01$, $k_2 = 0.01$, $k_3 = 0.01$, $k_4 = 0.01$, $k_5 = 0.01$, $k_M = 0.3$, $\gamma_1 = 1.5$, $\gamma_2 = 1.5$, $\gamma_3 = 1.5$, $\gamma_4 = 1.5$, $\gamma_5 = 1.5$, $\rho_1 = 0.001$, $\rho_2 = 0.00001$, $\rho_3 = 0.00001$, $\rho_4 = 0.00001$, $\rho_5 = 0.00001$, $\rho_6 = 0.00001$, $\eta = 0.6$, $\lambda_B = 30$, $\tau = 0.1$, $\theta_B = 1.2$, $p = 1.5$, $r = 16$ and $u = 1$.

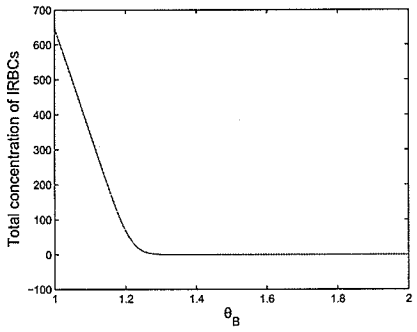


Figure 5.7: Simulations of the model (5.29) showing the total concentration of IRBCs as a function of parameter governing vaccine-induced enhanced immune response $\theta_B > 1$. Parameter values used are: $\lambda_X = 41664$, $\beta = 0.0008$, $\mu_X = 0.8$, $\mu_1 = 0.5$, $\mu_2 = 0.5$, $\mu_3 = 0.5$, $\mu_4 = 0.5$, $\mu_5 = 1.0$, $\mu_M = 3.0$, $\mu_B = 1.53$, $\mu_A = 0.4$, $k_1 = 0.01$, $k_2 = 0.01$, $k_3 = 0.01$, $k_4 = 0.01$, $k_5 = 0.01$, $k_M = 0.3$, $\gamma_1 = 1.5$, $\gamma_2 = 1.5$, $\gamma_3 = 1.5$, $\gamma_4 = 1.5$, $\gamma_5 = 1.5$, $\rho_1 = 0.001$, $\rho_2 = 0.00001$, $\rho_3 = 0.00001$, $\rho_4 = 0.00001$, $\rho_5 = 0.00001$, $\rho_6 = 0.00001$, $\eta = 0.6$, $\lambda_B = 30$, $\tau = 0.1$, $\psi = 0.5$, $p = 1.5$, $r = 16$ and $u = 1$.

# Chapter 6

# Population Model with Repeated Exposure to Malaria

## 6.1 Introduction

An important feature of malaria disease is that, in regions where it is endemic, humans develop natural immunity to malaria after several exposures; and such immunity has a large effect on how the disease spreads in such regions [9, 10, 32, 124]. In this state, the (immune) humans no longer show symptoms of malaria. The process of acquiring such immunity is slow, and may take years or decades to develop [70]. Low level exposure to infection acts as vaccination, leading to the development of immunity against the disease [46]. Humans are susceptible to re-infections because the acquired immunity may wane over time [134]. Children living in endemic areas become infected early in life, and experience more severe disease symptoms during the first five years of life

[124]. But as their immunity develops, the disease becomes less severe and the number of parasites circulating in the blood declines. The acquired immune response to malaria is strain-specific, and is lost if a person moves away from a malaria endemic area [124]. Owing to the aforementioned significance of natural immunity on disease spread, it is instructive, therefore, to carry out a detailed modelling study to quantify the impact of such immunity on the control of malaria transmission in a community.

Numerous mathematical models have been used to study the dynamics of malaria at population level (see, for instance, [6, 9, 10, 32, 75, 76, 107, 108]). Dietz *et al.* [32] studied the effect of acquired immunity in malaria using a deterministic model, by noting that the duration of acquired immunity in humans depends on repeated exposure (that is, immunity is boosted by exposure to infection repeatedly [9, 10]). Further, there are three aspects of immunity that are acquired at different rates; namely: loss of infectivity, increase in recovery, and decrease in detectability. This chapter extends some earlier malaria modelling studies by constructing a new comprehensive model that includes multiple infected and recovered classes (to account for the effect of repeated exposure to infection). The model can be formulated using $n$ exposure classes, but for mathematical tractability (of the associated mathematical analyses), three exposure classes will be considered in this thesis. Unlike in Aron [9], the model to be designed incorporates disease-induced death.

## 6.2 Formulation of Basic Repeated Exposure Model

To formulate the basic repeated exposure model for malaria transmission dynamics, the total human population at time $t$, denoted by $N_H(t)$, is sub-divided into seven mutually-exclusive sub-populations of susceptible humans ($S_H(t)$), first-time infected humans ($I_1(t)$), humans who recovered from first infection ($R_1(t)$), second-time infected humans ($I_2(t)$), humans who recovered from second infection ($R_2(t)$), third-time infected humans ($I_3(t)$) and humans recovered from third infection ($R_3(t)$), so that

$$N_H(t) = S_H(t) + I_1(t) + R_1(t) + I_2(t) + R_2(t) + I_3(t) + R_3(t).$$

Similarly, the total vector population at time $t$, denoted by $N_V(t)$, is split into susceptible ($S_V(t)$) and infected ($I_V(t)$) vectors. Hence,

$$N_V(t) = S_V(t) + I_V(t).$$

### Incidence Functions

Since mosquitoes bite both susceptible and infected humans, it is assumed that the average number of mosquito bites received by humans depends on the total sizes of the populations of mosquitoes and humans in the community [15]. Further, it is assumed that $C_{HV}$ represents the per capita biting rate of mosquitoes on a host; and the human hosts are always sufficient in abundance. Thus, it is reasonable to assume that the biting rate $C_{HV}$ is constant as female mosquitoes have a certain number of blood meals over their life time. Let $C_{VH}$ be the rate at which bites are received by a single host per

unit time. Thus, for the number of bites to be conserved, the following conservation law must hold (i.e., the total number of bites by mosquitoes equals to the total number of bites received by humans),

$$C_{HV}N_V = C_{VH}(N_H, N_V)N_H, \tag{6.1}$$

so that,

$$N_V = \frac{C_{VH}(N_H, N_V)}{C_{HV}}N_H. \tag{6.2}$$

Let $\beta_M C_{VH}$ be the effective contact rate between a susceptible human and infectious mosquitoes, where $\beta_M$ is the transmission probability per contact from an infectious mosquito to a susceptible human. Similarly, let $\beta_H C_{HV}$ be the effective contact rate between a susceptible mosquito and infectious humans, where $\beta_H$ is the transmission probability per contact from an infectious human to a susceptible mosquito. Thus, susceptible humans acquire infection, following effective contact with an infectious vector, at a rate $\lambda_M$, given by

$$\lambda_M = \frac{\beta_M C_{VH}(N_H, N_V)}{N_V}I_V. \tag{6.3}$$

Using (6.2) in (6.3) gives

$$\lambda_M = \frac{\beta_M C_{HV}}{N_H}I_V. \tag{6.4}$$

Similarly, susceptible mosquitoes can acquire infection following contact with infected humans in classes $I_1$, $I_2$ and $I_3$. Let $\beta_H C_{HV}$ be the effective contact rate between a

susceptible mosquito and infectious humans (where $\beta_H$ and $C_{HV}$ are as defined before). It is assumed that individuals who are re-infected are less infectious than those with primary infection. Thus, the rate at which mosquitoes acquire infection from infectious human hosts is given by

$$\lambda_H = \frac{\beta_H C_{HV}}{N_H}(I_1 + \phi_1 I_2 + \phi_2 I_3), \tag{6.5}$$

where $0 < \phi_1 < 1$ and $0 < \phi_2 < 1$ account for the assumed reduction of infectiousness of individuals who have had second or third infection, respectively, in comparison to individuals who were infected only once (*i.e.*, it is assumed that individuals with enhanced immunity, due to repeated exposure, are less infectious than first-time infected individuals).

The susceptible human population is generated by the recruitment of humans (by birth or immigration; and assumed susceptible) into the community (at a rate $\Pi_H$) and the loss of infection-acquired immunity by individuals who recovered from first (primary) infection (at a rate $\psi_1$). The susceptible population is decreased by infection (at the rate $\lambda_M$) and natural death (at a rate $\mu_H$; all human sub-populations are assumed to suffer natural death at the rate $\mu_H$). Thus, the rate of change of the susceptible human population is given by

$$\frac{dS_H}{dt} = \Pi_H + \psi_1 R_1 - \lambda_M S_H - \mu_H S_H.$$

The population of first-time infected humans is increased by the infection of sus-

ceptible humans (at the rate $\lambda_M$) and diminished by natural death (at the rate $\mu_H$), disease-induced death (at a rate $\delta_H$) and recovery or acquisition of infection-acquired immunity (at a rate $\gamma_1$), so that

$$\frac{dI_1}{dt} = \lambda_M S_H - \mu_H I_1 - \delta_H I_1 - \gamma_1 I_1.$$

First-time infected individuals who recovered (acquire immunity) from the disease are moved to a new compartment ($R_1$) of individuals who recovered from the first infection (at the rate $\gamma_1$). Furthermore, individuals who recovered from second infection ($R_2$ class) lose their infection-acquired immunity (at a rate $\psi_2$) and move to the $R_1$ class. The $R_1$ population is decreased by natural death (at the rate $\mu_H$), loss of immunity (at the rate $\psi_1$), and by re-infection (at a rate $\sigma_1\lambda_M$, with the modification parameter $0 < \sigma_1 < 1$ accounting for the reduced probability of acquisition of infection by recovered individuals due to their prior infection-acquired immunity). Hence,

$$\frac{dR_1}{dt} = \gamma_1 I_1 + \psi_2 R_2 - \mu_H R_1 - \psi_1 R_1 - \sigma_1 \lambda_M R_1.$$

The population of second-time infected humans is increased by the re-infection of individuals who recovered from first infection (at the rate $\sigma_1\lambda_M$) and diminished by natural death (at the rate $\mu_H$), disease-induced death rate (at a reduced rate $\theta_1\delta_H$, where $0 < \theta_1 < 1$ accounts for the assumed reduction in mortality of individuals with second infection in relation to those with first infection; in other words, it is assumed that repeated exposure (infection) reduces mortality rate) and by acquisition of immunity

or recovery (at a rate $\gamma_2$). Thus,

$$\frac{dI_2}{dt} = \sigma_1 \lambda_M R_1 - \mu_H I_2 - \theta_1 \delta_H I_2 - \gamma_2 I_2.$$

Second-time infected individuals acquire immunity (at the rate $\gamma_2$) and move to the class of individuals who recovered from the second infection ($R_2$). Recovered individuals in the class $R_3$ lose their immunity (at a rate $\psi_3$) and move to the $R_2$ class. The population of individuals who recovered from the second infection is reduced by natural death (at the rate $\mu_H$), loss of immunity (at the rate $\psi_2$) and by re-infection (at a rate $\sigma_2 \lambda_M$, where $0 < \sigma_2 < 1$ is a modification parameter), so that

$$\frac{dR_2}{dt} = \gamma_2 I_2 + \psi_3 R_3 - \mu_H R_2 - \psi_2 R_2 - \sigma_2 \lambda_M R_2.$$

It should be mentioned that the modification parameters $\sigma_1$ and $\sigma_2$ are such that $0 < \sigma_2 < \sigma_1 < 1$, due to the assumption that second-time recovered individuals get re-infected at a lower rate than first-time recovered individuals (because of the repeated exposure-enhanced immunity status of the former in comparison to the latter).

The population of third-time infected humans is increased by the re-infection of recovered individuals in the $R_2$ class (at the rate $\sigma_2 \lambda_M$) and is reduced by natural death (at the rate $\mu_H$), disease-induced death rate (at a reduced rate $\theta_2 \delta_H$, with $0 < \theta_2 < \theta_1 < 1$) and by the acquisition of immunity (at a rate $\gamma_3$). Thus,

$$\frac{dI_3}{dt} = \sigma_2 \lambda_M R_2 - \mu_H I_3 - \theta_2 \delta_H I_3 - \gamma_3 I_3.$$

Third-time infected individuals acquire immunity (at the rate $\gamma_3$) and move to the $R_3$ class. The population of individuals in the $R_3$ class is reduced by natural death (at the rate $\mu_H$) and loss of immunity (at the rate $\psi_3$, assumed negligible). Hence,

$$\frac{dR_3}{dt} = \gamma_3 I_3 - \mu_H R_3 - \psi_3 R_3.$$

Thus, it is assumed that individuals in the $R_3$ class have the highest possible exposure-induced immunity (and would take long time before such immunity is completely lost). Further, unlike in [9, 10], it is assumed that recovered individuals (in the $R_1$, $R_2$ and $R_3$ classes) do not transmit infection (while they are in these classes).

Susceptible mosquitoes are generated at a rate $\Pi_V$ and reduced by infection, following effective contact with infected humans, at the rate $\lambda_H$. All vector populations suffer natural death at a rate $\mu_V$. Thus, the rate of change of the susceptible vector population is given by

$$\frac{dS_V}{dt} = \Pi_V - \lambda_H S_V - \mu_V S_V.$$

Infected vectors are generated by the infection of susceptible mosquitoes (at the rate $\lambda_H$) and reduced by natural death (at the rate $\mu_V$) and disease-induced death (at a rate $\delta_V$). Thus,

$$\frac{dI_V}{dt} = \lambda_H S_V - \mu_H I_V - \delta_V I_V.$$

In summary, the repeated exposure immunity model for malaria is given by the following deterministic system of non-linear differential equations (see Figure 6.1 for a flow diagram and Tables 6.1 and 6.2 for the description of the variables and parameters

of the model).

$$
\begin{aligned}
\frac{dS_H}{dt} &= \Pi_H + \psi_1 R_1 - \lambda_M S_H - \mu_H S_H, \\
\frac{dI_1}{dt} &= \lambda_M S_H - \mu_H I_1 - \delta_H I_1 - \gamma_1 I_1, \\
\frac{dR_1}{dt} &= \gamma_1 I_1 + \psi_2 R_2 - \mu_H R_1 - \psi_1 R_1 - \sigma_1 \lambda_M R_1, \\
\frac{dI_2}{dt} &= \sigma_1 \lambda_M R_1 - \mu_H I_2 - \theta_1 \delta_H I_2 - \gamma_2 I_2, \\
\frac{dR_2}{dt} &= \gamma_2 I_2 + \psi_3 R_3 - \mu_H R_2 - \psi_2 R_2 - \sigma_2 \lambda_M R_2, \\
\frac{dI_3}{dt} &= \sigma_2 \lambda_M R_2 - \mu_H I_3 - \theta_2 \delta_H I_3 - \gamma_3 I_3, \\
\frac{dR_3}{dt} &= \gamma_3 I_3 - \mu_H R_3 - \psi_3 R_3, \\
\frac{dS_V}{dt} &= \Pi_V - \lambda_H S_V - \mu_V S_V, \\
\frac{dI_V}{dt} &= \lambda_H S_V - \mu_V I_V - \delta_V I_V.
\end{aligned}
\tag{6.6}
$$

The model (6.6) extends some other models in the literature, such as those in [9, 32, 134], by:

(i) incorporating three compartments for infected and recovered human populations, to account for repeated exposure to malaria;

(ii) incorporating that infectious individuals with second or third infections transmit the disease at a lower rate than those with primary infection;

(iii) incorporating that re-infection of recovered individuals occur at a lower rate ($0 < \sigma_1, \sigma_2 < 1$) than primary infection (i.e., probability of re-infection decreases with increasing number of exposure);

(iv) incorporating that infectious individuals with second or third infection suffer disease-induced mortality at a lower rate than those with primary infection (i.e., repeated exposure reduces mortality rate).

Further, unlike in the aforementioned modelling studies, detailed rigorous mathematical analysis of the model (6.6) will be provided.

### 6.2.1 Basic properties

Since the model (6.6) monitors human and mosquito populations, all its associated parameters and state variables are assumed to be non-negative for $t \geq 0$. We claim the following result.

**Lemma 6.1.** *The closed set*

$$\mathcal{D} = \left\{ (S_H, I_1, R_1, I_2, R_2, I_3, R_3, S_V, I_V) \in \mathbb{R}_+^9 : \right.$$
$$\left. S_H + I_1 + R_1 + I_2 + R_2 + I_3 + R_3 \leq \frac{\Pi_H}{\mu_H};\ S_V + I_V \leq \frac{\Pi_V}{\mu_V} \right\}$$

*is positively-invariant and attracting.*

*Proof.* Adding the first seven and the last two equations of the model (6.6) gives, respectively,

$$\begin{aligned} \frac{dN_H}{dt} &= \Pi_H - \mu_H N_H - (\delta_H I_1 + \theta_1 \delta_H I_2 + \theta_2 \delta_H I_3), \\ \frac{dN_V}{dt} &= \Pi_V - \mu_V N_V - \delta_V I_V. \end{aligned} \tag{6.7}$$

Since $dN_H/dt \leq \Pi_H - \mu_H N_H$ and $dN_V/dt \leq \Pi_V - \mu_V N_V$, it follows that $dN_H/dt \leq 0$ and $dN_V/dt \leq 0$ if $N_H(t) \geq \frac{\Pi_H}{\mu_H}$ and $N_V(t) \geq \frac{\Pi_V}{\mu_V}$, respectively. Thus, $N_H(t) \leq N_H(0)e^{-\mu_H t} + \frac{\Pi_H}{\mu_H}(1 - e^{-\mu_H t})$ and $N_V(t) \leq N_V(0)e^{-\mu_V t} + \frac{\Pi_V}{\mu_V}(1 - e^{-\mu_V t})$. In particular, $N_H(t) \leq \frac{\Pi_H}{\mu_H}$ if $N_H(0) \leq \frac{\Pi_H}{\mu_H}$ and $N_V(t) \leq \frac{\Pi_V}{\mu_V}$ if $N_V(0) \leq \frac{\Pi_V}{\mu_V}$, respectively. Thus, the region $\mathcal{D}$ is positively-invariant. Further, if $N_H(0) > \frac{\Pi_H}{\mu_H}$ and $N_V(0) > \frac{\Pi_V}{\mu_V}$, then either the solution enters $\mathcal{D}$ in finite time, or $N_H(t)$ approaches $\frac{\Pi_H}{\mu_H}$ and $N_V(t)$ approaches $\frac{\Pi_V}{\mu_V}$ asymptotically [52]. Hence, the region $\mathcal{D}$ attracts all solutions in $\mathbb{R}^9_+$. □

Since the region $\mathcal{D}$ is positively-invariant and attracting, it is sufficient to consider the dynamics of the flow generated by the model (6.6) in $\mathcal{D}$.

### 6.2.2 Stability of DFE

The DFE of the model (6.6) is given by

$$E_0 = (S_H^*,\ I_1^*,\ R_1^*,\ I_2^*,\ R_2^*,\ I_3^*,\ R_3^*,\ S_V^*,\ I_V^*) = (\Pi_H/\mu_H,\ 0,\ 0,\ 0,\ 0,\ 0,\ 0,\ \Pi_V/\mu_V,\ 0). \tag{6.8}$$

The local stability of $E_0$ will be explored using the next generation operator method [136]. The associated non-negative matrix, $F$, of new infection terms and the $M$-matrix, $V$, of the transition terms associated with the model (6.6) are given, respectively, by

$$F = \begin{pmatrix} 0 & 0 & 0 & \beta_M C_{HV} \\ 0 & 0 & 0 & 0 \\ 0 & 0 & 0 & 0 \\ \frac{\beta_H C_{HV} S_V^*}{N_H^*} & \frac{\beta_H C_{HV} \phi_1 S_V^*}{N_H^*} & \frac{\beta_H C_{HV} \phi_2 S_V^*}{N_H^*} & 0 \end{pmatrix},$$

and

$$V = \begin{pmatrix} \mu_H + \delta_H + \gamma_1 & 0 & 0 & 0 \\ 0 & \mu_H + \theta_1\delta_H + \gamma_2 & 0 & 0 \\ 0 & 0 & \mu_H + \theta_2\delta_H + \gamma_3 & 0 \\ 0 & 0 & 0 & \mu_V + \delta_V \end{pmatrix}.$$

It follows that the *basic reproduction number*, denoted by $\mathcal{R}_0 = \rho(FV^{-1})$, where $\rho$ denotes the spectral radius, is given by

$$\mathcal{R}_0 = \sqrt{\frac{\beta_M \beta_H C_{HV}^2 \Pi_V \mu_H}{(\mu_H + \delta_H + \gamma_1)(\mu_V + \delta_V)\Pi_H \mu_V}}. \tag{6.9}$$

Using Theorem 2 of [136], the following result is established.

**Lemma 6.2.** *The DFE of the model* (6.6), *given by* (6.8), *is LAS if* $\mathcal{R}_0 < 1$, *and unstable if* $\mathcal{R}_0 > 1$.

The epidemiological implication of Lemma 6.2 is that the disease can be eliminated from the community (when $\mathcal{R}_0 < 1$) if the initial sizes of the sub-population of the model are in the basin of attraction of $E_0$.

### 6.2.3 Backward bifurcation

The phenomenon of backward bifurcation has been described in Section 2.9. It is instructive, therefore, to explore whether or not the basic model (6.6) also exhibits such phenomenon. This is considered below.

Suppose,

$$E_1 = (S_H^{**},\ I_1^{**},\ R_1^{**},\ I_2^{**},\ R_2^{**},\ I_3^{**},\ R_3^{**},\ S_V^{**},\ I_V^{**}), \tag{6.10}$$

represents any arbitrary endemic equilibrium of the model (6.6) (that is, an equilibrium in which at least one of the infected components is non-zero). The existence of backward bifurcation in the model (6.6) will be explored using the Centre Manifold theory [17, 21, 136]. To apply this theory, it is convenient carry out the following change of variables.

Let $S_H = x_1,\ I_1 = x_2,\ R_1 = x_3,\ I_2 = x_4,\ R_2 = x_5,\ I_3 = x_6,\ R_3 = x_7,\ S_V = x_8,\ I_V = x_9$, so that $N_H = x_1 + x_2 + x_3 + x_4 + x_5 + x_6 + x_7$ and $N_V = x_8 + x_9$. By using vector notation $X = (x_1, x_2, \cdots, x_9)^T$, the model (6.6) can be re-written in the form $\frac{dX}{dt} = (f_1, f_2, \cdots, f_9)^T$, as follows:

$$\begin{aligned}
\frac{dx_1}{dt} &= f_1 = \Pi_H + \psi_1 x_3 - \lambda_M x_1 - \mu_H x_1,\\
\frac{dx_2}{dt} &= f_2 = \lambda_M x_1 - k_1 x_2,\\
\frac{dx_3}{dt} &= f_3 = \gamma_1 x_2 + \psi_2 x_5 - k_2 x_3 - \sigma_1 \lambda_M x_3,\\
\frac{dx_4}{dt} &= f_4 = \sigma_1 \lambda_M x_3 - k_3 x_4,\\
\frac{dx_5}{dt} &= f_5 = \gamma_2 x_4 + \psi_3 x_7 - k_4 x_5 - \sigma_2 \lambda_M x_5,\\
\frac{dx_6}{dt} &= f_6 = \sigma_2 \lambda_M x_5 - k_5 x_6,\\
\frac{dx_7}{dt} &= f_7 = \gamma_3 x_6 - k_6 x_7,\\
\frac{dx_8}{dt} &= f_8 = \Pi_V - \lambda_H x_8 - \mu_V x_8,\\
\frac{dx_9}{dt} &= f_9 = \lambda_H x_8 - k_7 x_9,
\end{aligned} \tag{6.11}$$

where, $k_1 = \mu_H + \delta_H + \gamma_1, k_2 = \mu_H + \psi_1,\ k_3 = \mu_H + \theta_1 \delta_H + \gamma_2,\ k_4 = \mu_H + \psi_2,$

$k_5 = \mu_H + \theta_2\delta_H + \gamma_3$, $k_6 = \mu_H + \psi_3$ and $k_7 = \mu_V + \delta_V$.

The Jacobian of the transformed system (6.11) at the DFE, $E_0$, is given by

$$J(E_0) = \begin{pmatrix} -\mu_H & 0 & \psi_1 & 0 & 0 & 0 & 0 & 0 & -\beta_M C_{HV} \\ 0 & -k_1 & 0 & 0 & 0 & 0 & 0 & 0 & \beta_M C_{HV} \\ 0 & \gamma_1 & -k_2 & 0 & \psi_2 & 0 & 0 & 0 & 0 \\ 0 & 0 & 0 & -k_3 & 0 & 0 & 0 & 0 & 0 \\ 0 & 0 & 0 & \gamma_2 & -k_4 & 0 & \psi_3 & 0 & 0 \\ 0 & 0 & 0 & 0 & 0 & -k_5 & 0 & 0 & 0 \\ 0 & 0 & 0 & 0 & 0 & \gamma_3 & -k_6 & 0 & 0 \\ 0 & -\frac{\beta_H C_{HV} S_V^*}{S_H^*} & 0 & -\frac{\beta_H C_{HV}\phi_1 S_V^*}{S_H^*} & 0 & -\frac{\beta_H C_{HV}\phi_2 S_V^*}{S_H^*} & 0 & -\mu_V & 0 \\ 0 & \frac{\beta_H C_{HV} S_V^*}{S_H^*} & 0 & \frac{\beta_H C_{HV}\phi_1 S_V^*}{S_H^*} & 0 & \frac{\beta_H C_{HV}\phi_2 S_V^*}{S_H^*} & 0 & 0 & -k_7 \end{pmatrix}.$$

Consider the case when $\mathcal{R}_0 = 1$. Suppose, further, that $\beta_H = \beta_H^*$ is chosen as a bifurcation parameter. Solving for $\beta_H$ from $\mathcal{R}_0 = 1$, gives

$$\beta_H = \beta_H^* = \frac{k_1 k_7 \Pi_H \mu_V}{\beta_M C_{HV}^2 \Pi_V \mu_H}.$$

The right eigenvector of $J(E_0)\Big|_{\beta_H=\beta_H^*}$ is given by $\mathbf{w} = (w_1, w_2, w_3, w_4, w_5, w_6, w_7, w_8, w_9)^T$, where,

$$w_1 = \frac{\beta_M C_{HV} w_9 - \psi_1 w_3}{-\mu_H}, \quad w_2 = \frac{\beta_M C_{HV} w_9}{k_1}, \quad w_3 = \frac{\gamma_1 w_2}{k_2}, \quad w_4 = w_5 = w_6 = w_7 = 0,$$
$$w_8 = \frac{-\beta_H^* C_{HV} S_V^* w_2}{\mu_V S_H^*}, \quad w_9 = w_9 > 0.$$

Similarly, $J(E_0)\Big|_{\beta_H=\beta_H^*}$ has a left eigenvector $\mathbf{v} = (v_1, v_2, v_3, v_4, v_5, v_6, v_7, v_8, v_9)$, where

$$v_1 = 0, \quad v_2 = \frac{k_7 v_9}{C_{HV}\beta_M}, \quad v_3 = 0, \quad v_4 = \frac{\phi_1 \beta_H^* C_{HV} S_V^* v_9}{S_H^* k_3}, \quad v_5 = 0, \quad v_6 = \frac{\phi_2 \beta_H^* C_{HV} S_V^* v_9}{S_H^* k_5},$$
$$v_7 = 0, \quad v_8 = 0, \quad v_9 = v_9 > 0.$$

The transformed system (6.11) with $\beta_H = \beta_H^*$ has at least one zero eigenvalue (and all other eigenvalues having negative real parts). Hence, the Centre Manifold theory [17, 21, 136] can be used to analyze the dynamics of (6.11). In particular, the following theorem (Theorem 4.1 in [21]), reproduced below for convenience, will be used.

**Theorem 6.1.** (Castillo-Chavez and Song [21]). *Consider the following general system of ordinary differential equations with a parameter* $\phi$

$$\frac{dx}{dt} = f(x, \phi), \ f : \mathbb{R}^n \times \mathbb{R} \to \mathbb{R}, \ \textit{and} \ f \in \mathbb{C}^2(\mathbb{R} \times \mathbb{R}). \tag{6.12}$$

*Without loss of generality, it is assumed that 0 is an equilibrium for system* (6.12) *for all values of the parameter* $\phi$*, (that is* $f(0, \phi) \equiv 0$ *for all* $\phi$*). Assume*

*A1:* $A = D_x f(0,0) = (\frac{\partial f_i}{\partial x_j}, 0, 0)$ *is the linearize matrix of system* (6.12) *around the equilibrium 0 with* $\phi$ *evaluated at 0. Zero is a simple eigenvalue of* $A$ *and all other eigenvalues of* $A$ *have negative real parts;*

*A2: Matrix* $A$ *has a nonnegative right eigenvector* $w$ *and a left eigenvector* $v$ *corresponding to the zero eigenvalue.*

*Let* $f_k$ *be the kth component of* $f$ *and*

$$a = \sum_{k,i,j=1}^{n} v_k w_i w_j \frac{\partial^2 f_k}{\partial x_i \partial x_j}(0,0),$$

$$b = \sum_{k,i=1}^{n} v_k w_i \frac{\partial^2 f_k}{\partial x_i \partial \phi}(0,0),$$

*The local dynamics of system* (6.12) *around 0 are totally determined by a and b.*

*i.* $a > 0$, $b > 0$. *When* $\phi < 0$ *with* $|\phi| \ll 1$, *0 is locally asymptotically stable and there exists a positive unstable equilibrium; when* $0 < \phi \ll 1$, *0 is unstable and there exists a negative and locally asymptotically stable equilibrium;*

*ii.* $a < 0$, $b < 0$. *When* $\phi < 0$, *with* $|\phi| \ll 1$, *0 is unstable; when* $0 < \phi \ll 1$, *0 is locally asymptotically stable, and there exists a positive unstable equilibrium;*

*iii.* $a > 0$, $b < 0$. *When* $\phi < 0$ *with* $|\phi| \ll 1$, *0 is unstable and there exists a locally asymptotically stable negative equilibrium; when* $0 < \phi \ll 1$, *0 is stable and a positive unstable equilibrium appears;*

*iv.* $a < 0$, $b > 0$. *When* $\phi$ *changes from negative to positive, 0 changes its stability from stable to unstable. Correspondingly a negative unstable equilibrium becomes positive and locally asymptotically stable.*

*Particularly, if* $a > 0$ *and* $b > 0$, *then a backward bifurcation occurs at* $\phi = 0$.

For the system (6.11), the associated non-zero partial derivatives of the right-hand

side functions, $f_i$, $i = 1, \cdots, 9$, are given by

$$\frac{\partial^2 f_2}{\partial x_2 \partial x_9} = \frac{\partial^2 f_2}{\partial x_9 \partial x_2} = \frac{\partial^2 f_2}{\partial x_3 \partial x_9} = \frac{\partial^2 f_2}{\partial x_9 \partial x_3} = \frac{-\beta_M C_{HV} \mu_H}{\Pi_H},$$
$$\frac{\partial^2 f_4}{\partial x_3 \partial x_9} = \frac{\partial^2 f_4}{\partial x_9 \partial x_3} = \frac{\sigma_1 \beta_M C_{HV} \mu_H}{\Pi_H},$$
$$\frac{\partial^2 f_6}{\partial x_5 \partial x_9} = \frac{\partial^2 f_6}{\partial x_9 \partial x_5} = \frac{\sigma_2 \beta_M C_{HV} \mu_H}{\Pi_H},$$
$$\frac{\partial^2 f_9}{\partial x_1 \partial x_2} = \frac{\partial^2 f_9}{\partial x_2 \partial x_1} = \frac{\partial^2 f_9}{\partial x_2 \partial x_3} = \frac{\partial^2 f_9}{\partial x_3 \partial x_2} = \frac{-\beta_H^* C_{HV} \mu_H^2 \Pi_V}{\Pi_H^2 \mu_V},$$
$$\frac{\partial^2 f_9}{\partial {x_2}^2} = \frac{-2\beta_H^* C_{HV} \mu_H^2 \Pi_V}{\Pi_H^2 \mu_V}, \quad \frac{\partial^2 f_9}{\partial x_2 \partial x_8} = \frac{\partial^2 f_9}{\partial x_8 \partial x_2} = \frac{\beta_H^* C_{HV} \mu_H}{\Pi_H},$$
$$\frac{\partial^2 f_9}{\partial x_2 \partial \beta_H^*} = \frac{C_{HV} \mu_H \Pi_V}{\Pi_H \mu_V}.$$

Thus, it follows from the above expressions that

$$a_1 = \sum_{k,i,j=1}^{9} v_k w_i w_j \frac{\partial^2 f_k}{\partial x_i \partial x_j}(0,0)$$

$$= \frac{2C_{HV}\mu_H}{\Pi_H^2 \mu_V}\Big(-v_2 w_2 w_9 \beta_M \Pi_H \mu_V - v_2 w_3 w_9 \beta_M \Pi_H \mu_V + v_4 w_3 w_9 \beta_M \sigma_1 \Pi_H \mu_V - v_9 w_1 w_2 \beta_H^* \mu_H \Pi_V$$
$$- v_9 w_2^2 \beta_H^* \mu_H \Pi_V - v_9 w_2 w_3 \beta_H^* \mu_H \Pi_V + v_9 w_2 w_8 \beta_H^* \Pi_H \mu_V\Big),$$

and,

$$b_1 = \sum_{k,i=1}^{9} v_k w_i \frac{\partial^2 f_k}{\partial x_i \partial \phi}(0,0) = \frac{v_9 w_2 C_{HV} \mu_H \Pi_V}{\Pi_H \mu_V} > 0.$$

Since the coefficient $b_1$ is always positive, it follows from Theorem 6.1 that the transformed model (6.11) (or, equivalently, the model (6.6)) will undergo backward bifurca-

tion at $\mathcal{R}_0 = 1$ if

$$\sigma_1 > \frac{1}{v_4 w_3 w_9 \beta_M \Pi_H \mu_V}(v_2 w_2 w_9 \beta_M \Pi_H \mu_V + v_2 w_3 w_9 \beta_M \Pi_H \mu_V + v_9 w_2^2 \beta_H^* \mu_H \Pi_V + v_9 w_2 w_3 \beta_H^* \mu_H \Pi_V - v_9 w_2 w_8 \beta_H^* \Pi_H \mu_V + v_9 w_1 w_2 \beta_H^* \mu_H \Pi_V), \tag{6.13}$$

(so that $a_1 > 0$). The above result is summarized below:

**Theorem 6.2.** *The model* (6.6) *exhibits backward bifurcation at* $\mathcal{R}_0 = 1$ *whenever the inequality* (6.13) *holds.*

This (backward bifurcation) phenomenon is illustrated by simulating the model (6.6), using a set of parameter values given in Table 6.2 (such that the inequality (6.13) is satisfied). The results obtained are depicted in Figure 6.2. With the set of parameter values used in these simulations, the bifurcation coefficients $a_1 = 1.374377915 > 0$ and $b_1 = 0.3052671186 > 0$. The parameter values are chosen only to illustrate the backward bifurcation phenomenon and these values may not be realistic epidemiologically (there are some discussions, in the context of mycobacterium tuberculosis [89], as to whether or not backward bifurcation can occur with realistic parameter values).

Further, the effect of the first re-infection parameter ($\sigma_1$) and the transmission probability from an infectious human to a susceptible vector ($\beta_H$) on the associated backward bifurcation region is investigated, as a function of the average life span of mosquitoes ($1/\mu_V$), by simulating the model (6.6) using the parameter values in Table 6.2 (unless otherwise stated). It should be noted that the parameter values are chosen such that $a_1 > 0, b_1 > 0$ and $\mathcal{R}_0 < 1$ (so that backward bifurcation occurs).

The backward bifurcation region for $\beta_H$ is then obtained by solving for $a > 0$ in

terms of $0 \leq \sigma_1 \leq 1$ and $\beta_H > 0$ (i.e., fixing all parameters in the expression for $\alpha$ except $\beta_H$ and $\sigma_1$). The results obtained for $\sigma_1 = 0.5$, depicted in Figure 6.3, show that the region for backward bifurcation (for $\beta_H$) increases as the average life span of mosquitoes $(1/\mu_V)$ decreases. For instance, when the average life span of vectors is 20 days ($\mu_V = 0.05$), the backward bifurcation region for $\beta_H$ is $\beta_H \in [0.00347, 0.1285]$, as shown in Figure 6.3a. When the average life span of vectors is decreased to 10 days ($\mu_V = 0.1$), the backward bifurcation region for $\beta_H$ increases to $\beta_H \in [0.00986, 0.3641]$ (Figure 6.3b). Furthermore, when the average life span of vectors is decreased to 5 days ($\mu_V = 0.2$), the backward bifurcation region for $\beta_H$ increases to $\beta_H \in [0.031326, 1.15665]$ (Figure 6.3c). Similar results are obtained for the cases $\sigma_1 = 0.6$ (Figure 6.4) and $\sigma_1 = 1$ (Figure 6.5), from which it is evident that the backward bifurcation regions for $\beta_H$ increase with increasing values of the re-infection rate $\sigma_1$. These results are tabulated in Table 6.3.

## 6.3 Effect of Re-infection on Malaria Transmission Dynamics

The objective here is to qualitatively analyse the impact of repeated exposure $(\sigma_1, \sigma_2)$ in malaria transmission dynamics. To do so, the re-infection parameters ($\sigma_1$ and $\sigma_2$)

in (6.6) are set to zero to get the following (reduced) basic model.

$$\begin{aligned}
\frac{dS_H}{dt} &= \Pi_H + \psi_H R_H - \lambda_M S_H - \mu_H S_H, \\
\frac{dI_H}{dt} &= \lambda_M S_H - \gamma_H I_H - \mu_H I_H - \delta_H I_H, \\
\frac{dR_H}{dt} &= \gamma_H I_H - \mu_H R_H - \psi_H R_H, \\
\frac{dS_V}{dt} &= \Pi_V - \lambda_H S_V - \mu_V S_V, \\
\frac{dI_V}{dt} &= \lambda_H S_V - \mu_V I_V - \delta_V I_V,
\end{aligned} \tag{6.14}$$

where, now, $\lambda_M = \frac{\beta_M C_{HV} I_V}{N_H}$ and $\lambda_H = \frac{\beta_H C_{HV} I_H}{N_H}$. For the reduced model (6.14), it can be shown (using the approach in Section 6.2.1) that the region

$$\mathcal{D}_r = \left\{ (S_H, I_H, R_H, S_V, I_V) \in \mathbb{R}^5_+ : S_H + I_H + R_H \leq \frac{\Pi_H}{\mu_H};\ S_V + I_V \leq \frac{\Pi_V}{\mu_V} \right\}$$

is positively-invariant and attracting.

### 6.3.1 Stability of DFE

The DFE of the reduced model (6.14) is given by

$$E_{01} = (S_H^*,\ I_H^*,\ R_H^*,\ S_V^*,\ I_V^*) = (\Pi_H/\mu_H,\ 0,\ 0,\ \Pi_V/\mu_V,\ 0). \tag{6.15}$$

Here, the associated next generation matrices ($F_1$ and $V_1$) are given by

$$F_1 = \begin{pmatrix} 0 & \beta_M C_{HV} \\ \frac{\beta_H C_{HV} S_V^*}{N_H^*} & 0 \end{pmatrix}, \quad V_1 = \begin{pmatrix} q_1 & 0 \\ 0 & q_3 \end{pmatrix},$$

where, $q_1 = \mu_H + \delta_H + \gamma_H$, $q_2 = \mu_H + \psi_H$, and $q_3 = \mu_V + \delta_V$. It follows that the corresponding reproduction number, denoted by $\mathcal{R}_{01} = \rho(F_1 V_1^{-1})$, is given by

$$\mathcal{R}_{01} = \sqrt{\frac{\beta_M \beta_H C_{HV}^2 \Pi_V \mu_H}{q_1 q_3 \Pi_H \mu_V}}. \tag{6.16}$$

Using Theorem 2 of [136], the following result is established.

**Lemma 6.3.** *The DFE of the reduced model* (6.14)*, given by* $E_{01}$*, is LAS if* $\mathcal{R}_{01} < 1$*, and unstable if* $\mathcal{R}_{01} > 1$.

### 6.3.2 Endemic equilibria and backward bifurcation

Let,

$$E_2 = (S_H^{**},\ I_H^{**},\ R_H^{**},\ S_V^{**},\ I_V^{**}) \tag{6.17}$$

represent any arbitrary equilibrium of the reduced model (6.14). Further, let

$$\lambda_M^{**} = \frac{\beta_M^{**} C_{HV} I_V^{**}}{N_H^{**}} \quad \text{and} \quad \lambda_H^{**} = \frac{\beta_H^{**} C_{HV} I_H^{**}}{N_H^{**}} \tag{6.18}$$

be the forces of infection of vector and human population, respectively, at steady state. It follows that, by setting the right-hand sides of the equations in (6.14) to zero,

$$\begin{aligned}
S_H^{**} &= \frac{q_1 q_2 \Pi_H}{(q_1 q_2 - \gamma_H \psi_H)\lambda_M^{**} + q_1 q_2 \mu_H}, \\
I_H^{**} &= \frac{q_2 \lambda_M^{**} \Pi_H}{(q_1 q_2 - \gamma_H \psi_H)\lambda_M^{**} + q_1 q_2 \mu_H}, \\
R_H^{**} &= \frac{\gamma_H \lambda_M^{**} \Pi_H}{(q_1 q_2 - \gamma_H \psi_H)\lambda_M^{**} + q_1 q_2 \mu_H}, \\
S_V^{**} &= \frac{\Pi_V}{\lambda_H^{**} + \mu_V}, \\
I_V^{**} &= \frac{\lambda_H^{**} \Pi_V}{q_3(\lambda_H^{**} + \mu_V)}.
\end{aligned} \tag{6.19}$$

where $q_1 q_2 - \gamma_H \psi_H = \mu_H(\mu_H + \delta_H + \gamma_H) + \psi_H(\mu_H + \delta_H) > 0$. Substituting (6.19) into the expressions of $\lambda_M^{**}$ and $\lambda_H^{**}$ in (6.18), gives

$$\begin{aligned}
\lambda_M^{**} &= \frac{\beta_M^{**} C_{HV} I_V^{**}}{N_H^{**}} \equiv \frac{\beta_M^{**} C_{HV} \lambda_H^{**} \Pi_V}{(\lambda_H^{**} + \mu_V) q_3 N_H^{**}}, \\
\lambda_H^{**} &= \frac{\beta_H^{**} C_{HV} I_H^{**}}{N_H^{**}} \equiv \frac{\beta_H^{**} C_{HV} q_2 \lambda_M^{**} \Pi_H}{[(q_1 q_2 - \gamma_H \psi_H)\lambda_M^{**} + q_1 q_2 \mu_H] N_H^{**}},
\end{aligned} \tag{6.20}$$

where,

$$N_H^{**} = S_H^{**} + I_H^{**} + R_H^{**}.$$

Substituting the expression of $\lambda_H^{**}$ into that of $\lambda_M^{**}$ gives

$$a_0(\lambda_M^{**})^2 + b_0 \lambda_M^{**} + c_0 = 0, \tag{6.21}$$

with,

$$a_0 = \Pi_H q_3(q_2+\gamma_H)[q_2(\beta_H^{**}C_{HV}+\mu_V)+\gamma_H\mu_V],$$

$$b_0 = q_2\{q_1q_3\Pi_H[q_2(2\mu_V+\beta_H^{**}C_{HV})+2\mu_V\gamma_H]-\Pi_V\beta_M^{**}\beta_H^{**}C_{HV}^2(q_1q_2-\gamma_H\psi_H)\},$$

$$c_0 = q_1^2q_2^2q_3\Pi_H\mu_V(1-\mathcal{R}_{01}^2).$$

It is worth noting that the coefficient $a_0$, of the quadratic (6.21), is always positive, and $c_0$ is positive (negative) if $\mathcal{R}_{01}$ is less than (greater than) unity. Hence, the following result is established.

**Theorem 6.3.** *The reduced model* (6.14) *has:*

*(i) a unique endemic equilibrium if* $c_0 < 0 \Longleftrightarrow \mathcal{R}_{01} > 1$;

*(ii) a unique endemic equilibrium if* $b_0 < 0$ *and* $c_0 = 0$ *or* $b_0^2 - 4a_0c_0 = 0$;

*(iii) two endemic equilibria if* $c_0 > 0$ $(\mathcal{R}_{01} < 1)$, $b_0 < 0$ *and* $b_0^2 - 4a_0c_0 > 0$;

*(iv) no endemic equilibrium otherwise.*

Case (iii) of Theorem 6.3 indicates the possibility of backward bifurcation in the reduced model (6.14) (where the stable DFE may co-exist with a stable endemic equilibrium when $\mathcal{R}_{01} < 1$). In other words, like in the case of the basic model (6.6), the reduced model (6.14) also undergoes backward bifurcation. This can be rigorously established by using the technique in Section 6.2.3 for the reduced model (6.14), from

which it can be shown that the associated backward bifurcation coefficients ($a_2$ and $b_2$) are given by

$$\begin{aligned} a_2 &= -\frac{2C_{HV}\mu_H}{\Pi_H^2\mu_V}(v_2w_2w_5\beta_M\Pi_H\mu_V + v_2w_3w_5\beta_M\Pi_H\mu_V + v_5w_1w_2\beta_H^*\mu_H\Pi_V + v_5w_2^2\beta_H^*\mu_H\Pi_V \\ &+ v_5w_2w_3\beta_H^*\mu_H\Pi_V - v_5w_2w_4\beta_H^*\Pi_H\mu_V), \end{aligned}$$

$$b_2 = \frac{v_5w_2C_{HV}\mu_H\Pi_V}{\Pi_H\mu_V},$$

and backward bifurcation occurs if $a_2 > 0$.

In summary, it is shown that the absence of re-infection (or repeated exposure) in the model (6.6) does not affect its backward bifurcation property (although not reported here, the functional form of the incidence function is responsible for the backward bifurcation in the reduced model (6.14) [110]). It should be noted that, in the case of TB transmission dynamics, the absence of (exogenous) re-infection is known to remove its backward bifurcation property (see, for instance, [126]). Further, it is worth stating that even if $\psi_H = 0$, the reduced model (6.14), with $\sigma_1 = \sigma_2 = 0$, still exhibits backward bifurcation.

## 6.4 Summary

In this chapter, a new deterministic model for the transmission dynamics of malaria in a population, which incorporates the role of repeated exposure to infection, is designed and analyzed. The main findings of this chapter are as follows:

(i) the model (6.6) exhibits the phenomenon of backward bifurcation;

(ii) unlike in the case of TB transmission dynamics with exogenous re-infection, the absence of re-infection in the malaria model (6.6) does not remove its backward bifurcation property;

(iii) the region for backward bifurcation of the model (6.6) increases with decreasing average life span of the malaria vector. Numerical simulations suggest that the region increases with increasing rate of re-infection of first-time infected humans.

| Variable | Description |
|---|---|
| $S_H(t)$ | Susceptible human population |
| $I_1(t)$ | First-time infected human population |
| $R_1(t)$ | Population of individuals who recovered from the first infection |
| $I_2(t)$ | Second-time infected human population |
| $R_2(t)$ | Population of individuals who recovered from the second infection |
| $I_3(t)$ | Third-time infected humans |
| $R_3(t)$ | Population of humans who recovered from the third infection |
| $S_V(t)$ | Susceptible vector population |
| $I_V(t)$ | Infected vector population |

Table 6.1: Description of the variables of the model (6.6).

| Parameter | Description | Value | References |
|---|---|---|---|
| $\Pi_H$ | Recruitment rate into the susceptible human population | 0.0015875/day | [44] |
| $\Pi_V$ | Recruitment rate into the susceptible vector population | 0.071/day | [44] |
| $\mu_H$ | Natural death rate of human population | 0.00004/day | [27] |
| $\mu_V$ | Natural death rate of vector population | 0.05/day | [90] |
| $C_{HV}$ | Per capita biting rate of mosquitoes on a host | 0.29/day | [72] |
| $\beta_M$ | Transmission probability from an infectious mosquito to a susceptible human | 0.8333/day | [23] |
| $\beta_H$ | Transmission probability from an infectious human to a susceptible mosquito | variable | variable |
| $\psi_1$ | Rate of loss of infection-acquired immunity for the first-time infected individuals | 0.000017/day | [72] |
| $\psi_2$ | Rate of loss of infection-acquired immunity for the second-time infected individuals | $10\psi_1$/day | Assumed |
| $\psi_3$ | Rate of loss of infection-acquired immunity for the third-time infected individuals | $10\psi_2$/day | Assumed |
| $\phi_1, \phi_2, \theta_1, \theta_2$ | Modification parameters | 0-1 | – |
| $\delta_H$ | Disease-induced mortality for humans | 0.0003454/day | [23] |
| $\delta_V$ | Disease-induced mortality for vectors | 0.07/day | Assumed |
| $\gamma_1$ | Rate of acquisition of immunity due to first infection | $0.0023 \pm 0.0005$/day | [32] |
| $\gamma_2$ | Rate of acquisition of immunity due to second time infection | 0.0001/day | Assumed |
| $\gamma_3$ | Rate of acquisition of immunity due to third time infection | $0.00019 \pm 0.00001$/day | [32] |
| $\sigma_1, \sigma_2$ | Modification parameters for re-infection | 0.5 | Assumed |

Table 6.2: Description of the parameters of the model (6.6).

| Average Life Span of Vectors ($1/\mu_V$) | $\sigma_1 = 0.5$ | $\sigma_1 = 0.6$ | $\sigma_1 = 1$ |
|---|---|---|---|
| 20 days | $\beta_H \in [0.00347, 0.1285]$ | $\beta_H \in [0.00344, 0.1285]$ | $\beta_H \in [0.003302, 0.1285]$ |
| 10 days | $\beta_H \in [0.00986, 0.3641]$ | $\beta_H \in [0.00975, 0.3641]$ | $\beta_H \in [0.009357, 0.3641]$ |
| 5 days | $\beta_H \in [0.031326, 1.1567]$ | $\beta_H \in [0.03099, 1.1567]$ | $\beta_H \in [0.02973, 1.1567]$ |

Table 6.3: Backward bifurcation ranges for $\beta_H$ for various values of $1/\mu_V$ and $\sigma_1$. *

* Note that since $\beta_H$ is a probability, we only consider $\beta_H \in [0, 1]$.

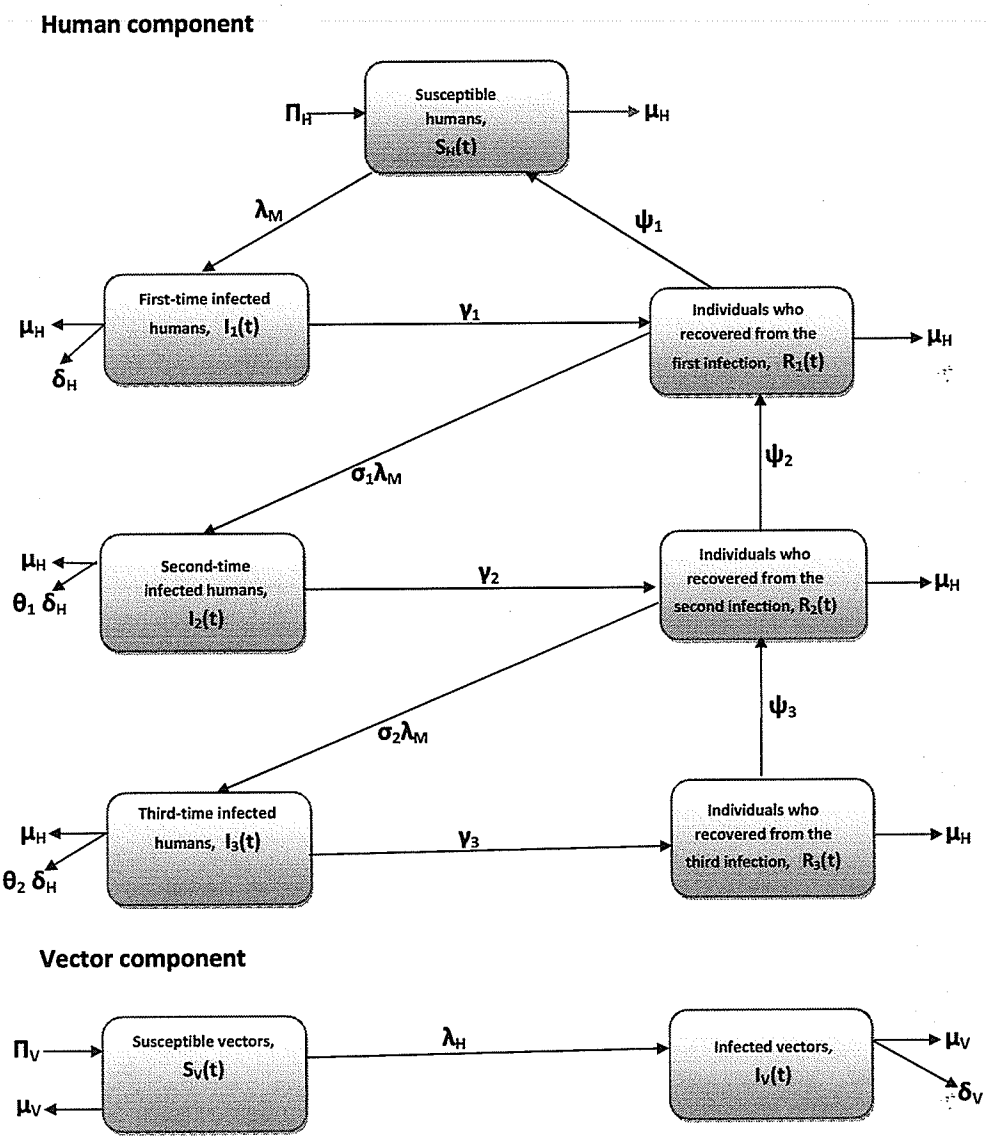


Figure 6.1: Schematic diagram of the malaria model (6.6).

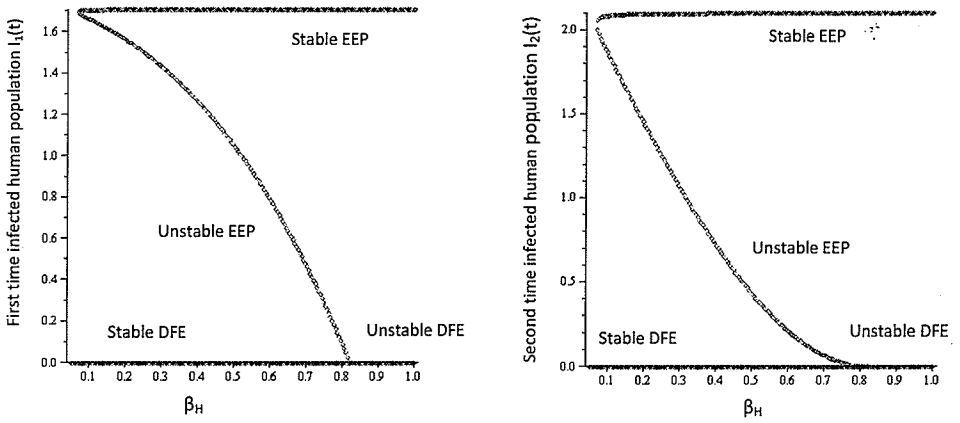


Figure 6.2: Simulations of the model (6.6). Backward bifurcation for the first-time infected and the second-time infected human populations using: $\Pi_H = 0.0099$, $\mu_H = 0.00004$, $\Pi_V = 0.071$, $\mu_V = 0.05$, $\delta_H = 0.003454$, $\delta_V = 0.007$, $\gamma_1 = 0.0023$, $\gamma_2 = 0.0001$, $\gamma_3 = 0.00019$, $\psi_1 = 0.000017$, $\psi_2 = 0.00017$, $\psi_3 = 0.0017$, $\sigma_1 = 0.5$, $\sigma_2 = 0.5$, $\theta_1 = 0.5$, $\theta_2 = 0.3$, $\phi_1 = 0.5$, $\phi_2 = 0.3$, $\beta_M = 0.8333$, and $C_{HV} = 0.29$ (so that, $a_1 = 1.374377915$, $b_1 = 0.3052671186$ and $\mathcal{R}_0 = 0.9459535$).

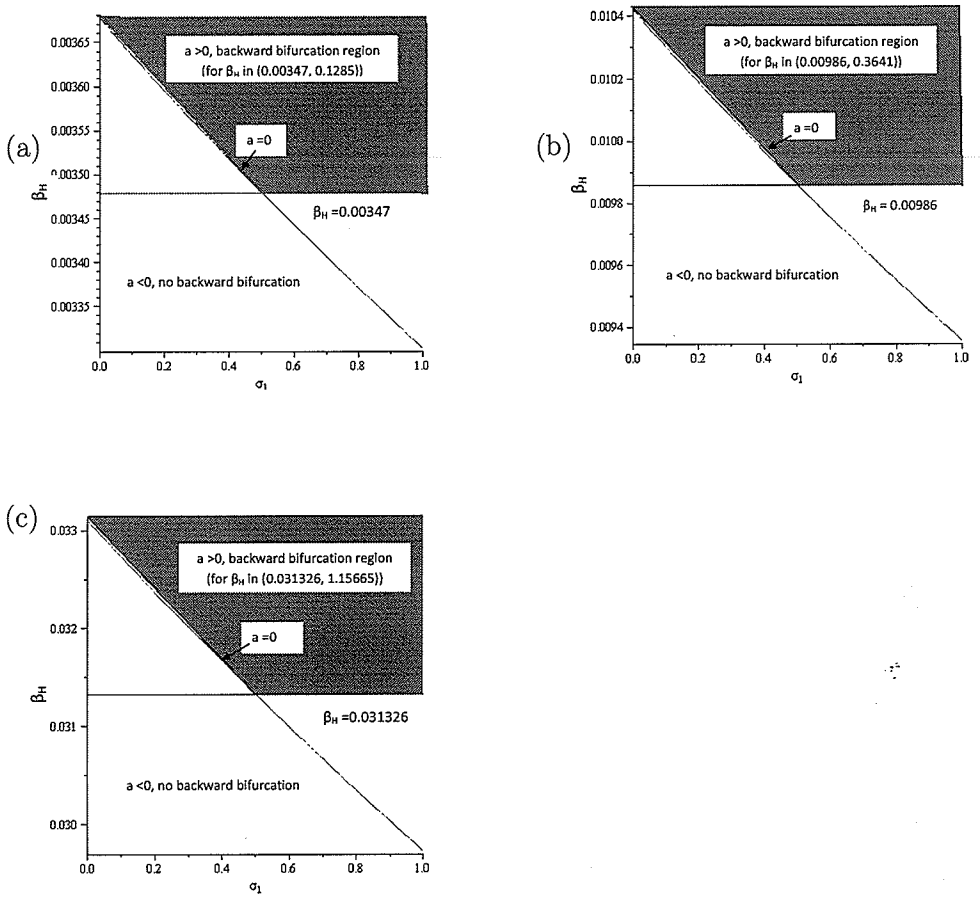


Figure 6.3: Backward bifurcation regions for the model (6.6) in the $\sigma_1 - \beta_H$ parameter space corresponding to $\sigma_1 = 0.5$ and various ranges of $\beta_H$. Parameter values used are: $\Pi_H = 0.0015875$, $\mu_H = 0.00004$, $\Pi_V = 0.071$, $\delta_H = 0.0003454$, $\delta_V = 0.07$, $\gamma_1 = 0.0023$, $\gamma_2 = 0.0001$, $\gamma_3 = 0.00019$, $\psi_1 = 0.000017$, $\psi_2 = 0.00017$, $\psi_3 = 0.0017$, $\sigma_2 = 0.5$, $\theta_1 = 0.5$, $\theta_2 = 0.3$, $\phi_1 = 0.5$, $\phi_2 = 0.3$, and $\beta_M = 0.8333$, $C_{HV} = 0.29$. (a) $\mu_V = 0.05$ (backward bifurcation region for $\beta_H$ is $\beta_H \in [0.00347, 0.1285]$), (b) $\mu_V = 0.1$ (backward bifurcation region for $\beta_H$ is $\beta_H \in [0.00986, 0.3641]$) and (c) $\mu_V = 0.2$ (backward bifurcation region for $\beta_H$ is $\beta_H \in [0.031326, 1.15665]$). With the above set of parameter values, the inequalities $a_1 > 0, b_1 > 0$ and $\mathcal{R}_0 < 1$ always hold.

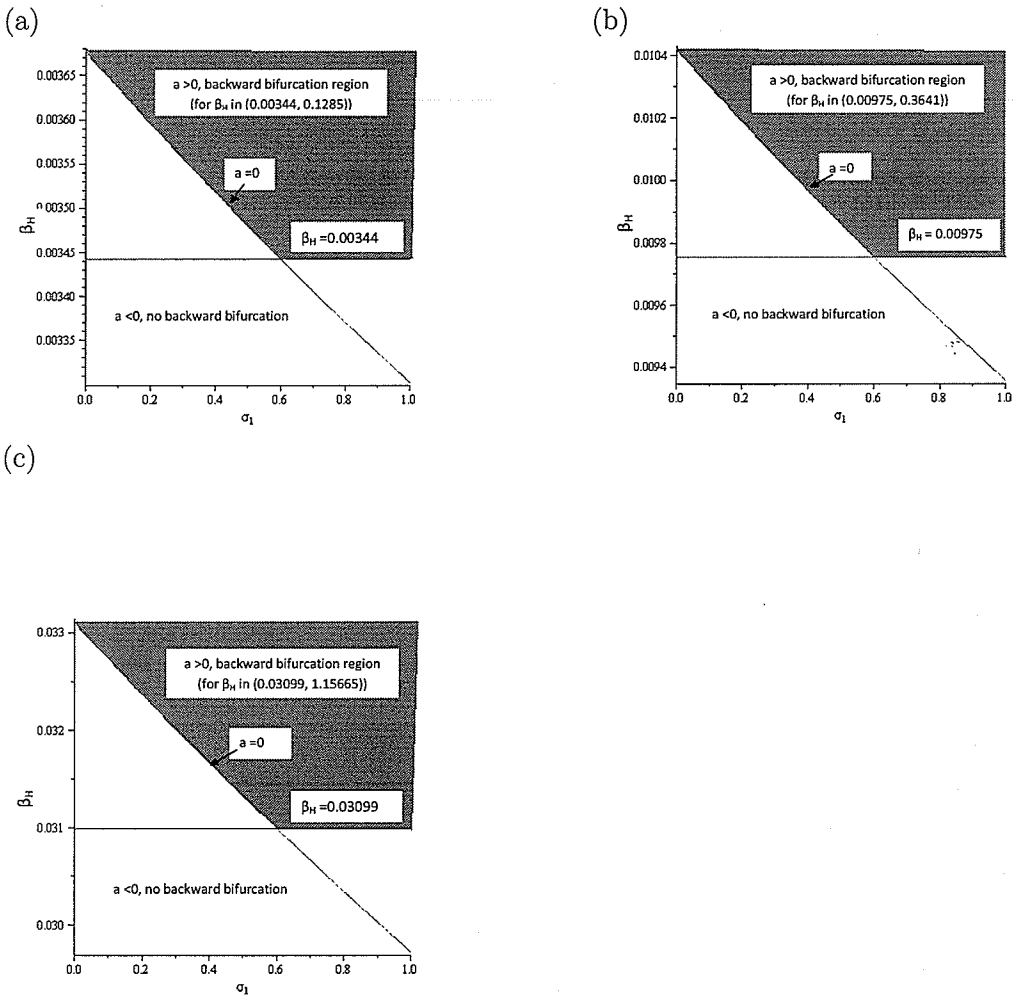


Figure 6.4: Backward bifurcation regions for the model (6.6) in the $\sigma_1 - \beta_H$ parameter space corresponding to $\sigma_1 = 0.6$ and various ranges of $\beta_H$. Parameter values used are: $\Pi_H = 0.0015875$, $\mu_H = 0.00004$, $\Pi_V = 0.071$, $\delta_H = 0.0003454$, $\delta_V = 0.07$, $\gamma_1 = 0.0023$, $\gamma_2 = 0.0001$, $\gamma_3 = 0.00019$, $\psi_1 = 0.000017$, $\psi_2 = 0.00017$, $\psi_3 = 0.0017$, $\sigma_2 = 0.5$, $\theta_1 = 0.5$, $\theta_2 = 0.3$, $\phi_1 = 0.5$, $\phi_2 = 0.3$, $\beta_M = 0.8333$, and $C_{HV} = 0.29$. (a) $\mu_V = 0.05$ (backward bifurcation region for $\beta_H$ is $\beta_H \in [0.00344, 0.1285]$), (b) $\mu_V = 0.1$ (backward bifurcation region for $\beta_H$ is $\beta_H \in [0.00975, 0.3641]$) and (c) $\mu_V = 0.2$ (backward bifurcation region for $\beta_H$ is $\beta_H \in [0.03099, 1.15665]$). With the above set of parameter values, the inequalities $a_1 > 0, b_1 > 0$ and $\mathcal{R}_0 < 1$ always hold.

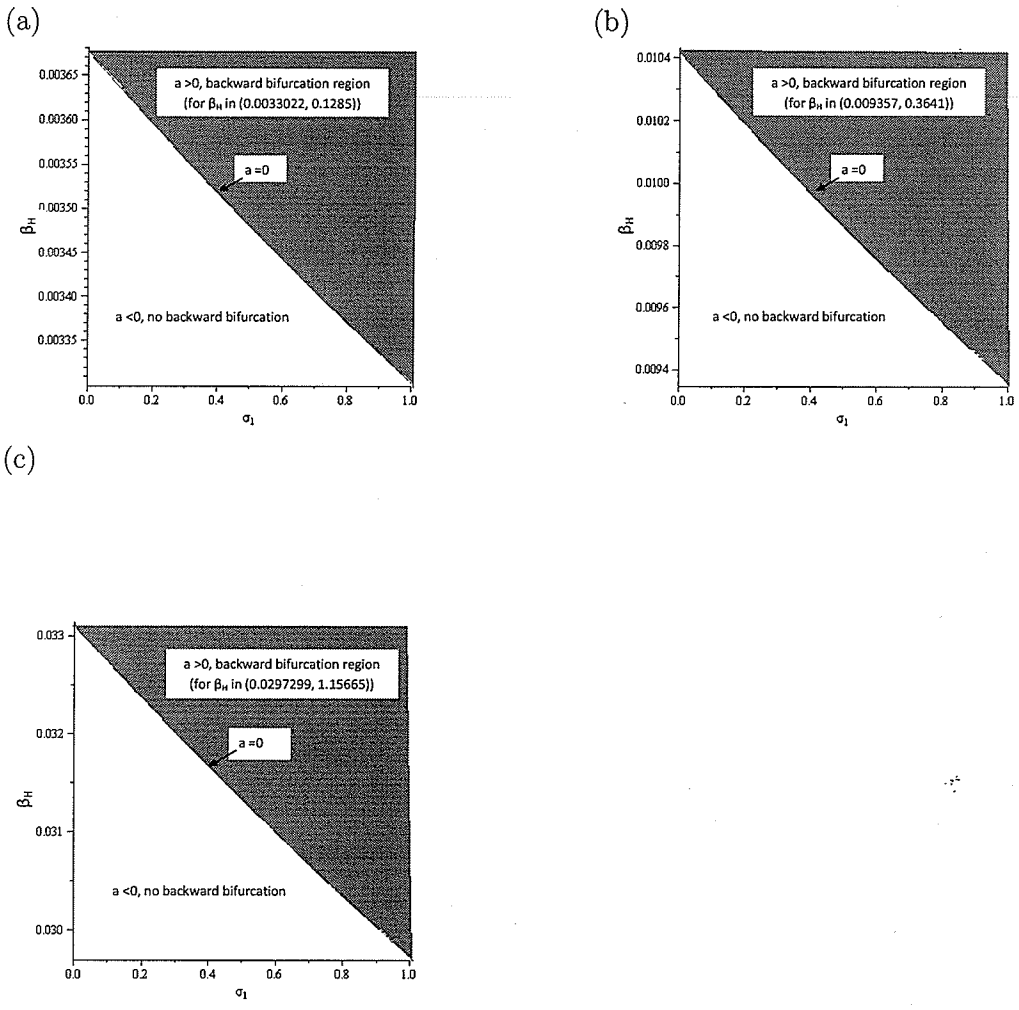


Figure 6.5: Backward bifurcation regions for the model (6.6) in the $\sigma_1 - \beta_H$ parameter space corresponding to $\sigma_1 = 1$ and various ranges of $\beta_H$. Parameter values used are: $\Pi_H = 0.0015875$, $\mu_H = 0.00004$, $\Pi_V = 0.071$, $\delta_H = 0.0003454$, $\delta_V = 0.07$, $\gamma_1 = 0.0023$, $\gamma_2 = 0.0001$, $\gamma_3 = 0.00019$, $\psi_1 = 0.000017$, $\psi_2 = 0.00017$, $\psi_3 = 0.0017$, $\sigma_2 = 0.5$, $\theta_1 = 0.5$, $\theta_2 = 0.3$, $\phi_1 = 0.5$, $\phi_2 = 0.3$, $\beta_M = 0.8333$, and $C_{HV} = 0.29$. (a) $\mu_V = 0.05$ (backward bifurcation region for $\beta_H$ is $\beta_H \in [0.0033022, 0.1285]$), (b) $\mu_V = 0.1$ (backward bifurcation region for $\beta_H$ is $\beta_H \in [0.009357, 0.3641]$) and (c) $\mu_V = 0.2$ (backward bifurcation region for $\beta_H$ is $\beta_H \in [0.02973, 1.15665]$). With the above set of parameter values, the inequalities $a_1 > 0, b_1 > 0$ and $\mathcal{R}_0 < 1$ always hold.

# Chapter 7

# Contributions of the Thesis

The main novel contributions of this thesis can be classified into three main categories, namely, model formulation, mathematical analysis and contributions to public health (in terms of the ecology of the malaria vector and the epidemiology and parasitology of the disease). These are summarized as follows.

## 7.1 Model Formulations

(i) A new multi-parasitic stage model for assessing the impact of immune response and an imperfect vaccine on malaria dynamics *in vivo* is designed. The model is based on the progressive refinements of some existing models;

(ii) a new population model for assessing the role of infection-acquired immunity, due to repeated host exposure to malaria is designed.

## 7.2 Mathematical Analysis

### 7.2.1 Chapters 3 and 4

A detailed rigorous analysis of the vector population model (with or without time delay), subject to Verhulst-Pearl logistic growth function and Beverton-Holt function, is carried out.

(i) The global asymptotic stability of the trivial equilibria of the vector population models (with and without time delay) are established subject to any arbitrary birth function satisfying Assumptions **A1** – **A3**. This is based on using the fluctuation method. Further, the existence and the asymptotic stability of the associated non-trivial equilibria are established;

(ii) conditions for Hopf bifurcation are provided for both the delayed and the non-delayed models (using each of the two birth rate functions);

(iii) the amplitude of oscillation increases with increasing values of $T > T_c$;

(iv) the use of time delay in modelling vector population dynamics contributes in sustaining vector dynamics.

### 7.2.2 Chapter 5

(i) Provided complete global analysis of the Anderson *et al.* model (5.1) and the multiple parasitic stage model (5.10) for malaria dynamics *in vivo* (using linear

and non-linear Lyapunov functions, in conjunction with the LaSalle's Invariance Principle);

(ii) proving the global asymptotic stability of the disease-free equilibrium of the extended model with immune response (5.20) for a special case. This is based on using Lyapunov function theory, in conjunction with the LaSalle's Invariance Principle;

(iii) determined a threshold quantity for assessing the potential impact of an imperfect malaria vaccine *in vivo*.

### 7.2.3 Chapter 6

(i) Established the existence and local stability of the endemic equilibria of the repeated exposure models ((6.6),(6.14)) for malaria transmission dynamics;

(ii) proving the presence of the phenomenon of backward bifurcation in the repeated exposure model and showing that the phenomenon arises due to repeated exposure to infection or the use of standard incidence in modelling the infection term.

## 7.3 Public Health

The study provides some important ecological and epidemiological insight into malaria transmission dynamics and control strategies as follows:

(i) the use of Beverton-Holt function seems to be more suitable for modelling the population dynamics of the malaria vector in comparison to using the Verhulst-Pearl logistic growth function;

(ii) a future malaria vaccine with increasing efficacy will reduce the concentration of IRBCs *in vivo*;

(iii) a potential malaria vaccine that increases immune response will decrease the concentration of IRBCs;

(iv) a malaria vaccine that reduces the number of merozoites released per bursting IRBC would have significant impact on reducing the infection;

(v) numerical simulations suggest that a future malaria vaccine (with characteristics listed in Section 5.4) can lead to the elimination of the parasite *in vivo* if its efficacy is at least 87.85%.

(vi) the repeated exposure to malaria infection induces the phenomenon of backward bifurcation in malaria transmission dynamics. The associated region of backward bifurcation increases with decreasing average life span of the mosquito.

# Appendix A: Proof of Lipschitzian property of $f$

**Lemma 7.1.** *Consider the delayed system* (4.1) *which has the general form:*

$$\dot{X}(t_1) = f(t_1, X_{t_1}).$$

*Then $f$ is Lipschitzian.*

*Proof.* The following steps are taken to show that the function $f$ is Lipschitzian.

$$|f_1(X_1) - f_1(X_2)| = \Big|[p\tau HW_1 - (a+\mu)U_1] - [p\tau HW_2 - (a+\mu)U_2]\Big|,$$

$$\leq p\tau H|W_1 - W_2| + (a+\mu)|U_1 - U_2|; \quad \text{using} \quad |A-B| \leq |A| + |B|$$

$$\leq p\tau H \max\|X_1 - X_2\| + (a+\mu)\max\|X_1 - X_2\|,$$

$$\leq 2C_1 \max\|X_1 - X_2\|, \quad \text{where } C_1 = \max\{p\tau H,\ a+\mu\}.$$

Furthermore,

$$|f_2(X_1) - f_2(X_2)| = \left| \left[ aB(U_1)U_1 e^{-\mu_e T} + aU_1 - \left(\mu + \frac{bH}{H+K}\right) V_1 \right] \right.$$
$$\left. - \left[ aB(U_2)U_2 e^{-\mu_e T} + aU_2 - \left(\mu + \frac{bH}{H+K}\right) V_2 \right] \right|,$$

$$= \left| ae^{-\mu_e T}[B(U_1)U_1 - B(U_2)U_2] + a(U_1 - U_2) - \left(\mu + \frac{bH}{H+K}\right)(V_1 - V_2) \right|,$$

$$\leq a|B(U_1)U_1 - B(U_2)U_2| + a|U_1 - U_2| + \left(\mu + \frac{bH}{H+K}\right)|V_1 - V_2|,$$

$$|f_2(X_1) - f_2(X_2)| \leq a|B(U_2)U_1 - B(U_2)U_2| + a|U_1 - U_2| + \left(\mu + \frac{bH}{H+K}\right)|V_1 - V_2|,$$
$$\text{if } U_2 < U_1, \quad B(U_1)U_1 < B(U_2)U_1,$$

$$\leq a|B(U_2)||U_1 - U_2| + a|U_1 - U_2| + \left(\mu + \frac{bH}{H+K}\right)|V_1 - V_2|,$$

$$\leq aB_0 \max \|X_1 - X_2\| + a \max \|X_1 - X_2\| + \left(\mu + \frac{bH}{H+K}\right) \max \|X_1 - X_2\|,$$

$$\leq 3C_2 \max \|X_1 - X_2\|, \quad \text{where} \quad C_2 = \max\left\{ aB_0,\ a,\ \mu + \frac{bH}{H+K} \right\}.$$

Similarly,

$$|f_3(X_1) - f_3(X_2)| = \left| \left[ \frac{bH}{H+K} V_1 - (\mu + \tau H) W_1 \right] - \left[ \frac{bH}{H+K} V_2 - (\mu + \tau H) W_2 \right] \right|,$$

$$\leq \frac{bH}{H+K} |V_1 - V_2| + (\mu + \tau H) |W_1 - W_2|,$$

$$\leq \frac{bH}{H+K} \max \|X_1 - X_2\| + (\mu + \tau H) \max \|W_1 - W_2\|,$$

$$\leq 2C_3 \max \|X_1 - X_2\|, \quad \text{where} \quad C_3 = \max\left\{ \frac{bH}{H+K},\ \mu + \tau H \right\}.$$

Thus,

$$\|f(X_1) - f(X_2)\| \leq C_4 \|X_1 - X_2\|; \quad C_4 = \max\{C_1, C_2, C_3\}.$$

□

# Appendix B: Proof of Lemma 4.6

*Proof.* Using the expression for **B1** from (4.42) in the characteristic equation (4.40) gives

$$\lambda^3 + Q\lambda^2 + R\lambda + P = 2Pe^{-\lambda T} - AB_0e^{-(\mu_s+\lambda)T}. \tag{7.1}$$

Differentiating (7.1) with respect to $T$ gives

$$\left[3\lambda^2+2Q\lambda+R+2PTe^{-\lambda T}-AB_0Te^{-(\mu_s+\lambda)T}\right]\frac{d\lambda}{dT} = -2P\lambda e^{-\lambda T}+AB_0(\mu_s+\lambda)e^{-(\mu_s+\lambda)T}.$$

The above expression can be further simplified to give

$$\left(\frac{d\lambda}{dT}\right)^{-1} = \frac{3\lambda^2 + 2Q\lambda + R + e^{-\lambda T}(2PT - AB_0Te^{-\mu_sT})}{e^{-\lambda T}[-2P\lambda + AB_0(\mu_s + \lambda)e^{-\mu_sT}]},$$

$$= \frac{(3\lambda^2 + 2Q\lambda + R)(2P - AB_0e^{-\mu_sT}) + (\lambda^3 + Q\lambda^2 + R\lambda + P)(2PT - AB_0Te^{-\mu_sT})}{(\lambda^3 + Q\lambda^2 + R\lambda + P)[-2P\lambda + (\mu_s + \lambda)P\mathcal{R}_{0d}]},$$

$$= \frac{(2P - AB_0e^{-\mu_sT})[3\lambda^2 + 2Q\lambda + R + T(\lambda^3 + Q\lambda^2 + R\lambda + P)]}{(\lambda^3 + Q\lambda^2 + R\lambda + P)[-2P\lambda + (\mu_s + \lambda)P\mathcal{R}_{0d}]},$$

$$= \frac{P(2 - \mathcal{R}_{0d})[3\lambda^2 + 2Q\lambda + R + T(\lambda^3 + Q\lambda^2 + R\lambda + P)]}{(\lambda^3 + Q\lambda^2 + R\lambda + P)[-2P\lambda + (\mu_s + \lambda)P\mathcal{R}_{0d}]}.$$

It follows that (see also [22, 28, 41, 131]),

$$\begin{aligned}
\operatorname{sign}\left\{\frac{d(\mathrm{Re}\lambda)}{dT}\right\}_{T=T_c} &= \operatorname{sign}\left\{\mathrm{Re}\left(\frac{d\lambda}{dT}\right)^{-1}\right\}_{T=T_c}, \\
&= \operatorname{sign}\left\{\mathrm{Re}\left[\frac{P(2-\mathcal{R}_{0d})[3\lambda^2+2Q\lambda+R+T(\lambda^3+Q\lambda^2+R\lambda+P)]}{(\lambda^3+Q\lambda^2+R\lambda+P)[-2P\lambda+(\mu_s+\lambda)P\mathcal{R}_{0d}]}\right]_{T=T_c}\right\}, \qquad (7.2) \\
&= \operatorname{sign}\Bigg\{P(2-\mathcal{R}_{0d}) \\
&\quad \times \mathrm{Re}\left[\frac{[3(i\omega)^2+2Q(i\omega)+R+T((i\omega)^3+Q(i\omega)^2+R(i\omega)+P)]}{((i\omega)^3+Q(i\omega)^2+R(i\omega)+P)[-2P(i\omega)+(\mu_s+(i\omega))P\mathcal{R}_{0d}]}\right]_{T=T_c}\Bigg\}.
\end{aligned}$$

The last equation of (7.2) can be further simplified to:

$$\operatorname{sign}\left\{\frac{d(\mathrm{Re}\lambda)}{dT}\right\}_{T=T_c} = \operatorname{sign}\left\{P(2-\mathcal{R}_{0d})\mathrm{Re}\left[\frac{A_1+iB_1}{(C_1+iD_1)(C_2+iD_2)}\right]_{T=T_c}\right\}, \qquad (7.3)$$

where

$$A_1 = R - 3\omega^2 + T(P - Q\omega^2),$$

$$B_1 = 2Q\omega + T\omega(R - \omega^2),$$

$$C_1 = (P - Q\omega^2),$$

$$D_1 = \omega(R - \omega^2),$$

$$C_2 = P\mathcal{R}_{0d}\mu_s,$$

$$D_2 = P\omega(\mathcal{R}_{0d} - 2).$$

Rationalizing the denominator of (7.3) gives

$$\text{sign}\left\{\frac{d(\text{Re}\lambda)}{dT}\right\}_{T=T_c} = \text{sign}\left\{P(2 - \mathcal{R}_{0d})\frac{A_1(C_1C_2 - D_1D_2) + B_1(C_1D_2 + C_2D_1)}{(C_1C_2 - D_1D_2)^2 + (C_1D_2 + C_2D_1)^2}\right\}_{T=T_c}.$$

Since, $P(2-\mathcal{R}_{0d}) < 0$ (noting that $\mathcal{R}_{0d} > 3$ from (4.58)) and $(C_1C_2-D_1D_2)^2+(C_1D_2+C_2D_1)^2 > 0$, the sign of $[A_1(C_1C_2-D_1D_2)+B_1(C_1D_2+C_2D_1)]$ will determine the sign of the real part of $\frac{d\lambda}{dT}$ at $T = T_c$. Now,

$$\begin{aligned} A_1(C_1C_2 - D_1D_2) + B_1(C_1D_2 + C_2D_1) = \Big\{&[R - 3\omega^2 + T(P - Q\omega^2)][P\mathcal{R}_{0d}\mu_s(P - Q\omega^2) \\ &- P\omega^2(R - \omega^2)(\mathcal{R}_{0d} - 2)] + [2Q\omega + T\omega(R - \omega^2)] \\ &\times [P\omega(P - Q\omega^2)(\mathcal{R}_{0d} - 2) + P\mathcal{R}_{0d}\mu_s\omega(R - \omega^2)]\Big\}_{T=T_c,\omega=\omega_c}. \end{aligned}$$

Thus, $\left\{\frac{d(\text{Re}\lambda)}{dT}\right\}_{T=T_c} > 0$ if the inequalities in (4.62) hold. □

# Appendix C: Proof of Lemma 4.7

*Proof.* Using the birth function **B2** in the characteristic equation (4.40) gives

$$\lambda^3 + Q\lambda^2 + R\lambda + P = P(1-n)e^{-\lambda T} + \frac{P^2}{AB_0}e^{-(\mu_s+\lambda)T}. \tag{7.4}$$

Differentiating (7.4) with respect to $T$ gives

$$\left[3\lambda^2+2Q\lambda+R+P(1-n)Te^{-\lambda T}+\frac{P^2T}{AB_0}e^{-(\mu_s+\lambda)T}\right]\frac{d\lambda}{dT} = -P(1-n)\lambda e^{-\lambda T}-\frac{P^2}{AB_0}(\lambda-\mu_s)e^{-(\lambda-\mu_s)T},$$

so that,

$$\left(\frac{d\lambda}{dT}\right)^{-1} = \frac{3\lambda^2 + 2Q\lambda + R + e^{-\lambda T}[PT(1-n) + \frac{P^2T}{AB_0e^{-\mu_s T}}]}{e^{-\lambda T}[-P(1-n)\lambda - \frac{P^2}{AB_0e^{-\mu_s T}}(\lambda-\mu_s)]},$$

$$= \frac{3\lambda^2 + 2Q\lambda + R + e^{-\lambda T}[PT(1-n) + \frac{P^2T}{P\mathcal{R}_{0d}}]}{e^{-\lambda T}[-P(1-n)\lambda - \frac{P^2}{P\mathcal{R}_{0d}}(\lambda-\mu_s)]},$$

$$= \frac{3\lambda^2 + 2Q\lambda + R + e^{-\lambda T}[PT(1-n) + \frac{PT}{\mathcal{R}_{0d}}]}{e^{-\lambda T}[-P(1-n)\lambda - \frac{P}{\mathcal{R}_{0d}}(\lambda-\mu_s)]},$$

$$= \frac{3\lambda^2 + 2Q\lambda + R + \left\{\frac{\lambda^3+Q\lambda^2+R\lambda+P}{P[1-n(1-\frac{1}{\mathcal{R}_{0d}})]}\right\}[PT(1-n) + \frac{PT}{\mathcal{R}_{0d}}]}{\left\{\frac{\lambda^3+Q\lambda^2+R\lambda+P}{P[1-n(1-\frac{1}{\mathcal{R}_{0d}})]}\right\}[-P(1-n)\lambda - \frac{P}{\mathcal{R}_{0d}}(\lambda-\mu_s)]}.$$

Hence,

$$\left(\frac{d\lambda}{dT}\right)^{-1} = \frac{(3\lambda^2 + 2Q\lambda + R)[\mathcal{R}_{0d}(1-n)+n] + T(\lambda^3 + Q\lambda^2 + R\lambda + P)[\mathcal{R}_{0d}(1-n)+n]}{(\lambda^3 + Q\lambda^2 + R\lambda + P)[(n-1)\lambda\mathcal{R}_{0d} + n(\mu_s - \lambda)]}. \tag{7.5}$$

Substituting $\lambda = i\omega$ in (7.5) gives

$$\left(\frac{d\lambda}{dT}\right)^{-1} = \frac{[\mathcal{R}_{0d}(1-n)+n]\{R - 3\omega^2 + T(P - Q\omega^2) + i[2Q\omega + T\omega(R-\omega^2)]\}}{[P - Q\omega^2 + i\omega(R-\omega^2)]\{n\mu_s + i[\omega\mathcal{R}_{0d}(n-1) - n\omega]\}},$$

which can be re-written as

$$\left(\frac{d\lambda}{dT}\right)^{-1} = \frac{[\mathcal{R}_{0d}(1-n)+n](G_1 + iH_1)}{(M_1 + iN_1)(M_2 + iN_2)},$$

where,

$$G_1 = R - 3\omega^2 + T(P - Q\omega^2),$$

$$H_1 = 2Q\omega + T\omega(R - \omega^2),$$

$$M_1 = P - Q\omega^2,$$

$$N_1 = \omega(R - \omega^2),$$

$$M_2 = n\mu_s,$$

$$N_2 = \omega\mathcal{R}_{0d}(n-1) - n\omega.$$

Thus,

$$\text{sign}\left\{\frac{d(\text{Re}\lambda)}{dT}\right\}_{T=T_c} = \text{sign}\left\{\text{Re}\left(\frac{d\lambda}{dT}\right)^{-1}\right\}_{T=T_c},$$

$$= \text{sign}\left\{[\mathcal{R}_{0d}(1-n)+n]\text{Re}\left[\frac{(G_1+iH_1)}{(M_1+iN_1)(M_2+iN_2)}\right]_{T=T_c}\right\},$$

$$= \text{sign}\left\{[\mathcal{R}_{0d}(1-n)+n]\left[\frac{G_1(M_1M_2-N_1N_2)+H_1(M_1N_2+M_2N_1)}{(M_1M_2-N_1N_2)^2+(M_1N_2+M_2N_1)^2}\right]_{T=T_c}\right\}.$$

Since $\mathcal{R}_{0d} > \dfrac{n}{n-2}$ (from (4.59)), it follows that $n > 2$ (for $\mathcal{R}_{0d} > 1$). Noting that $\mathcal{R}_{0d} > 1$ for $E_1$ to exist, it is easy to show that the term $\mathcal{R}_{0d}(1-n)+n < 0$. Furthermore, $(M_1M_2 - N_1N_2)^2 + (M_1N_2 + M_2N_1)^2 > 0$. Thus, $\left\{\dfrac{d(\text{Re}\lambda)}{dT}\right\}_{T=T_c} > 0$ if the following inequality holds:

$$G_1(M_1M_2 - N_1N_2) + H_1(M_1N_2 + M_2N_1) < 0. \tag{7.6}$$

The inequality (7.6) can be simplified to,

$$[R - 3\omega_c^2 + T_c(P - Q\omega_c^2)]\left\{n\mu_s(P - Q\omega_c^2) - \omega_c^2(R - \omega_c^2)[\mathcal{R}_{0d}(n-1) - n]\right\}$$
$$+ [2Q\omega_c + T_c\omega_c(R - \omega_c^2)]\left\{(P - Q\omega_c^2)[\omega_c\mathcal{R}_{0d}(n-1) - n\omega_c] + n\mu_s(R - \omega_c^2)\right\} < 0,$$

so that,

$$
\begin{aligned}
&n\mu_s T_c(P - Q\omega_c^2)^2 + n\mu_s T_c\omega_c^2(R - \omega_c^2)^2 + 2Qn\mu_s\omega_c^2(R - \omega_c^2) \\
&- 3\omega_c^2\Big\{n\mu_s(P - Q\omega_c^2) + \omega_c^2(R - \omega_c^2)[\mathcal{R}_{0d}(1 - n) + n]\Big\} \\
&< \omega_c^2[\mathcal{R}_{0d}(1 - n) + n][2Q(P - Q\omega_c^2) - R(R - \omega_c^2)] - n\mu_s R(P - Q\omega_c^2),
\end{aligned}
$$

which is equivalent to,

$$\frac{F_1}{F_2} < 1.$$

□

# Appendix D: Proof of Theorem 5.5

*Proof.* Consider the Lyapunov function

$$\mathcal{F}_3 = M + rY_n + \sum_{m=1}^{n-1} r \prod_{i=m}^{n-1} \frac{\gamma_i}{Q_i} Y_m,$$

with Lyapunov derivative given by

$$\begin{aligned}
\dot{\mathcal{F}}_3 &= r(\mu_n + \gamma_n)Y_n - \mu_M M - u\beta XM + r(\gamma_{n-1}Y_{n-1} - Q_n Y_n) \\
&\quad + \left(\frac{r\gamma_1\gamma_2\cdots\gamma_{n-1}}{Q_1Q_2\cdots Q_{n-1}}\right)(\beta XM - Q_1Y_1) + \left(\frac{r\gamma_2\gamma_3\cdots\gamma_{n-1}}{Q_2Q_3\cdots Q_{n-1}}\right)(\gamma_1Y_1 - Q_2Y_2) \\
&\quad + \cdots + \left(\frac{r\gamma_{n-1}}{Q_{n-1}}\right)(\gamma_{n-2}Y_{n-2} - Q_{n-1}Y_{n-1}), \\
&= \left(\frac{\beta r\gamma_1\gamma_2\cdots\gamma_{n-1}X}{Q_1Q_2\cdots Q_{n-1}} - \mu_M\right)M - u\beta XM, \\
&= \beta XM\left(\frac{r\gamma_1\gamma_2\cdots\gamma_{n-1}}{Q_1Q_2\cdots Q_{n-1}} - u\right) - \frac{\mu_M}{\beta}M, \\
&= \beta\left(\frac{r\gamma_1\gamma_2\cdots\gamma_{n-1}}{Q_1Q_2\cdots Q_{n-1}} - u\right)\left[X - \frac{\mu_M}{\beta\left(\frac{r\gamma_1\gamma_2\cdots\gamma_{n-1}}{Q_1Q_2\cdots Q_{n-1}} - u\right)}\right]M, \\
&= \beta\left(\frac{r\gamma_1\gamma_2\cdots\gamma_{n-1}}{Q_1Q_2\cdots Q_{n-1}} - u\right)(X - X^{**})M.
\end{aligned}$$

We consider the following cases for the sign of $\dot{\mathcal{F}}_3$.

**Case 1**: If $R_S < 1$ and $(\frac{r\gamma_1\gamma_2\cdots\gamma_{n-1}}{Q_1Q_2\cdots Q_{n-1}} - u) < 0$, then it follows from the expression for $X^{**}$ in Section 5.2.2 that $X^{**} < 0$, so that $X - X^{**} > 0$. Hence, $\dot{\mathcal{F}}_3 \leq 0$.

**Case 2**: If $(\frac{r\gamma_1\gamma_2\cdots\gamma_{n-1}}{Q_1Q_2\cdots Q_{n-1}} - u) > 0$, then using inequality (5.18) and the fact that $X \leq X^*$ in $\mathcal{D}_1^*$, we have $\dot{\mathcal{F}}_3 \leq 0$.

Thus, $\dot{\mathcal{F}}_3 \leq 0$ if $\mathcal{R}_S \leq 1$ with $\dot{\mathcal{F}}_3 = 0$ if and only if $M = 0$. Further, the largest compact invariant set in $\{(X, Y_1, Y_2, \cdots, Y_n, M) \in \mathcal{D}_1^* : \dot{\mathcal{F}}_3 = 0\}$ is the singleton $\{E_{01}\}$. It follows from the LaSalle's Invariance Principle [56, 86] that every solution to the system (5.10) with initial conditions in $\mathcal{D}_1^*$ converge to the DFE $E_{01}$ as $t \to \infty$. That is, $(Y_1(t), Y_2(t), \cdots, Y_n(t), M(t)) \to (0, 0, \cdots, 0)$ as $t \to \infty$. Substituting these in the equations for $dX/dt$ gives $X(t) \to X^*$ as $t \to \infty$. Hence, the DFE, $E_{01}$, of the model (5.10) is GAS in $\mathcal{D}_1^*$ if $\mathcal{R}_S \leq 1$. □

# Appendix E: Proof of Theorem 5.6

*Proof.* Consider the following Lyapunov function (with non-negative coefficients $a$, $b_i$ and $c$)

$$\mathcal{F}_4 = a(X - X^{**}\ln X) + \sum_{i=1}^{n} b_i(Y_i - Y_i^{**}\ln Y_i) + c(M - M^{**}\ln M),$$

with Lyapunov derivative given by

$$\dot{\mathcal{F}}_4 = a\left(\dot{X} - \frac{X^{**}}{X}\dot{X}\right) + \sum_{i=1}^{n} b_i\left(\dot{Y}_i - \frac{Y_i^{**}}{Y_i}\dot{Y}_i\right) + c\left(\dot{M} - \frac{M^{**}}{M}\dot{M}\right).$$

Following the approach in Adda *et al.* [1], the coefficients $a, b_i$ and $c$ are chosen such that, in the computation of $\dot{\mathcal{F}}_4$, the linear terms in $Y_i$ and $M$ and the bilinear terms in $XM$ cancel out. This entails using the following relations (obtained from equating the linear terms from the system (5.10)):

$$\begin{aligned} a + uc &= b_1, \\ b_1 Q_1 &= \gamma_1 b_2, \\ b_2 Q_2 &= \gamma_2 b_3, \\ &\cdots\cdots\cdots \\ b_{n-1} Q_{n-1} &= \gamma_{n-1} b_n, \\ b_n Q_n &= cr(\gamma_n + \mu_n). \end{aligned} \tag{7.7}$$

It follows from the above relations that

$$b_n = \frac{cr(\gamma_n + \mu_n)}{Q_n},$$

$$b_{n-1} = \frac{cr(\gamma_n + \mu_n)\gamma_{n-1}}{Q_n Q_{n-1}},$$

.....

$$b_i = \frac{cr(\gamma_n + \mu_n)\gamma_{n-1}\cdots\gamma_i}{Q_n Q_{n-1}\cdots Q_i}, \tag{7.8}$$

.....

$$b_1 = \frac{cr(\gamma_n + \mu_n)\gamma_{n-1}\cdots\gamma_1}{Q_n Q_{n-1}\cdots Q_1},$$

$$a = \frac{cr(\gamma_n + \mu_n)\gamma_{n-1}\cdots\gamma_1}{Q_n Q_{n-1}\cdots Q_1} - uc = c\frac{\mu_M}{\beta X^{**}} > 0.$$

Collecting the linear terms in $M$ gives $(a\beta X^{**} - c\mu_M)M$. The terms in $M$ cancel out for any value of $c$. Consider $c = 1$, without loss of generality. Thus,

$$\dot{\mathcal{F}}_4 = a\left[(\lambda_X - \mu_X X) - \frac{X^{**}}{X}(\lambda_X - \mu_X X)\right] - b_1\beta Y_1^{**}\frac{XM}{Y_1} - \sum_{i=2}^{n} b_i\gamma_{i-1}Y_{i-1}\frac{Y_i^{**}}{Y_i}$$
$$+ \sum_{i=1}^{n} b_i Q_i Y_i^{**} - r(\gamma_n + \mu_n)Y_n\frac{M^{**}}{M} + u\beta M^{**}X + \mu_M M^{**}.$$

It follows from the system of equations (5.10), and the relation among the coefficients ($a$, $b_i$ and $c$) given in (7.7) and (7.8) that

$$b_1\beta X^{**}M^{**} = b_iQ_iY_i^{**} = b_i\gamma_{i-1}Y_{i-1}^{**} = r(\gamma_n+\mu_n)Y_n^{**}, \tag{7.9}$$

and,

$$\begin{aligned}\mu_M M^{**} &= r(\gamma_n+\mu_n)Y_n^{**} - u\beta X^{**}M^{**},\\ &= b_1\beta X^{**}M^{**} - u\beta X^{**}M^{**},\\ &= (b_1-u)\beta X^{**}M^{**} = aQ_1Y_1^{**}.\end{aligned} \tag{7.10}$$

Using the relations in (7.9) and (7.10) gives

$$\begin{aligned}\dot{\mathcal{F}}_4 &= kr(\gamma_n+\mu_n)Y_n^{**} + 2a\lambda_X - a\lambda_X\frac{X^{**}}{X} + [r(\gamma_n+\mu_n)Y_n^{**} - a\lambda_X]\frac{X^{**}}{X}\\ &\quad - r(\gamma_n+\mu_n)Y_n^{**}\frac{X}{X^{**}}\frac{M}{M^{**}}\frac{Y_1^{**}}{Y_1} - \sum_{i=2}^{n} r(\gamma_n+\mu_n)Y_n^{**}\frac{Y_{i-1}}{Y_{i-1}^{**}}\frac{Y_i^{**}}{Y_i} - r(\gamma_n+\mu_n)Y_n^{**}\frac{Y_n}{Y_n^{**}}\frac{M^{**}}{M},\\ &= r(\gamma_n+\mu_n)\left(n + \frac{X}{X^{**}} - \frac{X}{X^{**}}\frac{M}{M^{**}}\frac{Y_1^{**}}{Y_1} - \sum_{i=2}^{n}\frac{Y_{i-1}}{Y_{i-1}^{**}}\frac{Y_i^{**}}{Y_i} - \frac{Y_n}{Y_n^{**}}\frac{M^{**}}{M}\right)Y_n^{**}\\ &\quad + a\lambda_X\left(2 - \frac{X^{**}}{X} - \frac{X}{X^{**}}\right),\\ &= r(\gamma_n+\mu_n)\left(n+2 - \frac{X^{**}}{X} - \frac{X}{X^{**}}\frac{M}{M^{**}}\frac{Y_1^{**}}{Y_1} - \sum_{i=2}^{n}\frac{Y_{i-1}}{Y_{i-1}^{**}}\frac{Y_i^{**}}{Y_i} - \frac{Y_n}{Y_n^{**}}\frac{M^{**}}{M}\right)Y_n^{**}\\ &\quad + (b_1\mu_X X^{**} - u\lambda_X)\left(2 - \frac{X^{**}}{X} - \frac{X}{X^{**}}\right).\end{aligned}$$

The terms in the bracket of the last equation are non-positive, since the arithmetic mean exceeds the geometric mean. Thus, $\dot{\mathcal{F}}_4 \leq 0$ if

$$b_1 \mu_X X^{**} - u\lambda_X \geq 0,$$

which is equivalent to

$$b_1 \geq \frac{u\lambda_X}{\mu_X X^{**}}.$$

Hence, $\dot{\mathcal{F}}_4 \leq 0$ if $\mathcal{R}_S \geq 1$ and $b_1 \geq \frac{u\lambda_X}{\mu_X X^{**}}$ with $\dot{\mathcal{F}}_4 = 0$ if and only if $(X, Y, M) = (X^{**}, Y^{**}, M^{**})$. The proof is concluded as in the case for the proof of Theorem 5.5.

□

# Bibliography

[1] Adda, P., Dimi, J. L., Iggidr, A., Kamgang, J. C., Sallet, G. and Tewa, J. J. (2007). General models of host-parasite systems. Global analysis. *Discrete and Continuous Dynamical Systems-Series B.* **8**: 1-17.

[2] Anderson, R. M. and May, R. M. eds. (1982). Population of Biology of Infectious Diseases, Springer-Verlag, Berlin, Heidelberg, New York.

[3] Anderson, R. M., May, R. M. and Gupta, S. (1989). Non-linear phenomena in host-parasite interactions. *Parasitology.* **99**: 59-79.

[4] Anderson, R. M. and May, R. M. eds. (1991). Infectious Diseases of Humans: Dynamics and Control, Oxford Univ. Press, London/New York.

[5] Anderson, R. M. (1998). Complex dynamic behaviours in the interaction between parasite population and the host's immune system. *Int. Journal of Parasitol.* **28**: 551-566.

[6] Aneke, S. J. (2002). Mathematical modelling of drug resistant malaria parasites and vector population. *Mathematical Methods in the Applied Sciences.* **90**: 385-396.

[7] Arino, J., Cooke, K. L., van den Driessche, P. and Velasco-Hernández, J. (2004). An epidemiology model that includes a leaky vaccine with a general waning function. *Discrete and Continuous Dynamical Systems-B.* **4**: 479-495.

[8] Arino, J. and van den Driessche, P. (2006). Time delays in epidemic models: modeling and numerical considerations. Pages 539-578 in Delay Differential Equations and Applications, O. Arino, M.L. Hbid and E. Ait Dads, editors, Springer Verlag.

[9] Aron, J. L. (1988). Acquired immunity dependent upon exposure in an SIRS epidemic model. *Math. Biosci.* **88**: 37-47.

[10] Aron, J. L. (1988). Mathematical modelling of immunity to malaria. *Math. Biosci.* **90**: 385-396.

[11] Bailey, N. T. J. (1982). The Biomathematics of Malaria. Malaria, Charles Griffin Co. Ltd., London. 1-93.

[12] Baird, J. (2000). Resurgent malaria at the millennium: control strategies in crisis. *Drugs.* **59**: 719-743.

[13] Ballou, W. R., Alo-Herrera, M. A., Carucci, D., Richie, T. L., Corradin, G., Diggs, C., Druilhe, P., Giersing, B., Saul, A., Heppner, D. G., Kester, K. E., Lanar, D. E., Lyon, J., Hill, A. V. S., Pan, W. and Cohen, J. D. (2004). Update on the clinical development of candidate malaria vaccines. *Am. J. Trop. Med. Hyg.* **71**: 239-247.

[14] Ballou, W. R. *et al.* (2004). Update on the Clinical Development of Candidate Malaria Vaccines. In The Intolerable Burden of Malaria: II. What's New, What's Needed. The American Society of Tropical Medicine and Hygiene, Northbrook, IL. Joel G. Breman, Martin S. Alilio, and Anne Mills, Editors.

[15] Bowman, C., Gumel, A. B., van den Driessche, P., Wu, J. and Zhu, H. (2005). A mathematical model for assessing control strategies against West Nile virus. *Bull. of Math. Bio.* **67**: 1107-33.

[16] Brännström, Å. and Sumpter, D. J. T. (2005). The role of competition and clustering in population dynamics. *Proc. R. Soc. B.* **272**: 2065-2072.

[17] Carr, J. (1981). Applications of Centre Manifold Theory. Springer-Verlag, New York.

[18] Castanera, M. B., Aparicio, J. P. and Gurtler, R. E. (2003). A stage-structured stochastic model of the population dynamics of *Triatoma infestans*, main vector of Chagas disease. *Ecol. Model.* **162**: 33-53.

[19] Castillo-Chavez, C., Cooke, K., Huang, W. and Levin, S. A. (1989). Results on the dynamics for models for the sexual transmission of the human immunodeficiency virus. *Appl. Math. Letters.* **2**: 327-331.

[20] Castillo-Chavez, C., Cooke, K., Huang, W. and Levin, S. A. (1989). The role of long incubation periods in the dynamics of HIV/AIDS.part 2: Multiple group models, In Carlos Castillo-Chavez, ed., Mathematical and Statistical Approaches

to AIDS Epidemiology, Lecture Notes in Biomathematics, Springer-Verlag. **83**: 200-217.

[21] Castillo-Chavez, C. and Song, B. (2004). Dynamical models of tuberculosis and their applications. *Math. Biosci. Engrg.* **2**: 361-404.

[22] Celik, C. (2008). The stability and Hopf bifurcation for a predator-prey system with time delay. *Chaos, Solitons and Fractals.* **37**: 87-99.

[23] Chitnis, N., Cushing, J. M. and Hyman, J. M. (2006). Bifurcation analysis of a mathematical model for malaria transmission. *SIAM J. of Appl. Math.* **67**(1): 24-45.

[24] Chiyaka, C., Garira, W. and Dube, S. (2008). Modelling immune response and drug therapy in human malaria infection. *Computational and Mathematical Methods in Medicine.* **9**:143-163.

[25] Cooke, K., van den Driessche, P. and Zou, X. (1999). Interaction of maturation delay and nonlinear birth in population and epidemic models. *J. Math. Biol.* **39**: 332-352.

[26] Costantino, R. F., Desharnais, R. A., Cushing, J. M. and Brian, D. (1998). Chaotic dynamics in an insect population. *Science.* **275**: 389-391.

[27] Coutinho, F. A. B., Burattini, M. N., Lopez, L. F. and Massad, E. (2005). An approximate threshold condition for non-autonomous system: an application to a vector-borne infection. *Mathematics and Computers in Simulation.* **70**: 149-158.

[28] Culshaw, R. V. and Ruan, S. (2000). A delay-differential equation model of HIV infection of $CD4^+$ T-cells. *Mathematical Biosciences.* **165**: 27-39.

[29] Depinay, J. O., Mbogo, C. M., Killeen, G., Knols, B., Beier, J., Carlson, J., Dushoff, J., Billingsley, P., Mwambi, H., Githire, J., Toure, A. M. and Mckenzie, F. E. (2004). A simulation model of African *Anopheles* ecology and population dynamics for the analysis of malaria transmission. *Malaria Journal.* **3**: 29.

[30] Diebner, H. H., Eincher, M., Molineaux, L., Collins, W. E., Jefferey, G. M. and Dietz, K. (2000). Modelling the transition of sexual blood stages of Plasmodium falciparum to gameatocytes. *J. Theor. Biol.* **202**: 113-127.

[31] Diekmann, O., Heesterbeek, J. A. P. and Metz, J. A. J. (1990). On the definition and computation of the basic reproduction ratio $\mathcal{R}_0$ in models for infectious disease in heterogeneous population. *J. Math. Biol.* **28**: 365-382.

[32] Dietz, K., Molineaux, L. and Thomas, A. (1974). A malaria model tested in the African Savannah. *Bull. World Health Association.* **50**: 347-357.

[33] Dietz, K. (1975). Transmission and control of arbovirus disease, In Epidemiology, K. L. Cooke, ed. *SIAM*, Philadelphia.

[34] Dieudonné, J. (1969). Foundations of Modern Analysis. Academic Press, London.

[35] Druilhe, P., Spertini, F., Soesoe, D., Corradin, G., Mejia, P., Singh, S., Audran, R., Bouzidi, A., Oeuvray, C. and Roussilhon, C. (2005). A malaria vaccine that

elicits in humans antibodies able to kill *Plasmodium falciparum. PLoS Medicine.* **2**: 1135-1144.

[36] Dubovsky, F. (2001). Creating a Vaccine Against Malaria. Malaria Vaccine Initiative at PATH. 1-5.

[37] Elbasha, E. H. and Gumel, A. B. (2006). Theoretical assessment of public health impact of imperfect Prophylactic HIV-1 vaccines with therapeutic benefits. *Bull. Math. Biol.* **68**: 577-614.

[38] Engwerda, C. R. and Good, M. F. (2005). Interactions between malaria parasites and the host immune system. *Current Opinion in Immunology.* **17**: 381-387.

[39] Esteva, L., Gumel, A. B. and de Leon, C. V. (2009). Qualitative study of transmission dynamics of drug-resistant malaria. *Mathematical and Computer Modelling.* **50**:611-630.

[40] Feng, Z., Castillo-Chavez, C. and Capurro, F. (2000). A model for tuberculosis with exogeneous reinfection. *Theor. Pop. Biol.* **57**: 235-247.

[41] Forde, J. and Nelson, P. (2004). Applications of Strum sequences to bifurcation analysis of delay differential equation models. *J. Math. Anal. and Appl.* **300**: 273-284.

[42] Freedman, H. I. and So, J. W. H. (1985). Global stability and persistence of simple food chains. *Math. Biosci.* **76**: 69-86.

[43] Garba, S. M., Gumel, A. B. and Abu Bakar, M. R. (2008) Backward bifurcation in dengue transmission dynamics. *Math. Biosci.* **215**: 11-25.

[44] Gemperli, A., Vounatsou, P., Sogoba, N. and Smith, T. (2006). Malaria mapping using transmission models: application to survey data. *American Journal of Epidemiology.* **163**: 289-297.

[45] Genton, B. and Reed, Z. H. (2007). Asexual blood-stage malaria vaccine development: facing the challenges. Tropical and travel-associated diseases. *Current Opinion in Infectious Diseases.* **20**: 467-475.

[46] Ghosh, A. K., Chattppadhyay, J. and Tapaswi, P. K. (1996). Immunity boosted by low exposure to infection in an SIRS model. *Ecological Modelling.* **87**: 227-233.

[47] Giles, H. M. and Warrel, D. A. (1993). Bruce-Chwatt's Essential Malariology, 3rd Edition. Heinemann Medical Books, Portsmouth, NH.

[48] Global Health Reporting. http://www.globalhealthreporting.org/malaria.asp?id=3494. (Accessed March 2009).

[49] Gravenor, M. B., McLean, A. R. and Kwiatkowski, D. (1995). The regulation of malaria parasitaemia: parameter estimates for a population model. *Parasitology.* **110**: 115-122.

[50] Gravenor, M. B. and Lloyd, A. L. (1998). Reply to: Models for the in-host dynamics of malaria revisited: Errors in some basic models lead to large over-estimates of growth rates. *Parasitology.* **117**: 409-410.

[51] Gravenor, M. B., Lloyd, A. L., Kremsner, P.G., Missinou, M. A., English, M., Marsh, K. and Kwiatkowski, D. (2002). A model for estimating total parasite load in falciparum malaria patients. *J. Theor. Biol.* **217**: 137-148.

[52] Gumel, A. B., McCluskey, Connell C. and Watmough, J. (2006). An SVEIR model for assessing potential impact of an imperfect anti-SARS vaccine. *Math. Biosci. Engrg.* **3**: 485-512.

[53] Gumel, A. B. (2009). Global dynamics of a two-strain avian influenza model. *International Journal of Computer Mathematics.* **86**: 85-108.

[54] Guo, H. and Li, M. Y. (2006). Global dynamics of a staged progression model for infectious diseases. *Mathematical Biosciences and Engineering.* **3**: 513-525.

[55] Hadeler, K. P. and Castillo-Chavez, C. (1995). A core group model for disease transmission. *Mathematical Biosciences.* **128**: 41-55.

[56] Hale, J. K. (1969). Ordinary Differential Equations. John Wiley and Sons, New York.

[57] Hale, J. K. (1977). Theory of Functional Differential Equations. Springer-Verlag, New York.

[58] Hassard, B. D., Kazarinoff, N. D. and Wan, Y. N. (1981). Theory and Application of Hopf Bifurcations. Cambridge University Press, Cambridge.

[59] Hellriegel, B. (1992). Modelling the immune response to malaria with ecological concepts: Short-term behaviour against long-term equilibrium. *Proc. R. Soc. Lond. Ser. B.* **250**: 249-256.

[60] Hethcote, H. W. (1976). Qualitative analysis of communicable disease models. *Math. Biosci.* **28**: 335-356.

[61] Hethcote, H. W. and van Ark, J. W. (1987). Epidemiology models for heterogeneous populations: proportionate mixing, parameter estimation, and immunization programs. *Math. Biosci.* **84**: 85-118.

[62] Hethcote, H. W. (1994). A thousand and one epidemic models. In Frontiers in Theoretical Biology, S. A. Levin, ed. Lecture notes in Biomath. 100, Springer-Verlag, Berlin, 504-515.

[63] Hethcote, H. M. (2000). The mathematics of infectious diseases. *SIAM Rev.* **42**: 599-963.

[64] Hethcote, W. H. and van den Driessche, P. (2000). Two SIS epidemiologic models with delays. *J. Math. Biol.* **40**: 3-26.

[65] Hetzel, C. and Anderson, R. M. (1996). The within-host cellular dynamics of bloodstage malaria: Theoretical and experimental studies. *Parasitology.* **113**: 25-38.

[66] Hirsch, W. M., Hanisch, H. and Gabriel, J. P. (1985). Differential equation models for some parasitic infections; methods for the study of asymptotic behaviour. *Comm. Pure Appl. Math.* **38**: 733-753.

[67] Hoffman, S. L., Goh, L. M., Luke, T. C., Schneider, I., Le, T. P., Doolan, D. L., Sacci, J., de la Vega, P., Dowler, M., Paul, C., Gordon, D. M., Stoute, J. A., Church, L. W., Sedagah, M., Heppner, D. G., Ballou, W. R. and Richie, T. L. (2002). Protection of humans against malaria by immunization with radiation-attenuated *Plasmodium falciparum* sporozoites. *J. Infec. Dis.* **185**: 1155-1165.

[68] Holmes, P. and Guckenheimer, J. (1990). Nonlinear Oscillations, Dynamical Systems, and Bifurcations of Vector Fields, Springer-Verlag, New York Inc.

[69] Hoshen, M. B., Heinrich, R., Stein, W. D. and Ginsburg, H. (2001). Mathematical modelling of the within-host dynamics of *Plasmodium falciparum*. *Parasitology.* **121**: 227-235.

[70] Hviid, P. (2005). Natural acquired immunity to *Plasmodium falciparum* in Africa. *Acta Tropica.* **95**: 265-269.

[71] Iggidr, A., Kamgang, J.C., Sallet, G. and Tewa, J.J. (2006). Global analysis of new malaria intrahost models with a competitive exclusion principle. *SIAM J. Appl. Math.* **67**: 260-278.

[72] Ishikawa, H., Ishi, A., Nagai, N., Ohmae, H., Masakazu, H., Suguri, S. and Leafasia, J. (2003). A mathematical model for the transmission of *Plasmodium vivax* malaria. *Parasitology International.* **52**: 81-93.

[73] Jang, S. R.-J. (2005). Contest and scramble competition with a dynamic resource. *Nonlinear Analysis.* **63**: 109-118.

[74] Kermack, W. O. and McKendrick, A. G. (1927). A contribution to the mathematical theory of epidemic. *Proc. Roy. Soc. A.* **115**: 700-721.

[75] Koella, J. C. (1991). On the use of mathematical models of malaria transmission. *Acta Tropica.* **49**: 1-25.

[76] Koella, J. C. and Antia, R. (2003). Epidemiological models for the spread of anti-malarial resistance. *Malaria Journal.* **2**: 3.

[77] Korobeinikov, A. and Wake, G. C. (2002). Lyapunov functions and global stability for SIR, SIRS and SIS epidemiological models. *Appl. Math. Lett.* **15**: 955-960.

[78] Korobeinikov, A. and Maini, P. K. (2004). A Lyapunov function and global properties for SIR and SEIR epidemiological models with nonlinear incidence. *Mathematical Biosciences and Engineering.* **1**: 61-80.

[79] Korobeinikov, A. (2006). Lyapunov functions and global stability for SIR and SIRS epidemiological models with non-linear transmission. *Bull. Math. Biol.* **68**: 615-626.

[80] Kribs-Zaleta, C. M. (1999). Structured models for heterosexual disease transmission. *Mathematical Biosciences.* **160**: 83-108.

[81] Kribs-zaleta, C. and Valesco-Hernandez, J. (2000). A simple vaccination model with multiple endemic state. *Math. Biosci.* **164**: 183-201.

[82] Kuang, Y. (1993). Delay Differential Equations with Applications in Population Dynamics. Academic Press, Boston.

[83] Kwiatkowski, D. (1995). Malaria toxins and the regulation of parasite density. *Parasitology Today.* **11**: 206-212.

[84] Kwiatkowski, D. and Nowak, M. (1991). Periodic and chaotic host-parasite interactions in human malaria. *Proc. Natl. Acad. Sci. USA.* **88**: 5111-5113.

[85] Lambert, J. D. (1932). Numerical Methods for Ordinary Differential Systems. John Wiley and Sons, New York.

[86] LaSalle, J. P. (1976). The stability of dynamical system. Regional Conference Series in Applied Mathematics. *SIAM.* Philadelphia.

[87] Li, M. Y. and Muldowney, J. S. (1996). A geometric approach to global stability problems. *SIAM Journal on Mathematical Analysis.* **27**: 1070-1083.

[88] Linthicum, K. J., Anyamba, A., Tucker, C. J., Kelley, P. W., Myers, M. F. and Peters, C. J. (1999). Climate and satellite indicators to forest rift valley fever epidemics in Kenya. *Science.* **285**: 397-400.

[89] Lipsitch, M. and Murray, M.B. (2003). Multiple equilibria: tuberculosis transmission require unrealistic assumptions. *Theor. Popul. Biol.* **63**: 169-70.

[90] Macdonald, G. (1957). The Epidemiology and Control of Malaria. Oxford University Press, London.

[91] Malaria and the Human Immune System. (2002). http://malaria.wellcome.ac.uk/doc_WTD023881.html. (Accessed March, 2009).

[92] Malaria Site. http://malariasite.com (Accessed August, 2009).

[93] The Malaria Vaccine Initiative (MVI). http://www.malariavaccine.org/index.htm. (Accessed December, 2007).

[94] Marsden, J. E. and McCracken, M. F. (1976). The Hopf Bifurcation and its Applications. Springer-Verlag, New York.

[95] McCall, P. J. and David, W. K. (2002). Learning and memory in disease vectors. Research Update. *Trends Parasitol.* **18**: 429-433.

[96] McCluskey, C. Connell. (2008). Global stability for a class of mass action system allowing for latency in tuberculosis. *Journal of Mathematical Analysis and Applications.* **338**: 518-535.

[97] McQueen, P. G. and McKenzie, F. E. (2004). Age-structured red blood cell susceptibility and the dynamics of malaria infections. *Proc. Natl. Acad. Science. USA.* **101**: 9161-9166.

[98] McQueen, P. G. and McKenzie, F. E. (2008). Host control of malaria infections: constraints on immune and erythropoeitic response kinetics. *PLoS Computational Biology.* 4(8): e1000149.

[99] Mikolajczak, S. A., Aly, A. S. I. and Kappe, S. H. I. (2007). Pre-erythrocytic malaria vaccine development. Tropical and travel-associated diseases. *Current Opinion in Infectious Diseases.* **20**(5): 461-466.

[100] Molineaux, L. and Gramiccia, G. (1980). The Garki Project: Research on the Epidemiology and Control of Malaria in the Sudan Savanna of West Africa. World Health Organization, Geneva.

[101] Molineaux, L., Diebner, H. H., Eincher, M., Collins, W. E., Jefferey, G. M. and Dietz, K. (2001). *Plasmodium falciparum* parasitaemia described by a new mathematical model. *Parasitology.* **122**: 379-391.

[102] Molineaux, L. and Dietz, K. (1999). Review of intra-host models of malaria. *Parasitoligia.* **41**: 221-231.

[103] Moon, E. T. (1976). A statistical model for the dynamics of a mosquito vector (*Culex tarsalis*) population. *Biometrics.* **32**: 355-368.

[104] Muir, D. (1988). Anopheline mosquitoes: vectro-reproductions, life cycle and biotope. In: Malaria: Principles and Practice of Malariology (eds Wernsdorfer, W. and McGregor, I.). Churchill Livingstone, New York, pp: 431-452.

[105] Mukandavire, Z., Gumel, A. B., Garira, W. and Tchuenche, J. M. (2009). Mathematical analysis of a model for HIV-malaria co-infection. *Mathematical Biosciences and Engineering.* **6**: 333-362.

[106] Muldowney, J. S. (1990). Compound matrices and ordinary differential equations. *Rocky Mountain J. Math.* **20**: 857-872.

[107] Nedelman, J. (1984). Inoculation and recovery rates in the malaria model of Dietz, Molineaux and Thomas. *Mathematical Biosciences.* **69**: 209-233.

[108] Nedelman, J. (1985). Some new thoughts about some old malaria models-introductory review. *Mathematical Biosciences.* **73**: 159-182.

[109] Ngwa, G. A. (2005). On the population dynamics of the malaria vector. *Bull. Math. Biol.* **68**: 2161-2189.

[110] Niger, A. M. and Gumel, A. B. (2008). Mathematical analysis of the role of repeated exposure on malaria transmission dynamics. *Differential Equations and Dynamical Systems.* **16**: 251-287.

[111] Nussenzweig, R. S., Vanderberg, J., Most, H. and Orton, C. (1967). Protective immunity produced by the injection of x-irradiated sporozoites of *Plasmodium berghei. Nature.* **216**: 160-162.

[112] Pan American Health Organization. Annual Malaria Cases and Deaths in the Americas 1998-2006. http://www.paho.org/English/AD/DPC/CD/mal-cases-deaths-1998-2006.pdf (Accessed August, 2008).

[113] Perko, L. (2000). Differential Equations and Dynamical Systems. Text in Applied Mathematics. Volume **7**, Springer, Berlin.

[114] Plebanski, M. and Hill, A. V. S. (2000). The immunology of malaria infections. *Curr. Opin. Immunol.* **12**: 437-441.

[115] Porphyre, T., Bicout, D. J. and Sabatier, P. (2005). Modelling the abundance of mosquito vectors versus flooding dynamics. *Ecol. Model.* **183**: 173-181.

[116] Powell, A. J. and Logan, J. A. (2005). Insect seasonality: A circle map analysis of the temperature-driven life cycles. *Theor. Popul. Biol.* **67**: 161-179.

[117] Pykh, Y. A. (2002). Lyapunov functions as a measure of biodiversity: theoretical background. *Ecological Indicators.* **2**: 123-133.

[118] Robinson, R. C. (2004). An Introduction to Dynamical Systems: Continuous and Discrete. Pearson Education, Inc. New Jersey.

[119] Raffy, M. and Tran, A. (2005). On the dynamics of flying insects populations controlled by large scale information. *Theor. Popul. Biol.* **68**: 91-104.

[120] RBM Global Strategic Plan 2005-2015, November 2005, RBM Partnership. http://www.rollbackmalaria.org/multimedia/partnershippublications.html#2006, (Accessed March, 2009).

[121] Rowe, A. K. and Steketee, R. W. (2007). Prediction of the impact of malaria control efforts on all-cause child mortality in Sub-Saharan Africa. *Am. J. Trop. Med. Hyg.* **77**: 48-55.

[122] Saul, A. (1998). Models for the in-host dynamics of malaria revisited: Errors in some basic models lead to large over-estimates of growth rates. *Parasitology.* **117**: 405-407.

[123] Saul, A. (2007). Mosquito stage, transmission blocking vaccines for malaria. Tropical and travel-associated diseases. *Current Opinion in Infectious Diseases.* **20**: 476-481.

[124] Sharma, K. S., Chattopadhyay, R., Chakrabarti, K., Pati, S. and Chitnis, C. E. (2004). Epidemiology of malaria transmission and development of natural immunity in a malaria endemic village, San Dulakudar, in Orissa state, India. *American Journal of Tropical Medicine and Hygiene.* **71**: 457-465.

[125] Sharma, S. and Pathak, S. (2008). Malaria vaccine: a current perspective. *J. Vector Borne Dis.* **45**: 1-20.

[126] Sharomi, O., Podder, C. N., Gumel, A. B. and Song, B. (2008). Mathematical analysis of the transmission dynamics of HIV/TB coinfection in the presence of treatment. *Math. Biosci and Engrg.* **5**: 145-174.

[127] Simon, C. P. and Jacquez, J. A. (1992). Reproduction numbers and the stability of equilibrium of SI models for heterogeneous populations. *SIAM J. Appl. Math.* **52**: 541-576.

[128] Smith, T., Killeen, G. F., Maire, N., Ross, A., Molineaux, L., Tediosi, F., Hutton, G., Utzinger, J., Dietz, K. and Tanner, M. (2006). Mathematical modeling of the

impact of malaria vaccines on the clinical epidemiology and natural history of *Plasmodium falciparum* malaria: Overview. *Am. S. Trop. Med. and Hyg.* **75**(suppl 2): 1-10.

[129] Song, Y., Han, M. and Wei, J. (2005). Stability and Hopf bifurcation analysis on a simplified BAM neural network with delays. *Physica D.* **200**: 185-204.

[130] Strogatz, S. H. (2000). Nonlinear Dynamics and Chaos, With Applications to Physics, Biology, Chemistry, and Engineering. Westview Press, Cambridge.

[131] Sun, C., Lin, Y. and Han, M. (2006). Stability and Hopf bifurcation for an epidemic disease model with delay. *Chaos, Solitons and Fractals.* **30**: 204-216.

[132] Takahashi, L. T., Norberto, A. M., Wilson, C. F., Jr., Petronio, P. and Hyun, M. Y. (2005). Mathematical models for *Aedes aegypti* dispersal dynamics: Travelling waves by wing and wind. *Bull. Math. Biol.* **67**: 509-528.

[133] Thieme, H. R. (1993). Persistence under relaxed point dissipativity (with application to an epidemic model). *SIAM J. Math. Anal.* **24**: 407-435.

[134] Tumwiine, J., Mugisha, J. Y. T. and Luboobi, L. S. (2007). On oscillatory pattern of malaria dynamics in a population with temporary immunity. *Comp. and Math. Methods of Medicine.* **8**: 191-203.

[135] Udhayakumar, V. (1998). Immunogenicity of *Plasmodium falciparum* and *Plasmodium vivax* circumsporozoite protein repeat multiple antigen constructs (MAC). *Vaccine.* **16**: 982-988.

[136] van den Driessche, P. and Watmough, J. (2002). Reproduction numbers and subthreshold endemic equilibria for compartmental models of disease transmission. *Math. Biosci.* **180**: 29-48.

[137] Wang, R., Doolan, D. L., Le, T. P., Hedstrom, R. C., Coonan, K. M., Charoenvit, Y., Jones, T. R., Hobart, P., Margalith, M., Ng, J., Weiss, W. R., Sedegah, M., de Taisne, C., Norman, J. A. and Hoffman, S. L. (1998). Induction of antigen-specific cytotoxic T lymphocytes in humans by a malaria DNA vaccine. *Science.* **282**: 476-479.

[138] Wiggins, S. (1983). Introduction to Applied Nonlinear Dynamical Systems and Chaos. Springer-Verlag, New York.

[139] World Health Organization (2005). World Malaria Report. *www.rbm.who.int.* (accessed July, 2008).

[140] Yandell, S. B. and Hogg, B. D. (1988). Modelling insect natality using splines. *Biometrics.* **44**: 385-395.